

Isocyanate-free approaches to polyurea dispersions and coatings

Citation for published version (APA):

Ma, S. (2017). *Isocyanate-free approaches to polyurea dispersions and coatings*. [Phd Thesis 1 (Research TU/e / Graduation TU/e), Chemical Engineering and Chemistry]. Technische Universiteit Eindhoven.

Document status and date:

Published: 29/11/2017

Document Version:

Publisher's PDF, also known as Version of Record (includes final page, issue and volume numbers)

Please check the document version of this publication:

- A submitted manuscript is the version of the article upon submission and before peer-review. There can be important differences between the submitted version and the official published version of record. People interested in the research are advised to contact the author for the final version of the publication, or visit the DOI to the publisher's website.
- The final author version and the galley proof are versions of the publication after peer review.
- The final published version features the final layout of the paper including the volume, issue and page numbers.

[Link to publication](#)

General rights

Copyright and moral rights for the publications made accessible in the public portal are retained by the authors and/or other copyright owners and it is a condition of accessing publications that users recognise and abide by the legal requirements associated with these rights.

- Users may download and print one copy of any publication from the public portal for the purpose of private study or research.
- You may not further distribute the material or use it for any profit-making activity or commercial gain
- You may freely distribute the URL identifying the publication in the public portal.

If the publication is distributed under the terms of Article 25fa of the Dutch Copyright Act, indicated by the "Taverne" license above, please follow below link for the End User Agreement:

www.tue.nl/taverne

Take down policy

If you believe that this document breaches copyright please contact us at:

openaccess@tue.nl

providing details and we will investigate your claim.

Isocyanate-free approaches to polyurea dispersions and coatings

PROEFSCHRIFT

ter verkrijging van de graad van doctor aan de Technische Universiteit Eindhoven, op
gezag van de rector magnificus prof.dr.ir. F.P.T. Baaijens,
voor een commissie aangewezen door het College voor Promoties, in het openbaar te
verdedigen op donderdag 29 november 2017 om 14:00 uur

door

Shuang Ma

geboren te Zhejiang, China

Dit proefschrift is goedgekeurd door de promotoren en de samenstelling van de promotiecommissie is als volgt:

voorzitter:	prof.dr.ir. N. A. J. M. Sommerdijk
1 ^e promotor:	prof.dr.ir. C. E. Koning
2 ^e promotor:	prof.dr.ir. R. A. T. M. van Benthem
copromotor(en):	dr.ir. R. J. Sablong
leden:	prof.dr.ir. K. U. Loos (Rijksuniversiteit Groningen)
	prof.dr. H. Cramail (Université de Bordeaux)
	prof.dr. R. Tuinier
	prof.dr.ir. A. P. H. J. Schenning

Het onderzoek of ontwerp dat in dit proefschrift wordt beschreven is uitgevoerd in overeenstemming met de TU/e Gedragscode Wetenschapsbeoefening.

The most beautiful thing we can experience is the mysterious. It is the source of all true art and science.

Albert Einstein

Shuang Ma

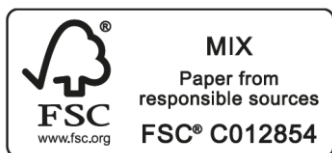
Isocyanate-free approaches to polyurea dispersions and coatings

Eindhoven University of Technology, 2017

This research forms part of the research programme of the Dutch Polymer Institute (DPI), project #759.

A catalogue record is available from the Eindhoven University of Technology Library
ISBN: 978-90-386-4392-2

Printed by: Gildeprint – www.gildeprint.nl



Copyright © 2017 by Shuang Ma

Cover design by Pengcheng An and Shuang Ma

Table of content

Chapter 1. Non-isocyanate polyurethane/ureas	1
1.1 General introduction of polyurethanes and polyureas.....	1
1.2 Isocyanate-free approaches to polyurethanes	3
1.2.1 Poly(alkyl urethane)s	3
1.2.2 Poly(hydroxyl urethanes) from bis-cyclic carbonates ([m,n]-PUR).....	9
1.3 Isocyanate-free approaches to polyureas (PUs, [n]-PU).....	14
1.4 Catalysts for the isocyanate-free polyurethane chemistry	15
1.5 Water-borne polyurethane/urea dispersions and coatings	16
1.6 Research aim and scope	17
1.7 References	19
Chapter 2. Catalysts for isocyanate-free polyurethane/urea synthesis: mechanism and application	25
2.1 Introduction	26
2.2 Experimental Section	27
2.2.1 Materials	28
2.2.2 Reactions and synthesis	28
2.2.3 Characterizations	29
2.3 Results and discussion.....	30
2.3.1 General observations	30
2.3.2 Reaction order and transition states of the alkali bases- and TBD-catalyzed model reaction	32
2.3.3 Activation energy of urethane formation.....	34
2.3.4 Activation energy of urea formation	35
2.3.5 Comparison with computational modeling	38
2.3.6 Application in polymerization.....	40
2.4 Conclusions	42
2.5 References	43
Appendix	46

Chapter 3. Preparation of cationically stabilized water-borne polyurea dispersions via an isocyanate-free route	53
3.1 Introduction	54
3.2 Experimental Section	57
3.2.1 Materials	57
3.2.2 Reactions and synthesis	57
3.2.3 Characterizations	59
3.3 Results and discussion.....	61
3.3.1 Model reaction study of diamine-functional IDAs (IDAAs) and dicarbamate-functional IDAs (IDAcS)	61
3.3.2 Polyureas with IDAAs	64
3.3.3 PU dispersions and coatings.....	66
3.4 Conclusion.....	71
3.5 References	72
Chapter 4. Investigation and mitigation of a side reaction during carbamate aminolysis: N-alkylation.....	75
4.1 Introduction	76
4.2 Experimental Section	77
4.2.1 Materials	77
4.2.2 Reactions and synthesis	77
4.2.3 Characterizations	79
4.3 Results and discussion.....	79
4.3.1 Preliminary observations.....	79
4.3.2 N-alkylation in carbamate aminolysis	81
4.3.3 Mitigation of the side reaction: N-alkylation	83
4.3.4 M_n optimization	91
4.4 Conclusions	93
4.5 References	94
Chapter 5. Isocyanate-free polyurethane/urea coatings with di-tert-butyl carbamates as monomer	95
5.1 Introduction	96
5.2 Experimental section	97
5.2.1 Materials	97
5.2.2 Reactions and synthesis	98
5.2.3 Characterizations	100
5.3 Results and discussion	102

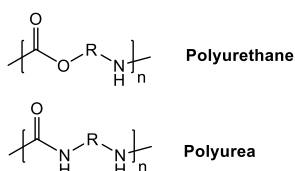
5.3.1 Model reaction of dicarbamates and HEX.....	102
5.3.2 Polyurea synthesis.....	108
5.3.3 Polyurethane synthesis	110
5.3.4. Preparation of water-borne polyurea (PU) and polyurethane urea (PUU) dispersions	113
5.4 Conclusions	120
5.5 References	121
Chapter 6. Anionic polyurea dispersions with ethylenediaminetetraacetic dianhydride as internal dispersing agent	123
6.1 Introduction	124
6.2 Experimental Section	126
6.2.1 Materials	126
6.2.2 Reactions and synthesis	126
6.2.3 Characterization.....	127
6.3 Results and discussion.....	129
6.3.1 Model reaction study with diamine and dianhydride	129
6.3.2 Poly(amic acid urea) dispersions (PAAUDs)	132
6.3.3 Effect of the TEA/-COOH molar neutralization ratio on the PAAUD particle sizes.....	134
6.3.4 Effect of PUda/EDTAD molar ratio on the PAAUD particle size	135
6.3.5 Effect of the molecular weight of PUda on the PAAUD particle size	136
6.3.6 Water-borne poly(amic acid urea) coatings.....	139
6.4 Conclusions	140
6.5 References	141
Chapter 7. Curing of polyurea coatings.....	143
7.1 Introduction	144
7.2 Experimental Section	146
7.2.1 Materials	146
7.2.2 Reactions and synthesis	147
7.2.3 Characterization.....	149
7.3 Results and discussion.....	151
7.3.1 Catalysts for amic acid/amine reaction	151
7.3.2 Crosslinking of anionically stabilized PUDs	157
7.3.3 Crosslinking of cationically stabilized PUDs	160
7.4 Conclusions	165
7.5 References	166

Appendix	167
Chapter 8. Epilogue	169
8.1 Highlights	169
8.2 Technology assessment.....	170
8.3 Outlook.....	171
Glossary	173
Summary	177
Acknowledgement.....	180
List of publications	183
Curriculum Vitae.....	184

Chapter 1. Non-isocyanate polyurethane/ureas

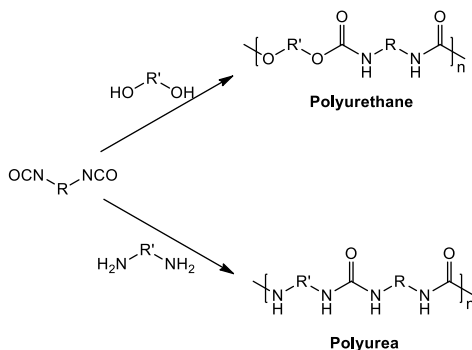
1.1 General introduction of polyurethanes and polyureas

Polyurethanes (PURs) are a class of polymers in which the segments are connected by urethane (or carbamate) groups, while the polymers bridged by urea moieties are referred to as polyureas (PUs, Scheme 1). The two types of polymers have similar structures and exhibit comparable physical properties. Therefore, in many cases, they are both referred to as polyurethanes, even for those with only urea moieties in the chains.¹



Scheme 1. Structure of polyurethane and polyurea.

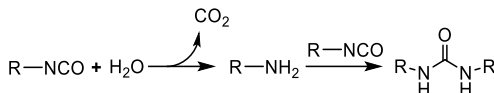
The history of PU(R)s dates back to 1937, when Otto Bayer, inspired by the work of Wallace Carothers on polyesters and polyamides, first synthesized PURs by polyaddition of hexane-1,6-diisocyanate (HDI) and 1,4-butanediol (BDO).² Similarly, PUs can be generated from diamines and diisocyanates (Scheme 2).³ Like polyamides, these PU(R)s are categorized as [m,n]-PU(R)s, while [n]-PURs can be synthesized from α -hydroxy- ω -isocyanato alkanes.⁴



Scheme 2. PUR and PU formations from diisocyanates and diols and diamines.

PU(R) products are widely employed in numerous applications, such as (dispersion-based) coatings, plastics, fibers, foams, adhesives, paints, sealants and elastomers. The superior mechanical properties of PU(R)s stem from the abundant hydrogen bonds between the polymer chains (Scheme 3). Such intermolecular hydrogen bonds can act as physical crosslinks and significantly improve the mechanical properties of the materials. The energy of the hydrogen bonding interaction between the urethane moieties is about 18.4 kJ/mol, which is much higher than the interaction energy between urethanes and aliphatic chain parts (7.5 kJ/mol).⁵ Therefore, the urethane moieties tend to rearrange and form ordered local

foams are produced via the reaction of diisocyanates with water, which generates primary amines and the blowing agent CO₂.⁴ While the amines can further react with diisocyanates to form ureas (Scheme 4), which bear even stronger hydrogen bond interactions between the chains compared to urethanes,⁵ CO₂ forms empty areas or pores inside the material. Nowadays, such porous material finds wide applications in rigid car dash boards, flexible car seats and mattresses, insulating panels, seals and packages.^{7,8}



Scheme 4. Urea and CO₂ formation from isocyanates in aqueous environment.

1.2 Isocyanate-free approaches to polyurethanes

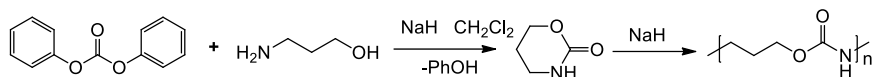
Despite the high popularity of PU(R)s in global markets, their industrial production has some drawbacks. A major issue is the use of the toxic diisocyanates. For instance, Peters et al. studied the cumulative pulmonary effects of toluene diisocyanate (TDI) and observed acute changes in ventilatory capacity of workers upon exposure to TDI.⁹ Other diisocyanates such as 1,6-hexamethylene diisocyanate (HDI) and isophorone diisocyanate (IPDI) also have similar effects on human health and therefore, request measures to prevent their direct contact with skins during operation. One of the most notorious event demonstrating the hazardous nature of the isocyanates was the tragic Bhopal disaster, which took thousands of lives after a methyl isocyanate leakage.¹⁰ This catastrophe not only shocked the local governments, but also chemists, who thereupon strove to develop non-isocyanate routes for PU(R) synthesis. Two categories of PURs are obtained via isocyanate-free strategies, namely poly(alkyl urethane)s, produced from (bis)carbamates as monomers, and poly(hydroxyl urethane)s, generated from bis-cyclic carbonates (BCCs) and diamines.

1.2.1 Poly(alkyl urethane)s

Different categories of monomers were reported for the synthesis of poly(alkyl urethane)s, namely cyclic urethanes, hydroxyl carbamates (HCs), bis-hydroxyalkylcarbamates (BHCs) and bis-alkylcarbamates (BACs). The application of these monomers in PUR production is discussed in this section.

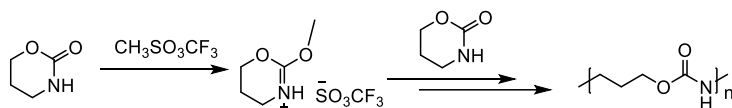
1.2.1.1 Cyclic urethanes as monomers ([n]-PUR)

The first PUR synthesis with cyclic urethane as monomers was described in 1958 by Hall and Schneider.¹¹ In their report, amino propanol and di-*p*-cresyl carbonate were used as starting materials to synthesize a cyclic urethane. The polymerization of this cyclic trimethylene urethane was catalyzed by NaH at 80 °C (Scheme 5). The resulting PUR had a melting point of 148 °C. However, due to the limited analytical instruments, in-depth studies on the ring-opening polymerization (ROMP) of cyclic urethane or microstructures of the materials were not performed.



Scheme 5. Ring opening polymerization of cyclic urethane synthesized from di-*p*-cresyl carbonate and amino propanol with NaH as catalyst.¹¹

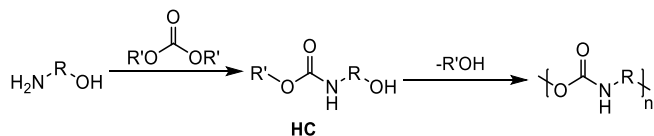
In 1996, the group of Höcker conducted a more detailed study on the ROMP of cyclic urethanes (Scheme 6).¹² They showed that polymerizations with anionic initiators, like NaH or other strong bases such as *sec*-butyl lithium, generated PURs with non-uniform microstructures. On the contrary, the cationic initiation of the cyclic monomers by methyl triflate at 100-120 °C over 24 hours produced a more uniform polymer microstructure with a number average molecular weight (M_n) of 22 kDa (Scheme 6).



Scheme 6. Ring opening polymerization of cyclic urethane with methyl triflate as initiator.

1.2.1.2 Hydroxyl carbamates as monomers ([n]-PUR)

Hydroxyl carbamates (HCs) are another important type of monomers in isocyanate-free PUR synthesis. These compounds could be self-condensed into PURs (Scheme 7).¹³

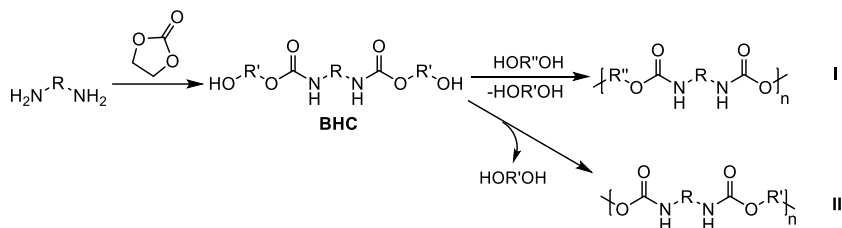


Scheme 7. PUR synthesis from self-condensation of HC.¹³

HCs can be prepared either via the reaction of amino alcohols and ϵ -caprolactam or via reaction between diamines and ϵ -caprolactone, followed by modification with diphenyl carbonate. Since phenol is a good leaving group, the self-condensation of the phenyl-bearing HCs can proceed at a rather low temperature (90 °C).¹⁴ Thus, Höcker et al. reported the synthesis of thermoplastic PURs with M_w values up to 60 kDa using such monomers and $\text{Bu}_2\text{Sn}(\text{OCH}_3)_2$ as catalyst.^{15,16}

1.2.1.3 Bis-hydroxyalkylcarbamates as monomers ([m,n]-PUR)

BHCs can either copolymerize with diols or self-polymerize to form PURs. Scott et al. described the preparation of PURs via self-condensation of bis-(2-hydroxyethyl)-1,6-hexanedicarbamate with BaO as catalyst at 150 °C.¹⁷ They also showed that the addition of high boiling point diols could lead to the transurethanization product (**I** in Scheme 8), with only a minor quantity of self-polymerized product (**II**).

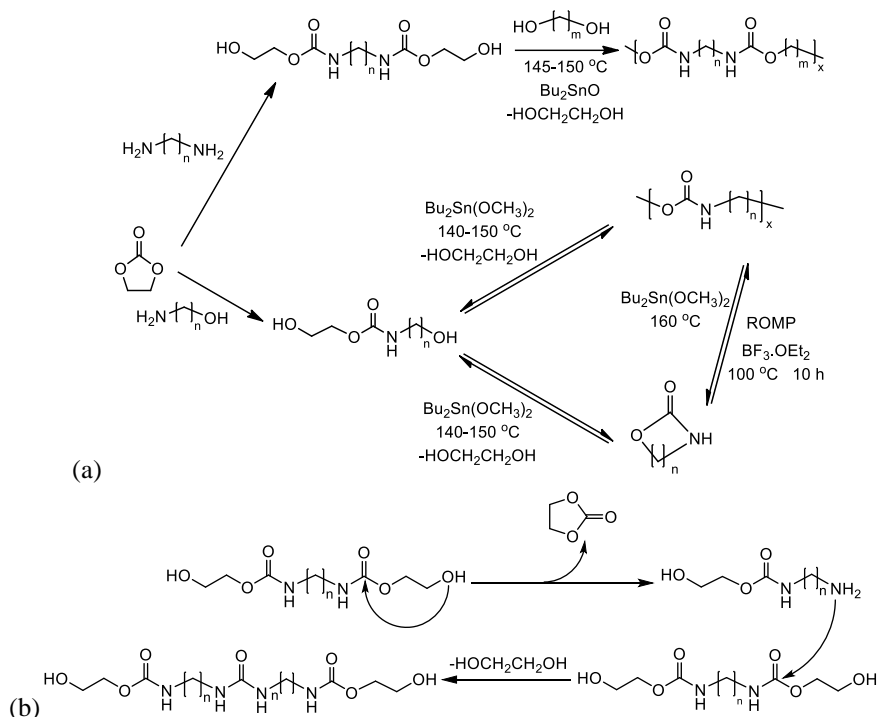


Scheme 8. PUR synthesis from BHC.¹⁷

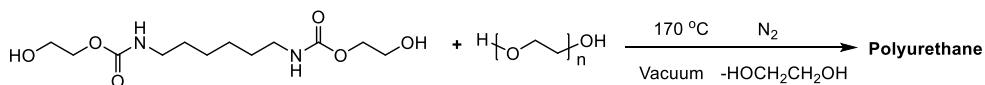
Detailed investigations on the mechanism of BHC polymerizations were carried out by Rokicki and Piotrowska, who modified the diamines or the amino alcohols with ethylene carbonate to produce bis-hydroxylalkylcarbamates or BHCs, which were subsequently polymerized with diols or self-polymerized to form PURs (Scheme 9a).¹⁸ The polymerization utilized $\text{Bu}_2\text{Sn}(\text{OMe})_2$ or Bu_2SnO as catalysts and xylene as azeotropic solvent to facilitate the removal of the ethylene glycol by-product from the reaction mixture. The presence of urea in these PURs was confirmed by both NMR and MALDI, and was identified as the result of transurethanization reactions between the hydroxyl urethanes and the amines. The latter are generated via the backbiting of the hydroxyl groups on the carbamates (Scheme 9b). Further optimization of such transurethanization polymerization was carried out by Ochiai et al, who showed that the urea formation between amine and carbamate was suppressed at elevated temperatures.¹⁹ The self-condensation of hydroxyl carbamates took place at 140–150 °C, resulting in either PURs or cyclic urethanes. The yields of the latter depend both on the stabilities of the rings (6-membered more stable than 7-membered) and the concentration of the monomers (dilution of the monomers favors the generation of cyclic urethane). The hydroxyl carbamates can also ring-close at 160 °C to form cyclic urethanes, which can further self-condense to produce high M_n PURs in the presence of $\text{BF}_3\cdot\text{OEt}_2$.

More recently, Yang et al. prepared PURs of M_n s up to 45 Da with BHCs and diols.^{20,21} They first polymerized BHCs with diols at 170 °C under N_2 with SnCl_2 as catalyst, followed by a gradual reduction of pressure to remove the traces of ethylene glycol and increase the conversion of the end-groups (Scheme 10).²² By varying the soft and hard segments, the T_g s of these semi-crystalline PURs could vary from -40 to 30 °C and their T_m s from 100 to 180 °C, which is suitable for thermoplastic applications.²³

As mentioned above, one favorable property of high molecular weight PPC is the large elongation at break, which allows the enhancement of the elastic modulus by using (inorganic) fillers or blending with other polymers without severe loss of toughness. By blending polyhydroxybutyrate with PPC, Siemens and BASF have developed an alternative material to styrene-based acrylonitrile-butadiene-styrene (ABS) plastic. Empower Materials is producing PPC on a pilot scale, which is used as sacrificial binder for high quality products in advanced ceramics, powder metals and sealing glasses.⁷



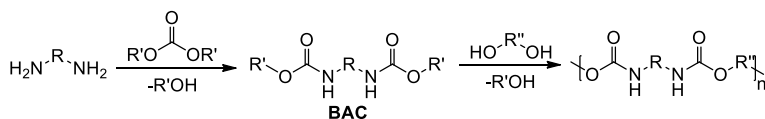
Scheme 9. (a) PUR formation with ethylene carbonate and amino alcohol or diamine. (b) Urea formation during polymerization.¹⁸



Scheme 10. High M_n PUR synthesis with BHCs and diols.²¹

1.2.1.4 Bis-alkylcarbamates as monomers ([m,n]-PUR)

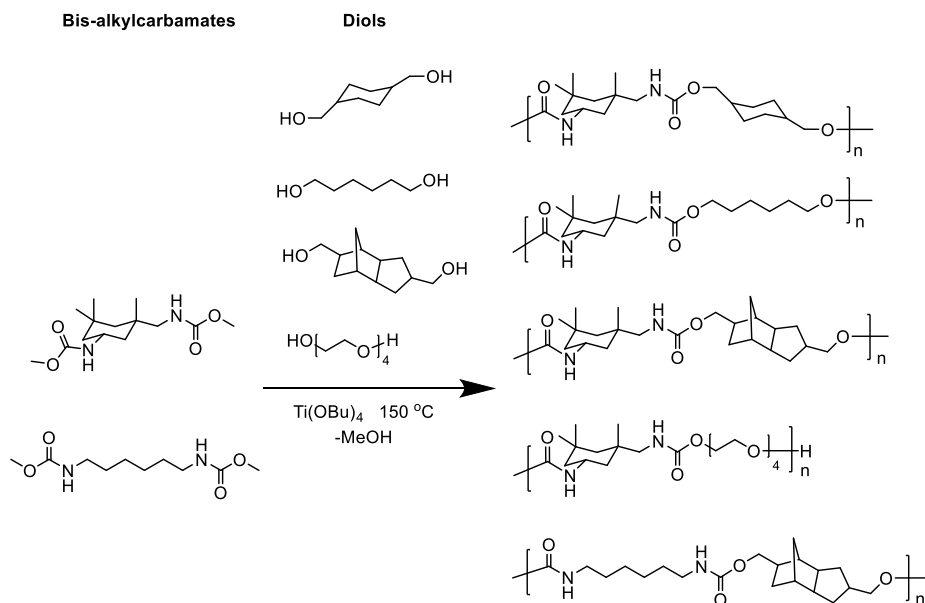
Bis-alkylcarbamates (BACs) form another type of versatile monomers for isocyanate-free PUR synthesis. The most common ones are bis-methyl-(BMCs) and bis-phenylcarbamates (BPCs), which can condense with polyols to yield PURs with methanol and phenol as by-products (Scheme 11).



Scheme 11. High M_n PUR synthesis with BHCs and diols.

Deepa et al. synthesized PURs with BMCs and various diols at 150 °C with $\text{Ti}(\text{O}i\text{Bu})_4$ as catalyst (Scheme 12).^{24,25} The BMCs employed were prepared via the reaction between dimethyl carbonate (DMC) and diamines in the presence of strong bases. By tuning the structure of the two building blocks, PURs with various material properties and microstructures were obtained. The T_g s of the materials could be modulated from -30 °C to

120 °C and their M_n s ranged from 3-20 kDa. BMCs with cycloaliphatic structures such as isophorone dimethylcarbamate (IPDMC) increased the rigidity of the polymers and thus, their T_g s. The authors also indicated a higher reactivity of primary hydroxyl groups towards the BMCs compared with secondary ones due to steric effects, while the influence of the structure of the BMCs on their reactivity towards diols was rather limited.



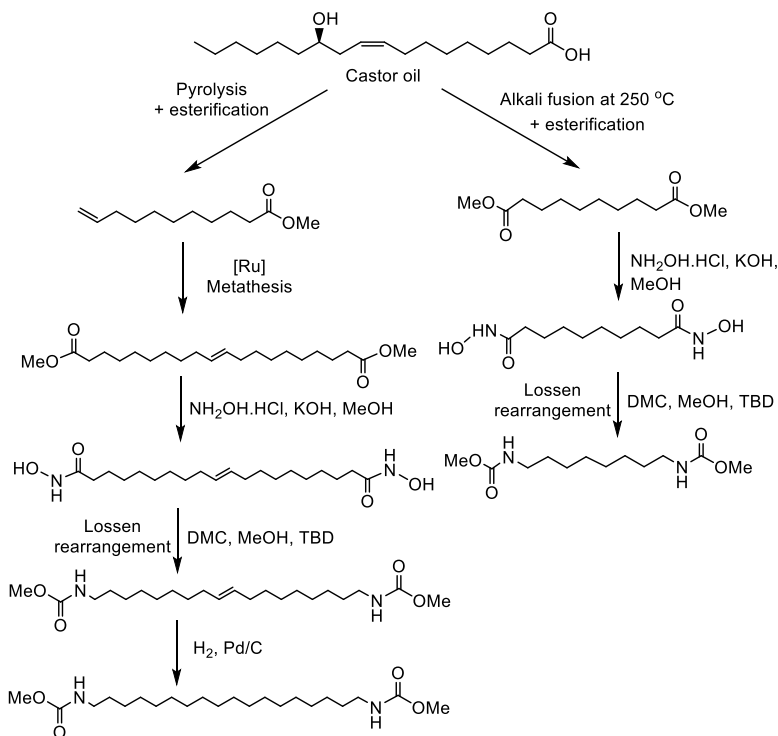
Scheme 12. PURs formation with different diols and biscarbamates.²⁴

The use of bio-based BMCs was reported by several groups.^{26,27} For example, Meier et al. described the synthesis of BMCs with limonene-modified monomers, prepared by reaction with thiol amine and DMC.²⁸ These BMCs were polymerized with various diols to form amorphous or semi-crystalline PURs with T_g s between 10-20 °C and melting points around 50-240 °C. The syntheses of both BMCs and PURs employed 1,5,7-triazabicyclo-[4.4.0]dec-5-ene (TBD), a known catalyst for various reactions including esterification and amide formation, which lowered the reaction temperature to 120 °C.²⁹ Similarly, Burel et al. employed a dimer fatty acid-based diamine (Priamine 1074 from Croda) and methyl ricinoleate as renewable starting materials for preparing BMCs. Both TBD and K_2CO_3 displayed high catalytic activities towards the BMC/diol polymerizations.³¹ The K_2CO_3 -catalyzed BMC/diol polymerization at 200 °C resulted in PURs with higher M_n s than those produced with TBD at 160 °C. The dangling aliphatic segments in the Priamine-based PURs limited the intermolecular interaction between the polymer chains, resulting in amorphous polymers with T_g s below -20 °C.

Tian et al. prepared PURs with 1,6-hexamethylene dicarbamate (HDC) and a high MW poly(carbonate macrodiol) (PCMD) as monomers and Bu_2SnO as catalyst.³² The polymerization conditions were optimized via monitoring the intrinsic viscosity of the reaction mixture during polymerization at different catalyst loadings, temperatures and

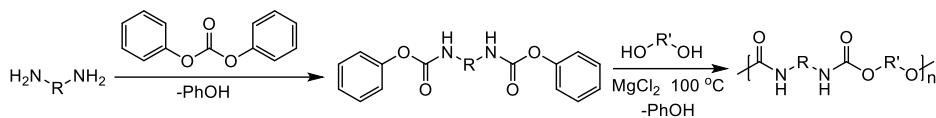
reaction times. The optimized conditions minimized the undesired side reactions and degradations. The M_n s of the PURs ranged from 35 to 51 Da, with D_M values between 1.3 and 1.6.

A new non-isocyanate approach to produce BMCs was also reported by Meier et al.³³ The authors employed castor oil as the raw material, which was modified into diesters by alkali fusion or pyrolysis followed by metathesis. The diesters were then treated with hydroxylamine under basic conditions, followed by Lossen rearrangement in the presence of dimethyl carbonate to obtain BMCs (Scheme 13). Despite the relatively high number of synthetic steps, this method can be industrially relevant, since castor oil is cheap and environmentally benign.



Scheme 13. PUR formation with castor oil as starting material.³³

BPCs were employed by Yamazaki et al. as monomers for isocyanate-free PUR synthesis.³⁴ The BPCs were prepared by modifying diamines with diphenyl carbonate. The polymerizations proceeded at 100 °C for 20 hours, and the phenol was removed by N_2 flow (Scheme 14). $MgCl_2$ was reported to be most active metal salt catalyst for such polymerization, as evidenced by the highest viscosity of the reaction mixtures obtained in the presence of this compound.

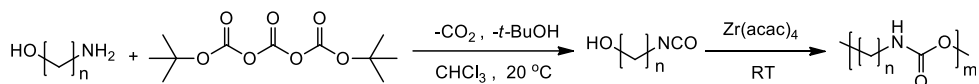


Scheme 14. PUR formation with BPC and diol as monomers.³⁴

In fact, those transurethanization reactions generally proceed at high temperatures with a catalyst due to the low reactivity of dicarbamates towards diols. In order to perform the polymerization under milder conditions, more reactive monomers or more active catalysts must be employed.

1.2.1.5 Other monomers ([n]-PUR)

The group of Meijer also reported the synthesis of aliphatic PURs by employing amino alcohols modified in situ with di-*tert*-butyl-tricarbonate to α,ω -isocyanato alcohols as monomers (Scheme 15).³⁵ The latter were then polymerized at room temperature with $\text{Zr}(\text{acac})_4$ as the catalyst. This one-pot polymerization provides a facile route to aliphatic PURs on a laboratory scale. However, due to the possible side reaction between the α,ω -isocyanato- and the amino alcohols, which could alter the stoichiometry of the polymerization, such synthetic method seems to be less suitable for industrial application.

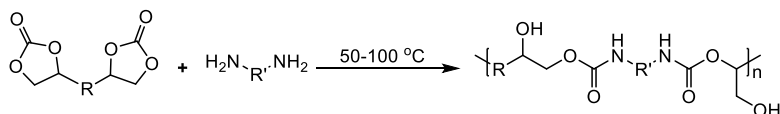


Scheme 15. PUR formation with amino alcohols as monomers.³⁵

1.2.2 Poly(hydroxyl urethanes) from bis-cyclic carbonates ([m,n]-PUR)

1.2.2.1 General description

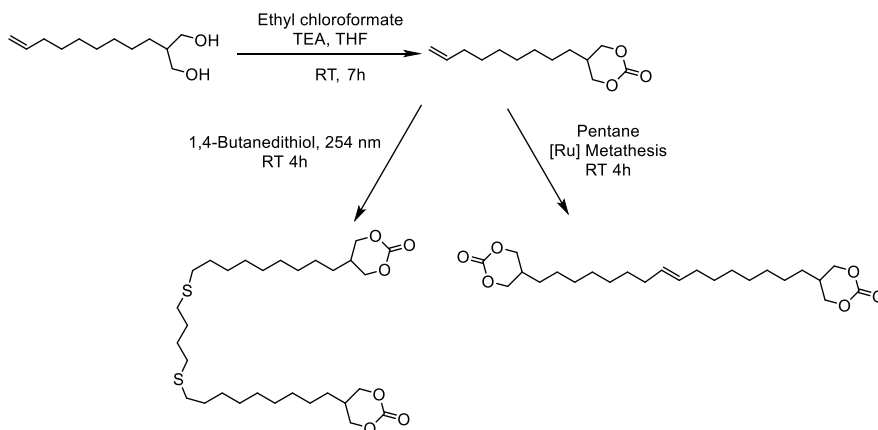
Bis-cyclic carbonates (BCCs) are reactive towards nucleophiles such as amines or thiols owing to the ring tension of the carbonate cycles. The energy of the ring strain is released during the ring opening process, thereby lowering the activation energy of the reaction. This results in mild reaction conditions (50-100 °C), even in the absence of catalyst, for the synthesis of poly(hydroxyl urethane)s (PHUs) with BCCs and diamines as monomers (Scheme 16). Thus, the BCC-diamine polymerizations have been one of the most investigated isocyanate-free routes to PURs.³⁶



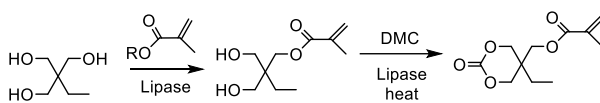
Scheme 16. General PHU synthesis with diamine and BCC as monomers.

BCCs can be obtained by various methods. For example, Mülhaupt et al. described the synthesis of BCC from bio-based limonene dioxide and CO_2 .³⁷ Cramail et al. reported the preparation of 6-membered BCCs by the reaction between alkene-carrying diols and ethyl chloroformate, followed by coupling via thiol-ene reaction or metathesis (Scheme 17).³⁸ Similarly, Pyo et al. described the production of methacrylic cyclic carbonates via a lipase-catalyzed reaction between trimethylolpropane (TMP), an alkyl methacrylate and dimethyl

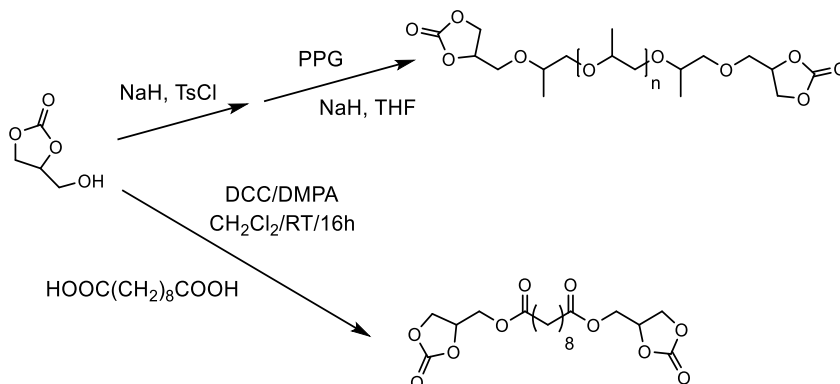
carbonate, a much less toxic route than the one using ethyl chloroformate (Scheme 18).³⁹ Another interesting route to BCCs involves the coupling of glycerol carbonate with diacids or diols to generate BCCs based on diesters⁴⁰ or polyethers^{41,42}, respectively (Scheme 19). Such methods requires reactive coupling agents like sodium hydride^{41,43} or dicyclohexylcarbodiimide (DCC),^{40, 44} due to the slow esterification and etherification of the BCCs.



Scheme 17. BCC synthesis through thiol-ene reaction or metathesis.³⁸



Scheme 18. 6-Membered cyclic carbonate synthesis from TMP, alkyl methacrylate and DMC.³⁹

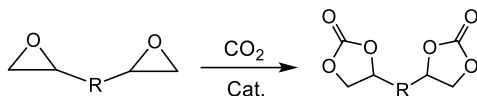


Scheme 19. BCC synthesis from glycerol carbonate and diol or diacid.^{40,41}

1.2.2.2 Synthesis of BCCs

The most popular method for BCC synthesis is via the reaction between CO₂ and di-epoxides. This is related to the inexpensive and renewable nature of CO₂ (Scheme 20).^{45,46} The addition of CO₂ to epoxides often requires harsh conditions such as high pressure and high temperature,

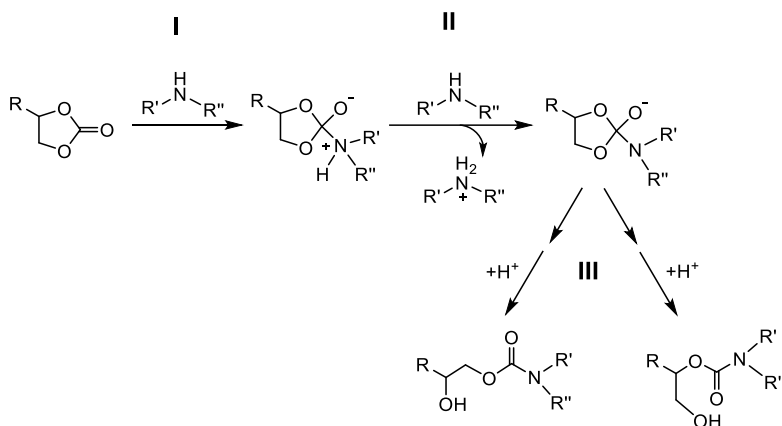
which could be mitigated via addition of efficient catalysts. For such reaction, a wide range of catalysts is available, including alkali halides,^{47,48} metal complexes,⁴⁹⁻⁵¹ and ionic liquids.⁵²⁻⁵⁵



Scheme 20. General route to BCC formation using di-epoxide and CO₂.

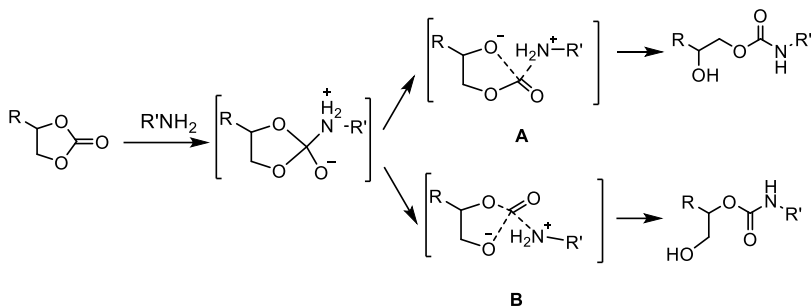
1.2.2.3 Mechanism of BCC aminolysis

The mechanism of the five-membered cyclic carbonate aminolysis was proposed by Garipov et al. as a three-step process (Scheme 21): the first stage (**I**) is considered to be the rate limiting step of the reaction, and consists of the nucleophilic attack on the carbonyl by the amine to yield a tetrahedral transition state. In the next stage (**II**), the charged transition state is deprotonated by a second amine molecule. The high electron density in the deprotonated tetrahedral intermediate initiates the cleavage of the carbon-oxygen bond in the last stage (**III**) and forms a hydroxyurethane with either a primary or a secondary alcohol.⁵⁶



Scheme 21. Mechanism of cyclic carbonate aminolysis.⁵⁶

The reactivity and the selectivity of the cyclic carbonate aminolysis are affected by a number of factors, including the nature of the substituents of the carbonate, the structure of the carbonate and the amine, the nature of the solvent and the catalyst. In their study on the aminolysis of 5-membered cyclic carbonates by hexylamine, Tomita et al. revealed an increase of the aminolysis rate when a strong electron-withdrawing group (EWG) is connected to the cyclic carbonate (Scheme 22).⁵⁷ The authors attribute the enhancement of the aminolysis rate to the inductive effect of the EWG on the negatively charged oxygen that stabilizes the intermediates **A** and **B**. Additionally, the closer distance between the substituent and the negatively charged oxygen in **A** is inductively more effective than that in **B**, leading to a lower primary/secondary alcohol ratio when a strong EWG is introduced.



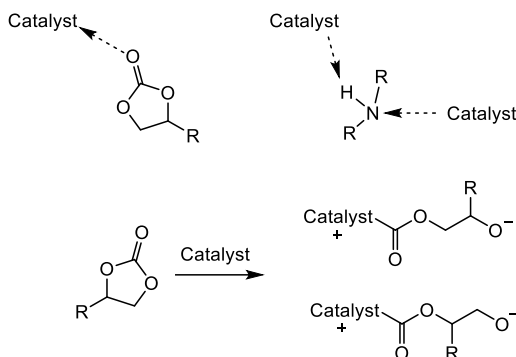
Scheme 22. Mechanism of primary and secondary hydroxyl group formation from cyclic carbonate and amine.⁵⁷

The influence of the cyclic carbonate structure on the aminolysis rate was investigated by the group of Endo.⁵⁸ They revealed that the aminolysis rates of cyclic carbonates follow the order seven-membered > six-membered > five membered ones. This was attributed to a higher strain in seven-membered cyclic carbonates with a heat of formation $\Delta H = -8.56$ kcal/mol compared to six- ($\Delta H = -5.58$ kcal/mol) and five-membered cyclic carbonates ($\Delta H = -2.74$ kcal/mol). Based on environmental considerations, five-membered cyclic carbonates are favored over the six- and seven-membered analogues, as the latter are prepared from phosgene or chloroformates.^{59,60}

The structure of the amines has a strong influence on the aminolysis rates of cyclic carbonates. Generally, primary amines with the highest nucleophilicity are the most reactive towards cyclic carbonates,^{61,62} while aromatic and secondary ones are inert for this reaction at room temperature.^{63,64} Furthermore, primary amines attached to a primary carbon are more reactive than those attached to a secondary one due to the steric effect.⁶⁵ Nohra et al. also showed that an increase of the alkyl chain length of the aliphatic amines resulted in a reduced reactivity. This is attributed to the less stable charged transition state with increasing hydrophobicity of the amines, caused by longer alkyl chains (Scheme 21).⁶²

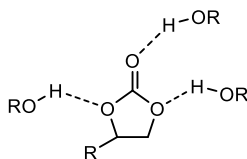
1.2.2.4 Catalysts and solvents for BCC aminolysis

Catalysts are often employed during the aminolysis of cyclic carbonates. The catalysts activate the reaction via increasing either the nucleophilicity of the amine or the electrophilicity of the carbonyl, or via ring-opening of the cyclic carbonate (Scheme 23). These catalysts include Lewis bases like triethylenediamine,⁶⁶ phosphines⁶⁷ and dimethylaminopyridine (DMAP),^{68,69} Lewis acids such as LiBr,⁴² ZnCl₂^{70,71} and Sc(OTf)₃,⁷² guanidine derivatives such as TBD,⁹⁹ 7-methyl-TBD (MTBD)⁷³ and 1,8-diazabicyclo(5.4.0)undec-7-ene (DBU),⁷⁴ thioureas^{75,76} and enzymes.^{77,78}



Scheme 23. Different catalytic mechanisms of cyclic carbonate aminolysis.⁴⁵

The polarity of the solvent also influences the kinetics of the cyclic carbonate aminolysis. As indicated in Scheme 21, the transition state of the reaction is charged, and hence more stable in polar solvents. The higher polarity of the solvent results in a lower activation energy and a faster reaction. Garipov et al. evidenced a similar feature in protic compared to aprotic solvents, which is attributed to the formation of hydrogen bonds between the solvent and the oxygens in the cyclic carbonate, increasing the electrophilicity of the carbonyl groups (Scheme 24).⁵⁵



Scheme 24. Increasing of electrophilicity of cyclic carbonate in presence of protic solvent.⁵⁵

Most of the BCC/diamine polymerizations are performed in polar solvents such as dimethyl sulfoxide (DMSO),⁷⁹ dimethylacetamide (DMAc)⁸⁰ and dimethylformamide (DMF)⁸¹ at 25 to 100 °C. In the absence of catalysts, the M_n s of the PHUs prepared in these solvents generally range from 3-20 kDa.^{82,83} However, the M_n s of the PHUs reach 30-50 kDa when catalysts such as TBD⁷⁸ or thioureas⁸⁴ are employed. Prömpers et al. reported that the polymerization of BCCs and diamines in less polar solvents such as tetrahydrofuran (THF) or CH_2Cl_2 could lead to M_n s up to 87 kDa, probably due to the precipitation of the PHUs in these solvents, preventing them from degradation via reverse or side reactions.⁸⁵ The authors also showed that both higher concentrations of monomers and higher temperatures led to an increase of M_n , owing to the higher aminolysis rates and lower viscosities under these conditions. Ochiai et al. described the synthesis of PHUs in a mixture of water and an ionic liquid. The low M_n s of 4 kDa or less were attributed to the hydrolysis of the BCCs in water.⁸⁶

Bulk polymerizations of BCCs and diamines were also investigated for enhancing the molecular weight of the polymers. Sheng et al. synthesized PHUs with M_n s around 30 kDa using different BCCs and diamines in bulk at 80 °C for 2h,⁸⁷ while the production of PHUs with M_n s up to 68 kDa, from a diamine-functional macromonomer based on poly(propylene

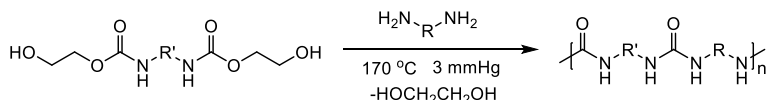
glycol) (PPG) with an M_n of 2000, was reported by Annunziata et al.⁸⁸

As mentioned earlier, the high rates of the aminolysis of BCCs allow BCC/diamine copolymerizations to generate PHUs of high M_n s under mild conditions. However, those PHUs are more hygroscopic compared with standard, non-hydroxyl PURs due to the high polarity of the pendent hydroxyl groups and therefore, are not suitable for outdoor applications or for automotive coatings.⁹⁹ Side reactions, such as carbonation of the amine,⁸⁹ in-situ formation of CO_2 ⁹⁰ and oxazolidinone formation,^{91,92} also occur during BCC/diamine polymerizations, further limiting the M_n s of the PHUs.

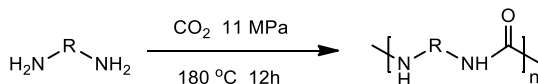
1.3 Isocyanate-free approaches to polyureas (PUs, [n]-PU)

PUs are good alternatives to PURs, due to their comparable material properties such as abrasion resistance, elongation at break, water resistance and outdoor durability as a result of the presence of abundant hydrogen bonds in both materials. In addition, the urea moiety has a much better stability against degradation compared to the urethane bond.^{93,94}

Several research teams reported the synthesis of PUs via isocyanate-free approaches. Yang et al. synthesized thermoplastic PUs from diamines and bis(hydroxyethyl) diurethanes at 170 °C under N_2 . PUs with M_n s up to 12 kDa were obtained with T_g s between 3 and 18 °C and T_m s of 140-150 °C (Scheme 25).⁹⁵ An interesting pathway to oligoureas was introduced by Zhao et al., who synthesized PUs with M_n values of 2 kDa from CO_2 and diamines at 180 °C (Scheme 26).⁹⁶ Despite the use of renewable CO_2 , the complex synthesis of BCCs prohibit a larger scale production.⁷⁹ The synthesis of dendritic PUs with carbonyl diimidazole or carbonyl biscaprolactam as carbonyl sources was reported by Loontjens and Davis.^{97,98} This method could also be applied to the preparation of linear PUs.

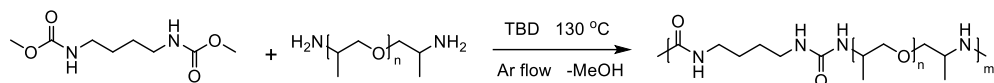


Scheme 25. Urea synthesis from azide and isothiocyanate.⁹⁶



Scheme 26. Urea synthesis from diamine and CO_2 .⁹⁷

Recently, our group described the synthesis of PUs from dicarbamates and poly(propylene glycol) bis(2-aminopropyl ether)s (PPGdas) as monomers and TBD as catalyst (Scheme 27).⁹⁹ This procedure afforded materials with M_n values around 30 kDa, which is sufficiently high to obtain satisfactory mechanical properties.⁵ The investigation also revealed an increase of the T_g s of the polymers as well as their mechanical properties, such as the E-Modulus, with higher hard segment content, the length of which also affects the flow temperature of the materials.



Scheme 27. PU formation with butane dicarbamate and PPGda as comonomers.¹⁰⁰

1.4 Catalysts for the isocyanate-free polyurethane chemistry

Several catalysts were employed in the carbamate aminolysis or alcoholysis, including TBD¹⁰⁰ and potassium *tert*-butoxide.²³ Other catalysts utilized in esterification reactions, amidations or isocyanate chemistry could also be potentially employed in carbamate/amine or carbamate/alcohol reactions. A series of commercially available catalysts including strong bases such as phosphazenes,^{19,20} guanidine derivatives,^{19,99} organo-metallic compounds,^{23,111,112} alkaline oxides,¹⁰⁴⁻¹⁰⁷ and transition metal compounds^{30,109,110} is depicted in Table 1.

Table 1. Commercially available catalysts for esterification, carbonate or ester aminolysis and urethane formation reported in literature.

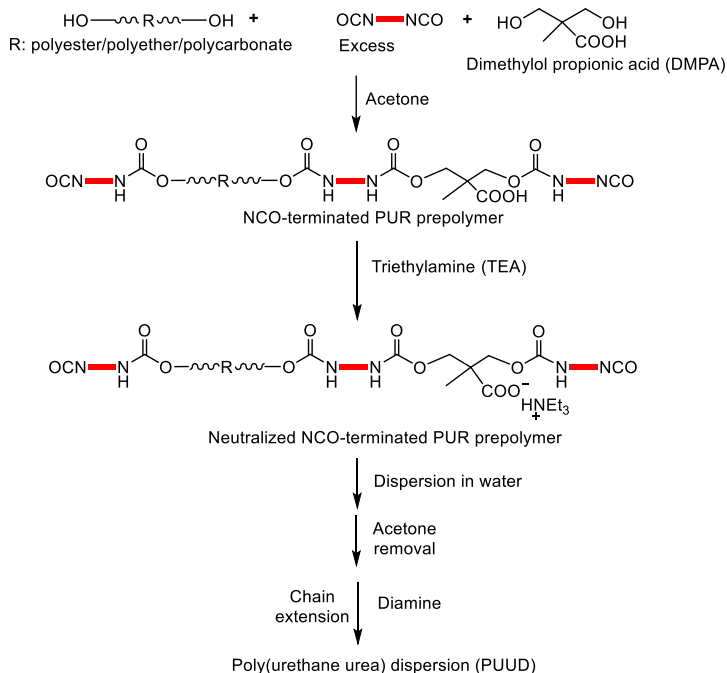
Catalysts	Structure	Reactions*	References
Phosphazenes		Carbonate aminolysis Esterification	68, 100
1,5,7-Triazabicyclo-[4.4.0]dec-5-ene (TBD)		Carbonate aminolysis	99
1,8-Diazabicyclo-(5.4.0)undec-7-ene (DBU)		Carbonate aminolysis Amidation	74
Potassium <i>tert</i> -butoxide (KO ^{<i>t</i>} -Bu)		Esterification	103
Strontium oxide	SrO	Esterification	104
Calcium oxide	CaO	Esterification	105
Titanium butoxide		Urethane formation Esterification	24, 25
Di-butyltin-dilaurate (DBTDL)		Urethane formation	110, 111, 112
Scandium triflate		Esterification	30

* Most relevant reactions

1.5 Water-borne polyurethane/urea dispersions and coatings

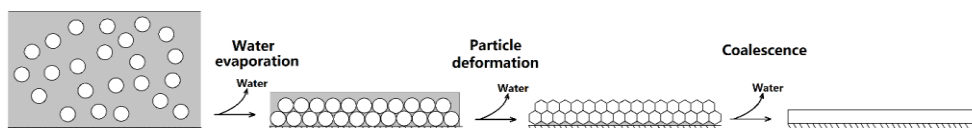
Solvent-borne PU(R)s coatings have so far dominated the coating market thanks to their fast-drying and excellent mechanical properties.¹¹³ However, the high demand for such coatings during the last decades led to the implementation of environmental regulations to limit the amount of volatile organic compounds (VOCs) in their coating formulations.¹¹⁴ Therefore, water-borne PU(R) coating systems have gained growing attention due to their low VOC contents. Furthermore, the water-borne polyurethane/urea dispersions (PUUDs) have significantly lower viscosities compared with the solvent-borne solutions, especially at high solid contents and accordingly prevent wrinkling during coating application.^{115,116} PUUDs consist of PU(R) particles dispersed in water and are generally stabilized by an internal dispersing agent (IDA) chemically incorporated within the PU(R) chains. The IDAs are either of cationic (quaternized ammonium salts¹¹⁷), anionic (carboxylates^{118,119} or sulfonates¹²⁰ neutralized by volatile acids) or non-ionic (water soluble polyethers like polyethylene glycol)^{121,122} nature. Although the PUUDs with non-ionic IDAs exhibit higher stabilities compared to the ionic ones at freezing temperatures, high shear forces and high salt concentrations, the resulting coatings are more hygroscopic and sensitive to water due to the presence of water-soluble polyether chains in the parent resins.¹²⁰ Conventional methods for PUUD preparation employ diisocyanates and diols as comonomers, together with diol-functional IDAs, typically dimethylolpropionic acid (DMPA). The resulting diisocyanate-functional prepolymers are then dissolved in volatile solvents (like acetone or butanone) and neutralized with tertiary amines (anionic IDAs, implying e.g. neutralized DMPA) or acids (cationic IDAs, implying e.g. neutralized tertiary amines) before mixing in water. The mixtures are then chain-extended with diamines to form high molecular weight PUUDs (Scheme 28).^{43,44}

This multi-step procedure prevents the direct dispersion of a high molecular weight polymer into water, which would be very difficult due to high viscosity of the mixtures. However, the mixing of the prepolymer solutions with water leads to the reaction between the isocyanate end-groups and water before or during the addition of the diamine chain extender (Scheme 4).¹²³



Scheme 28. Industrial synthesis of high molecular weight poly(urethane urea) dispersions.

The PUUDs can be applied on a wide range of rigid and flexible substrates to form thin films or coatings. The PU(R) coatings are produced by evaporating the water from the PUUDs (Scheme 29).¹²⁴ The particles in the PUUDs become more densely packed as water evaporates and deform into closely-packed hexagonal structures.¹²⁵ The deformation of the particles is caused by various factors such as the capillary forces, inter-particle cohesion and dry sintering. The latter is driven by the polymer-air surface tension lowering the particle surface area.¹²⁶⁻¹²⁹ In the last stage, inter-diffusion of the polymer chains takes place between the deformed particles, which eventually coalesce into a smooth polymer film.¹³⁰ PU(R)s with T_g s up to 40 °C can form coating films at room temperature due to the plasticizing effect of water, which lowers the T_g of the particles.^{131,132} For PU(R)s with high T_g s (> 40 °C), higher temperatures (or small amounts of organic solvent, so-called coalescent agent) are required to form smooth films.¹³³⁻¹³⁵



Scheme 29. Coating formation process from water-borne PUUDs.¹¹⁵

1.6 Research aim and scope

The main objective of this study is to develop an isocyanate-free route for preparing water-borne polyurea (PU) dispersions (PUDs) for coating applications. In this work, 4,9-dioxa-

1,12-dodecane- diamine (DODD), 4,7,10-trioxa-1,13-tridecanediamine (TOTDDA), diamine-functional poly(tetrahydrofuran) with molecular weight of 1000 Da (pTHFda1000) and poly(propylene glycol) bis(2-aminopropyl ether) (PPGda) with molecular weights of 230, 400 and 2000 Da (PPGda230, PPGda400 and PPGda2000, respectively) are used as diamines monomers to increase the flexibility of the material, while isophorone dimethylcarbamate (IPDMC) is incorporated to increase the T_g of the PUs as well as their solubility in volatile solvents such as alcohols.

Catalysts suitable for carbamate aminolysis reactions are screened and evaluated in Chapter 2. The reaction mechanisms occurring in the presence of the most active catalysts are studied with both kinetic experiments and computational simulation. The application of these catalysts in isocyanate-free polyurea synthesis is carried out with PPGda2000 as diamine and butane dicarbamate.

In Chapter 3, cationically stabilized PUDs are prepared with secondary/tertiary amine-containing IDAs including diethylene triamine (DETA), bis(3-aminopropyl)amine (BAPA), 3,3'-diamino-*N*- methyl dipropylamine (DMDPA) and their dicarbamate counterparts. The properties of these PUDs and the resulting PU coatings are investigated.

In Chapter 4, the *N*-alkylation of amine as side reaction during carbamate aminolysis is studied in detail. Mitigation of this side reaction by increasing the rate of methanol removal, the addition of catalyst or the use of alternative dicarbamates is discussed. Optimization of the M_n s of the produced PUs is performed using various ratios diamines/dicarbamates.

In Chapter 5, di-*tert*-butyl dicarbamate (DiBoc-carbamate) is evaluated as a potential monomer for isocyanate-free PU synthesis. The mechanism of *tert*-butyl carbamate (Boc-carbamate) aminolysis is studied, and cationically stabilized PU(R)Ds with high M_n s are prepared from di-*tert*-butyl isophorone dicarbamate (DiBoc-IPDC), MeBAPA and diamines or diols. The properties of the resulting coatings are evaluated using standardized industrially relevant methods, e.g. pencil hardness and reverse impact test and solvent resistance.

In Chapter 6, anionically stabilized PUDs are developed by polymerizing diamine-functional polyureas with dianhydrides to form water-dispersible poly(amic acid urea)s (PAAUs). Factors that affect the M_n s of the PAAUs and the particle sizes of these PUDs are studied. The properties of the PAAU coatings prepared from different diamines are evaluated and optimized.

In Chapter 7, high temperature curing of the PU or PAAU coatings prepared in Chapter 3 and 6 are studied. Suitable catalysts for accelerating the curing process was screened and investigated. The properties of the cured coatings prepared from different diamines are evaluated.

In Chapter 8, a technology assessment of the possible industrial application of isocyanate-free PU(R) synthesis described in this thesis is presented, together with comments and outlook for future research in this field.

1.7 References

- (1) Schmelzer, H. G.; Mafoti, R. M.; Sanders, J.; Slack, W. E. *J. Prak. Chem. Chem. Ztg.* **1994**, 336, 483-491.
- (2) Bayer, O.; Rinke, H.; Siefken, W.; Ortner, L.; Schild, H. German Patent 728981, **1937**.
- (3) Bayer, O. *Angew. Chem.*, **1947**, 59, 257-272.
- (4) Neffgen, S.; Kusân, J.; Fey, T.; Keul, H.; Hocker, H. *Macromol. Rapid Commun.* **2000**, 201, 2108-2114.
- (5) Yilgör, E.; Burgaz, E.; Yurtsever, E.; Yilgor, I. *Polymer* **2000**, 41, 849-857.
- (6) Wool, R. P. *Macromolecules* **1993**, 26, 1564-1569.
- (7) Paabo, M.; Levin, B. C. *Fire and Material* **1987**, 11, 1-29.
- (8) Orzel, R. A.; Womble, S. E.; Ahmed, F.; Brasted, H. S. *J. Am. Coll. Toxicol.* **1989**, 8, 1139-1175.
- (9) Peters, J. M. *J. R. Soc. Med.* **1970**, 63, 372-375.
- (10) Broughton, E. *Environ. Health.* **2005**, 4, 1-6.
- (11) Hall, H. K.; Schneider, A. K. *J. Am. Chem. Soc.* **1958**, 80, 6409-6412.
- (12) Neffgen, S.; Keul, H.; Hocker, H. *Macromol. Rapid Commun.* **1996**, 17, 373-382.
- (13) Maisonneuve, L.; Lamarzelle, O.; Rix, E.; Grau, E.; Cramail, H. *Chem. Rev.* **2015**, 115, 12407-12439.
- (14) Sharma, B.; Ubaghs, L.; Keul, H.; Höcker, H.; Loontjens, T.; van Benthem, R. *Polymer* **2004**, 45, 5427-5440.
- (15) Sharma, B.; Keul, H.; Höcker, H.; Loontjens, T.; van Benthem, R. *Polymer* **2005**, 46, 1775-1783.
- (16) Neffgen, S.; Keul, H.; Höcker, H. *Macromol Chem. Phys.* **1998**, 199, 197-206.
- (17) Dyer, E.; Scott, H. *J. Am. Chem. Soc.* **1957**, 79, 672-675.
- (18) Rokicki, G.; Piotrowska, A. *Polymer* **2002**, 43, 2927-2935.
- (19) Ochiai, B.; Utsuno, T. *J. Polym. Sci., Part A: Polym. Chem.* **2013**, 51, 525-533.
- (20) Deng, Y.; Li, S.; Zhao, J. B.; Zhang, Z.; Zhang, J.; Yang, W. *RSC Adv.* **2014**, 4, 43406-43414.
- (21) Li, C.; Li, S.; Zhao, J.; Zhang, Z.; Zhang, J.; Yang, W. *J. Polym. Res.* **2014**, 21, 1-10.
- (22) Li, S.; Zhao, J.; Zhang, Z.; Zhang, J.; Yang, W. *RSC Adv.* **2014**, 4, 23720-23729.
- (23) Deng, Y.; Li, S.; Zhao, J.; Zhang, Z.; Zhang, J.; Yang, W. *Chin. J. Polym. Sci.* **2015**, 33, 880-889.
- (24) Deepa, P.; Jayakannan, M. *J. Polym. Sci., Part A: Polym. Chem.* **2007**, 45, 2351-2366.
- (25) Deepa, P.; Jayakannan, M. *J. Polym. Sci., Part A: Polym. Chem.* **2008**, 46, 5897-5915.
- (26) Hablot, E.; Graiver, D.; Narayan, R. *PU Magazine International* **2012**, 9, 255-257.
- (27) Palaskar, D. V.; Boyer, A. I.; Cloutet, E.; Alfes, C.; Cramail, H. *Biomacromolecules* **2010**, 11, 1202-1211.
- (28) Firdaus, M.; Meier, M. A. R. *Green Chem.* **2013**, 15, 370-380.
- (29) Simón, L.; Goodman, J. M. *J. Org. Chem.* **2007**, 72, 9656-9662.
- (30) Remme, N.; Koschek, K.; Schneider, C. *Synlett*, **2007**, 491-493.
- (31) Duval, C.; Kébir, N.; Charvet, A.; Martin, A.; Burel, F. *J. Polym. Sci., Part A: Polym. Chem.* **2015**, 53, 1351-1359.
- (32) Pan, D.; Tian, H. *J. Appl. Polym. Sci.* **2015**, 132, 41377-41385.

- (33) Unverferth, M.; Kreye, O.; Prohammer, A.; Meier, M. A. R. *Macromol. Rapid Commun.* **2013**, *34*, 1569-1574.
- (34) Yamazaki, N.; Icuchi, T. *J. Polym. Sci., Part A: Polym. Chem.* **1979**, *17*, 835-841.
- (35) Versteegen, R. M.; Sijbesma, R. P.; Meijer, E. W. *Angew. Chem. Int. Ed.* **1999**, *111*, 3095-3097.
- (36) Maisonneuve, L.; Lamarzelle, O.; Rix, E.; Grau, E.; Cramail, H. *Chem. Rev.* **2015**, *115*, 12407-12439.
- (37) Bahr, M.; Bitto, A.; Mülhaupt, R. *Green Chem.* **2012**, *14*, 1447-1454.
- (38) Maisonneuve, L.; Wirotius, A. -L.; Alfos, C.; Graua, E.; Cramail, H. *Polym. Chem.* **2014**, *5*, 6142-6147
- (39) Sayed, M.; Gaber, Y.; Bornadel, A.; Pyo, S.-H. *Biotechnol. Prog.* **2016**, *32*, 83-88.
- (40) Duval, C.; Kébir, N.; Jauseau, R.; Burel, F. *J. Polym. Sci., Part A: Polym. Chem.* **2016**, *54*, 758-764.
- (41) Annunziata, L.; Diallo, A. K.; Fouquay, S.; Michaud, G.; Simon, F.; Brusson, J. -M.; Carpentier, J. -F.; Guillaume, S. M. *Green Chem.* **2014**, *16*, 1947-1956.
- (42) Helou, M.; Carpentiera, J. -F.; Guillaume, S. M. *Green Chem.* **2011**, *13*, 266-271.
- (43) Sörensen, K.; Lundmark, S.; Hatti-Kaul, R.; Bornadel, A.; Pyo, S. -H. *Biotechnol. Prog.* **2013**, *29*, 66-73.
- (44) Pyo, S. -H.; Persson, P.; Mollaahmad, M. A.; Sörensen, K.; Lundmark, S.; Hatti-Kaul, R. *Pure Appl. Chem.* **2012**, *84*, 637-661.
- (45) Cornille, A.; Auvergne, R.; Fouquay, S.; Boutevin, B.; Caillo, S. *Eur. Polym. J.* **2016**, *87*, 535-552.
- (46) For a review on preparation of cyclic carbonates, see Shaikh, A. -A. G.; Sivaram, S. *Chem. Rev.* 1996, *96*, 951-976.
- (47) Rokicki, G.; Kuran, W. *Bull. Chem. Soc. Jpn.* **1984**, *57*, 1662-1666.
- (48) Liang, S.; Liu, H.; Jiang, T.; Song, J.; Yang, G.; Han, B. *Chem. Commun.* **2011**, *47*, 2131-2133.
- (49) Paddock, R. L.; Nguyen, S. T. *J. Am. Chem. Soc.* **2001**, *123*, 11498-11499.
- (50) Kilic, A.; Ulusoy, M.; Durgun, M.; Tasci, Z.; Yilmaz, I.; Cetinkaya, B. *Appl. Organomet. Chem.* **2010**, *24*, 446-453.
- (51) Buchard, A.; Kember, M. R.; Sandeman, K. G.; Williams, C. K. *Chem. Commun.* **2011**, *47*, 212-214.
- (52) Kim, Y. J.; Varma, R. S. *J. Org. Chem.* **2005**, *70*, 7882-7891.
- (53) Peng, J. J.; Deng, Y. Q. *New J. Chem.* **2001**, *25*, 639-641.
- (54) Calo, V.; Nacci, A.; Monopoli, A.; Fanizzi, A. *Org. Lett.* **2002**, *4*, 2561-2563.
- (55) Wang, J. Q.; Yue, X. D.; Cai, F.; He, L. N. *Catal. Commun.* **2007**, *8*, 167-172.
- (56) Garipov, R.M.; Sysoev, V. A.; Mikheev, V. V.; Zagidullin, A. I.; Deberdeev, R. Y.; Irzhak, V. I.; Berlin, A. A. A. *Doklady Phys. Chem.* **2003**, *393*, 289-292.
- (57) Tomita H, Sanda, F.; Endo T, *J. Polym. Sci., Part A: Polym. Chem.* **2001**, *39*, 3678-3685.
- (58) Tomita H, Sanda, F.; Endo T, *J. Polym. Sci., Part A: Polym. Chem.* **2001**, *39*, 4091-4100.
- (59) He, Y.; Keul, H.; Möller, M. *React Funct. Polym.* **2001**, *71*, 175-186.
- (60) Boyer, A.; Cloutet, E.; Tassaing, T.; Gadenne, B.; Alfos, C.; Cramail, H. *Green Chem.*

- 2010**, *12*, 2205-2213.
- (61) Diakoumakos, C. D.; Kotzev, D. L. *Macromol. Symp.* **2004**, *216*, 37-46.
 - (62) Nohra, B.; Candy, L.; Blanco, J. -F.; Raoul, Y.; Mouloungui, Z. *J. Am. Oil. Chem. Soc.* **2012**, *89*, 1125-1133.
 - (63) Webster, D.C.; Crain, A.L. *Progr. Organ. Coat.* **2000**, *40*, 275-282.
 - (64) Bürgel, T.; Fedtke, M.; Franzke, M. *Polym. Bull.* **1993**, *30*, 155-162.
 - (65) Tabushi, I.; Oda, R. *Nippon Kagaku Zasshi* **1963**, *84*, 162-167.
 - (66) Murayama, M.; Sanda, F.; Endo, T.; *Macromolecules* **1998**, *31*, 919-923.
 - (67) Kiesewetter, M. K.; Shin, E. J.; Hedrick, J. L.; Waymouth, R. M. *Macromolecules* **2010**, *43*, 2093-2107.
 - (68) Kamber, N. E.; Jeong, W.; Waymouth, R. M.; Pratt, R. C.; Lohmeijer, B. G. G.; Hedrick, J. L. *Chem. Rev.* **2007**, *107*, 5813-5840.
 - (69) Ashton, P. R.; Calcagno, P.; Spencer, N.; Harris, K. D. M.; Philp, D. *Org. Lett.* **2000**, *2*, 1365-1368.
 - (70) Corma, A.; Garcia, H. *Chem Rev.* **2003**, *103*, 4307-4365.
 - (71) Lombardo, V. M.; Dhulst, E.A.; Leitsch, E. K.; Wilmot, N.; Heath, W. H.; Gies, A. P.; Miller, M. D.; Torkelson, J. M.; Scheidt, K. A. *Eur. J. Org. Chem.* **2015**, *1*, 2791-2795.
 - (72) Dobrzynski, P.; Pastusiak, M.; Bero, M. *J. Polym. Sci., Part A: Polym. Chem.* **2005**, *43*, 1913-1922.
 - (73) Nederberg, F.; Lohmeijer, B. G. G.; Leibfarth, F.; Pratt, R. C.; Choi, J.; Dove, A. P.; Waymouth, R. M.; Hedrick, J. L. *Biomacromolecules* **2007**, *8*, 153-160.
 - (74) Lambeth, R. H.; Henderson, T. J. *Polymers* **2013**, *54*, 5568-5573.
 - (75) Schreiner, P. R.; Wittkopp, A. *Org. Lett.* **2004**, *4*, 217-220.
 - (76) Sohtome, Y.; Tanatani, A.; Hashimoto, Y.; Nagasawa, K. *Tetrahedron Lett.* **2004**, *45*, 5589-5592.
 - (77) Kobayashi, S.; Kikuchi, H.; Uyama, H. *Macromol. Rapid Commun.* **1997**, *18*, 575-579.
 - (78) Bisht, K. S.; Svirkin, Y. Y.; Henderson, L. A.; Gross, R. A.; Kaplan, D. L.; Swift, G. *Macromolecules* **1997**, *30*, 7735-7742.
 - (79) Maisonneuve, L.; Lamarzelle, O.; Rix, E.; Grau, E.; Cramail, H. *Chem. Rev.* **2015**, *115*, 12407-12439.
 - (80) Kihara, N.; Endo, T. *J. Polym. Sci., Part A: Polym. Chem.* **1993**, *31*, 2765-2773.
 - (81) Steblyanko, A.; Choi, W.; Sanda, F.; Endo, T. *J. Polym. Sci., Part A: Polym. Chem.* **2000**, *38*, 2375-2380.
 - (82) Kim, M.-R.; Kim, H.-S.; Ha, C.-S.; Park, D.-W.; Lee, J.-K. *J. Appl. Polym. Sci.* **2001**, *81*, 2735-2743.
 - (83) Tomita, H.; Sanda, F.; Endo, T. *J. Polym. Sci., Part A: Polym. Chem.* **2001**, *39*, 860-867.
 - (84) Chen, Q.; Gao, K.; Peng, C.; Xie, H.; Zhao, Z. K.; Bao, M. *Green Chem.* **2015**, *17*, 4546-4551.
 - (85) Prömpers, G.; Keul, H.; Höcker, *Des. Monomers Polym.* **2005**, *8*, 547-569.
 - (86) Ochiai, B.; Satoh, Y.; Endo, T. *J. Polym. Sci., Part A: Polym. Chem.* **2009**, *47*, 4629-4635.
 - (87) Sheng, X.; Ren, G.; Qin, Y.; Chen, X.; Wang, X.; Wang, F. *Green Chem.* **2015**, *17*,

373-379.

- (88) Annunziata, L.; Diallo, A. K.; Fouquay, S.; Michaud, G.; Simon, F.; Brusson, J. -M.; Carpentier, J. -F.; Guillaume, S. M. *Green Chem.* **2014**, *16*, 1947-1956.
- (89) Caplow, M. *J. Am. Chem. Soc.* **1968**, *90*, 6795-6803.
- (90) Astarita, G.; Marrucci, G.; Gioia, F. *Chem. Eng. Sci.* **1964**, *19*, 95-103.
- (91) Besse, V.; Camara, F.; Mechin, F.; Fleury, E.; Caillol, S.; Pascault, J.-P.; Boutevina, B. *Eur. Polym. J.* **2015**, *71*, 1-11.
- (92) Clements, J. H. *Ind. Eng. Chem. Res.* **2003**, *42*, 663-674.
- (93) Querat, E.; Tighzert, L.; Pascault, J. P.; Dusek, K. *Angew. Makromol. Chem.* **1996**, *242*, 1-36.
- (94) Spirkova, M.; Dusek, K. *Polym. Bull.* **1989**, *22*, 191-198.
- (95) Li, S.; Sang, Z.; Zhao, J.; Zhang, Z.; Zhang, J.; Yang, W. *Ind. Eng. Chem. Res.* **2016**, *55*, 1902-1911.
- (96) Wu, C.; Wang, J.; Chang, P.; Cheng, H.; Yu, Y.; Wu, Z.; Dong, D.; Zhao F. *Phys. Chem. Chem. Phys.* **2012**, *14*, 464-468.
- (97) Xiang, F.; Loontjens, T.; Geladé, E.; Vorenkamp, J. *Macromol. Chem. Phys.* **2012**, *213*, 1841-1850.
- (98) Rannard, S.; Davis, N. *Polym. Mater. Sci. Eng.* **2001**, *84*, 2-5.
- (99) Tang, D.; Mulder, D. J.; Noordover, B. A. J.; Koning, C. E. *Macromol. Rapid Commun.* **2011**, *32*, 1379-1385.
- (100) Quaranta, E.; Carafa, M.; Trani, F. *Appl. Catal. B: Environ.* **2009**, *91*, 380-388.
- (101) Zhang, L. *Macromolecules* **2007**, *40*, 4154-4158.
- (102) Jin, L.; Wu, Y.; Kim, C. -K.; Xue, Y. *J. Mol. Struc-THEOCHEM* **2010**, *942*, 137-144.
- (103) Kim, B. R.; Lee, H. -G.; Kang, S. -B.; Sung, G. H.; Kim, J. -J.; Park, J. K.; Lee, S. -G.; Yoon, Y. -J. *Synthesis* **2012**, *44*, 42-50.
- (104) Nayebezhadeh, H. *Chem. Biochem. Eng. Q.* **2013**, *27*, 267-273.
- (105) Liu X.; He, H.; Wang, Y.; Zhu, S.; Piao, X. *Fuel* **2008**, *87*, 216-221.
- (106) Seshu-Babu, N.; Sree, R.; Prasad, P. S.; Lingaiah, N. *Energy & Fuels* **2008**, *22*, 1965-1971.
- (107) Thitsartarn, W.; Kawi, S. *Green Chem.* **2011**, *13*, 3423-3430.
- (108) Distaso, M.; Quarant, E. *J. Catal.* **2008**, *253*, 278-288.
- (109) Santhanaraj, A.; Manickam, J. *J. Polym. Sci., Part A Polym. Chem.* **2016**, *54*, 1065-1077.
- (110) Fabbri, M.; Soccio, M.; Costa, M.; Lotti, N.; Gazzano, M.; Siracusa, V.; Gamberini, R.; Rimini, B.; Munari, A.; García-Fernandez, L.; Vazquez-Lasa, B.; Roman, J. S. *Polym. Degrad. Stab.* **2016**, *132*, 169-180.
- (111) Wang, S.; Wang, Y.; Yang, P.; Li, T. *Appl. Mech. Mater.* **2012**, *11*, 3938-3941.
- (112) Luo, S.; Liu, C.; Gong, G. *Adv. Mater. Res.* **2011**, *1*, 197-198.
- (113) Fragata, F.; Ahneida, E.; Santos, D.; de la Fueme, D.; Morcillo, M. *Surf. Coat. Int. Part B Coat. Trans.* **2006**, *89*, 237-244.
- (114) Noble, K. -L. *Progr. Org. Coat.* **1997**, *32*, 131-136.
- (115) Dieterich, D. *Progr. Org. Coat.* **1981**, *9*, 281-340.
- (116) Xia, Y.; Larock, R. C. *ChemSusChem* **2011**, *4*, 386-391.
- (117) Barni, A.; Levi, M. *J. Appl. Polym Sci* **2003**, *88*, 716-723.

- (118) Chattopadhyay, D. K.; Raju, K. V. S. N. *Prog. Polym. Sci.* **2007**, *32*, 352-418.
- (119) Li, Y.; Noordover, B. A. J.; van Benthem, R. A. T. M.; Koning, C. E. *Eur. Polym. J.* **2014**, *52*, 12-22.
- (120) Athavale, V. D.; Kulkarni, M. A. *JCT Research Publisher* **2010**, *7*, 2-10.
- (121) Rosthauser, J. W.; Nachtkamp, K.; *Adv. Ureth. Sei. Tech.* **1987**, *10*, 121-162.
- (122) Bleutge, J. C.; Koeckert, A. H.; Gil, J. C. US Patent 3905929, **1975**.
- (123) Kim, B. K. *Colloid Polym. Sci.* **1996**, *274*, 599-611.
- (124) Oh, J. K.; Anderson, J.; Erdem, B.; Drumright, R.; Meyers, G. *Prog. Org. Coat.* **2011**, *72*, 253-259.
- (125) Stewarda, P. A.; Hearn, J.; Wilkinson, M.C. *Adv. Colloid Interface Sci* **2000**, *86*, 195-267.
- (126) Dillon, R.E.; Matheson, L. A.; Bradford, E. B. *J. Colloid Sci.* **1951**, *6*, 108-117.
- (127) Frenkel, J. *J. Phys. (USSR)* **1943**, *9*, 385-1338.
- (128) Brown, G. L. *J. Polym. Sci.* **1956**, *22*, 423-434.
- (129) Kendall, K.; Padget, J. C. *Int. J. Adhes. Adhesives* **1982**, *2*, 149-154.
- (130) de Gennes, P. G. *J. Chem. Phys.* **1971**, *55*, 572-579.
- (131) Ellgood, B. *J. Oil Colour Chem. Assoc.* **1985**, *68*, 164-169.
- (132) Eckersley, S. T.; Rudin, A. *J. Appl. Polym. Sci.* **1993**, *48*, 1369-1381.
- (133) Feng, J.; Winnik, M. A.; Siemiarczuk, A. *J. Polym. Sci., Part B Polym. Phys.* **1998**, *36*, 1115-1128.
- (134) Hoy, K. L. *J. Paint Technol.* **1973**, *45*, 51-56.
- (135) Toussaint, A.; DeWilde, M.; Molenaar, F.; Mulvihill, J. *Prog. Org. Coat.* **1997**, *30*, 179-184.

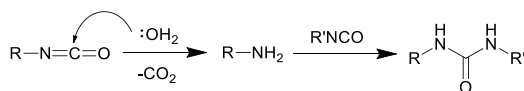
Chapter 2. Catalysts for isocyanate-free polyurethane/urea synthesis: mechanism and application

Summary

In this chapter, catalysts for carbamate and carbonate aminolysis were screened and investigated. Four catalysts, *viz.* 1,5,7-triazabicyclo[4.4.0]dec-5-ene (TBD), potassium bis(trimethylsilyl)amide (KHMDs), potassium methoxide (KOMe) and potassium *tert*-butoxide (KO*t*-Bu) were screened for a low toxicity route towards (poly)urethane/ureas preparation from carbonate/carbamate esters. Based on similar kinetics, the catalytically active species for KHMDs, KO*t*-Bu and KOMe was inferred to be the alkoxide anion RO⁻, depending on the R group in the carbonate/carbamate. Its activity was much higher than that of TBD. The low activity of TBD-catalyzed carbamate aminolysis was attributed to the formation of stable intermediate between carbamate and TBD molecules during the reaction. Computational simulation for MeO⁻-catalyzed urethane/urea formation was carried out using density functional theory. The activation energies calculated were in close match with the experimental results for the three MeO⁻-based catalysts. TBD and KOMe were applied in the isocyanate-free polyurea preparation by polycondensation. Again, KOMe exhibited a higher efficiency than TBD.

2.1 Introduction

Polyurethanes and polyureas have found wide applications in construction, packaging, vehicle parts, and coatings due to their versatile material properties. In comparison with polyurethanes, polyureas have superior mechanical properties due to the stronger intermolecular interaction between polyurea chains. Furthermore, the urea moiety has a much better stability against degradation.^{1,2} Polyurethanes and polyureas can be rigid,^{3,4} semirigid,^{5,6} or flexible⁵ depending on the monomers and the polymer microstructures. The industrial synthesis of polyurethanes and polyureas is based on isocyanate chemistry, where multifunctional isocyanates are polymerized with either diol- or diamine-functional monomers, respectively. The main disadvantage of this approach lies in the notorious toxicity of isocyanates and the required raw materials phosgene and chloroformates,^{7,8} all of which can cause severe damage to the environment and health. Additionally, although the high reactivity of isocyanates facilitates fast polymerization, which is highly appreciated in practical applications, they can be quite problematic in some specific scenarios such as the preparation of water-borne polyurethane/urea dispersions applied in coating materials, adhesives, and membranes.⁹ Indeed, the isocyanate groups can easily react with water to form amines and CO₂ (Scheme 1). This will change the stoichiometry between the isocyanates and diols or diamines, leading to an uncontrolled polymerization.



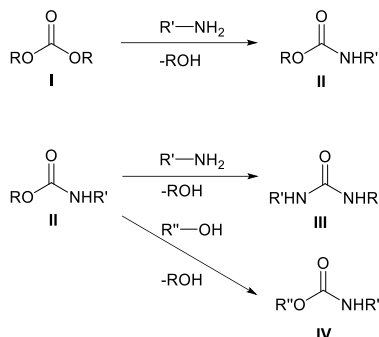
Scheme 1. Consumption of isocyanate by water in aqueous medium.

During the past decades, exploring new, nontoxic routes to prepare polyurethanes (PUs) has become a hotspot for both academic and industrial research. Most of these isocyanate-free routes, however, are based on cyclic species such as cyclic carbonates,¹⁰⁻¹² urethanes,¹³ or ureas,^{14,15} the synthesis of which often requires harsh conditions or toxic reagents such as chloroformate¹⁶⁻¹⁸ and oxiranes.^{19,20} Furthermore, the reaction between dicyclic carbonates and diamines results in poly(hydroxyurethanes) carrying hydroxyl side groups, which can lead to undesired properties such as low water resistance and poor material properties due to insufficient packing of neighboring chains.^{21,22}

Recently, a new isocyanate-free route (Scheme 2) for preparing polyurethanes (**IV**) or polyureas (**III**) was proposed by several groups,^{3,23,24} using dicarbamates (**II**) and diols (R''OH) or diamines (R'NH₂) as monomers. The dicarbamates are synthesized from potentially sustainable raw materials such as dimethyl carbonate (**I**) and diamines.

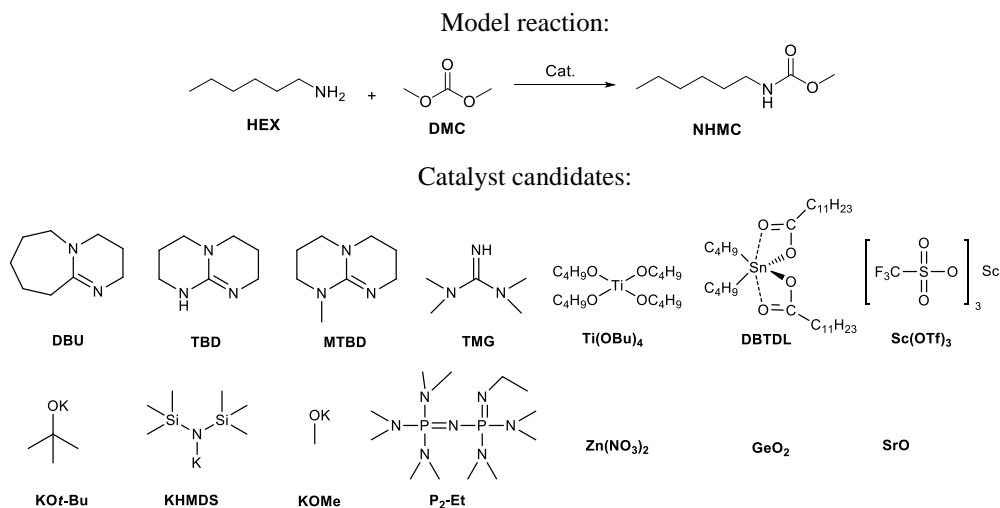
Since carbamates or carbonates are less reactive than isocyanates, especially towards water, a controlled polymerization should be possible even in an aqueous environment. This is particularly relevant when aqueous polyurethane or polyurethane/urea dispersions are targeted.

However, the lower reactivity of the carbonate/ carbamate-amine/alcohol chemistry implies a lower polymerization rate in comparison to isocyanate-amine/alcohol reactions. To overcome this reactivity issue, efficient catalysts must be employed.



Scheme 2. Isocyanate-free routes to urethane/urea formation through a carbamate intermediate.

Various catalysts utilized in esterification reactions or isocyanate chemistry have been screened as potential candidates for carbonate/carbamate-amine/alcohol reactions. They include strong bases such as phosphazenes,^{25,26} guanidine derivatives such as 1,5,7-triazabicyclo[4.4.0]dec-5-ene (TBD),²⁷⁻³⁰ organo-alkali-metal catalysts,³¹ alkaline oxides,^{32,33} and transition-metal compounds³⁴⁻³⁶ (Scheme 3). They are all active for esterification or (cyclic) carbonate-amine/alcohol reactions. The four most promising catalysts have been selected for a more detailed study in this chapter, and their application in polymerization reactions is evaluated.



Scheme 3. Carbonate aminolysis model reaction with DMC and HEX as substrates and catalyst candidates.

2.2 Experimental Section

2.2.1 Materials

All reagents are commercially available unless specified otherwise. Hexylamine (HEX, Acros Organics 99%) was purified by distillation from potassium hydroxide. Dimethyl carbonate (DMC, Reagent Plus, 99% Sigma Aldrich) and diethyl carbonate (DEC, 99% Sigma Aldrich) were purified by drying over 4 Å molecular sieves and subsequent fractional distillation. Poly(propylene glycol) bis(2-aminopropyl ether) with an average M_n of 200 Da (PPGda2000), hexylamine (HEX, 99%), toluene (anhydrous, 99.8%), germanium(IV) oxide (GeO_2 , 99.99%), zinc nitrate ($\text{Zn}(\text{NO}_3)_2$, 99.99%), 1,5,7-triazabicyclo[4.4.0]dec-5-ene (TBD, 98%), 7-methyl-1,5,7-triazabicyclo[4.4.0]dec-5-ene (MTBD, 98%), 1,1,3,3-tetramethylguanidine (TMG, 99%), 1,8-diazabicyclo [5.4.0]undec-7-ene (DBU, 99.0%), tetramethyl(tris(dimethylamino)phosphoranylidene) phosphorictriamid-Et-imine ($\text{P}_2\text{-Et}$, 98%), titanium(IV) butoxide ($\text{Ti}(\text{OBu})_4$), scandium triflate ($\text{Sc}(\text{OTf})_3$, 99.995%), dibutyltin dilaurate (DBTDL, 95%), 1,4-diaminobutane (DAB, 99%), strontium oxide (SrO , 99.9%), potassium bis(trimethylsilyl)amide (KHMDs, 95%), potassium methoxide (KOMe, 95%) and potassium *tert*-butoxide ($\text{KO}t\text{-Bu}$, 99.99%) were bought from Sigma Aldrich. Deuterated solvents were purchased from Buchem BV. Other common solvents were purchased from Biosolve. All the chemicals were used without further purification.

2.2.2 Reactions and synthesis

Model reaction

Catalyst activities were assessed by monitoring the reaction between HEX and DMC (Scheme 3) or DEC. In a typical experiment, 0.25 mmol of catalyst and 25 mmol of DMC/DEC were introduced into a 20 mL crimp-cap vial. 0.4 g of toluene was added as an internal standard, followed by the injection of 25 mmol of HEX into the vial. The time of the injection of HEX was considered as the $t = 0$ of the reaction.

Synthesis of *N*-hexyl methylcarbamate (NHMC)

In a 100 mL flask, DMC (90 g, 1 mol), HEX (20.2 g, 0.2 mol), and TBD (0.69 g, 5 mmol) were stirred for 12 hours at room temperature. The reaction mixture was then concentrated by using a rotary evaporator and washed 3 times with a saturated aqueous NaCl solution. The organic phase was then dried with anhydrous sodium sulfate to obtain NHMC as a colorless oil (28.6 g, 90%).

^1H NMR (400 MHz, CDCl_3 , δ in ppm): 4.95 (s, broad, 1H, NH), 3.65 (s, 3H, OCH_3), 3.16 (m, 2H, NHCH_2), 1.49 (m, 2H, NHCH_2CH_2), 1.29 (m, 6H, $\text{CH}_3\text{CH}_2\text{CH}_2\text{CH}_2$), 0.89 (m, 2H, CH_2CH_3); $^{13}\text{C}\{^1\text{H}\}$ NMR (100.6 MHz, CDCl_3 , δ in ppm): 157.2 (C=O), 51.9 (OCH_3); 40.9 (NHCH_2); 31.5 ($\text{CH}_3\text{CH}_2\text{CH}_2$); 29.9 (NHCH_2CH_2); 26.2 ($\text{NHCH}_2\text{CH}_2\text{CH}_2$); 22.5 (CH_3CH_2); 14.0 (CH_2CH_3).

Synthesis of 1,4-butylenedicarbamate (BU2)²⁵

In a 500 mL flask, a mixture of DMC (90 g, 1 mol), molten DAB (35.2 g, 0.4 mol) and TBD (1.39 g, 10 mmol) was stirred for 1 hour at room temperature. During this period, 100 mL of diethylether (Et_2O) were added when precipitation was observed. The precipitate was then isolated by filtration. The residue was recrystallized from chloroform and dried in a vacuum oven overnight at 60 °C to obtain BU2 as a colorless crystalline solid (70 g, 86%).

^1H NMR (400 MHz, CDCl_3 , δ in ppm): 4.86 (s, broad, 1H, NH), 3.63 (s, 3H, OCH_3), 3.16 (m, 2H, NHCH_2); 1.51 (m, 2H, NHCH_2CH_2); $^{13}\text{C}\{^1\text{H}\}$ NMR (100.6 MHz, CDCl_3 , δ in ppm): 157.2 ($\text{C}=\text{O}$), 51.9 (OCH_3); 40.6 (NHCH_2); 27.2 (NHCH_2CH_2).

Polymerization of diamine and dicarbamate

Polymerization reactions were carried out by using PPGda2000 and BU2 as comonomers. In a typical experiment, 20 g (0.01) mol of PPGda2000 and 2.04 g (0.01) mol of BU2 were introduced into a 100 mL 3-neck flask subsequently flushed with argon. The reaction mixture was heated up to 130 °C prior to the addition of 0.5 mmol of catalyst. Samples were taken during the reaction to determine the molecular weight evolution by SEC measurements.

2.2.3 Characterizations

Gas chromatography with flame ionization detector (GC-FID)

A Varian CP-3800 equipped with an FID was used for analysis of the kinetic results. Samples were prepared by quenching 0.05 mL of the reaction mixture into 1 mL of chloroform.

The conversion of DMC was monitored by GC-FID measurement as follows:

$A_{\text{DMC}-t}$ and $A_{\text{toluene}-t}$ are the GC-FID peak areas attributed to DMC and toluene at time t , respectively.

The initial concentration ratio between DMC and toluene is designated by I_0 where

$$I_0 = A_{\text{DMC}-0} / A_{\text{toluene}-0}$$

The ratio between DMC and toluene after x minutes is designated by I_x , where

$$I_x = A_{\text{DMC}-x} / A_{\text{toluene}-x}$$

The concentration of DMC at time x is then:

$$C_x = I_x / I_0$$

The same calculation method holds when using DEC or NHMC as the carbonate source.

Attenuated total reflection Fourier transform infrared (ATR-FTIR) spectroscopy

ATR-FTIR was performed using a Bio-Rad Excalibur FTS3000MX infrared spectrometer (fifty scans per spectrum, spectral resolution of 4 cm^{-1}) with an ATR diamond unit (Golden Gate). The measurement was performed by applying the sample onto the ATR diamond. The spectra were taken between 4000-650 cm^{-1} .

Nuclear magnetic resonance (NMR)

$^{13}\text{C}\{^1\text{H}\}$ NMR (100.62 MHz) and ^1H NMR (400 MHz) spectra were recorded using a Varian Mercury Vx spectrometer at 25 °C. The samples were prepared by quenching 0.05 mL of the reaction mixture into 1 mL of deuterated chloroform (CDCl_3).

Size exclusion chromatography (SEC)

SEC in 1,1,1,3,3,3-hexafluoro-2-propanol (HFIP) was performed on a system equipped with a Waters 1515 Isocratic HPLC pump, a Waters 2414 refractive index detector (35 °C), a Waters 2707 autosampler and a PSS PFG guard column followed by 2 PFG-linear-XL (7 μm , 8*300 mm) columns in series at 40 °C. HFIP with potassium trifluoroacetate (3 g/L) was used as eluent at a flow rate of 0.8 mL/min. The molecular weights were calculated with

respect to poly(methyl methacrylate) standards (Polymer Laboratories, $M_p = 580$ g/mol up to $M_p = 7.1 \times 10^6$ g/mol).

Computational details

The mechanism of KOMe-catalyzed urethane/urea formation was studied by density functional theory (DFT) calculations. Geometry optimizations were performed using a hybrid B3LYP exchange-correlation functional and 6-31+G(d,p) basis set for all atoms.³⁹⁻⁴¹ Frequency calculations were carried out at the same level to verify the nature of the stationary points. All local minima configurations showed no imaginary frequencies, while the transition state (TS) structures showed single imaginary frequency corresponding to the displacements along the reaction coordinate. The attribution of the TS to a particular elementary step was further confirmed through the intrinsic reaction coordinate (IRC) calculations.⁴²⁻⁴⁴ To improve the accuracy of the estimated energies, single-point calculations were performed at the MP2/6-311++G(d,p) level of theory for all structures.⁴⁵⁻⁴⁷ Energies used for estimation of the reaction heats and barriers include the zero-point energies (ZPEs) from the DFT frequency calculations. All calculations were performed using the Gaussian 09 D.01 program package.⁴⁸

2.3 Results and discussion

2.3.1 General observations

The various candidates depicted in Scheme 1 were evaluated as catalysts for the model reaction (Scheme 3). The reaction rate constants for some of the active catalysts at different temperatures are shown in Table 1. The concentration changes of substrates in stoichiometric DMC/HEX or DEC/HEX model reactions with and without catalysts, *viz.* GeO₂, SrO, TMG, MTBD, DBU, P₂-Et, Ti(OBu)₄, Zn(NO₃)₂, DBTDL, Sc(OTf)₃, KOMe, KO*t*-Bu, KHMDS and TBD, can be found in Figures S1–S8 in the Appendix of this chapter. The rate constants were calculated by assuming second order reaction kinetics for all the catalysts. This assumption is validated in the later discussion.

In this model reaction, the most active catalysts identified are KOMe, KHMDS, KO*t*-Bu and TBD. The substitution of DMC by DEC leads to lower reaction rates in their presence. The activity difference can reach a factor from 3 to 10, depending on the temperature. A possible explanation for this rate difference lies in the larger steric effect of the ethyl groups in DEC compared to the methyl groups in DMC, hindering the nucleophilic attack of the amine on the carbonyl center. Compared to TBD, the alkali bases KHMDS and KO*t*-Bu exhibit a more pronounced change in activity with increasing reaction temperature. According to the Arrhenius equation, a less significant catalytic activity change upon temperature increase indicates that TBD has a lower activation energy (E_a) compared to the two alkali bases. This is probably resulting from a bi-functional activation mechanism of TBD (Scheme 4a),⁴⁹ where both nitrogen atoms of TBD are coordinated to the carbonate in the catalytic cycle. Such a mechanism is supported by the lack of activity of DBU (pK_a = 24) and methyl-TBD (MTBD, pK_a = 25.5), both of similar basicity as TBD but without NH group, towards the model reaction (Figure 1). This implies the importance of the secondary amine in TBD. Furthermore, the binding of substrates on the two sites results in a significant entropy

decrease in the transition state. According to the Eyring equation, such an entropy penalty compensates for the lower enthalpy of activation for TBD, which leads to a lower reaction rate compared to the alkali catalysts KHMDS and KO*t*-Bu.

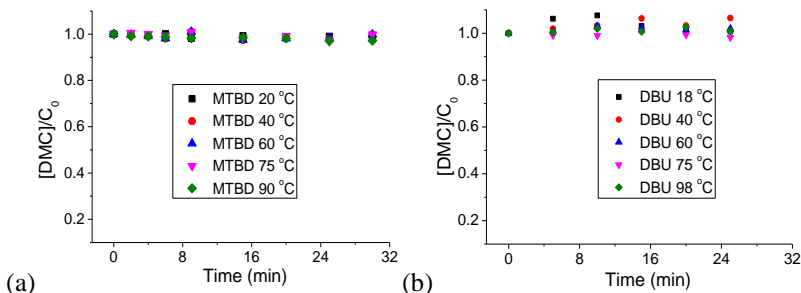
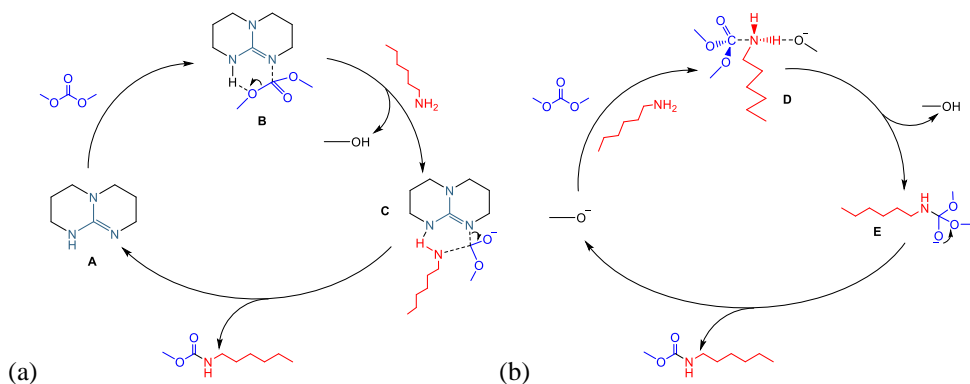


Figure 1. Concentration change of DMC in the model reaction at different temperatures with (a) MTBD and (b) DBU as catalysts.

Table 1. Reaction rate constants ($\text{mM}^{-1}\cdot\text{L}\cdot\text{s}^{-1}$) for active catalysts at different temperatures with DMC or DEC and HEX as substrates.

Carbamates	DMC					DEC				
T (°C)/ Catalyst	20	40	60	75	90	20	40	60	75	90
KOt-Bu	2.22	3.68	6.08	9.49	14.41	0.38	0.74	2.18	3.62	N.A
KHMDS	2.37	4.06	5.81	8.11	12.4	0.37	0.79	2.08	3.48	4.51
KOMe	2.29	3.82	6.01	8.68	12.98	0.37	0.78	2.12	3.55	4.55
TBD	2.21	2.81	3.97	4.65	6.04	0.38	0.54	0.61	1.00	1.50
Sc(OTf) ₃	0.34	0.40	0.48	0.62	0.72	0	0.20	0.25	0.30	0.34
DBTDL	0	0	0.11	0.20	0.005	N.A ^a	N.A	N.A	N.A	N.A
Zn(NO ₃) ₂	0	0	0	0.20	0.40	N.A	N.A	N.A	N.A	N.A
Ti(OBu) ₄	0	0	0	0	0.20	N.A	N.A	N.A	N.A	N.A
Blank	0	0	0	0	0	0	0	0	0	0

^{a)} Not available.



Scheme 4. Proposed mechanisms for (a) TBD and (b) KOMe as catalysts for the model reaction.

The proposed catalytic mechanism for alkali catalysts (Scheme 4b) is different compared to TBD. First, both KO t -Bu (pK $_a$ = 19) and KHMDS (pK $_a$ = 26) have higher basicities than KOMe (pK $_a$ = 15.5). Therefore, during the reaction, the byproduct methanol can easily react with KO t -Bu or KHMDS to generate methoxide anions.



Considering the relatively small amount (1 mol%) of catalyst compared to the substrates and the high tendency for the above equilibrium to move to the right, the conversion of 1 % of the substrate will generate 1 molar equivalent of methanol per catalyst. So both KO t -Bu and KHMDS will be rapidly converted into KOMe. Thus, we can consider the active catalytic species in both KO t -Bu- and KHMDS-catalyzed model reactions to be KOMe. Similarly, KOEt is the active catalytic species for reactions with DEC as substrate. A direct attack of a methoxide anion on the carbonyl of DMC will release a methoxide anion as the leaving group to form the same DMC molecule. Moreover, the methoxide anion is not basic enough to deprotonate amines. Hence, the following mechanism is proposed (Scheme 4b). During the catalytic cycle, HEX will attack the carbonate through activation by a methoxide anion, which activates the amine function by increasing its nucleophilicity to generate the dimethoxymethanolate **D**. The next step consists of the dissociation of methanol from the transition state **D**, generating the (hexylamino)-dimethoxymethanolate transition state **E**, which subsequently dissociates to a methoxide anion and the carbamate product.

2.3.2 Reaction order and transition states of the alkali bases- and TBD-catalyzed model reaction

The reaction order for each catalyst is required to determine the activation energy E_a and the frequency factor A . Therefore, the model reaction was carried out with KHMDS, KO t -Bu, KOMe and TBD at 40, 50, 60 and 70 °C. The concentration C of DMC was followed during 1 hour (Figure 2).

The plots of $\ln C$ vs. reaction time and the inverse DMC concentration vs. reaction time for data related to TBD and KOMe at 40, 50, 60 and 70 °C are presented in Figure 2a,b (data

from KHDMS and KO*t*-Bu are omitted, as the latter convert rapidly to KOMe as discussed previously).

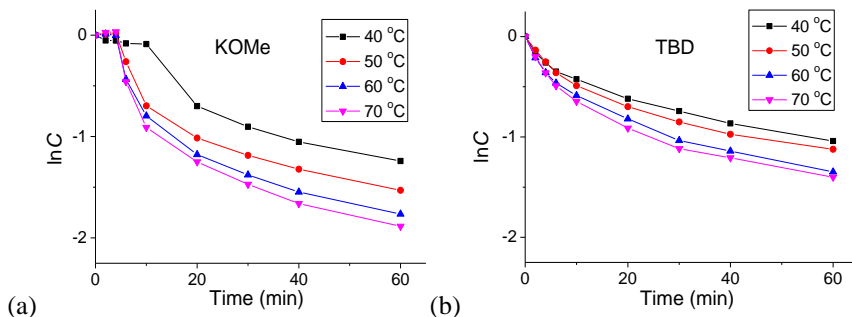


Figure 2. Logarithm of DMC concentration vs. time for (a) KOMe and (b) TBD as catalysts in HEX/DMC model reaction.

The limited conversion of DMC during the first 3 minutes can be attributed to the very low solubility of KOMe in the initial reaction mixture. However, the MeOH produced gradually dissolves the catalyst, leading to an increase of the reaction rate. The steeper slopes of the plots observed before 20 minutes of reaction time are probably resulting from the exothermic nature of the aminolysis with KOMe, as the exothermic reaction results in a temperature increase of 15 °C above the set temperature. A lower temperature increment of 5 °C is also observed with TBD at the beginning of the reaction, but leads to limited slope change. A linear relation between $1/C$ and reaction time compared with non-linear $\ln C$ vs. reaction time plot after 20 minutes indicates that the reaction is of second order.

To determine the transition state with the highest energy level for the KOMe-catalyzed HEX/DMC reaction, and thereby identifying the rate-determining step, DMC was substituted by the more reactive cyclic propylene carbonate (PC) in the model reaction (Figure 3a). During the aminolysis of PC, the ring tension lowers the activation energy. As a result, the reaction can proceed without catalyst at a moderate rate to obtain the ring opening product. The conversions of PC and DMC into their aminolysis products were determined by GC-FID and are displayed in Figure 3.

Figures 3b and 3c reveal a faster conversion of PC compared to DMC in the presence of TBD. This is caused by the reduction of activation energy in state **B** of the TBD catalytic cycle due to the release of the ring tension in PC. By contrast, KOMe generates similar rates for both DMC and PC.

A reasonable explanation is that the potential beneficial effect of the PC ring tension towards the reaction may only occur during the nucleophilic attack of the carbonate by the MeO⁻-activated amine. However, the release of ring tension takes place after the amine activation (transition state **D** in Scheme 4b), which is the rate determining step for the KOMe-catalyzed reaction. The total reaction rate thus remains similar when the more reactive PC is used instead of DMC.

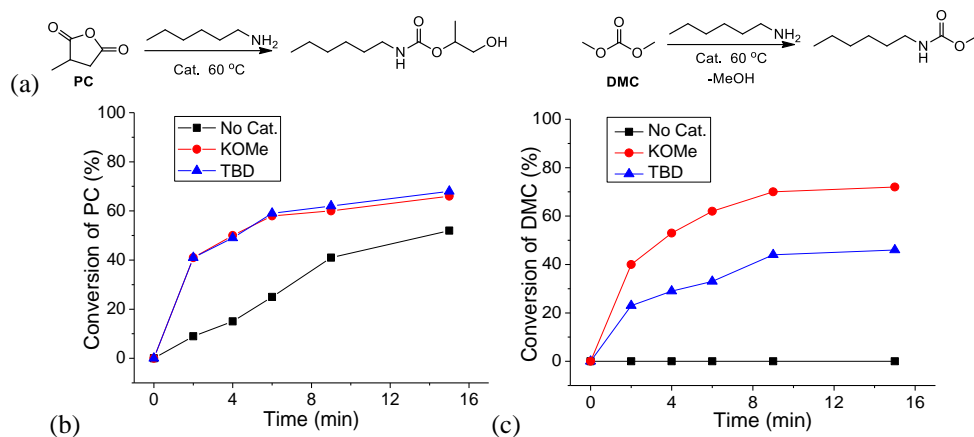


Figure 3. (a) Reaction scheme of PC and DMC with HEX. (b) Conversion of PC in the PC/HEX model reaction. (c) Conversion of DMC in the DMC/HEX reaction at 60 °C with TBD or KOMe (1 mol%) as catalyst or without catalyst.

2.3.3 Activation energy of urethane formation

The reaction rate constant k was determined for each catalyst at the four temperatures. The plot of $\ln k$ vs. $1/RT$ gives reasonably straight lines, from which the activation energy E_a and the frequency factor A were obtained (Arrhenius equation). The results are reported in Table 2.

The lower activation energy and higher entropy change of the TBD-catalyzed reaction compared with the three alkali alkoxides further validates the bi-functional mechanism of TBD, where a significant entropy change is taking place during the transition state.

The activation energy for the non-catalyzed HEX/DMC model reaction was determined for comparison. As shown previously by the catalysts screening (Table 1, blank entry), a stoichiometric ratio of substrates gives negligible conversion in the absence of catalyst in a closed environment, which may lead to inaccurate conversion determination by GC. The accuracy of the measurement is enhanced by using one reactant (DMC) in large excess (20 equivalents) and monitoring the concentration of the other (HEX) along the reaction.

The Arrhenius plot related to the non-catalyzed reaction (Figure 4) leads to an activation energy of 85.6 kJ/mol, considerably higher than in the presence of TBD (12.2 kJ/mol) or alkali bases (23-24 kJ/mol, Table 2), indicating the high efficiency of those catalysts towards the carbonate aminolysis.

Table 2. Activation energy, frequency factor and entropy change for each catalyst of the HEX-DMC model reaction.*

Catalyst	E_a (kJ/mol)	$\ln A$	$\Delta^\ddagger S$ (J/mol)
KOMe	24.2	4.2	-55.3
KO <i>t</i> -Bu	23.3	4.3	-55.2
KHMDS	24.3	4.4	-55.0
TBD	12.2	0.2	-60.3
No Cat.	85.6	24.1	-54.2

*The reaction constants are calculated from the slope after 20 minutes, where k become constant.

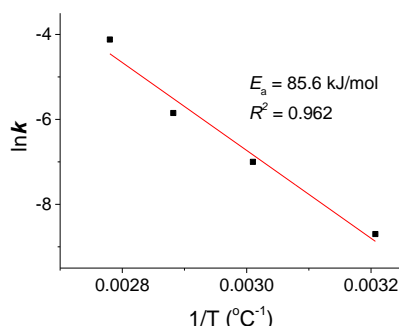
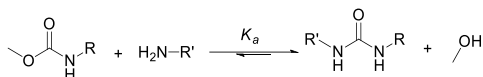


Figure 4. Arrhenius plot of HEX/DMC reaction with no catalyst.

2.3.4 Activation energy of urea formation

Interestingly, the concentration of HEX continued to decrease even after nearly complete conversion of DMC, as evidenced by the outcome of the signals attributed to the methyl (DMC, δ at 3.72 ppm) and methylene (HEX, δ at 2.61 ppm) protons in the ^1H NMR spectrum (Figure S9). Such non-stoichiometric reaction behavior can be explained by urea formation as side reaction (Scheme 2, where R = Methyl and R' = *n*-Hexyl). Each DMC molecule consumes two HEX moieties, to form one urea product (**III**). In addition, the HEX/DMC ratio decreases much faster with the alkali bases than with TBD (Figure S10).

Further experiments were carried out to evaluate the performance of the catalysts in the aminolysis of the N-hexyl methylcarbamate (NHMC, synthesized from HEX and DMC, see experimental part) by HEX, which is related to urea formation. A stoichiometric ratio between the amine and the carbamate resulted in almost no consumption of the substrates in a closed environment, as indicated by a reaction between HEX and DMC in a 2/1 molar ratio. In such a reaction mixture (Figure S11), half of HEX was converted into NHMC within 1 hour, while its concentration remained almost constant during the next 24 hours. This suggests that the equilibrium of the carbamate aminolysis (Scheme 5) is strongly shifted to the left, i.e. $K_a \ll 1$. The reaction can be reversed by removing the condensation product methanol from the reaction vessel, as observed earlier by our group during copolymerizations between dicarbamates and diamines to polyureas.²⁰



Scheme 5. Reaction scheme of the carbamate aminolysis reaction.

To monitor the concentration change of NHMC in the reaction mixture with higher accuracy, 20/1 or 100/1 ratios of HEX and NHMC were mixed in a closed set-up with 1 mol % (relative to the amount of HEX) of TBD or KOMe. The conversion of NHMC was monitored by GC-FID (Figure 5).

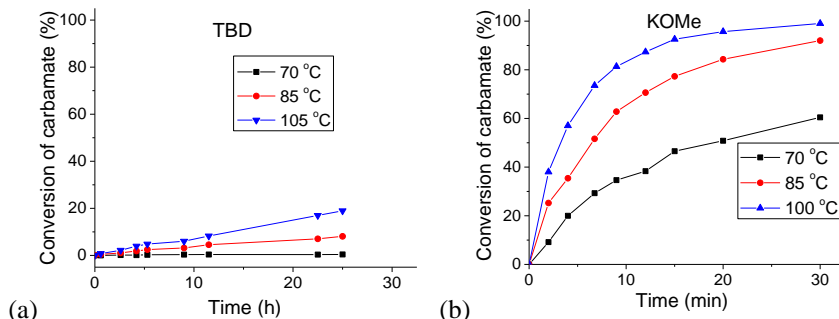
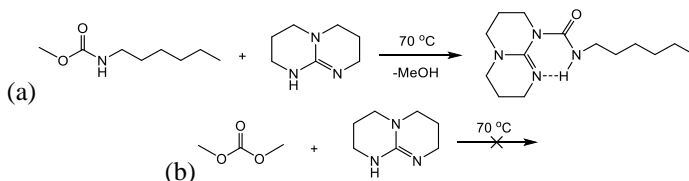


Figure 5. (a) Conversion of carbamate in NHMC-HEX mixture (1/100) with TBD as catalyst at different temperatures. (b) Conversion of NHMC in NHMC-HEX mixture (1/20) with KOMe as catalyst at different temperatures.

Figure 5a indicates a moderate activity for TBD at 105 °C. This is in agreement with our previous observations, where TBD-catalyzed diamine-dicarbamate polymerizations proceeded only above 120 °C.²⁵ Interestingly, the reaction between TBD and NHMC in a stoichiometric ratio at 70 °C under an argon flow generated the TBD-urea derivative depicted in Scheme 6a. The synthesis of similar substances by reactions between isocyanates and TBD was also reported previously.⁴⁹ This relatively stable intermediate of the NHMC-HEX reaction (melting point 120 °C) can drastically increase the activation energy for NHMC-HEX reaction, thereby retarding it. The assignment of the signals in the ¹H NMR spectrum of the intermediate to the corresponding protons is shown in Figure 6a. The signal at m/z = 267.4 in the mass spectrum of the intermediate (Figure 6b) is in agreement with its molar mass. In contrast, no stable intermediate was detected for the TBD-DMC reaction (Scheme 6b), which is in agreement with the low activation energy of a TBD-catalyzed DMC-HEX reaction (Table 2).



Scheme 6. Reaction between TBD and (a) NHMC and (b) DMC at 70 °C.

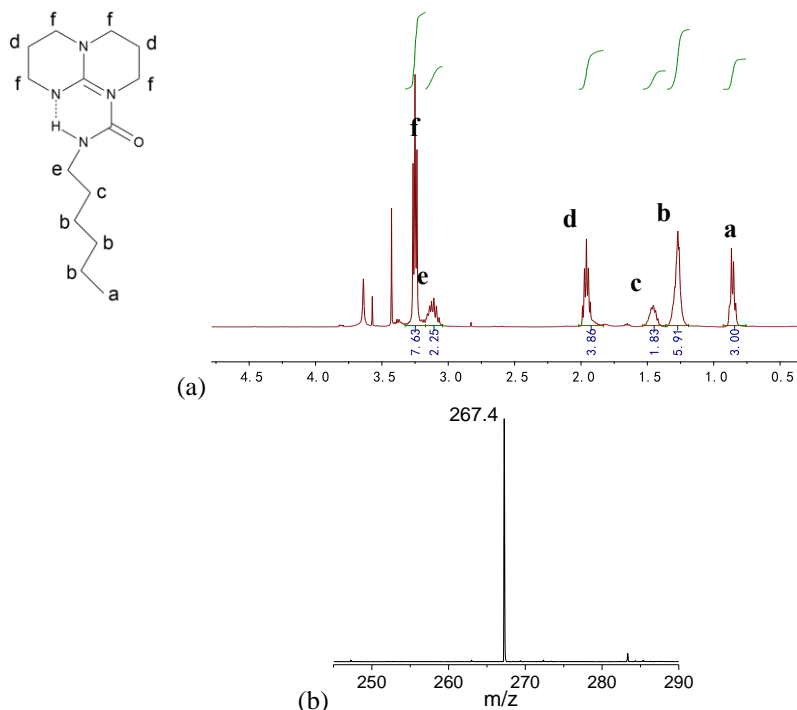


Figure 6. (a) ^1H NMR and (b) mass spectrum ($[\text{H}^+ + \text{M}] = 267.4$) of TBD/NHMC intermediate.

In comparison to TBD, KOMe is a much more efficient catalyst, leading to carbamate conversion above 75% within 1 h at 70 °C. Such a result is not surprising, due to the comparable structures of carbamate and carbonate. Thus, a similar mechanism may apply for both carbonate and carbamate aminolyses.

The urea formation during the reaction has been confirmed by ATR-IR, as indicated by the growth of a new peak at 1640 cm^{-1} attributed to a urea carbonyl vibration, combined with the gradual disappearance of the carbamate peak at 1750 cm^{-1} (Figure 7a). The relatively low intensity of the urea peak in comparison with the $-\text{NH}_2$ peak of HEX at 1584 cm^{-1} is due to the much higher concentration of HEX with regard to NHMC (20/1). The monitoring of this reaction by $^{13}\text{C}\{^1\text{H}\}$ NMR also shows a gradual decrease of the carbamate signal at 158 ppm, while the urea peak at 160 ppm increases over time (Figure 7b).

According to the corresponding Arrhenius plots (Figure 8), the activation energies are 73.2 kJ/mol for KOMe and 94.8 kJ/mol for TBD as the catalyst, respectively. The activation energy of the carbamate aminolysis is clearly higher in comparison to the carbonate reaction reported in Table 2.

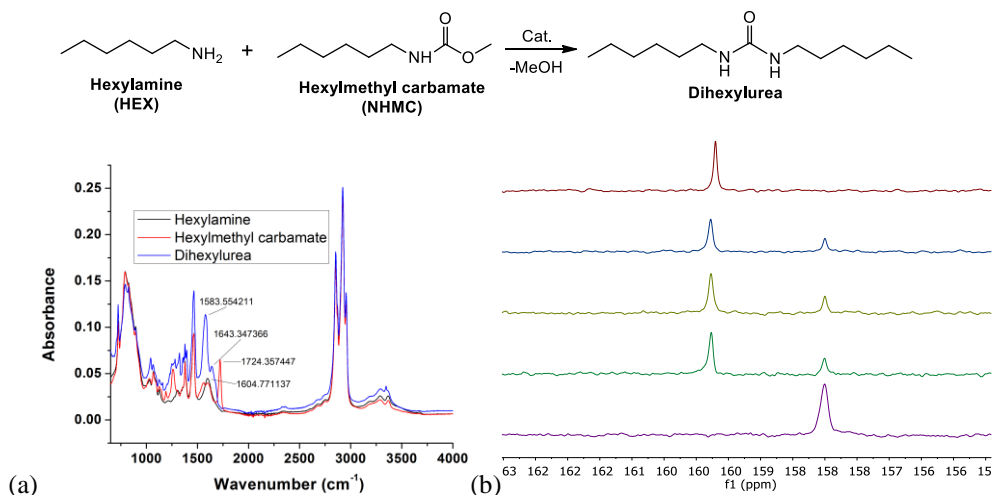


Figure 7. (a) ATR-FTIR spectra of substrates (HEX and NHMC) and products (dihexylurea with HEX in excess). (b) ¹³C{¹H} NMR spectra (DMSO-*d*₆) of a HEX/NHMC (20/1) reaction mixture at 70 °C with KOMe as catalyst.

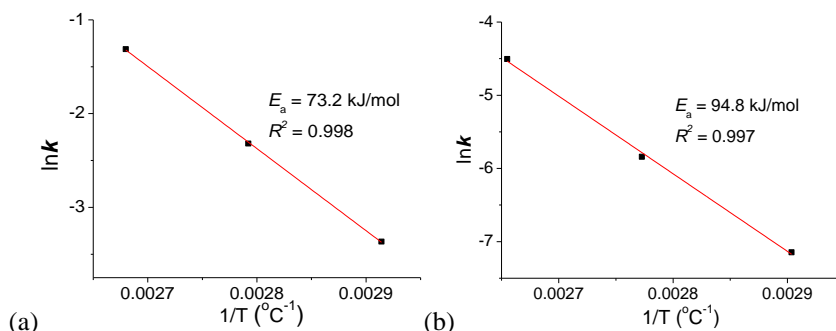


Figure 8. Arrhenius plots of HEX/NHMC (20/1) model reactions with (a) KOMe and (b) TBD as the catalyst.

2.3.5 Comparison with computational modeling

The mechanism of urethane/urea formation with KOMe has been further studied by DFT calculations. The methoxide anion is considered as the catalytically active species for the reaction of DMC and HEX. Figure 9 shows the corresponding reaction energy diagram (Figure 9a) and its transition states (Figure 9c).

The reaction is initiated by the coordination of the methoxide anion and the reactants. Assisted by the methoxide anion, the amine nucleophile attacks the C=O in DMC via the transition state TS1 to yield the tetrahedral intermediate IM1. This step is exothermic with a reaction energy (ΔE) of -46 kJ/mol and shows a barrier (ΔE[‡]) of 23 kJ/mol. At the next step, IM1 is isomerized to form intermediate IM2 (ΔE = -1 kJ/mol), from which the methoxide anion can be released. The elimination of the catalytic methoxide anion and the formation of the coupling product closes the catalytic cycle via the transition state TS2. This step is also

strongly exothermic with an energy of -69 kJ/mol and shows a very low barrier of only 9 kJ/mol. These computational results indicate that the first C-N bond formation is the rate-determining step in the catalytic cycle. The calculated barrier of 23 kJ/mol is in good agreement with the experimental value of 24.2 kJ/mol.

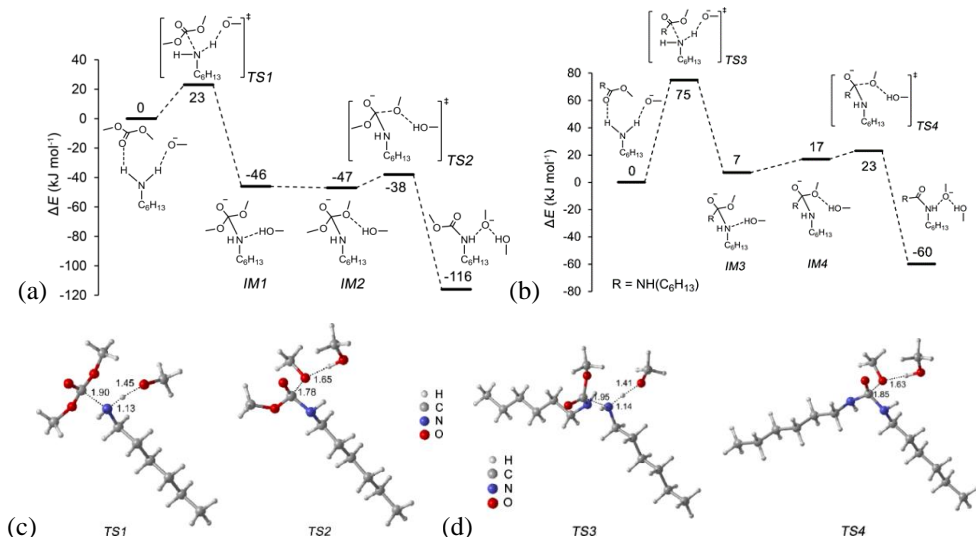


Figure 9. (a) DFT-calculated reaction energy diagram for KOME-catalyzed urethane formation. (b) DFT-calculated reaction energy diagram for KOME-catalyzed urea formation. (c) Ball-stick model of transition states (TS1 and TS2) of HEX+DMC system. (d) Ball-stick model of transition states (TS3 and TS4) of HEX+NHMC system.

Likewise, the activation energy calculated for the NHMC/HEX reaction with KOME of 75 kJ/mol (Figure 9b) is comparable to the experimental value (73.2 kJ/mol). Sardon et al. demonstrated that the aminolysis of cyclic carbonates occurred with the presence of two amines rather than one.⁴⁸ Similarly, an additional amine could stabilize the transition states by extra hydrogen-bonding interactions (Figure 10).

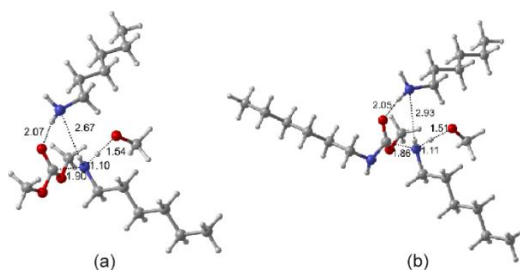


Figure 10. Ball-stick model of transition states for KOME-catalyzed (a) HEX/DMC and (b) HEX/NHMC reactions.

The estimated activation barriers for the HEX/DMC and HEX/NHMC systems are 18 and 70 kJ/mol, respectively. However, considering the relatively high entropy gain due to the involvement of four molecules, such transition state is unlikely to exist in the catalytic cycle.

The DMC-HEX reaction without catalyst was also studied by DFT calculations. The urethane formation can proceed via a four-membered-ring transition state (Figure 11a). The calculated activation barrier is 126 kJ/mol. The presence of an additional amine molecule can stabilize the transition state by forming a six-membered ring structure (Figure 11b), which decreases the activation energy barrier to 106 kJ/mol. The reaction activation energies from both the DFT calculations (ca. 100 kJ/mol) and the kinetic experiments (ca. 90 kJ/mol) are much lower than the values for the alkali base and TBD catalyzed reactions, indicating the efficiency of these catalysts.

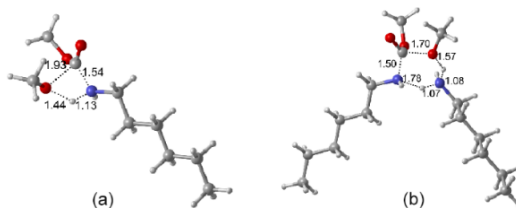


Figure 11. Ball-stick model of transition states of HEX/DMC system without catalyst: (a) 4-membered ring structure; (b) 6-membered ring structure.

One might also consider the interaction between KOMe with the carbonate carbonyl groups. There are two possibilities involving the interaction of the potassium cation with the oxygen of the carbonyl (Figure 12a) or the attack of MeO⁻ on the carbonyl to form the trimethoxymethanolate intermediate followed by reaction with HEX (Figure 12b). However, according to DFT calculations, the energy barriers for the two possibilities are 40 and 248 kJ/mol, respectively, both significantly higher than the activation energy (23 kJ/mol) of the mechanism described in Figure 9, which is therefore more likely to take place.

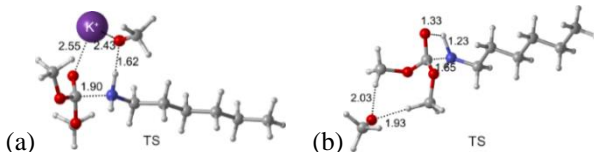


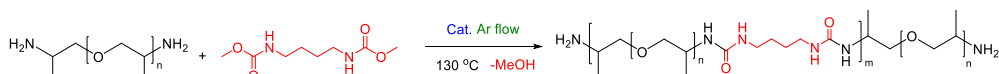
Figure 12. Ball-stick model of interaction between KOMe and DMC in the KOMe catalyzed DMC/HEX model reaction: (a) situation 1: interaction of potassium with oxygen in carbonyl group; (b) situation 2: attack of HEX on the trimethoxymethanolate intermediate.

2.3.6 Application in polymerization

The insights obtained from the model studies described above were employed in polyurea synthesis. To test the catalysts in polymerization reactions, the diamine-functionalized polyether poly(propylene glycol) bis(2-aminopropyl ether), with an M_n of approximately 2000 g/mol (PPGda2000) and butylene biscarbamate (BU2), were used as comonomers. These components were polymerized at 130 °C in the presence of TBD, KOMe, and KO^{*t*}-Bu (Scheme 7) under a flow of argon to remove MeOH. M_n values were determined by HFIP-SEC and monitored as a function of polymerization time, as shown in Figure 13. The urea formation during polymerization was confirmed by ¹³C{¹H} NMR, as indicated by the reduction of the carbamate signal at 157 ppm and the emergence of a resonance at 158 ppm

assigned to the urea moieties (Figure 13a). The growth of urea carbonyl vibration at 1640 cm^{-1} was also observed from ATR-IR over a period of 10 hours (Figure 13b).

The results indicate a faster M_n increase with KOMe and KO*t*-Bu in comparison to TBD, in accordance with the results of the model reactions. In addition, the similar molecular weight growth rates observed with KOMe- and KO*t*-Bu catalyzed polymerizations further corroborate the formation of KOMe from methanol. MeO^- is therefore the proposed active catalytic species for those systems.



Scheme 7. Copolymerization of PPGda2000 and BU2 with different catalysts.

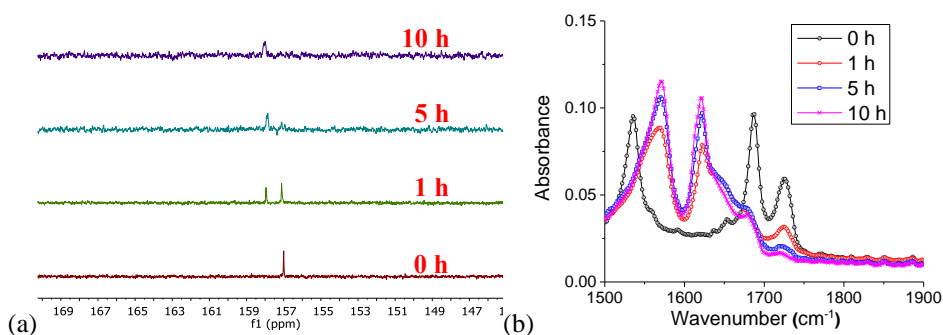


Figure 13. Reaction of a stoichiometric ratio of BU2/PPGda2000 at 130 °C with KOMe as catalyst under argon flow, monitored by (a) $^{13}\text{C}\{^1\text{H}\}$ NMR and (b) ATR-IR.

During the polymerizations with KOMe and KO*t*-Bu, the mixture became solid within 5 h. Such solid formation leads to a slower polymerization rate due to a reduced mobility of the reacting species (Figure 14a).

Although TBD is significantly less active than KOMe and KO*t*-Bu, it is much less sensitive to water. Therefore, the copolymerization was also carried out under a non-dried air flow (Figure 14b).

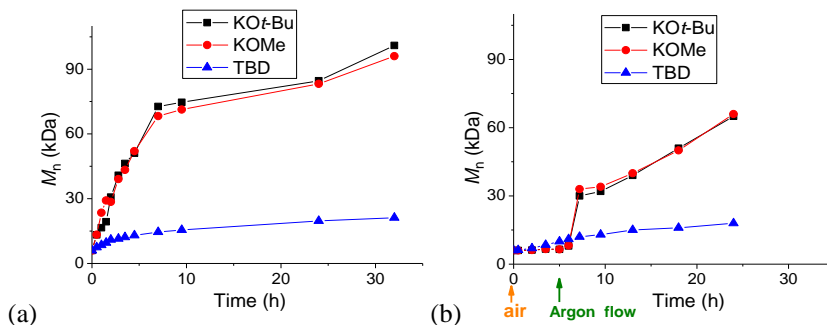
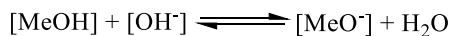


Figure 14. M_n of (a) the polymer mixture during polymerization with PPGda2000 and BU2 as comonomers and TBD, KOMe or KOt-Bu as catalysts under argon flow, (b) the polymer mixture during polymerization with PPGda2000 and BU2 as comonomers, under non-dried air (before 5 hours) and argon (after 5 hours) flow.

The molecular weight increase rate of the TBD-catalyzed polymerization under air was very similar to the reaction under argon, as shown by Figure 14b, indicating a lack of reactivity towards moisture. In contrast, polymerizations with KOMe and KOt-Bu proved to undergo a significant drop in activity under non-dried air, illustrated by a very slow increase of M_n . This can be explained by the reaction of the catalysts with H_2O to produce KOH, completely inactive towards amine-carbamate reactions.

After 5 h, the air flow was replaced by argon. The polymerization catalyzed by TBD was barely affected by such a change. This further indicates the very low moisture sensitivity of this organic catalyst. In contrast, the reactions with KOMe and KOt-Bu were subjected to significant M_n increase rates, from 1 to 2.5 h upon switching to argon. The rates are comparable to those issued from Figure 14a, indicating almost a full recovery of the catalytic efficiency. This sharp increase of polymerization rate may result from the production of MeOH followed by subsequent reaction with KOH to form the KOMe catalyst. The following equilibrium reaction shifts to the right side since the argon flow will gradually remove water, while methanol is continuously generated by the reaction:



The equilibrium suggests that, despite their sensitivity towards water, alkali bases can be regenerated up to full efficiency once the moisture is removed. This is relevant for industrial production, since reactor exposure to air or hydrolysis of catalyst can be rectified by flushing an inert gas.

2.4 Conclusions

In this article, we evaluated a series of potential catalysts for carbonate and carbamate aminolysis, among which TBD and the alkali bases KHMDS, KOt-Bu, and KOMe were the most successful. The active catalytic species of the systems when using the alkali bases appeared to be the alkoxide anion, the nature of which is determined by the ROC(O) groups of the substrate. The experimental activation energies determined for the both DMC-HEX and NHMC-HEX model reactions with the alkali bases (23-24 and 73 kJ/mol, respectively)

were in good agreement with the computational simulation values (23 and 75 kJ/mol). The evaluation of these catalysts in polyurea production was carried out using PPGda2000 and BU2 as co-reacting building blocks. The results agreed with the investigations on the model reaction, where the alkali bases were much more efficient for carbonate/carbamate aminolysis in comparison to TBD. Finally, contrary to TBD, the alkali bases are much more sensitive to water, as illustrated by their very low activity under non-dried air. Their catalytic efficiency, however, can be recovered once the water is removed by flushing the reaction vessel with inert gas.

2.5 References

- (1) Querat, E.; Tighzert, L.; Pascault, J. P.; Dusek, K. *Angew. Makromol. Chem.* **1996**, 242, 1-36.
- (2) Spirkova, M.; Dusek, K. *Polym. Bull.* **1989**, 22, 191-198.
- (3) Deepa, P.; Jayakannan, M. *J. Polym. Sci., Part A: Polym. Chem.* **2008**, 46, 2445-2458.
- (4) Chattopadhyay, D. K.; Raju, K. V. S. N. *Prog. Polym. Sci.* **2007**, 32, 352-418.
- (5) Septevani, A. A.; Evans, D. A. C.; Chaleat, C.; Martin, D. J.; Annamalai, P. K. *Industrial Crops and Products* **2015**, 66, 16-26.
- (6) Zhang, M.; Zhang, J.; Chen, S. Zhou, Y. *Polym. Degrad. Stab.* **2014**, 110, 27-34.
- (7) Trovati, G.; Sanches, E.A.; Neto, S. C.; Mascarenhas, Y.P.; Chierice, G.O. *J. Appl. Polym. Sci.* **2010**, 115, 263-268.
- (8) Trovati, G.; Sanches, E. A.; de Souza, S. M.; dos Santos, A. L.; Neto, S. C.; Mascarenhas, Y. P.; Chierice, G. O. *J. Mol. Struct.* **2014**, 1075, 589-593.
- (9) Eastmond, G. C., Ledwith, A., Russo, S., Sigwalt, P., Eds.; Pergamon: Oxford, **1989**; Vol. 5, p 413.
- (10) Caraculacu, A. A.; Coseri, S. *Prog. Polym. Sci.* **2001**, 26, 799-851.
- (11) Klingenberg, E. H.; Fazel, S. N. US 7342068 B2 **2008**.
- (12) Hall, H. K.; Schneider, A. K. *J. Am. Chem. Soc.* **1958**, 80, 6409-6412.
- (13) Neffgen, S.; Keul, H.; Höcker, H. *Macromol. Rapid Commun.* **1996**, 17, 373-382.
- (14) Schmitz, F.; Keul, H.; Höcker, H. *Polymer* **1998**, 39, 3179-3186.
- (15) Miyagawa, T.; Shimizu, M.; Sanda, F.; Endo, T. *Macromolecules* **2005**, 38, 7944-7949.
- (16) Maisonneuve, L.; Lamarzelle, O.; Rix, E.; Grau, E.; Cramail, H. *Chem. Rev.* **2015**, 115, 12407-12439.
- (17) Sardon, H.; Pascual, A.; Mecerreyes, D.; Taton, D.; Cramail, H.; Hedrick, J. L. *Macromolecules* **2015**, 48, 3153-3165.
- (18) Su, W.; Luo, X. H.; Wang, H. F.; Li, L.; Feng, J.; Zhang, X. Z.; Zhuo, R. X. *Macromol. Rapid Commun.* **2011**, 32, 390-396.
- (19) Kühling, S.; Keul, H.; Höcker, H.; Buysch, H. J.; Schon, N. *Makromol. Chem.* **1991**, 192, 1193-1205.
- (20) Hu, X. L.; Chen, X. S.; Cheng, H. B.; Jing, X. B. *J. Polym. Sci., Part A: Polym. Chem.* **2009**, 47, 161-169.
- (21) Sakakura, T.; Kohno, K. *Chem. Commun.* **2009**, 11, 1312-1330.
- (22) Park, J. H.; Jeon, J. Y.; Lee, J. J.; Jang, Y.; Varghese, J. K.; Lee, B. Y. *Macromolecules* **2013**, 46, 3301-3308.

- (23) Delebecq, E.; Pascault, J. P.; Boutevin, B.; Ganachaud, F. *Chem. Rev.* **2013**, *113*, 80-118.
- (24) Tomita, H.; Sanda, F.; Endo, T. *J. Polym. Sci., Part A: Polym. Chem.* **2001**, *39*, 4091-4100.
- (25) Tang, D.; Mulder, D. J.; Noordover, B. A. J.; Koning, C. E. *Macromol. Rapid Commun.* **2011**, *32*, 1379-1385.
- (26) Unverferth, M.; Kreye, O.; Prohammer, A.; Meier, M. A. R. *Macromol. Rapid Commun.* **2013**, *34*, 1569-1574.
- (27) Quaranta, E.; Carafa, M.; Trani, F. *Appl. Catal. B- Environ.* **2009**, *91*, 380-388.
- (28) Zhang, L.; Nederberg, F.; Prat, R. C. Waymouth, R. M.; Hedrick, J. L.; Wade, C. G. *Macromolecules* **2007**, *40*, 4154-4158.
- (29) Jin, L.; Wu, Y.; Kim, C.; Xue, Y. *J Mol Struc-Thermochem.* **2010**, *942*, 137-144.
- (30) Lambeth, R. H.; Henderson, T. J. *Polymer* **2013**, *54*, 5568-5573.
- (31) Duval, C.; Kebir, N.; Charvet, A.; Martin, A.; Burel, F. *J. Polym. Sci., Part A: Polym. Chem.* **2015**, *53*, 1351-1359.
- (32) Duval, C.; Kebir, N.; Charvet, A.; Jauseau, R.; Burel, F. *J. Polym. Sci., Part A: Polym. Chem.* **2016**, *54*, 758-764.
- (33) Kim, B. R.; Lee, H.-G.; Kang, S.-B. Sung, G. H.; Kim, J.-J.; Park, J. K.; Lee, S.-G.; Yoon, Y.-J. *Synthesis* **2012**, *44*, 42-50.
- (34) Tamura, M.; Siddik, H. S. M. A.; Shimizu, K. *Green Chem.* **2013**, *15*, 1641-1646.
- (35) Liu, X.; He, H.; Wang, Y.; Zhu, S.; Piao, X. *Fuel* **2008**, *87*, 216-221.
- (36) Babu, N. S.; Sree, R.; Prasad, P. S. S.; Lingaiah, N. *Energy & Fuels* **2008**, *22*, 1965-1971.
- (37) Thitsartarn, W.; Kawi, S. *Green Chemistry* **2011**, *13*, 3423.
- (38) Distaso, M.; Quarant, E. *J. Catal.* **2008**, *253*, 278-288.
- (39) Lee, C.; Yang, W.; Parr, R. G. *Phys. Rev. B.* **1988**, *37*, 785-789.
- (40) Becke, A. D. *J. Chem. Phys.* **1993**, *98*, 5648-5652.
- (41) Becke, A. D. *J. Chem. Phys.* **1993**, *98*, 1372-1377.
- (42) Fukui, K. *Acc. Chem. Res.* **1981**, *14*, 363-368.
- (43) Gonzalez, C.; Schlegel, H. B. *J. Chem. Phys.* **1989**, *90*, 2154-2161.
- (44) Gonzalez, C.; Schlegel, H. B. *J. Chem. Phys.* **1990**, *94*, 5523-5527.
- (45) Head-Gordon, M.; Pople, J. A.; Frisch, M. J. *Chem. Phys. Lett.* **1988**, *153*, 503-506.
- (46) Frisch, M. J.; Head-Gordon, M.; Pople, J. A. *Chem. Phys. Lett.* **1990**, *166*, 281-289.
- (47) Frisch, M. J.; Head-Gordon, M.; Pople, J. A. *Chem. Phys. Lett.* **1990**, *166*, 275-280.
- (48) Frisch, M. J.; Trucks, G. W.; Schlegel, H. B.; Scuseria, G. E.; Robb, M. A.; Cheeseman, J. R.; Scalmani, G.; Barone, V.; Mennucci, B.; Petersson, G. A.; Nakatsuji, H.; Caricato, M.; Li, X.; Hratchian, H. P.; Izmaylov, A. F.; Bloino, J.; Zheng, G.; Sonnenberg, J. L.; Hada, M.; Ehara, M.; Toyota, K.; Fukuda, R.; Hasegawa, J.; Ishida, M.; Nakajima, T.; Honda, Y.; Kitao, O.; Nakai, H.; Vreven, T.; Montgomery Jr., J. A.; Peralta, J. E.; Ogliaro, F.; Bearpark, M. J.; Heyd, J.; Brothers, E. N.; Kudin, K. N.; Staroverov, V. N.; Kobayashi, R.; Normand, J.; Raghavachari, K.; Rendell, A. P.; Burant, J. C.; Iyengar, S. S.; Tomasi, J.; Cossi, M.; Rega, N.; Millam, N. J.; Klene, M.; Knox, J. E.; Cross, J. B.; Bakken, V.; Adamo, C.; Jaramillo, J.; Gomperts, R.; Stratmann, R. E.; Yazyev, O.; Austin, A. J.; Cam-mi, R.; Pomelli,

- C.; Ochterski, J. W.; Martin, R. L.; Morokuma, K.; Zakrzewski, V. G.; Voth, G. A.; Salvador, P.; Dannenberg, J. J.; Dapprich, S.; Daniels, A. D.; Farkas, Ö.; Foresman, J. B.; Ortiz, J. V.; Cioslowski, J.; Fox, D. J. Gaussian 09, Gaussian, Inc.
- (49) Pratt, R. C.; Lohmeijer, B. G. G.; Long, D. A.; Waymouth, R. M. J.; Hedrick, L. J. *Am. Chem. Soc.* **2006**, *128*, 4556-4557.

Appendix

Concentration changes of either DMC or DEC in model reactions with HEX

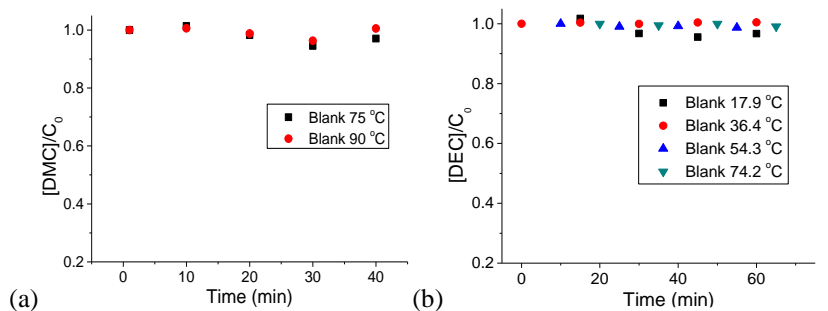
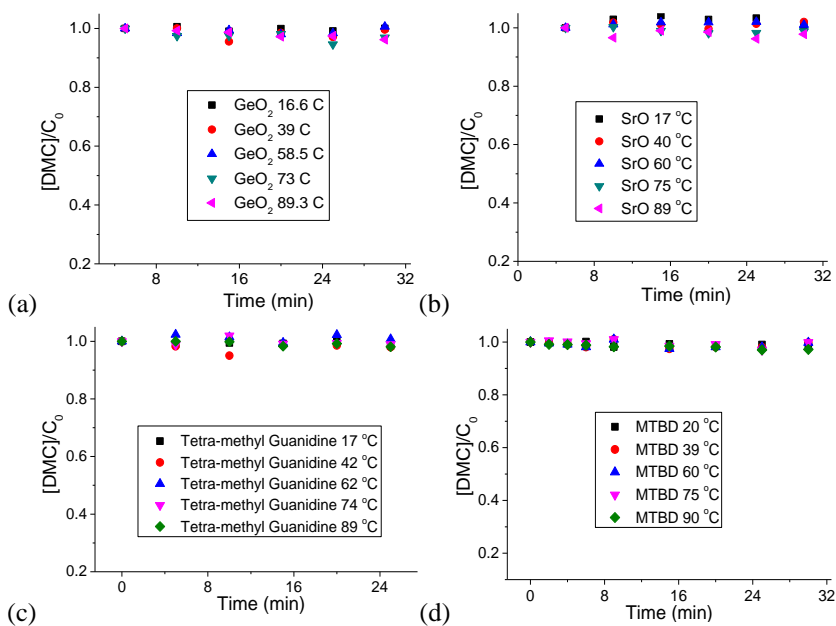


Figure S1. Concentration change of (a) DMC and (b) DEC in the model reaction with HEX at different temperatures without catalyst.



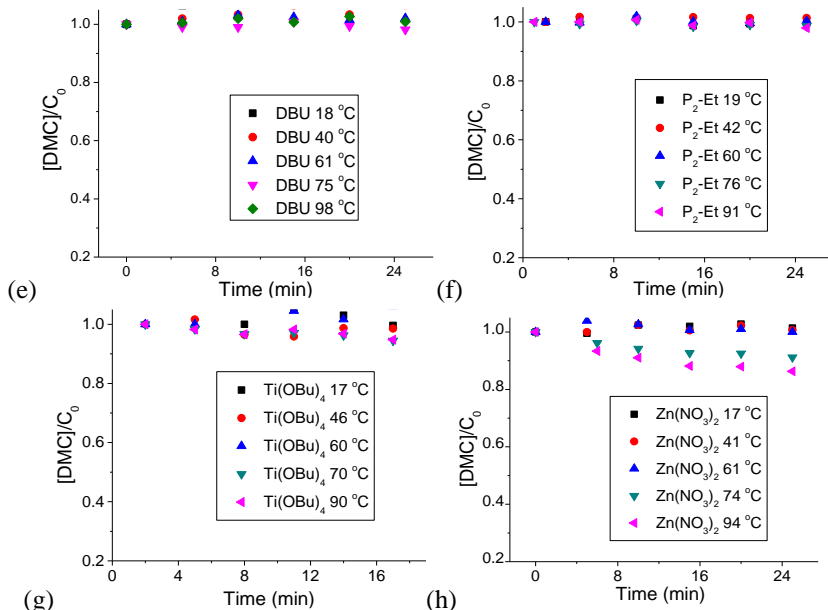


Figure S2. Concentration change of DMC in the model reaction with HEX at different temperatures with (a) GeO_2 , (b) SrO , (c) tetra-methyl guanidine, (d) MTBD, (e) DBU, (f) P_2 -Et, (g) $Ti(OBu)_4$ and (h) $Zn(NO_3)_2$ as catalysts.

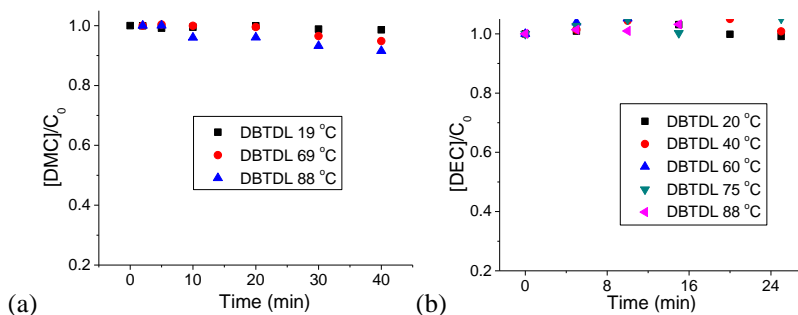


Figure S3. Concentration change of (a) DMC and (b) DEC in the model reaction with HEX at different temperatures with DBTDL as catalyst.

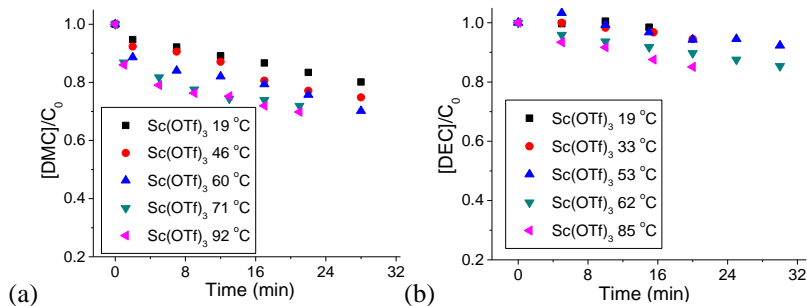


Figure S4. Concentration change of (a) DMC and (b) DEC in the model reaction with HEX at different temperatures with $\text{Sc}(\text{OTf})_3$ as catalyst.

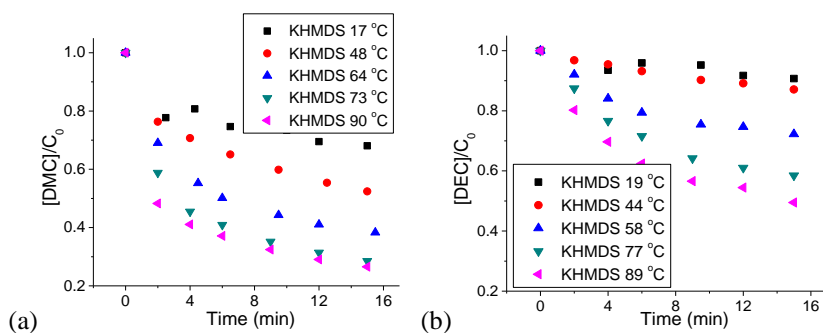


Figure S5. Concentration change of (a) DMC and (b) DEC in the model reaction with HEX at different temperatures with KHMDS as catalyst.

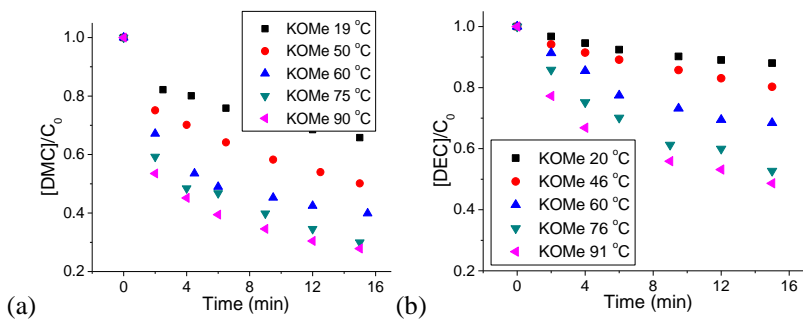


Figure S6. Concentration change of (a) DMC and (b) DEC in the model reaction with HEX at different temperatures with KOMe as catalyst.

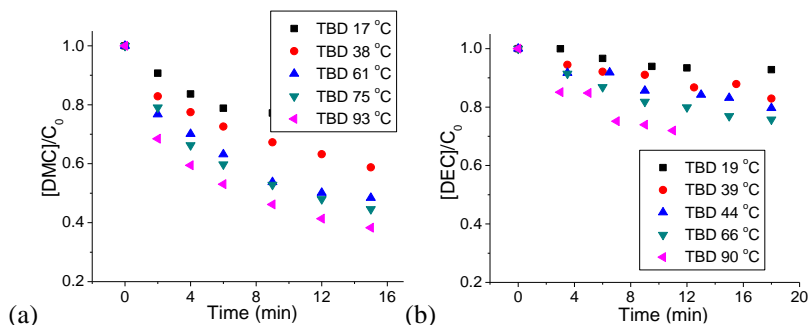


Figure S7. Concentration change of (a) DMC and (b) DEC in the model reaction with HEX at different temperatures with TBD as catalyst.

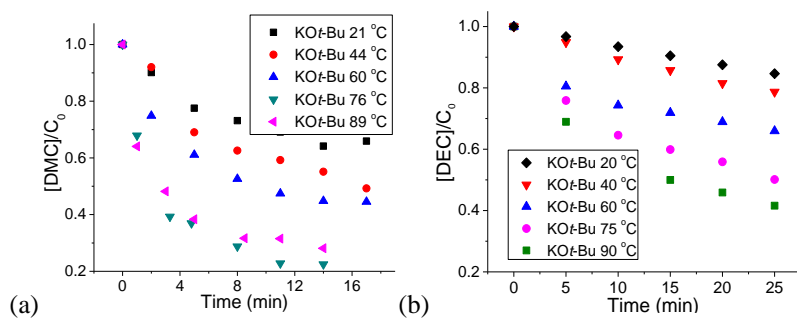


Figure S8. Concentration change of (a) DMC and (b) DEC in the model reaction with HEX at different temperatures with KOt-Bu as catalyst.

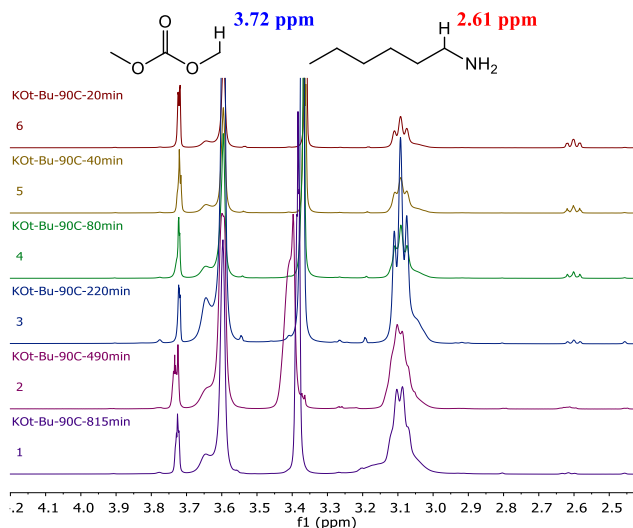


Figure S9. NMR spectra of the model reaction with KOMe. The resonance area at 3.72 ppm (methyl proton of DMC) is kept constant, whereas the methylene area of HEX at 2.62 ppm decreases over time.

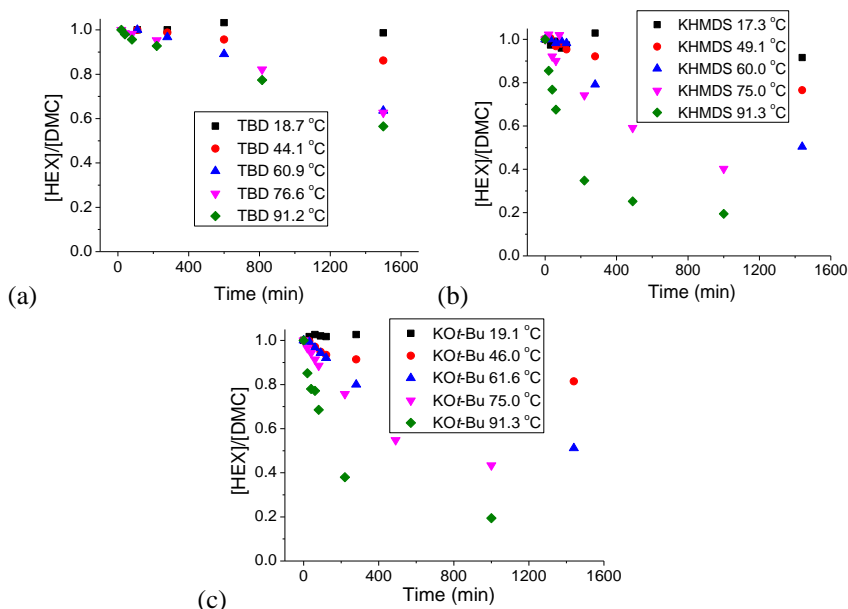


Figure S10. Concentration ratio change of HEX and DMC during the model reaction catalyzed by (a) TBD, (b) KHMDS and (c) KOt-Bu at different temperatures over 24 hours.

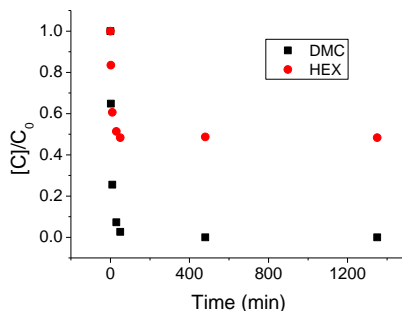


Figure S11. Concentration change of DMC and HEX in the reaction mixture (1/2 ratio of DMC and HEX with 1 mol% TBD as catalyst) at 90 °C, determined by 1H NMR.

Arrhenius equation:

$$\ln k = \ln A - \frac{E_a}{RT},$$

Where k is the rate constant of the reaction, A the pre-exponential factor, E_a the activation energy of the reaction, R the gas constant and T the absolute temperature.

Eyring equation:

$$\ln \frac{k}{T} = \frac{-\Delta H}{RT} + \ln \frac{k_B}{h} + \frac{\Delta S}{R},$$

Where k is the rate constant of the reaction, ΔH the enthalpy of activation, R the gas constant, T the absolute temperature, k_B the Boltzmann constant, h the Planck's constant and ΔS the entropy of activation.

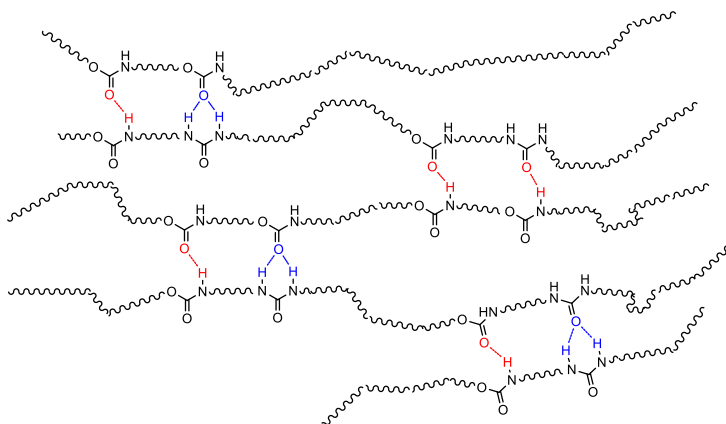
Chapter 3. Preparation of cationically stabilized water-borne polyurea dispersions via an isocyanate-free route

Summary

In this chapter, the synthesis of internal amine-containing polyureas (PUs) for coating applications and their evaluations in a water-borne coating system are reported. Internal amine-containing diamine monomers, *viz.* diethylene triamine (DETA), bis(3-aminopropyl)amine (BAPA), 3,3'-diamino-*N*-methyldipropylamine (DMDPA) and their dicarbamate counterparts were employed as internal dispersing agents (IDAs). A model reaction with IDA and *N*-hexyl methylcarbamate (NHMC) as substrates showed lower reactivity of the internal amine of the dicarbamate functional IDAs (IDAcS) compared to the primary ones, with the order BAPA > DETA >> DMDPA. The dicarbamate IDAs (IDAcS) exhibited significantly lower aminolysis rates compared to butane dicarbamate (BU2) due to the hydrogen bond formation between the carbamate and the internal amines, which sterically hinders the aminolysis reaction. Poly(propylene glycol) bis(2-aminopropyl ether) with an average M_n of 400 Da (PPGda400), 4,7,10-trioxa-1,13-tridecanediamine (TOTDDA), 4,9-dioxa-1,12-dodecanediamine (DODD) and isophorone dicarbamate (IPDMC) were employed for the synthesis of PUs. Branched and crosslinked PUs were obtained with either DETA or BAPA as IDAa. An increase of T_g was observed with increasing DMDPA content in the polyureas with PPGda400, while PUs prepared from DCMDPA and PPGda400 exhibited similar T_g with increasing IDA content. Stable dispersions were obtained from polyureas with either DCMDPA or DMDPA. The hardnesses of the coatings resulting from these dispersions were hardly affected by the neutralization agent. The hardnesses of the coatings from DMDPA-based polyureas (PUas) increase from 4B to 2B with increasing IDA concentration, while hardnesses of 6B were obtained with PU coatings prepared from DCMDPA (PUcs). PUcs with different IDA concentrations all passed the reverse impact test, while most PUas did not, with the notable exception of the PUa with 40 mol% of DMDPA in the diamine monomers and a high M_n about 48 kDa. These coatings also showed a satisfactory solvent resistance against acetone and water. In conclusion, the developed polyureas with internal amine containing IDAs are promising materials for coating applications.

3.1 Introduction

Over the past decades, polyurethanes (PURs) and polyureas (PUs) have gained increasing interest both from academia and industry due to their superior material properties, which stem from their strong intermolecular interactions caused by hydrogen bonds (Scheme 1). Such intermolecular hydrogen bonds can act as physical crosslinkers, which significantly improves the mechanical properties of the material.

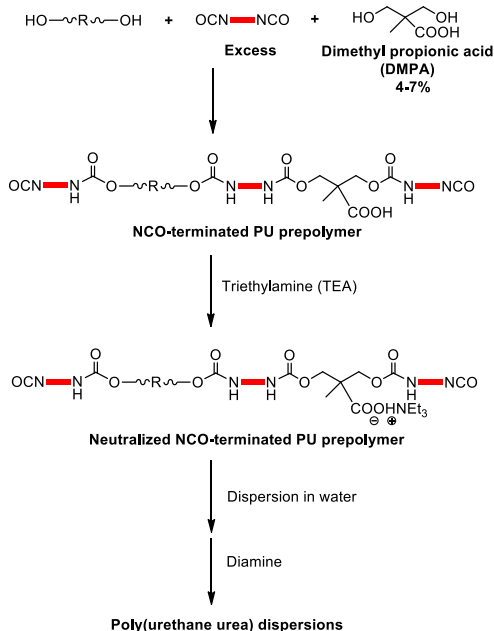


Scheme 1. Intermolecular Hydrogen bonds between urethane and urea moieties in PU(R)s.

Due to their excellent material properties and good chemical resistance, in recent years PU(R)s have gained a dominating role in the polymer materials markets. The quantities of PU(R)s produced in 2007 have reached 12 million metric tons, with an annual growth of about 5%.¹⁻³ PU materials have been utilized in various industrial applications such as fibers, foams, adhesives, coatings, elastomers and sealants.^{4,5} In the coating industry, PU(R)s can be applied on many substrates for protection purposes. For instance, they provide good exterior gloss, satisfactory color retention and they provide good scratch and corrosion resistance to vehicles, floors and furniture. The coatings are normally prepared from PU solutions in organic solvents or from PU dispersions in water (PUDs), which are dried on the substrate to form the final product. Due to environmental regulations to reduce volatile organic compounds (VOC), solvent-borne PUs are becoming less desired. Thus, the alternative water-borne polyurethane/urea dispersions (PUUDs) have gained increasing attention since the 1990s.⁶ Conventional isocyanate-based water-borne PUDs are prepared using cationic, anionic or non-ionic internal dispersing agents (IDAs). Non-ionic dispersions are stabilized by incorporating hydrophilic building blocks in the PUs to increase the hydrophilicity of the PUD particles and to introduce steric stabilization, while cationic or anionic dispersions are electrostatically stabilized by amine or acid groups, which are neutralized by volatile acids or amines, added before dispersing in water. The use of an excess of diisocyanate monomer results in a diisocyanate-functional prepolymer, which is then usually chain extended with a diamine to reach high M_n with good mechanical properties (Scheme 2). One of the most commonly used IDAs in the PU industry is dimethylol propionic acid (DMPA), used for the

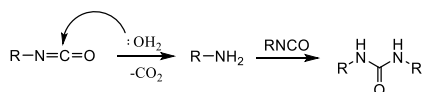
preparation of anionically stabilized PUUDs, which are more compatible with ingredients in the PUUDs compared to cationically stabilized ones.

The industrial PU synthesis involves highly toxic and hazardous diisocyanates (Scheme 2). Typical diisocyanates are methylene diphenyl diisocyanate (MDI) and toluene diisocyanate (TDI), which account for approximately 95% of the global isocyanate market.⁷ Another frequently used diisocyanate is isophorone diisocyanate (IPDI), which is non-aromatic. Diisocyanates are mostly synthesized via the reaction between primary amines and phosgene or chloroformates, both extremely toxic.



Scheme 2. Synthesis of water-borne polyurethane via isocyanate chemistry.

Additionally, although the isocyanates is highly appreciated in practical applications due to its high reactivity during polymerization, they can easily react with water in the aqueous medium to form carbamic acids, which easily decompose into primary amines and CO_2 during polyurethane/urea dispersion preparation (Scheme 3).⁸ In fact, since the generated amines can react with NCO end-groups, leading to a deviation from the stoichiometry between the isocyanates and the diols or diamines, thereby resulting in an uncontrolled polymerization. The toxicity of the diisocyanates and the growing interest in sustainable production of high performance materials as well as their high reactivity resulting in less controlled polymerizations have triggered researchers to investigate alternative non-toxic isocyanate-free pathways.

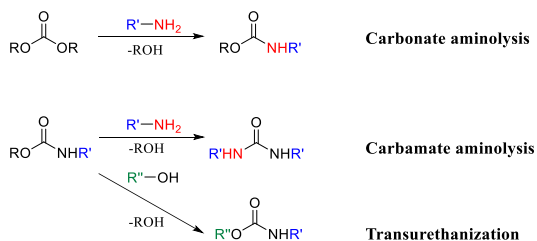


Scheme 3. Consumption of isocyanate by water.

Most of the isocyanate-free routes are based on cyclic species such as cyclic carbonates or cyclic urethanes and ureas,⁹⁻¹² the synthesis of which often requires harsh conditions or toxic reagents such as chloroformate and oxiranes.¹³⁻¹⁷ Furthermore, the reaction between dicyclic carbonates and diamines results in poly(urethane)s carrying hydroxyl side groups, the presence of which can lead to undesired properties such as low water-resistance and tensile strength due to insufficient packing of neighboring chains.^{18,19} Recently, a new method for preparing polyurethane/ureas was developed proposed by several groups, using dicarbamates and diols or diamines as monomers (Scheme 4).²⁰⁻²² The carbamates are synthesized from potentially sustainable raw materials such as dimethyl carbonate, cyclic carbonate, CO₂ and various diamines.

Compared with polyurethanes, polyureas have superior mechanical properties due to the stronger intermolecular interactions between polyurea chains. Furthermore, the urea moieties exhibit a much better stability against degradation.^{23,24} Additionally, the primary amine groups are stronger nucleophiles than hydroxyls, which makes their reaction with carbonyls much faster.^{6,20} Therefore, in this study, we will focus on preparing and investigating water-dispersible polyureas obtained via diamine/dicarbamate polymerization.

For the same reactivity reasons, DMPA is not employed in this study for the preparation of anionically stabilized PUDs. Instead, diamine-functional monomers with neutralizable secondary or tertiary amines in the backbone are incorporated in the PU as IDAs for synthesizing the cationically stabilized PUDs, which can potentially be applied in potentially antibiotic coatings.²⁹ The structure-properties relationships of these water-dispersible polyureas are investigated by studying their dispersion and coating properties.



Scheme 4. Non-isocyanate reactions resulting in urethane or urea linkages through a carbamate intermediate.

3.2 Experimental Section

3.2.1 Materials

All reagents were commercially available unless specified otherwise. Diethylenetriamine (DETA, 99%), bis(3-aminopropyl)amine (BAPA, 98%), 3,3'-diamino-*N*-methyldipropylamine (DMDPA, 96%), 4,7,10-Trioxa-1,13-tridecanediamine (TOTDDA, 97%), 4, 9-dioxa-1,12-dodecanediamine (DODD, 99%), 5-amino-1,3,3-trimethylcyclohexane-methylamine (IPDA, *cis* and *trans* mixture, 99%), 1,5,7-triazabicyclo [4.4.0]dec-5-ene (TBD, 98%), potassium methoxide (KOMe, 95%), dimethyl carbonate (DMC, 99%), triethylamine (TEA, 99%), 1,4-diaminobutane (DAB, 99%), 1,7-diaminoheptane (HDA, 98%), poly(propylene glycol) bis(2-aminopropyl ether) with an average M_n of 400 Da (PPGda400) and dimethylacetamide (DMAc, anhydrous) were purchased from Sigma Aldrich. Other common solvents were purchased from Biosolve. All the purchased chemicals were used without further purification.

3.2.2 Reactions and synthesis

Synthesis of *N*-hexyl methylcarbamate (NHMC)²⁵

In a 100 mL flask, DMC (90 g, 1 mol), HEX (20.2 g, 0.2 mol), and TBD (0.69 g, 5 mmol) were stirred for 12 hours at room temperature. The reaction mixture was then concentrated by using a rotary evaporator and washed 3 times with a saturated aqueous NaCl solution. The organic phase was then dried with anhydrous sodium sulfate to obtain NHMC as a colorless oil (28.6 g, 90%).

¹H NMR (400 MHz, CDCl₃, δ in ppm): 4.95 (s, broad, 1H, **NH**), 3.65 (s, 3H, OCH₃), 3.16 (m, 2H; NHCH₂), 1.49 (m, 2H; NHCH₂CH₂), 1.29 (m, 6H; CH₃CH₂CH₂CH₂), 0.89 (m, 2H; CH₂CH₃); ¹³C{¹H} NMR (100.6 MHz, CDCl₃, δ in ppm): 157.2 (C=O), 51.9 (OCH₃); 40.9 (NHCH₂); 31.5 (CH₃CH₂CH₂); 29.9 (NHCH₂CH₂); 26.2 (NHCH₂CH₂CH₂); 22.5 (CH₃CH₂); 14.0 (CH₂CH₃).

Synthesis of BU2²¹

In a 500 mL flask, a mixture of DMC (90 g, 1 mol), molten DAB (35.2 g, 0.4 mol) and TBD (1.39 g, 10 mmol) was stirred for 1 hour at room temperature. During this period, 100 mL of diethylether (Et₂O) were added when precipitation was observed. The precipitate was then isolated by filtration. The residue was recrystallized from chloroform and dried in a vacuum oven overnight at 60 °C to obtain BU2 as a colorless crystalline solid (70 g, 86%).

¹H NMR (400 MHz, CDCl₃, δ in ppm): 4.86 (s, broad, 2H, **NH**), 3.63 (s, 6H, OCH₃), 3.16 (m, 4H, NHCH₂), 1.51 (m, 4H, NHCH₂CH₂). ¹³C{¹H} NMR (100.6 MHz, CDCl₃, δ in ppm): 157.2 (C=O), 51.9 (OCH₃); 40.6 (NHCH₂); 27.2 (NHCH₂CH₂).

Synthesis of isophorone dicarbamate (IPDMC)²⁰

In a 2000 mL three-neck flask equipped with a condenser, 170 g (1 mol) of IPDA, 630 g (7 mol) of DMC and 70 g (1 mol) of sodium methoxide were mixed under argon flow and stirred at room temperature. After 4 hours, the mixture was heated up to 60 °C for another 6 hours. The solution was then cooled and poured into an excess of chloroform and then washed with brine. The organic layer was dried over anhydrous sodium sulfate. The solvent was

evaporated to obtain the product as a yellowish solid (150 g, 52%).

^1H -NMR (400 MHz, CDCl_3 δ in ppm): 4.75 (d, 1H, $-\text{NHCH}_2$), 4.6 (s, 1H, cy- NHCH), 3.8-3.6 (s, 1H, cy- CHNH , 6H, $-\text{OCH}_3$), 3.3, 2.9 (d, 2H, $-\text{CH}_2\text{NH}$), 1.7-0.7 (15H, cy- H). $^{13}\text{C}\{^1\text{H}\}$ NMR (100.6 MHz, CDCl_3 δ in ppm): 157.4, 156.3 ($\text{C}=\text{O}$), 54.8 and 52.1 (OCH_3), 51.8, 46.9, 46.3, 44.6, 42.5, 41.8, 36.3, 34.9, 31.7, 29.6, 27.5, and 23.1 (cy- C).

Synthesis of bis(2-aminoethyl) carbamate (BAEC)

In a 1000 mL flask, a mixture of DMC (225 g, 2.5 mol), molten DETA (103 g, 1 mol) and TBD (4.2 g, 30 mmol) was stirred for 1 hour at room temperature. During this period, 100 mL of diethylether (Et_2O) were added when precipitation was observed. The precipitate was then isolated by filtration. The residue was recrystallized from chloroform and dried in a vacuum oven overnight at 60 °C to obtain BAEC as a colorless crystalline solid (160 g, 73%).

^1H -NMR (400 MHz, CDCl_3 , δ in ppm): 5.21 (d, 2H, $-\text{CONHCH}_2$), 3.67 (s, 6H, $-\text{OCH}_3$), 3.3, 3.27 (d, 4H, $-\text{CH}_2\text{NHCO}$), 2.74 (t, 4H, $-\text{CH}_2\text{NHCH}_2-$), 1.11 (s, 1H, $-\text{CH}_2\text{NHCH}_2-$). $^{13}\text{C}\{^1\text{H}\}$ NMR (100.6 MHz, CDCl_3 , δ in ppm): 157.3 ($\text{C}=\text{O}$), 52.1 (OCH_3), 48.7 (CH_2NHCH_2), 40.8 (CONHCH_2).

Synthesis of bis(3-aminopropyl) carbamate (BAPC)

In a 1000 mL flask, a mixture of BAPA (131 g, 1 mol), DMC (180 g, 2mol) and TBD (2.8 g, 20 mmol) was stirred for 3 hours at room temperature. The mixture was then washed with brine and dried with sodium sulfate. The resulting solution was evaporated to obtain the product as a viscous light yellow liquid (177 g, 71.7%).

^1H -NMR (400 MHz, CDCl_3 δ in ppm): 5.48 (d, 2H, $-\text{CONHCH}_2$), 3.67 (s, 6H, $-\text{OCH}_3$), 3.24 (d, 4H, $-\text{CH}_2\text{NHCO}$), 2.67 (t, 4H, $-\text{CH}_2\text{NHCH}_2-$), 1.67 (m, 4H, $-\text{CH}_2\text{CH}_2\text{NHCH}_2-$), 1.27 (s, 1H, $-\text{CH}_2\text{NHCH}_2-$). $^{13}\text{C}\{^1\text{H}\}$ NMR (100.6 MHz, CDCl_3 δ in ppm): 157.3 ($\text{C}=\text{O}$), 52.0 (OCH_3), 47.5 (CH_2NHCH_2), 39.6 (CONHCH_2), 29.6 ($-\text{CH}_2\text{CH}_2\text{NHCH}_2-$).

Synthesis of 3,3'-dicarbamate-*N*-methyl-dipropylamine (DCMDPA)

In a 1000 mL flask, a mixture of DMDPA (145 g, 1 mol), DMC (180 g, 2mol) and TBD (2.8 g, 20 mmol) was stirred for 3 hours at room temperature. The mixture was then washed with brine and dried with sodium sulfate. The resulting solution was evaporated to obtain the product as an orange viscous liquid (195 g, 74.7%).

^1H -NMR (400 MHz, CDCl_3 δ in ppm): 5.62 (d, 2H, $-\text{CONHCH}_2$), 3.66 (s, 6H, $-\text{OCH}_3$), 3.24 (d, 4H, $-\text{CH}_2\text{NHCO}$), 2.40 (t, 4H, $-\text{CH}_2\text{NCH}_3\text{CH}_2-$), 2.17 (s, 3H, $-\text{CH}_2\text{NCH}_3\text{CH}_2-$), 1.67 (m, 4H, $-\text{CH}_2\text{CH}_2\text{NHCH}_3\text{CH}_2-$). $^{13}\text{C}\{^1\text{H}\}$ NMR (100.6 MHz, CDCl_3 δ in ppm): 157.3 ($\text{C}=\text{O}$), 56.0 (OCH_3), 52.0 (CH_2NHCH_2), 41.7 ($-\text{CH}_2\text{NCH}_3\text{CH}_2-$), 39.9 (CONHCH_2), 26.8 ($-\text{CH}_2\text{CH}_2\text{NCH}_3\text{CH}_2-$).

Reactivity test of the secondary amines in dicarbamate-functional IDAs (IDAcS)

The reactivity of the secondary amines in IDAcS towards carbamates was evaluated by monitoring the reaction between IDAcS and NHMC. In a typical experiment, 0.30 mmol of KOMe and 30 mmol of NHMC were introduced into a 20 mL crimp-cap vial, followed by the injection of 1 mmol of IDAc into the vial. The time of the injection of IDAc was considered as the $t = 0$ of the reaction.

Reactivity test of the carbamates in IDAcS

The reactivity of IDAcS towards amines was evaluated by monitoring the reaction between IDAs and hexylamine (HEX). In a typical experiment, 0.25 mmol of KOMe and 2.5 mmol of HEX were introduced into a 20 mL crimp-cap vial. 0.1 g of toluene was added as an internal standard, followed by the injection into the vial of a solution of 25 mmol of IDAc in 4 g anhydrous DMAc. The time of the injection of the IDAc solution was considered as the $t = 0$ of the reaction.

Preparation of diamine-terminated cationically dispersible polyureas

Water dispersible polyureas were prepared with poly(propylene glycol) bis(2-aminopropyl ether) (PPGda), isophorone dicarbamate (IPDMC) and various molar percentages of internal dispersing agent (IDA). In a typical experiment, a mixture of PPGda400 (6.40 g, 16 mmol), DETA (0.41 g, 4 mmol), IPDMC (5.72 g, 20 mmol) and TBD (0.14 g, 1 mmol) was added to a 100 mL 3-neck flask and stirred under argon flow at 130 °C for 12 hours. Then, the pressure in the flask was gradually reduced to 5 mmHg and maintained at this value for another 6 hours before quenching the mixture with water. Finally, the precipitated polymer was washed with water 3 times and dried in a vacuum oven for 12 hours to obtain the light yellowish polymer (8.30 g, 73.8%).

Preparation of water-borne polyurea dispersions

In a typical experiment, 1 gram of prepolymer was dissolved in 1 mL of methanol. An equivalent amount of acidic acid was added according to the concentration of the amines determined from the potentiometric titration. The mixture was stirred for 10 minutes and then slowly added to 8 mL of water under vigorous stirring.

3.2.3 Characterizations

Size exclusion chromatography (SEC)

SEC in 1,1,1,3,3,3-hexafluoro-2-propanol (HFIP) was performed at 40 °C on a system equipped with a Waters 1515 Isocratic HPLC pump, a Waters 2414 refractive index detector (35 °C), a Waters 2707 autosampler, a PSS PFG guard column followed by 2 PFG-linear-XL (7 μ m, 8*300 mm) columns in series. HFIP with potassium trifluoroacetate (3 g/L) was used as eluent at a flow rate of 0.8 mL/min. The molecular weights were calculated with respect to poly(methyl methacrylate) standards (Polymer Laboratories, $M_p = 580$ Da up to $M_p = 7.1 \times 10^6$ Da).

Atomic Force Microscopy (AFM)

AFM measurements were performed at room temperature ($\sim 20^\circ\text{C}$) on an NT-MDT NTegra Aura, in semi-contact mode, using NSG11 cantilevers (NT-MDT) with a typical spring constant of 5.5 N/m and a typical resonance frequency of 150 KHz. The sample scan size is $10 \times 10 \mu\text{m}$.

Potentiometric titration

Potentiometric titrations were carried out using a Metrohm Titrino 785 DMP automatic titration device fitted with an Ag-titrode. The sample solution was prepared by dissolving 1 gram of sample in 50 mL of methanol. The amount of the amine functionalities of the sample was measured by titrating the sample solution with a solution of HCl in isopropanol (0.1 M).

A blank experiment was carried out by titrating 50 mL of methanol with the HCl solution. The molar amount of amine per gram of sample was defined according to the following equation:

$$N_{\text{amine}} = \frac{(V_{\text{sample}} - V_{\text{blank}}) * 0.1}{1}$$

where the V_{sample} is the volume of HCl solution needed for the sample (mL) and V_{blank} the volume of HCl solution needed for the blank experiment (mL).

Nuclear magnetic resonance spectroscopy (NMR)

$^{13}\text{C}\{^1\text{H}\}$ NMR (100.62 MHz) and ^1H NMR (400 MHz) spectra were recorded using a Varian Mercury Vx spectrometer at 25 °C. The samples were prepared by dissolving 20 mg of polymer in 1 mL MeOH- d_4 or 50 mg/ml using dimethylsulfoxide (DMSO- d_6) or dimethylformamide (DMF- d_7) as a solvent.

Dynamic light scattering (DLS) and ζ -potential measurements

DLS and ζ -potential measurements were performed on a Malvern ZetaSizer Nano ZS (polyurethane refractive index: 1.59) at 25 °C to determine the dispersion characteristics. The average particle size and the particle size distribution of dispersions containing 0.1 wt% of solids were determined according to ISO 13321 (1996). The ζ -potential was calculated from the electrophoretic mobility (μ) using the Smoluchowski relationship $\zeta = \eta\mu/\epsilon$ with $\kappa\alpha \gg 1$,³¹ where η is the solution viscosity, ϵ the dielectric constant of the medium, and κ and α the Debye-Hückel parameter and the particle radius, respectively. Data acquisition was performed using the ZetaSizer Nano Software.

Gas chromatography with flame ionization detector (GC-FID)

A Varian CP-3800 equipped with an FID was used for analysis of the kinetic results. Samples were prepared by quenching 0.05 mL of the reaction mixture into 1 mL of chloroform.

Differential scanning calorimetry (DSC)

DSC measurements were performed on a TA Instruments DSC Q100. Samples were heated from -80 to 180 °C at a heating rate of 10 °C/min followed by an isothermal step for 5 min. A cooling cycle to -80 °C at a rate of 10 °C/min was performed prior to a second heating run to 180 °C at the aforementioned heating rate. The T_g was determined from the second heating run. The Universal Analysis 2000 software was used for data acquisition.

Coating evaluations

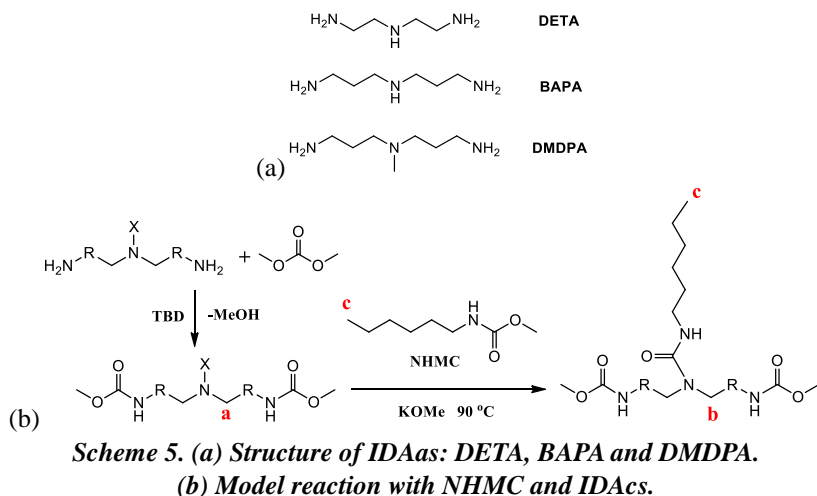
The acetone resistance was evaluated using the acetone rub test. Hereto, the sample was rubbed back and forth with a cloth drenched in acetone. If no damage was visible after more than 100 rubs, i.e. 50 ‘double rubs’, the acetone resistance of the coating was considered as good. The water resistance was evaluated by immersing the sample in water at room temperature, if no swelling or softening was observed after 1 hour, the water resistance of the coating was considered as good. The so-called reverse impact test is a rapid deformation test, performed by dropping a 1 kg ball on the backside of a coated panel from a 100 cm height, as described in ASTM D2794. Pencil hardness tests (ASTM D3363) were performed accordingly (from the hardest to the softest: 9H-1H, F, HB, 1B-9B). The thickness of the coatings was determined using a magnetic induction coating thickness measuring device

(Twin-Check by List-Magnetik GmbH).

3.3 Results and discussion

3.3.1 Model reaction study of diamine-functional IDAs (IDAAs) and dicarbamate-functional IDAs (IDAcS)

Ideally, the incorporation of the IDAAs take place via the reaction between their primary amines and the dicarbamate monomers, and generate linear PUs. However, the secondary amines of the IDAAs are also reactive towards the carbamates, leading to undesired branched or crosslinked structures during polymerization. Thus, model reactions were performed to investigate the reactivity of the secondary amines in IDAs towards carbamates. Since the equilibrium constant of the carbamate aminolysis is very small, an excess of IDAAs must be used to accurately determine the conversion of the carbamate.²⁵ Moreover, the secondary amines of the IDAAs are much less reactive towards carbamates compared with the primary ones. Thus, to determine the reactivity of the secondary amine, the primary amines are converted to methyl carbamates via reactions with dimethyl carbonate (DMC, Scheme 5b). The resulting dicarbamate functional IDAs (IDAcS) including bis(2-aminoethyl) carbamate (BAEC), bis(3-aminopropyl) carbamate (BAPC) and 3,3'-dicarbamate-*N*-methyl-dipropylamine (DCMDPA) are then reacted with an excess of *N*-hexyl methylcarbamate (NHMC) (1/20 ratio) at 90 °C with KOMe as catalyst in a closed set-up. The conversions of the secondary amines of the IDAcS are monitored by ¹H NMR (Figure 1a).



The proton signal **a** at 2.62 ppm is assigned to the methylene peak adjacent to the internal-amine of the IDAc. The signal shifts to 3.25 ppm (**b**) after reaction with NHMC, indicating the formation of urea moiety at the internal-amine. The signal **c** at 0.8 ppm is appointed to the methyl protons of the NHMC, and remains constant during the reaction. Thus, the conversions of the internal amines in IDAs are determined by the ratio of the intensities between the peaks **a** and **c** (Figure 2).

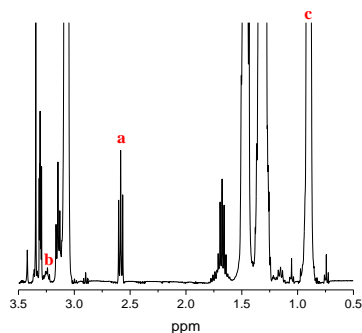


Figure 1. NMR spectrum of model reaction with BAPC and NHMC after 24 hours.

DCMDPA was inert towards NHMC due to the absence of active proton on the internal amine, while a faster conversion of the internal amine was observed with BAPC compared to BAEC. Such reactivity difference between the secondary amines could be attributed to the formation of hydrogen bonds between those amines and the carbamates, which reduces their nucleophilicity and slows down their attack on the carbonyl of NHMC (Scheme 6). Since the carbamate and the secondary amine within BAPC are separated by one additional methylene group compared with BAEC, the hydrogen bond of the carbamate analog is weaker, resulting in a higher reactivity with NHMC.

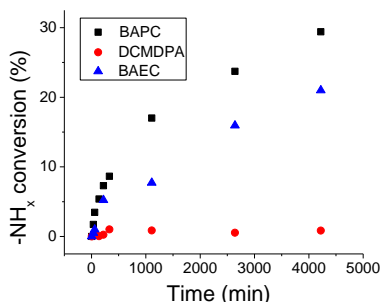
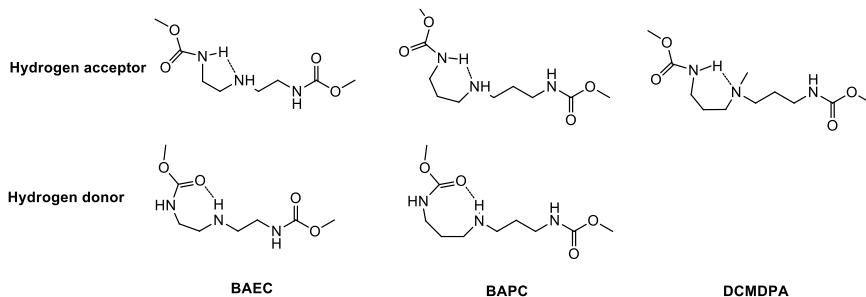
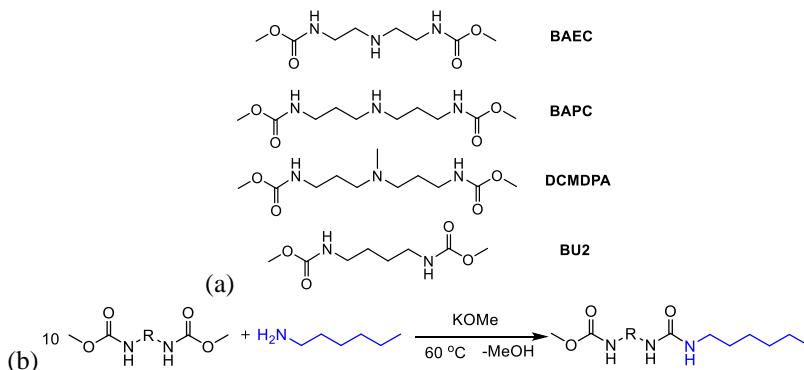


Figure 2. Conversions of internal-amines in IDAcS in the model reaction with NHMC under KOMe as catalyst at 90 °C.



Scheme 6. Possible intramolecular hydrogen bonds of IDAcS with the internal amines as either hydrogen donors or acceptors.

Similarly, various IDAcS were screened as substrates in aminolysis model reactions with hexylamine (HEX, Scheme 7). Thus, BAEC, BAPC and DCMDPA were reacted with HEX at 60 °C in the presence of KOMe as catalyst. The IDAcS were synthesized by reacting IDAAs with an excess DMC at room temperature in the presence of TBD. Butane dicarbamate (BU2) was employed as internal amine-free substrate for comparison with the IDAcS. Due to the very low reaction rate between carbamates and amines,²⁵ IDAcS and BU2 were reacted with HEX in a 10/1 ratio (Scheme 7b). The conversion of HEX in the reaction mixtures is shown in Figure 3.



Scheme 7. (a) Structure of IDAcS and BU2. (b) Aminolysis model reaction between HEX/dicarbamate (1/10 molar ratio) catalyzed by KOMe at 60 °C.

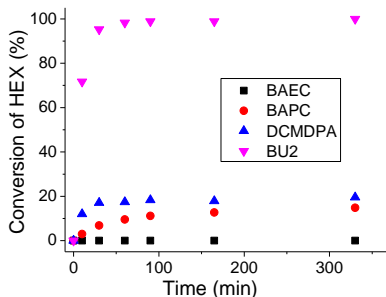


Figure 3. Conversion of HEX in the HEX/dicarbamate (1/10 molar ratio) aminolysis model reaction.

The IDAcS exhibit much lower reactivities towards hexylamine than BU2. This could be due to the formation of intramolecular hydrogen bonds between the carbamate functionalities and the internal amines, which could act as either the hydrogen donor or acceptor (Scheme 6). The hydrogen bonds enrich the electron density of the electron-deficient carbamate and therefore increase the activation energy of the amine-carbamate reaction, leading to a slower carbamate aminolysis rate. Additionally, such configuration change sterically hinders the nucleophilic attack of the amines on the carbamates, further reducing the reaction rate. A longer chain length between the internal amine and the carbamates weakens the hydrogen bonds, leading to a faster aminolysis of BAPC compared to BAEC. Due to the absence of hydrogen, the internal amine in DCMDPA can only act as hydrogen acceptor for the

carbamate. This leads to a weakened hydrogen bond compared with BAPC and BAEC, the internal amines of which can form hydrogen bonds with both the -NH and -C=O functions in the carbamate. Moreover, the methyl group of DCMDPA hinders the formation of the hydrogen bonds, thereby reducing the aminolysis rate to a lesser degree.

3.3.2 Polyureas with IDAAs

The model reactions showed a considerably lower reactivity of the internal amine in IDAAs compared with the primary ones. Thus, the dicarbamates preferentially react with the primary amines during their copolymerization with IDAAs, resulting in predominantly linear polyureas. To improve the mechanical properties, such as impact resistance and tensile strength, a combination of soft and hard segments is required for the polyureas. Therefore, the flexible diamines DODD, TOTDDA and PPGda400 were employed together with IDAAs as comonomers. Since the flexible diamines may lead to PUs with low T_g , isophorone dicarbamate (IPDMC) was used as dicarbamate to enhance the T_g of the polyurea. For conventional PUUDs, 4-7 wt% DMPA are incorporated in the PUUs, which corresponds to approximately 10-30 mol% IDAAs addition in the diamine feed in this approach.⁸ Thus, 10, 20, 30 and 40 mol% of IDAAs were mixed in the diamine monomer feed to investigate the effect of the IDAAs contents on the dispersion and coating properties. An excess of 1 mol% in diamines was used versus dicarbamate to obtain polyureas with controlled high M_n s (with degree of polymerization about 100). The molecular weight, molecular weight distribution (\bar{D}_M) and the thermal properties of the PUs were determined by NMR, HFIP-SEC and DSC, respectively. The results are summarized in Table 1.

The M_n s of the PPGda-based polyureas with DMDPA as IDAAs obtained by HFIP-SEC are about 30 kDa, while DODD and TOTDDA generate polymers with M_n values of 15-20 kDa. This difference is attributed to the higher molar mass of PPGDa. The M_n and \bar{D}_M values of the polyurea prepared with 10 mol% of DETA are significantly higher compared with those without IDA. The high M_n values are explained by the reaction of the secondary amine of DETA with IPDMC, which leads to branching, also illustrated by the high \bar{D}_M value of 4. A higher concentration of DETA (20 mol%) in the diamine and IDA feed results in a crosslinked polymeric system. A similar behavior is already observed with 10 mol% of BAPA, as anticipated from the model reaction results, which showed the higher reactivity of the secondary amine in BAPA towards carbonates. On the contrary, polyureas containing DMDPA have low \bar{D}_M values of 1.3-1.5, indicating linear polymers. Such low \bar{D}_M values in PU(R) synthesis were also observed in other studies,^{32,33} which could be explained by the interaction of the amine end-groups with the SEC column that lead to more exaggeration of the M_n s of the PUs with lower molecular weights (more amine end-groups) compared to PUs with higher ones, resulting in a reduction of \bar{D}_M . Thus, DMDPA is used as the IDAA for further investigations.

Table 1. Molecular weight of PUs, synthesized from IDAAs, diamines and IPDMC, determined by NMR and HFIP-SEC (amine monomers/dicarbamate = 1.01/1).

IDAAs (mol% in diamine)	PPGda400 (mol% in diamine)	TOTDDA (mol% in diamine)	DODD (mol% in diamine)	M_n (kDa, NMR) ^a	M_n (kDa, D_M) ^b
DETA (10)	90	0	0	N.A.	45 (4)
DETA (20)	80	0	0	N.A.	N.A. ^c
BAPC (10)	90	0	0	N.A.	N.A.
DMDPA (40)	60	0	0	N.A.	32 (1.46)
DMDPA (30)	70	0	0	N.A.	30 (1.40)
DMDPA (0)	100	0	0	N.A.	31 (1.42)
DMDPA (40)	0	60	0	18	19 (1.33)
DMDPA (30)	0	70	0	17	17 (1.34)
DMDPA (0)	0	100	0	18	21 (1.33)
DMDPA (40)	0	0	60	17	18 (1.35)
DMDPA (30)	0	0	70	15	19 (1.33)
DMDPA (0)	0	0	100	18	15 (1.34)

^a) Determined by NMR; ^b) determined by SEC in HFIP; ^c) not available due to gelation.

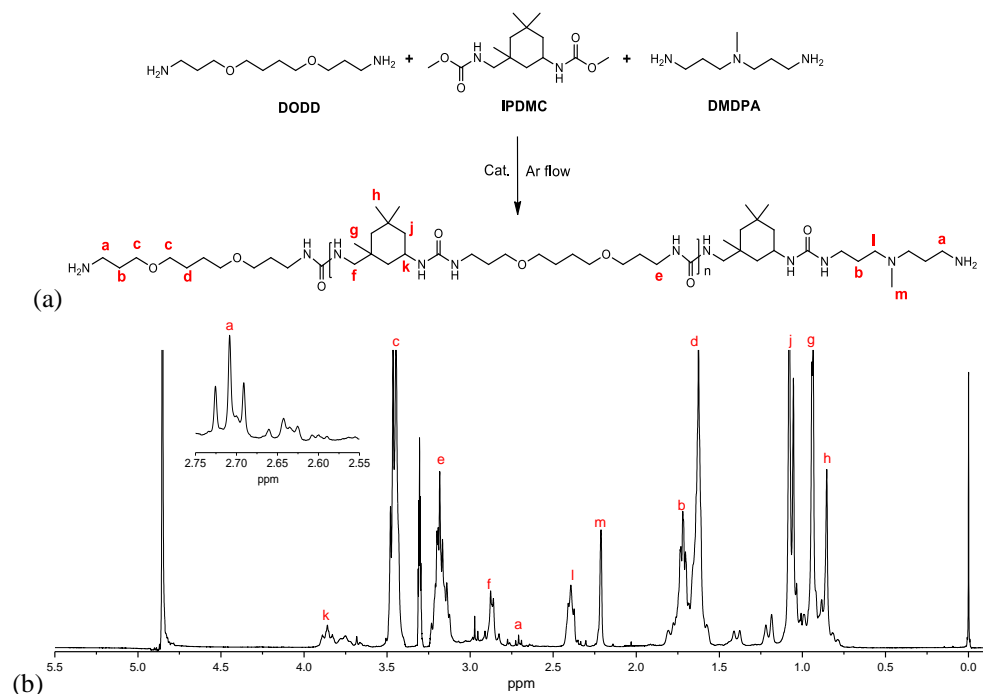


Figure 4. (a) Scheme of DODD, IPDMC and DMDPA polymerization. (b) NMR spectrum of the prepared polyurea with 30 mol% of DMDPA in the monomer feed.

An overlapping of the proton signals of the PPGda400 methyl end groups and the IPDMC cyclic ring is observed in the ^1H NMR spectra of the polyureas with PPGda400, prohibiting an accurate determination of NMR-based M_n values. The M_n s of the polyureas with TOTDDA and DODD were obtained via the methylene protons adjacent to the amine end-groups (peak **a** in Figure 4a) and the methylene protons adjacent to the urea moieties (peak **e**). The M_n values of these polyureas are situated between 15 to 19 kDa, lower than the theoretical ones ($100 \times (220 + 222) = 44$ kDa). This was caused by the side reaction of amine alkylation that consume the amine end-groups during the polymerization, leading to a deviation from the stoichiometry (see Chapter 4). Such alkylation reactions have also been observed during the synthesis of polyamides via diamine/dimethylester polycondensation.²⁶

3.3.3 PU dispersions and coatings

The above mentioned internal-amine carrying PUs could be dispersed in water to form water-borne PU dispersions, which were then applied on aluminum panels to obtain PU coatings. However, the PU coatings prepared from TOTDDA or DODD, DMDPA and IPDMC showed poor acetone and water resistance, probably due to the hydrophilicity of the TOTDDA and DODD blocks. Therefore, the more hydrophobic monomer PPGda400 was employed as diamine. The M_n s, D_{MS} and T_g s of polyureas with different concentrations of IDAas are presented in Table 2. The molecular weights were determined by SEC in HFIP, as ^1H NMR is not an appropriated method due to overlap of signals of IPDMC and of the end group of PPGDa400.

The M_n and D_M values of the polyurea prepared with 10 mol% of DETA are significantly higher compared with those of the IDA-free PU. This can be explained by the reaction of the secondary amine of DETA with IPCD, which leads to branching. A higher concentration of DETA (20 mol%) in the diamine feed even results in a crosslinked polymeric system. A similar behavior is observed with 10 mol% of BAPA, in agreement with the model reaction results, which demonstrate the higher reactivity of the secondary amine in BAPA towards carbonates.

The M_n s of polyureas with various DMDPA contents (10-40 mol% in diamine) range from 30-32 kDa, with D_{MS} ranging from 1.4-1.5. No gelation was observed with even 40 mol% DMDPA addition, indicating the inertness of the internal amine. The T_g s of the PUs increase with the content of DMDPA from 12 to 39 °C. This is explained by the higher urea density in the materials prepared with higher content of DMDPA, which has a lower molar mass (145 g/mol) than PPGDa400. A high urea density leads to stronger hydrogen bonding which limits the chain mobility, and thus gives a higher T_g .

Table 2. Properties of PUs synthesized from PPGDa400 and IPDMC with various concentrations of different IDAAs in the monomer feed (primary amine/carbamate = 1.01/1).

IDAa (mol% in amine monomers)	M_n (kDa) ^a	\bar{D}_M^a	T_g (°C) ^b
0	31	1.5	7
DETA (10)	45	4	42
DETA (20)	N.A. ^c	N.A.	56
BAPA (10)	N.A.	N.A.	53
DMDPA (10)	30	1.5	12
DMDPA (20)	31	1.5	23
DMDPA (30)	30	1.5	33
DMDPA (40)	32	1.5	39

^a) Determined by SEC in HFIP; ^b) determined by DSC; ^c) not available.

To form stable particles in water, cationically stabilized dispersions could be prepared by neutralization of the internal amines of the IDAAs by volatile acids, which are easily evaporated during coating applications. Thus, cationically stabilized polyurea dispersions were prepared with DMDPA-based polyureas, by first dissolving the polyurea in methanol, then neutralizing with acetic acid (equivalent amount to the molar amount of internal and chain-end amines in the polyurea), and dispersing the solution in water followed by evaporation of methanol. The dispersions were then casted on aluminum panels to evaluate the properties of the coatings. The composition of the PUs as well as the properties of the dispersions and of the resulting coatings are summarized in Table 3.

Table 3. Dispersion and coating properties of PUs with DMDPA as IDA, PPGda400 as diamine and IPDMC as dicarbamate (primary amine/carbamate = 1.01/1).

DMDPA (mol% in amine monomers)	M_n (kDa) ^a	T_g (°C) ^b	Av. particle size (nm) ^c	ζ -potential (mV) ^c	Pencil hardness	Impact test	Acetone resistance	Water resistance ^d
10	30	12	400	48	4B	-	-	+
20	31	23	26	52	3B	-	-	+
30	30	33	17	49	2B	-	-	+
40	32	39	17	51	2B	-	-	+
40 ^e	48	43	18	48	B	+	+	+

^a) Determined by SEC in HFIP; ^b) determined by DSC; ^c) determined by DLS; ^d) +: no swelling, ±: swelling without softening; ^e) prepared from 1/1.04 ratio of amine monomers/dicarbamate.

The thickness of the coatings are about 20-30 μm . The PUs with more DMDPA moieties incorporated, and thus more tertiary amines, yield aqueous dispersions with a higher concentration of charges on the particle surface. This leads to a higher particle surface area

or smaller particle sizes when dispersed in water.²⁷ The ζ -potentials of the dispersions are around 50 mV, indicating that the repulsions between the particles are strong enough to prevent the aggregation and coalescence, and therefore resulting in stable dispersions.²⁷ Due to the higher T_g and density of the hydrogen bonds in PUs with higher DMDPA contents, their coating hardnesses are also higher compared to those with lower DMDPA contents.^{28,29} The coating prepared from the PU of higher M_n (48 kDa) has sufficient resistance against acetone and water and can pass the reverse impact test, unlike the coatings obtained from the other PUs with M_n values around 30 kDa. These results can be explained by the more efficient entanglement network of the PU with higher MW which enhances its mechanical strength and solvent resistance. For the lower MW samples, cross-linking would be required to enhance the acetone and impact resistance.

Further experiments were carried out with different neutralization agent concentrations (NACs) to investigate their effect on the dispersion stabilities and coating properties. During the dispersion preparation process, the neutralization agent (acetic acid, formic acid or propionic acid) was added to neutralize the amines. Since most probably only the neutralized amine groups stay at the particle surface to stabilize the particle, a higher NAC leads to more of these stabilizing groups on the surface, and thus to smaller particles, as shown in Table 4.²⁸

Table 4. Dispersion properties and coating hardness of PUs using DMDPA as IDA, PPGda400 as diamine and IPDMC as dicarbamate, with different concentrations (and types) of neutralization agent.

Essay	DMDPA (mol% in amine monomers)	CH ₃ COOH/NH _x ^a	Av. particle size (nm)	ζ -potential (mV)	Pencil hardness
1	40	0.2/1	precipitates	N.A	N.A.
2	40	0.4/1	300~1000	49	3B
3	40	0.6/1	38	53	2B
4	40	0.75/1	20	52	2B
5	40	1/1	17	51	2B
6	20	0.75/1	50	48	3B
7	20	0.9/1	28	53	3B
8	20	1/1	26	52	3B
9	20	1.25/1	24	48	3B
10	20	1.4/1	22	56	3B
11	20	1/1 (C ₂ H ₅ COOH)	40	48	3B
12	20	1/1 (HCOOH)	25	46	3B

^{a)} Determined by potentiometric titration.

All coatings exhibit quite similar pencil hardnesses (2B-3B). Obviously, the chemical compositions of the essays listed in Table 4 are not sufficiently different to influence the coating hardness. The large particles and broad particle size distribution of essay **2** compared

to essays **3-5** might result in higher surface roughness after coating formation, if there is insufficient coalescence during the allowed time for film formation.³⁰ This was examined using AFM equipment. The AFM image of coating **2** indeed exhibits a much higher surface roughness compared to coatings **3-5**, which exhibit all a comparable roughness as shown in Figure 5. Next to acetic acid, other volatile neutralization agents such as formic acid and propionic acid were also tested in the preparation of dispersions (essays **11** and **12**). The particle sizes as well as the ζ -potentials of the dispersions and the coating hardnesses are all in the range of the values obtained with acetic acid.

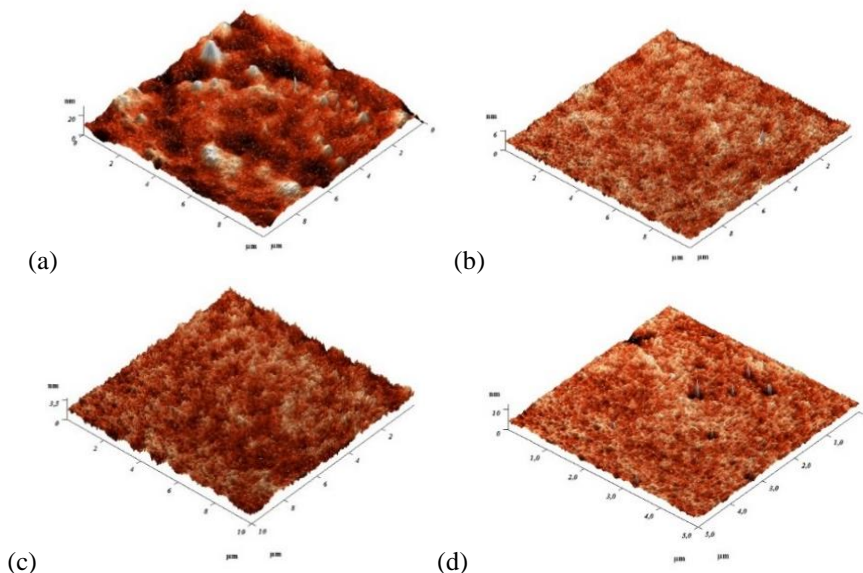


Figure 5. AFM images of the coatings prepared from essays (a) 2, (b) 3, (c) 4, (d) 5 listed in Table 4.

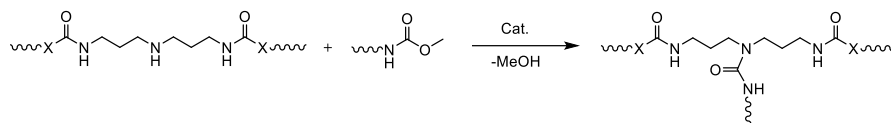
Figure 3 showed that the aminolysis rates of the internal amine of IDAc are significantly lower compared with BU2. Thus, their copolymerization with amines must be performed at temperatures up to 160 °C (vs. 130 °C with BU2). The M_n s and the T_g values of the polyureas prepared from PPGda400 and DCMDPA or BAPC in combination with IPDMC are shown in Table 5. BEPC was not used as IDAc because of its lack of reactivity towards amines.

Table 5. Properties of the PUs prepared with DCMDPA and BAPC as IDAs, PPGda400 as diamine and IPDMC as dicarbamate (primary amine/carbamate = 1.01/1).

Essay	IDAcS (mol% in dicarbamates)	M_n (kDa, \bar{D}_M) ^a	T_g (°C)
1	0	30 (1.5)	7
2	BAPC (10)	22 (1.9)	5
3	BAPC (20)	16 (1.8)	-1
4	BAPC (30)	13 (1.6)	-10
5	BAPC (40)	8 (1.5)	-11
7	DCMDPA (10)	28 (1.3)	6
8	DCMDPA (20)	28 (1.4)	8
9	DCMDPA (30)	34 (1.5)	7
10	DCMDPA (40)	35 (1.6)	8

^a) Determined by SEC in HFIP.

Essays 1-5 show a decreasing trend of M_n with increasing BAPC monomer feed. This decrease of M_n is caused by the aminolysis of carbamates by the secondary amine of BAPC (Scheme 8). This results in an increase of the primary amine/carbamate ratio (and in an increasing deviation from the optimum primary amine/carbamate ratio) with higher BAPC content during polymerization, leading to a decreasing M_n . This prompted us to focus our further investigations on PUs based on DCMDPA. The decreasing trend in T_g with increasing BAPC content is probably caused by the corresponding decrease in M_n .



Scheme 8. Aminolysis of secondary amines during polymerization between BAPC, IPDMC and PPGda400.

The T_g s of the polyureas based on DCMDPA (PUcs) are barely affected by the IDA content, possibly due to a similar contribution of the DCMDPA and IPDMC units to the T_g of the polymer (Figure 6). An increase of DCMDPA content in the PUcs leads to more substitution of HS2 with HS1, while the overall hardness segment concentration is constant. Moreover, the molecular weights of all DCMDPA-based PUcs are in the same order of magnitude.

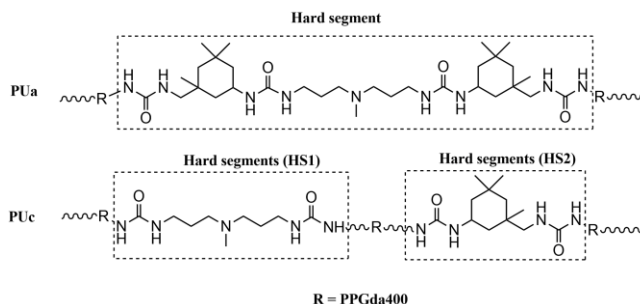


Figure 6. Hard segments in PUa and PUc.

Table 6. Dispersion properties and coating hardness of polyureas with IPDMC, PPGda400 and DCMDPA as IDA (primary amine/carbamate = 1.01/1).

DCMDPA (mol% in dicarbamate)	M_n (kDa) ^a	T_g (°C) ^b	Av. particle size (nm) ^c	ζ - potential (mV) ^c	Pencil hardness	Impact test	Acetone resistance	Water resistance ^d
10	27	6	55	51	6B	+	-	+
20	28	8	30	50	6B	+	-	+
30	34	7	19	49	6B	+	-	+
40	35	8	13	55	6B	+	-	+

^{a)} Determined by SEC in HFIP; ^{b)} determined by DSC; ^{c)} determined by DLS; ^{d)} +: swelling without softening.

The properties of the dispersions and coatings obtained from the PUCs compiled in Table 6 are very similar to those found for the PUAs (Table 3), namely small particle size, high ζ -potential and poor acetone resistance and good water resistance. However, the hardnesses of the resulting coatings are lower due to the lower T_g s (6-7 °C) compared to the coatings based on PUAs. The coatings based on PUCs pass the reverse impact test, most probably thanks to their flexibility, which originates from the flexible PPGda400 spacer between two hard segments. It is obvious that the molecular weights of these PUCs are too low in order to provide good solvent resistance without curing the coatings. Cured coatings will be discussed in the rest of this thesis.

3.4 Conclusion

In this chapter, water-dispersible polyureas were synthesized via an isocyanate-free approach from 4,9-dioxa-1,12-dodecanediamine (DODD), poly(propylene glycol) bis(2-aminopropyl ether) with average M_n of 400 Da (PPGda400), 4,7,10-trioxa-1,13-tridecanediamine (TOTDDA) and isophorone dicarbamate (IPDMC) and internal dispersing agents (IDAs). Model reactions with dicarbamate functional IDAs (IDAcS) including bis(2-aminoethyl) carbamate (BAEC), bis(3-aminopropyl) carbamate (BAPC) and 3,3'-dicarbamate-*N*-methyl- dipropylamine (DCMDPA) and *N*-hexylmethylcarbamate (NHMC) as substrates revealed that the secondary amine of BAPC reacted faster with NHMC compared to that of BAEC. The IDAcS (DCMDPA, BEPC and BAPC) containing internal amines induced a retarding effect on the aminolysis of the carbamate end-functions due to the hydrogen bond formation between carbamates and internal amine, which sterically hinders the reaction. This resulted in a much lower aminolysis rate of the IDAcS (DCMDPA > BAPC > BEPC) compared with butane dimethylcarbamate (BU2).

The polymerization of DETA or BAPA with IPDMC and PPGda400 resulted in cross-linked PUs, whereas PUs with DMDPA, TOTDDA or DODD and IPDMC had a relatively low \bar{M}_n . The carbamate aminolysis is accompanied by the methylation of amines, as identified by NMR, which limited the molecular weight build-up of the growing chains. M_n of polyureas prepared from DMDPA, PPGda400 and IPDMC ranged from 30 to 48 kDa, depending on the ratio between the comonomers. The T_g increased with increasing DMDPA content. Neither BEPC nor BAPC are suitable as IDA for polyurea preparation due to the lack of reactivity of BEPC towards the diamine monomers and the limited M_n increase with BAPC. The PUs prepared from DCMDPA, PPGda400 and IPDMC exhibited M_n s between 27 and 37 kDa,

with T_g s around 7 °C.

Stable dispersions with ζ -potentials around 50 mV and particle sizes lower than 100 nm could be prepared from polyureas with DCMDPA or DMDPA as IDAs. The hardness of the coatings resulting from these dispersions were hardly affected by the type of neutralization agents. The hardness of the coatings from the DMDPA-based polyureas (PUas) increased from 4B to 2B with increasing IDA concentration, which is significantly higher than the 6B hardness of those prepared from DCMDPA based polyureas (PUcs). PUcs with different IDA concentrations all passed the reverse impact test, while most PUas did not, with the notable exception of the PUa with 40 mol% of DMDPA in diamine monomers and a high M_n of about 48 kDa. These coatings also show a satisfactory solvent resistance against acetone and water. The other coatings studied in this chapter proved to have insufficiently high molecular weights to give solvent-resistant coatings without curing.

3.5 References

- (1) Szycher, M. *Szycher's Handbook of Polyurethanes*. CRC Press. **2012**, 5-15.
- (2) Avar, G. *Polyurethanes (PU)*. *Kunststoffe International*. **2008**, 10, 123-127.
- (3) Krol, P. *Prog. Mater. Sci.* **2007**, 52, 915-1015.
- (4) Sonnenschein, M. F. *Polyurethanes Science, Technology, Markets, and Trends*. **2015**, 336-374.
- (5) Noble, K. L. *Prog. Org. Coat.* **1997**, 32, 131-136.
- (6) Chattopadhyay, D. K.; Raju, K. V. S. N. *Prog. Polym. Sci.* **2007**, 32, 352-418.
- (7) Kreye, O.; Mutlu, H.; Meier, M. A. R. *Green Chem.* **2013**, 15, 1431-1455.
- (8) Klingenberg, E. H.; Fazel, S. N. US 7342068 B2, **2008**.
- (9) Hall, H. K.; Schneider, A. K. *J. Am. Chem. Soc.* **1958**, 80, 6404-6409.
- (10) Neffgen, S.; Keul, H.; Hocker, H. *Macromol. Rapid Commun.* **1996**, 17, 373-382.
- (11) Schmitz, F.; Keul, H.; Höcker, H. *Polymer*, **1998**, 39, 3179-3186.
- (12) Miyagawa, T.; Shimizu, M.; Sanda, F.; Endo, T. *Macromolecules* **2005**, 38, 7944-7949.
- (13) Su, W.; Luo, X. H.; Wang, H. F.; Li, L.; Feng, J.; Zhang, X. Z.; Zhuo, R. X. *Macromol. Rapid Commun.* **2011**, 32, 390-396.
- (14) Kühling, S.; Keul, H.; Höcker, H.; Buysch, H. J.; Schon, N. *Makromol. Chem.* **1991**, 192, 1193-1205.
- (15) Hu, X. L.; Chen, X. S.; Cheng, H. B.; Jing, X. B. *J. Polym. Sci., Part A: Polym. Chem.* **2009**, 47, 161-169.
- (16) Sakakura, T.; Kohno, K. *Chem. Commun.* **2009**, 11, 1312-1330.
- (17) Lee, B. Y. *Macromolecules* **2013**, 46, 3301-3308.
- (18) Delebecq, E.; Pascault, J. P.; Boutevin, B.; Ganachaud, F. *Chem. Rev.* **2013**, 113, 80-118.
- (19) Tomita, H.; Sanda, F.; Endo, T. *J. Polym. Sci., Part A: Polym. Chem.* **2001**, 39, 4091-4100.
- (20) Deepa, P.; Jayakannan, M. *J. Polym. Sci., Part A: Polym. Chem.* **2008**, 46, 2445-2458.
- (21) Tang, D.; Mulder, D. J.; Noordover, B. A. J.; Koning, C. E. *Macromol. Rapid Commun.* **2011**, 32, 1379-1385.

- (22) Unverferth, M.; Kreye, O.; Prohammer, A.; Meier, M. A. R. *Macromol. Rapid Commun.* **2013**, *34*, 1569-1574.
- (23) Querat, E.; Tighzert, L.; Pascault, J. P.; Dusek, K. *Angew. Makromol. Chem.* **1996**, *242*, 1-36.
- (24) Spirkova, M.; Dusek, K. *Polym. Bull.* **1989**, *22*, 191-198.
- (25) Ma, S.; Liu, C.; Sablong, R. J.; Noordover, B. A. J.; Hensen, E. J. M.; van Benthem, R. A. T. M.; Koning, C. E. *ACS Catalysis*. **2016**, *6*, 6883-6891.
- (26) Malluche, J.; Hellmann, G. P.; Hewel, M.; Liedloff, H.-J. *Polym. Eng. & Sci.* **2007**, *47*, 1589-1599.
- (27) Larsson, M.; Hill, A.; Duffy, J. *Annual transactions of the Nordic phenology* **2012**, *20*, 209-214.
- (28) Fu, Z.; Hejl, A.; Swartz, A. *Euro. Coat. J.* **2009**, *1*, 1-12.
- (29) Wicks, Z. W.; Frank, N. J.; Pappas, S. P.; Wicks, D. A. *Organic Coatings. Wiley-Interscience*. **2007**, 77-78.
- (30) Demas, N.G. Martin, C. L.; Ajayi, O. O.; Erck, R. A.; Shareef, I. *Metall. Mater. Trans. A* **2016**, *47*, 1629-1640.
- (31) Clifford, P.; Green, N. J. B.; Pilling, M. J. *J. Phys. Chem.* **1984**, *88*, 4171-4176.
- (32) Li, C.; Li, S.; Zhao, J.; Zhang, Z.; Zhang, J.; Yang, W. *J. Polym. Res.* **2014**, *21*, 1-10.
- (33) Deng, Y.; Li, S.; Zhao, J. B.; Zhang, Z.; Zhang, J.; Yang, W. *RSC Adv.* **2014**, *4*, 43406-43414.

Chapter 4. Investigation and mitigation of a side reaction during carbamate aminolysis: *N*-alkylation

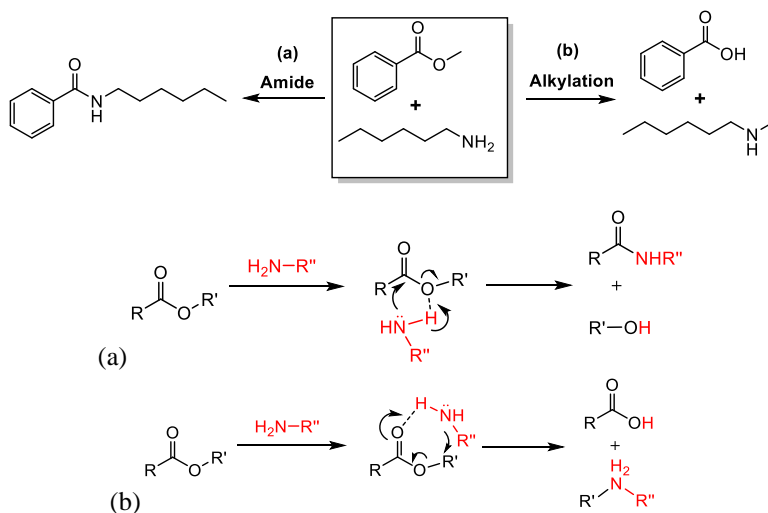
Summary

Investigations on the *N*-alkylation of amines during the aminolysis of carbamates and strategies to enhance the number average molecular weight (M_n) of polyureas produced from diamine/dicarbamate polymerizations are reported in this chapter. Poly(propylene glycol) bis(2-aminopropyl ether) with molecular weight of 230 Da (PPGda230), 4,7,10-trioxa-1,13-tridecanediamine (TOTDDA) and *N,N'*-dimethyl-1,6-hexanediamine (DMHD) were employed as the amine monomers, while butane dicarbamate (BU2) and isophorone dimethylcarbamate (IPDMC) were used as carbamate monomers to study the effect of the monomer structures on the rate of *N*-alkylation. Model reactions with stoichiometric amounts of diamine and dicarbamate in a closed set-up at 130 °C showed decreasing *N*-methylation rates with the order DMHD > TOTDDA > PPGda230, while similar rates were observed with IPDMC or BU2. The activation energy of the diamine/IPDMC reactions followed the order of PPGda230/IPDMC > TOTDDA/IPDMC > DMHD/IPDMC. The *N*-methylation could be efficiently suppressed by removal of methanol and addition of catalyst, which led to faster urea formation. The latter enhanced significantly with increasing argon flow rate when using TBD as catalyst, the absence of which resulted in a slower urea formation rate. The highest M_n was obtained for the copolymerization of TOTDDA and IPDMC with an optimum TOTDDA/IPDMC ratio of 0.95-0.96. A much lower *N*-alkylation rate was observed with isophorone diethylcarbamate (IPDEC), and the highest M_n was achieved for a stoichiometric copolymerization. No *N*-alkylation was detected during the copolymerization of isophorone di-*tert*-butylcarbamate (DiBoc-IPDC) and TOTDDA due to the steric effect of the *t*-butyl group. The reaction between TOTDDA and an excess of DiBoc-IPDC led to gelation, while the stoichiometric copolymerization between TOTDDA and DiBoc-IPDC resulted in a polyurea with high M_n and high polydispersity (D_M).

4.1 Introduction

The *N*-methylation of amines is a fundamental reaction in the synthesis of dyes, pharmaceuticals and synthetic intermediates.¹ Such reaction normally proceeds via nucleophilic attack of an amine on an electron deficient carbon to form a C-N covalent bond. Therefore most of the *N*-methylation agents contain reactive carbonyls or halides, e.g. the toxic formaldehyde and methylene chloride. More environmentally friendly CO₂, HCOOH and carbonates have also been reported in literature.²⁻¹⁷

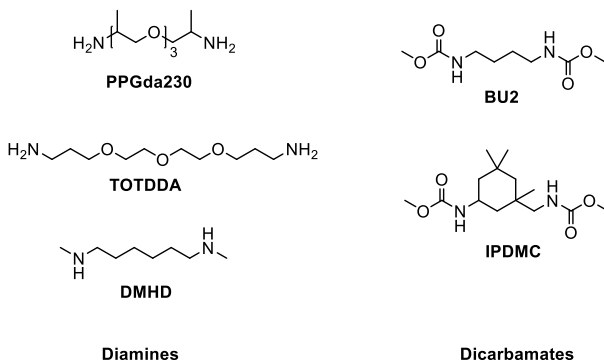
On the other hand, the *N*-methylation also occurs as a side reaction in diamine-diester polycondensations and potentially limits the molecular weight (MW) of the resulting polyamides. This is caused by the formation of less reactive monomers (secondary amines) and chain-stoppers (dimethylated amines) and accordingly, by disrupting the stoichiometric balance of the monomers.¹⁸⁻²² In their study of the model reaction between methyl benzoate and hexylamine or hexamethylene diamine, Hellmann et al. showed that the *N*-methylation rates of amines are only ten times lower than the rate of the amidations, and therefore should not be ignored (Scheme 1a).²⁰ The authors proposed a bimolecular mechanism involving the attack of the alkyl ester to form an alkylated amine and a carboxylic acid. The rate of *N*-alkylation is reduced when ethyl esters are employed instead of methyl esters (Scheme 1b).



Scheme 1. (a) Amidation and (b) *N*-alkylation reactions between hexylamine and methylbenzoate.²⁰

Similarly, the *N*-alkylation of amines could also take place during the aminolysis of carbamates, as indicated in Chapter 3. This could lead to an off-stoichiometry of the monomers during the diamine/dicarbamate polymerization, thereby resulting in PUs with lower molecular weight than expected. Thus, in the present chapter, this reaction is investigated in more detail. First, the influence of the structure of the monomers on the *N*-methylation rate is studied by employing butane- (BU2) and isophorone dimethylcarbamate (IPDMC), and the primary diamines 4,7,10-trioxa-1,13-tridecanediamine (TOTDDA) and

poly(propylene glycol) bis(2-aminopropyl ether) with an average M_n of 230 Da (PPGda230, Scheme 2). *N,N'*-Dimethyl-1,6-hexanediamine (DMHD) is employed as diamine to study specifically the dimethylation reaction. Limiting factors for the *N*-alkylation reactions such as methanol removal and addition of catalysts are also studied, and the MWs of the polyureas are optimized accordingly.



Scheme 2. Structures of the monomers employed in this study.

4.2 Experimental Section

4.2.1 Materials

All reagents were commercially available unless specified otherwise. Isophorone diamine (IPDA, *cis* and *trans* mixture, 99%), 1,5,7-triazabicyclo [4.4.0]dec-5-ene (TBD, 98%), di-*tert*-butyl dicarbonate (Boc₂O, 99%), diethyl carbonate (DEC, 99%), 1,4-diaminobutane (DAB, 99%), potassium methoxide (KOMe, 95%), dimethyl carbonate (DMC, 99%), poly(propylene glycol) bis(2-aminopropyl ether) with an average M_n of 230 Da (PPGda230), *N,N'*-dimethyl-1,6-hexanediamine (DMHD, 98%), 4,7,10-trioxa-1,13-tridecanediamine (TOTDDA, 97%) and sodium sulfate (99%, anhydrous) were purchased from Sigma Aldrich. Deuterated solvents were purchased from Buchem BV. Other common solvents were purchased from Biosolve. All the chemicals were used without further purification.

4.2.2 Reactions and synthesis

Synthesis of BU2

In a 500 mL flask, a mixture of DMC (90 g, 1 mol), molten DAB (35.2 g, 0.4 mol) and TBD (1.39 g, 10 mmol) was stirred for 1 hour at room temperature. During this period, 100 mL of diethylether (Et₂O) were added at the moment a precipitation was observed. The precipitate was then isolated by filtration. The residue was recrystallized from chloroform and dried overnight at 60 °C in a vacuum oven to obtain BU2 as a colorless crystalline solid (70 g, 86%).

¹H NMR (400 MHz, CDCl₃, δ in ppm): 4.9 (s, broad, 2H, NH), 3.6 (s, 6H, OCH₃), 3.2 (m, 4H, NHCH₂), 1.5 (m, 4H, NHCH₂CH₂). ¹³C { ¹H } NMR (100.6 MHz, CDCl₃, δ in ppm): 157.2 (C=O), 51.9 (OCH₃); 40.6 (NHCH₂); 27.2 (NHCH₂CH₂).

Synthesis of isophorone dimethylcarbamate (IPDMC)

In a 2000 mL three-neck flask equipped with a condenser, 170 g (1 mol) of IPDA, 630 g (7 mol) of DMC and 70 g (1 mol) of potassium methoxide were mixed under argon flow and stirred at room temperature. After 4 hours, the mixture was heated up to 60 °C for 6 hours. The solution was then cooled and poured into an excess of chloroform and subsequently washed with brine. The organic layer was dried over anhydrous sodium sulfate. The solvent was evaporated to dryness to obtain the product as a yellowish solid (196 g, 69%).

¹H-NMR (400 MHz, CDCl₃, δ in ppm): 4.8 (d, 1H, -NHCH₂), 4.6 (s, 1H, cy-NHCH), 3.8-3.6 (s, 1H, cy-CHNH, 6H, -OCH₃), 3.3, 2.9 (d, 2H, -CH₂NH), 1.7-0.7 (15H, cy-H). ¹³C{¹H} NMR (100.6 MHz, CDCl₃, δ in ppm): 157.4, 156.3 (C=O), 54.8 and 52.1 (OCH₃), 51.8, 46.9, 46.3, 44.6, 42.5, 41.8, 36.3, 34.9, 31.7, 29.6, 27.5, and 23.1 (cy-C).

Synthesis of isophorone diethylcarbamate (IPDEC)

In a 2000 mL three-neck flask equipped with a condenser, 170 g (1 mol) of IPDA, 826 g (7 mol) of DEC and 84 g (1 mol) of potassium ethoxide were mixed under argon flow and stirred at room temperature. After 4 hours, the mixture was heated up to 60 °C for 12 hours. The solution was then cooled and poured into an excess of chloroform and subsequently washed with brine. The organic layer was dried over anhydrous sodium sulfate. The solvent was evaporated to dryness to obtain the product as a brownish solid (230 g, 73%).

¹H-NMR (400 MHz, CDCl₃, δ in ppm): 4.7 (d, 1H, -NHCH₂), 4.5 (s, 1H, cy-NHCH), 4.11 (s, 4H, CH₃CH₂O) 3.75-2.9 (s, 1H, cy-CHNH, d, 2H, -CH₂NH), 1.2 (t, 6H, CH₃CH₂O) 1.7-0.7 (15H, cy-H). ¹³C{¹H} NMR (100.6 MHz, CDCl₃, δ in ppm): 157.4, 156.0 (C=O), 60.77 (OCH₂CH₃), 54.9, 47.2, 46.3, 42.8, 41.9, 36.4, 35.1, 31.8, 29.7, 27.7, and 23.2 (cy-C), 14.7 (OCH₂CH₃).

Synthesis of isophorone di-*tert*-butylcarbamate (DiBoc-IPDC)

In a 500 mL flask, 68 g (0.4 mol) of IPDA, 192 g (0.88 mol) of Boc₂O and 150 mL water were stirred at room temperature. After 12 hours, the mixture was dissolved in 200 mL chloroform and washed with water (3×200 mL). The organic layer was then dried over anhydrous sodium sulfate and evaporated to dryness to obtain a white powder (135 g, 91%).

¹H-NMR (400 MHz, CDCl₃, δ in ppm): 4.6 (d, 1H, -NHCH₂), 4.3 (s, 1H, cy-NHCH), 3.7 (s, 1H, cy-CHNH), 3.2, 2.9 (d, 2H, -CH₂NH), 1.7-0.7 (15H, cy-H, 18H, CCH₃). ¹³C{¹H} NMR (100.6 MHz, CDCl₃, δ in ppm): 157.4, 156.5 (C=O), 78.6 (C(CH₃)₃) 54.9 51.8, 46.9, 45.8, 43.7, 41.7, 41.4, 36.3, 34.3, 31.3, 28.8, 26.7, and 26.2 (cy-C), 27.4 (C(CH₃)₃).

Copolymerization between TOTDDA and dicarbamates

In a 50 mL crimp-capped vial, 4.29 g (15 mmol) of IPDMC (IPDEC or DiBoc-IPDC) and 3.30 g (15 mmol) of TOTDDA were mixed under argon flow and stirred at 130 °C until the mixture was homogeneous. 0.21 g (1.5 mmol) of TBD was then added to the mixture. The time of the addition of TBD was considered as the t = 0 of the reaction.

Model reaction of the *N*-methylation of a diamine

In a specific experiment, 4.29 g (15 mmol) of IPDMC and 3.30 g (15 mmol) of TOTDDA were mixed in a 50 mL crimp-capped vial and stirred at 130 °C until the mixture was homogeneous. The time of homogenous mixture formation was considered as t = 0 of the

reaction.

4.2.3 Characterizations

Size exclusion chromatography (SEC)

SEC in 1,1,1,3,3,3-hexafluoro-2-propanol (HFIP) was performed on a system equipped with a Waters 1515 Isocratic HPLC pump, a Waters 2414 refractive index detector (35 °C), a Waters 2707 autosampler, a PSS PFG guard column followed by 2 PFG-linear-XL (7 μ m, 8*300 mm) columns in series at 40 °C. HFIP with potassium trifluoroacetate (3 g/L) was used as eluent at a flow rate of 0.8 mL/min. The molecular weights were calculated with respect to poly(methyl methacrylate) standards (Polymer Laboratories, M_p = 580 Da up to M_p = 7.1×10^6 Da).

Nuclear magnetic resonance spectroscopy (NMR)

$^{13}\text{C}\{^1\text{H}\}$ NMR (100.62 MHz) and ^1H NMR (400 MHz) spectra were recorded using a Varian Mercury Vx spectrometer at 25 °C. Samples were prepared by dissolving 20 mg of polymer in 1 mL of MeOD- d_4 .

Matrix-assisted laser desorption ionization time-of-flight mass spectrometry (MALDI-ToF-MS)

MALDI-ToF-MS spectra were recorded on a Voyager DE-STR from Applied Biosystems. Calibrations were carried out with poly(ethylene oxide) standards for the lower mass range and polystyrene standards for the higher mass range. Trans-2-[3-(4-tert-butylphenyl)- 2-methyl-2-propenyldiene] malononitrile (DCTB) was used as a matrix. Polymer samples were dissolved in methanol at a concentration of 3-5 mg/mL. Potassium trifluoroacetate (KTFA, 5 mg/mL) was used as a cationization agent. The solutions of matrix (40 mg/mL), KTFA and polymer samples were premixed in a weight ratio of 4:1:4. The mixtures were subsequently hand-spotted on the target and left to dry. Spectra were recorded in the reflector mode at positive polarity.

Gas chromatography with flame ionization detector (GC-FID)

A Varian CP-3800 equipped with an FID was used for analysis of the kinetic results. Samples were prepared by quenching 0.05 mL of the reaction mixture into 1 mL of chloroform.

4.3 Results and discussion

4.3.1 Preliminary observations

We first observed the *N*-methylation of amine during the copolymerization between 4,7,10-trioxa-1,13-tridecanediamine (TOTDDA) and isophorone dimethylcarbamate (IPDMC) with a ratio of 1.01/1, as mentioned in Chapter 3. Since this side reaction may affect the molecular weight growth of the polyureas, we decided to carry out further investigations by monitoring this polymerization by ^1H NMR over 5 hours under the conditions mentioned in Chapter 3 (130 °C, argon flow and 5 mol% TBD as catalyst, Figure 1a,c). The spectra were characterized, between 2.0 and 2.8 ppm, by the decrease in time of the triplet at 2.71 ppm representing the methylene protons adjacent to the primary amine end groups (**d** in Figure 1c) and the rise of singlets at 2.23, 2.30, 2.35 and 2.62 ppm assigned to the methyl protons of the monomethylated amines, the decarboxylated carbamates, the methyl protons of dimethylated

amines and the methylene protons next to the monomethylated amines, respectively (**a**, **b**, **c**, **e** in Figure 1c).²¹ Thus, the *N*-methylation of a terminal amine by a methyl carbamate results in an unstable carbamic acid that quickly undergoes decarboxylation to form an isophorone moiety bearing a new amine. In other words, the *N*-methylation reaction consumes a carbamate group while producing an amine, thereby resulting in a polyurea with an M_n of 19 kDa, which is much lower than the theoretical value of 44 kDa.²⁶ Additional analysis of the TOTDDA/IPDMC polymerization with MALDI-TOF shows the existence of mono-, di-, tri- and tetramethylated TOTDDA at m/z of 235.4, 249.4, 263.1 and 277.3, respectively (Figure 1b,d), further confirming the *N*-methylation reaction during the diamine-dicarbamate polymerization.

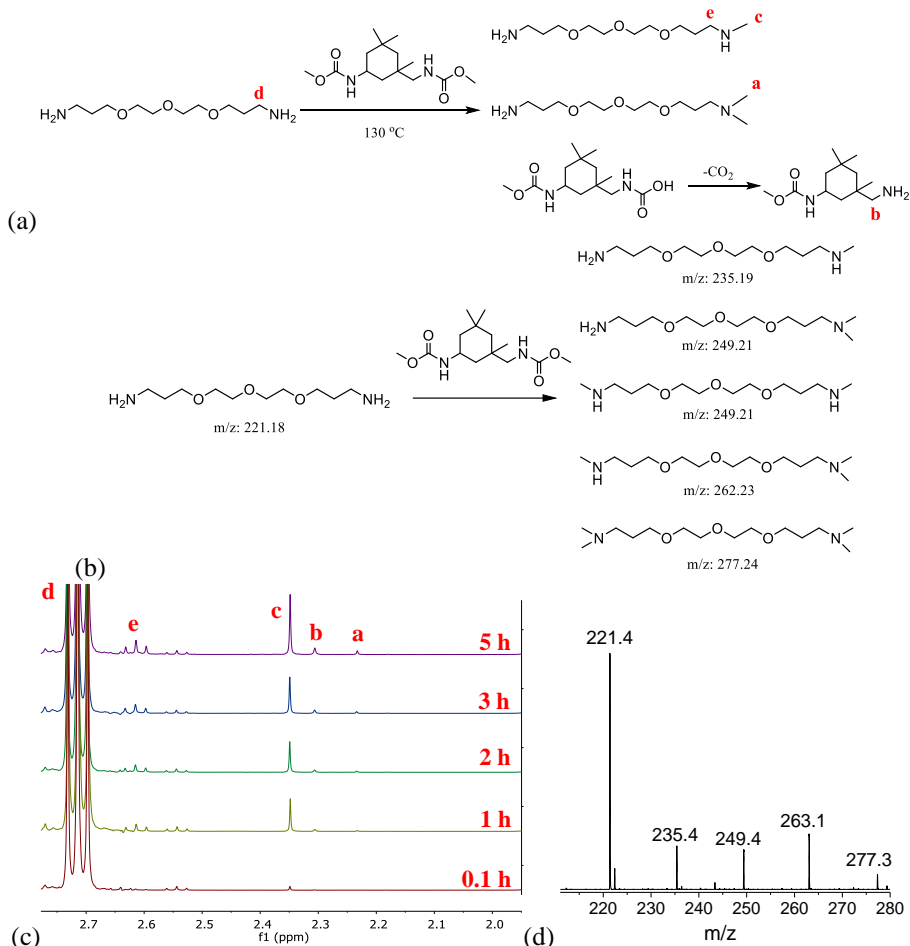


Figure 1. (a) Scheme of *N*-methylation of TOTDDA with IPDMC. (b) m/z values of mono-, di-, tri- and tetra methylated TOTDDA. (c) NMR spectra of a stoichiometric TOTDDA/IPDMC mixture at 130 °C at various reaction times (MeOD-d_4 as solvent). (d) Mass spectrum of a stoichiometric TOTDDA/IPDMC mixture at 130 °C after 1 hour.

4.3.2 *N*-alkylation in carbamate aminolysis

In this section, systematic investigations on the *N*-methylation were conducted with PPGda230, TOTDDA and DMHD as diamine monomers. PPGda230 contains primary amines on secondary carbons, while TOTDDA carries primary amines on primary carbons and DMHD bears secondary amines as end-groups. BU2 and the more sterically hindered IPDMC are employed as dicarbamates. The reactions between stoichiometric ratios of the diamines and the dicarbamates proceeded in a closed set-up to prevent the evaporation of methanol, and thus limit the urea formation. The conversion of the amine groups into the corresponding mono- and dimethylated amines in the reaction mixtures were determined by ^1H NMR (Figure 2).

A faster *N*-methylation rate is observed for the less sterically hindered amines in TOTDDA compared to the amine end groups in PPGda230. BU2 and IPDMC show similar *N*-methylation rates when reacting with the same amine, which indicates a limited steric effect of the carbamates. The dimethylation (*N*-methylation of a secondary amine) of DMHD by IPDMC is much faster than the *N*-methylation of TOTDDA, in agreement with the previous observations during diamine-diester polycondensations, where the $k_{2\text{Me}} = 2k_{\text{Me}}$ (Scheme 3).²³

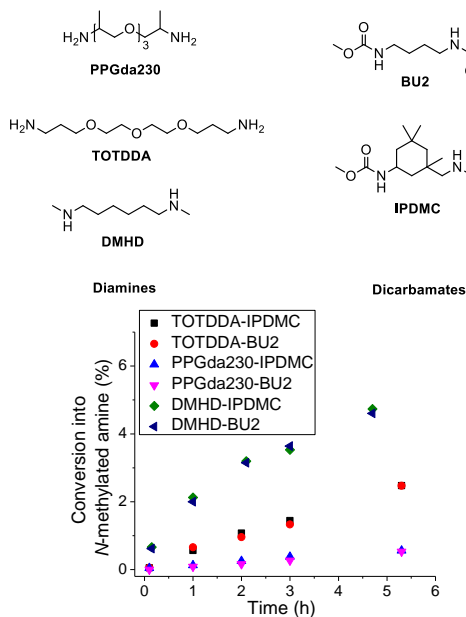
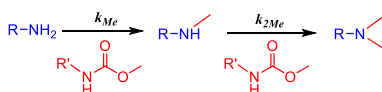
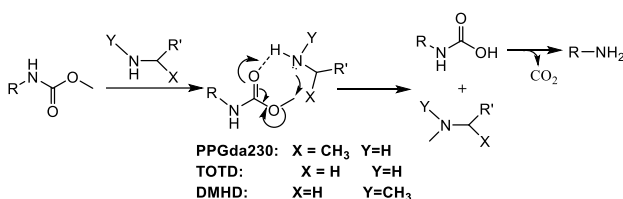


Figure 2. ^1H NMR-determined conversion of amine groups into the corresponding (di)methylated amines as a function of time in various diamine/dicarbamate stoichiometric mixtures at 130 °C.



Scheme 3. Mono- and dimethylation of a primary amine by a methyl carbamate.

Similarly to the aminolysis of esters, Scheme 4 shows the proposed mechanism of the *N*-methylation of an amine by a carbamate during which the nitrogen attacks the methyl group of the carbamate to form a covalent N-C bond, while the proton of the amine is transferred to the carbonyl oxygen.²⁰ This results in a methylated amine and an unstable carbamic acid, which immediately undergoes decarboxylation to form a primary amine and carbon dioxide. The methyl group next to the amine end-group in PPGda230 hinders the attack on the methyl group of the carbamate, leading to a lower *N*-methylation rate compared to TOTDDA. The methyl group of DMHD increases the electron density of the amine, which promotes the nucleophilic attack on the methyl group of the carbamate, leading to an even higher *N*-methylation rate than observed for TOTDDA. The steric effect of the R group in the carbamate is limited due to the distance to the site of the nucleophilic attack. This results in similar *N*-methylation rates for BU2 and IPDMC.



Scheme 4. Proposed mechanism for the *N*-methylation of an amine by a methyl carbamate.

The S_N2 nature of (di)methylation suggests that their rates can be calculated according to the reaction rate of a second order reaction:²³

$$\frac{d[A]}{dt} = k[A][C].$$

Where *k* is the reaction rate constant, [A] and [C] the concentrations of the amine and the carbamate, respectively, and *d*[A]/*dt* the slope of the concentration of the amine vs. time plot for each system in Figure 2. For stoichiometric reactions, *k_{Me}* and *k_{2Me}* equal the slope of the 1/[A] vs. time plot. The *k_{Me}* and *k_{2Me}* values, calculated for each system, are listed in Table 1. The *k_{Me}* values of the primary diamine/dimethylcarbamate reactions range from 0.3–1.2 mmol/L.h, which are comparable with those in the diamine/dimethylester reactions reported in the literature (*k_{Me}* = 0.2–1 mmol/L.h).²⁰

Table 1. *N*-methylation rate constants during diamine/dicarbamate reactions at 130 °C.

Diamine	Dicarbamate	<i>k_{Me}</i> (mmol/L.h)	<i>k_{2Me}</i> (mmol/L.h)
PPGda230	IPDMC	0.31	\
PPGda230	BU2	0.28	\
TOTDDA	IPDMC	1.32	\
TOTDDA	BU2	1.28	\
DMHD	IPDMC	\	4.53
DMHD	BU2	\	4.48

The *N*-methylation rate constants *k_{Me}* of the TOTDDA/IPDMC and PPGda230/IPDMC systems, and *k_{2Me}* with DMHD/IPDMC system were calculated at 130 °C, 140 °C, 150 °C and

160 °C. For the calculation of k_{Me} in the TOTDDA/IPDMC and PPGda230/IPDMC systems, the conversion of primary amines to monomethylated amine was calculated as the sum of the concentrations of mono- and dimethylated amines in the mixture determined by ^1H NMR, since the dimethylated amines are also converted from the monomethylated ones. In the DMHD/IPDMC system, the conversion of secondary amines to dimethylated amines was directly determined from the ^1H NMR measurements for k_{2Me} calculation. The corresponding activation energies were derived from the Arrhenius plots (Figure 3).

The activation energies follow the order PPGda230/IPDMC (109.9 kJ/mol) > TOTDDA/IPDMC (93.9 kJ/mol) > DMHD/IPDMC (73.1 kJ/mol). The higher activation energy of the PPGda230/IPDMC system compared to TOTDDA/IPDMC is in agreement with the proposed mechanism, where the steric effect of the methyl group in PPGda230 hinders the nucleophilic attack and raises the activation energy. Additionally, although the *N*-methyl group of DMHD generates a similar steric hindrance, it also enhances the nucleophilicity of amine, the effect of which is dominating over the former, leading to a lower activation energy of the DMHD/IPDMC system compared to the other two.

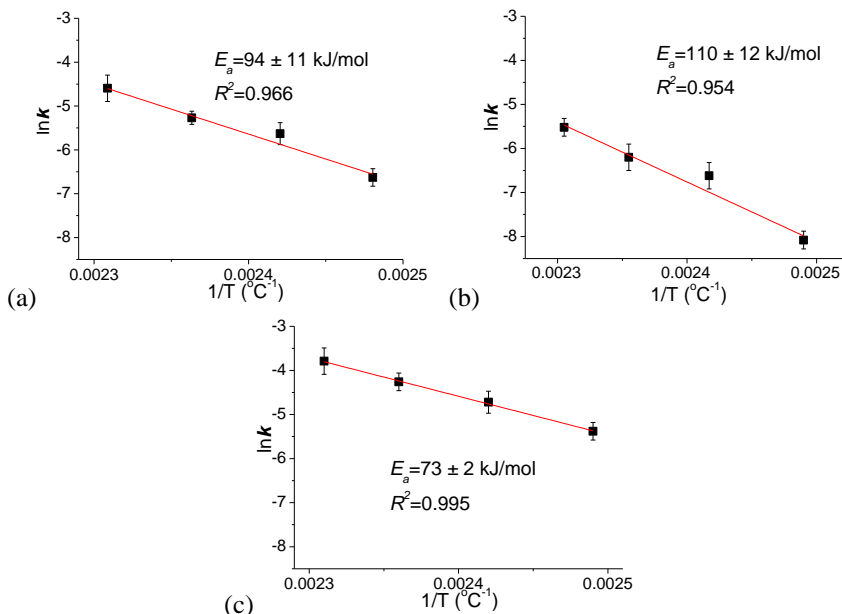


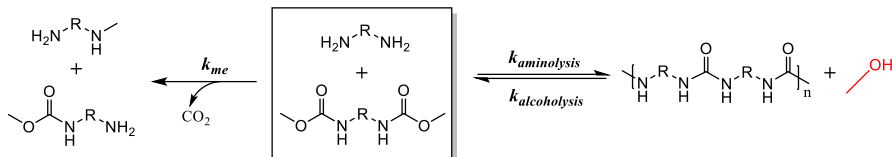
Figure 3. Arrhenius plots of *N*-methylation reactions in (a) TOTDDA/IPDMC system, (b) PPGda230/IPDMC system and (c) DMHD/IPDMC system.

4.3.3 Mitigation of the side reaction: *N*-alkylation

4.3.3.1 Removal of methanol

A practical route to limit *N*-methylation, and thereby obtaining high M_n polyureas, is by increasing the urea formation rate ($r_{\text{urea}} = k_{\text{aminolysis}}[\text{carbamate}][\text{amine}] - k_{\text{alcoholysis}}[\text{MeOH}][\text{urea}]$, Scheme 5). r_{urea} is considerably dependent on the removal of methanol and the use of a catalyst. Previous reports showed that the equilibrium of the

carbamate aminolysis (right side of Scheme 5) strongly favors the left side, i.e. the aminolysis rate is much lower than the urea alcoholysis ($k_{\text{aminolysis}} \ll k_{\text{alcoholysis}}$).²² Thus, the removal of the condensation product methanol is required to enhance the urea formation rate as well as the M_n of the polyurea.



Scheme 5. *N*-methylation of a diamine by a dicarbamate and polyurea formation with a dicarbamate and a diamine.

To investigate the effect of methanol removal on the polyurea formation, stoichiometric polymerizations of TOTDDA and IPDMC were first carried out under different argon flow rates (AFRs, 0.3, 0.8 and 1.2 L/min) in the absence of catalyst at 130 °C. The conversion of the amine groups into the monomethylated amines and the M_n of the polyureas were monitored by ¹H NMR and HFIP-SEC (Figure 4).

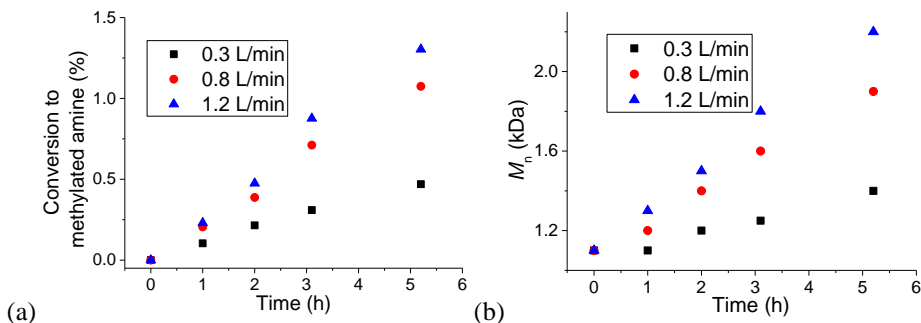


Figure 4. (a) ¹H NMR-determined conversion of the amine groups into methylated amines and (b) M_n of stoichiometric TOTDDA/IPDMC polymerization determined by HFIP-SEC under different argon flow rates at various reaction times.

A faster increase of the M_n and the urea concentration in the reaction mixtures was observed under higher AFRs, due to the more efficient methanol removal. However, the M_n of the mixture reached only 2 kDa after 5 hours, even under an AFR as high as 1.2 L/min, indicating a slow aminolysis of the carbamates in the absence of catalyst at 130 °C. Additionally, the absence of diamine signals from the GC-FID analysis of the blow outs from the argon flow indicates the monomer stoichiometry was not disrupted. Therefore, the reactions were also performed in the presence of TBD and KOMe as catalysts (see Chapter 2).

4.3.3.2 Addition of catalyst and removal of methanol

The results described in Chapter 2 showed that the alkali alkoxides are the most efficient catalysts for the carbamate aminolysis in the PPGdad2000/BU2 system. However, a faster M_n growth is observed for the TBD-catalyzed stoichiometric TOTDDA/IPDMC polymerization (5 mol% catalyst with regard to amines) compared with the KOMe-catalyzed one (Figure 5). This is attributed to the extremely low solubility of KOMe in this specific

TOTDDA/IPDMC combination (probably due to the hydrophobicity of the IPDMC), as indicated by the cloudy appearance of the reaction mixture.

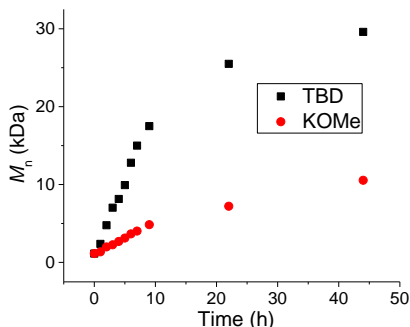


Figure 5. *M_n evolution during the TBD- and KOMe-catalyzed stoichiometric TOTDDA/IPDMC polymerizations at 130 °C under an AFR of 1.2 L/min.*

Additionally, a similar *N*-methylation rate of the TBD-catalyzed TOTDDA/IPDMC copolymerization compared to the catalyst-free reaction was observed, indicating that TBD does not catalyze the *N*-methylation reaction (Figure 6).

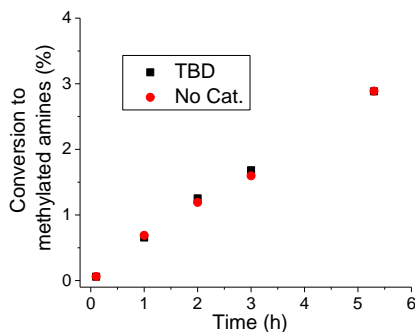


Figure 6. *¹H NMR-determined conversion of the amine groups into methylated amines for the stoichiometric TOTDDA/IPDMC polymerization system as a function of time with and without TBD at 130 °C in a closed set-up.*

Thus, TBD was employed as the catalyst in the stoichiometric polymerizations of TOTDDA and IPDMC. Again, different AFRs (0.3, 0.8, 1.2 L/min) were used to study the effect of the methanol removal efficiency on the *M_n* increase. Eight different moieties are distinguishable in the ¹H NMR spectrum, namely, the methyl group of the dimethylated amine (**a**), the methylene next to the primary amine end-group of the decarboxylated IPDMC (**b**), the methyl group of the monomethylated amine (**c**), the methylene adjacent to the monomethylated amine (**d**) or primary amine end-group (**e**), the methylene group in IPDMC (**f**), the methine group next to the carbamate (**g**) and the methylene next to the urea (**h**, Figure 7). The separate quantifications of **f** and **g** at 2.85 ppm is difficult, since these signals overlap. Therefore, the conversion of the carbamate next to the methine group into the corresponding amine was not separately monitored in this study.

The concentration of each moiety was calculated from the ratio of the integration of its NMR signal and the integration of the signals between 0.8 and 1.3 ppm, which results from the protons on the cyclic ring of the isophorone moieties, the concentration of which is constant ($C_{\text{isophorone}} = C_{0\text{-IPDMC}}/V = 0.015/0.00759 = 1.98 \text{ mol/L}$). The change of the concentration of these isophorone segments over time is plotted in Figure 8. At a low AFR of 0.3 L/min, the concentration of the mono- and dimethylated amines reaches 0.1 mol/L and 0.05 mol/L, accounting for 2.5% and 1.2% of the original amine end groups, respectively. Thus, approximately 5% of the carbamates had been converted into primary amines, leading to a significant deviation from the stoichiometric conditions and a low degree of polymerization. At AFRs of 0.8 and 1.2 L/min, the concentration of the monomethylated species dropped more than 20 times, while no dimethylated amine was detected. It should be noted that the intensities of the signal **a**, **b** and **c** are very low at high AFRs of 0.8 and 1.2 L/min, which could potentially lead to significant error during integration. Nevertheless, it is obvious that the intensities of these signals are much smaller at high AFRs compared to those at low AFRs of 0.3 L/min. Higher urea formation rates were observed at those AFRs (Figure 8a,c,e), as indicated by the faster increase of the urea concentration. The evolution of the urea groups is affected by both the carbamate aminolysis and the urea alcoholysis, the latter being proportional to the concentration of methanol (C_{MeOH}) in the mixture. At high AFRs, the low C_{MeOH} significantly limits this reaction and thereby enhancing the rate of urea production. The faster conversion of the carbamates into the urea groups at higher AFR also reduces the amine and the carbamate concentrations and therefore decreases the rate of *N*-methylation, as evidenced by the lower concentration of methylated species in the system. The concentration of amine generated by carbamates (**b**) reached a constant level after 20 hours, indicating the depletion of carbamates.

In order to assess the rate of urea formation, both contributions of the carbamate aminolysis and its reverse reaction, the urea alcoholysis, are taken into account, while the insignificant contribution from the methylation is neglected. Thus, the urea formation rate k_{urea} is calculated via the following equation:

$$k_{\text{urea}} = \frac{dC_{\text{urea}}}{dt} = \frac{k_{\text{aminolysis}}C_{\text{amine}}C_{\text{carbamate}} - k_{\text{alcoholysis}}C_{\text{urea}}C_{\text{MeOH}}}{C_{\text{amine}}C_{\text{carbamate}}} \\ = k_{\text{aminolysis}} - k_{\text{alcoholysis}} \frac{C_{\text{urea}}C_{\text{MeOH}}}{C_{\text{amine}}C_{\text{carbamate}}},$$

where C_{amine} , $C_{\text{carbamate}}$, C_{urea} and C_{MeOH} are the concentrations of amines, carbamates, urea groups and methanol in the mixture. $k_{\text{aminolysis}}$ and $k_{\text{alcoholysis}}$ are the rate constants of the carbamate aminolysis and the urea alcoholysis and k_{urea} represents the urea generation rate, which also includes the contribution of the urea alcoholysis (Table 2). k_{urea} at AFR of 0.3 L/min is only about 25 times higher than k_{Me} of the TOTDDA-IPDMC mixture at 130 °C in a closed set-up (Table 1). This results in a considerable degree of *N*-methylation during the polymerization (Figure 8b). k_{urea} increases by a factor of 10 and 30 at AFR of 0.8 L/min and 1.2 L/min, respectively. These k_{urea} values are about 150 (at an AFR of 0.8 L/min) and 500 times (at an AFR of 1.2 L/min) higher than k_{Me} . Thus, a faster removal of methanol successfully reduces the *N*-methylation, as indicated by the very low concentrations of methylated amines.

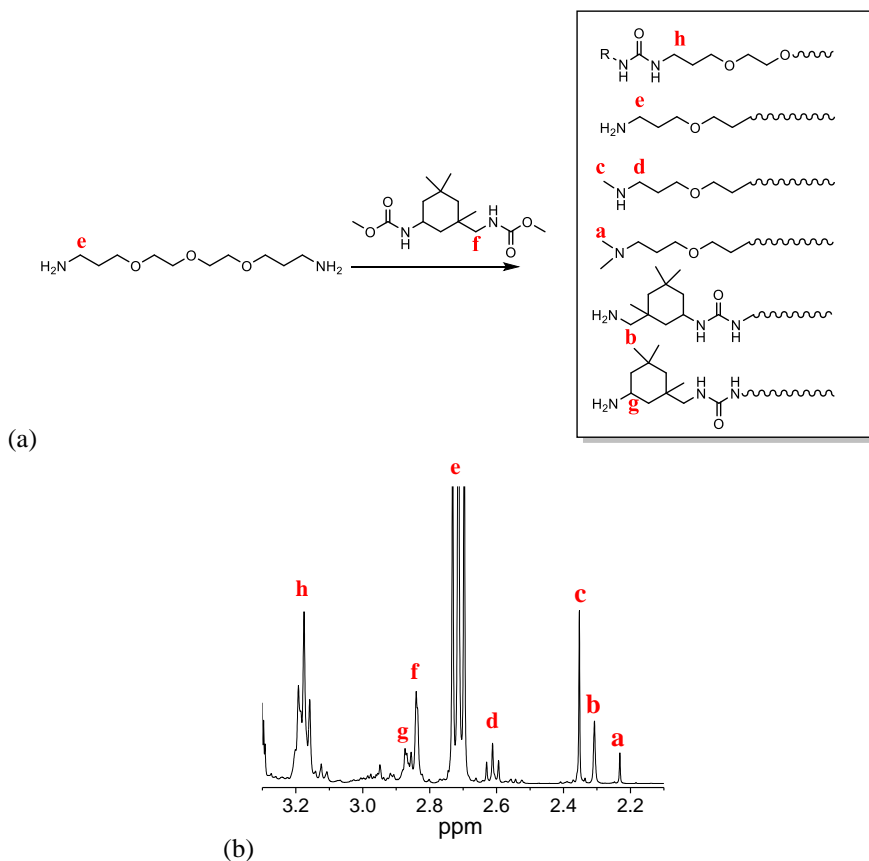


Figure 7. (a) Reaction products of the stoichiometric TOTDDA/IPDMC system.

(b) ^1H NMR spectrum of the stoichiometric TOTDDA/IPDMC mixture after 2 hours at 130 °C under an AFR of 0.3 L/min with TBD as catalyst.

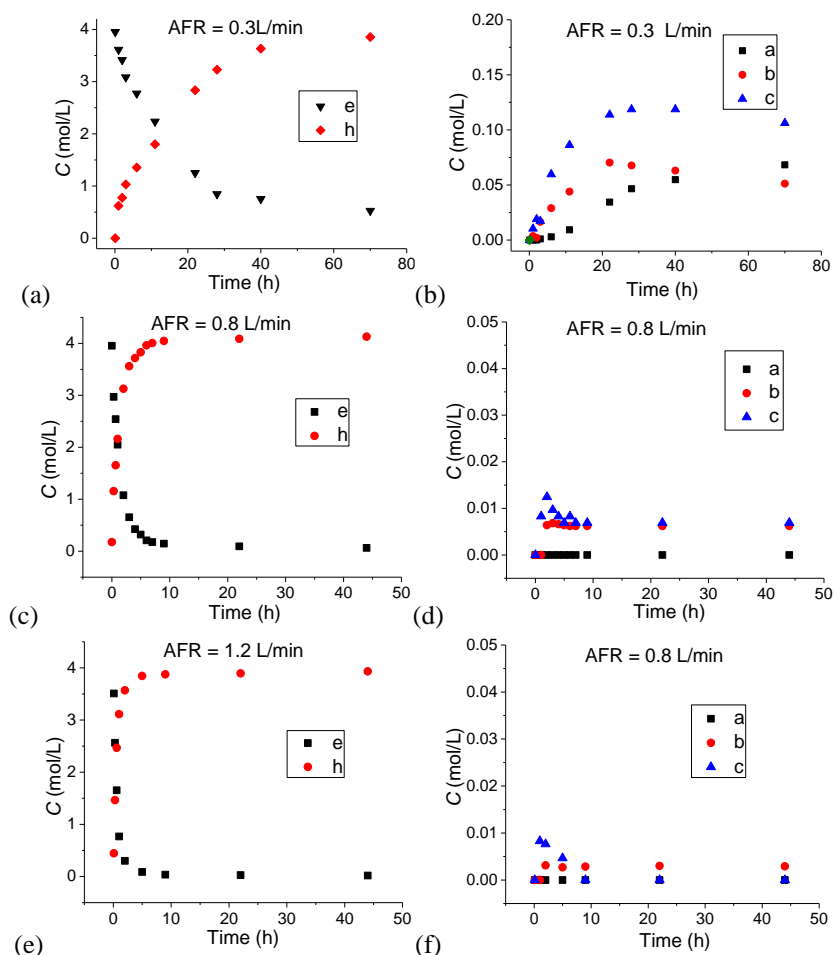


Figure 8. Concentration change of the various species in the TBD-catalyzed stoichiometric TOTDDA/IPDMC copolymerization at 130 °C with AFRs of (a) and (b) 0.3 L/min, (c) and (d) 0.8 L/min, (e) and (f) 1.2 L/min.

Table 2. Urea formation rate of stoichiometric TOTDDA/IPDMC mixtures at 130 °C under various AFRs.

AFR (L/min)	Urea formation rate k_{urea} (mmol/L.h)
0.3	23
0.8	229
1.2	647

The M_n growth of the stoichiometric TBD-catalyzed TOTDDA/IPDMC polymerizations at different AFRs measured by HFIP-SEC are plotted in Figure 9. A faster M_n growth was observed at higher AFRs, in agreement with the aminolysis rates listed in Table 2. After 44 hours, the M_n s of the polyureas prepared at AFRs of 1.2 L/min and 0.8 L/min are 32 kDa and

28 kDa, much higher than the M_n of the polyurea prepared at an AFR of 0.3 L/min (11 kDa). This indicates the significant impact of the AFR on the M_n of the polyureas.

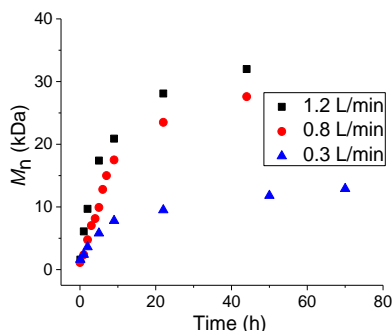


Figure 9. M_n growth of TBD-catalyzed stoichiometric TOTDDA/IPDMC stoichiometric polymerizations with different AFR at 130 °C as a function of time.

4.3.3.3 Alternative dicarbamates

Previous reports on amine-ester polymerizations described a limited *N*-alkylation with ethyl esters compared to methyl esters, which is caused by the higher *N*-alkylation activation energy due to the larger steric effect of the ethyl group.²⁰ Similarly, the *N*-alkylation rate was expected to be reduced during the polyurea formation by employing dicarbamates with bulkier alkyl substituents such as ethyl or *tert*-butyl.

Similar to the model reactions with IPDMC, a stoichiometric TOTDDA/IPDEC reaction was carried out at 130 °C in a closed set-up with 5 mol% TBD as catalyst. The concentration of the alkylated species in these reaction mixture proved to be considerably lower compared with that in the TOTDDA/IPDMC system (Figure 10) and the estimated *N*-alkylation rate constant is 18 times lower.

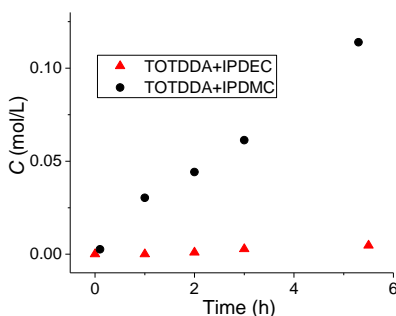


Figure 10. ^1H NMR determined concentration change of alkylated amine groups in the TOTDDA/IPDEC (black triangles) and TOTDDA/IPDMC (red spheres) stoichiometric mixtures at 130 °C as a function of time.

The copolymerization of TOTDDA and IPDEC catalyzed by TBD at 130 °C under an AFR of 1.2 L/min displays a slower M_n growth compared with the IPDMC/TOTDDA system under the same conditions, probably as a result of a lower aminolysis rate (Chapter 2).²² However, for the stoichiometric IPDMC/TOTDDA polymerization, the depletion of carbamates after

40 hours resulted in limited molecular weight growth, while continuous M_n growth was observed in the IPDEC/TOTDDA polymerization mixture (Figure 11). This indicates a low degree of alkylation in the IPDEC/TOTDDA system compared with IPDMC/TOTDDA, in agreement with the model reaction study in Figure 10.

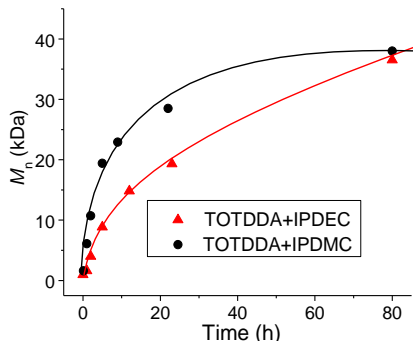


Figure 11. Evolution of M_n (HFIP-SEC) during the TBD-catalyzed stoichiometric IPDEC/TOTDDA and IPDMC/TOTDDA copolymerizations with an AFR of 1.2 L/min at 130 °C as a function of time.

No *N*-alkylation was detected in the stoichiometric mixture of isophorone di-*tert*-butyl carbamate (DiBoc-IPDC) and TOTDDA at 130 °C in a closed set-up, as the attack of the amine on the carbamate is hampered by the bulky *tert*-butyl group (Figure 12). The good solubility of alkali bases in the DiBoc-IPDC/TOTDDA mixture prompted us to perform polymerizations between DiBoc-IPDC and TOTDDA in the presence of KO*t*-Bu at 130 °C under an AFR of 1.2 L/min. Despite the much higher steric hindrance of the *t*-butyl group in DiBoc-IPDC compared to the methyl group in IPDMC, a high M_n of 120 kDa is reached with a stoichiometric ratio of TOTDDA and DiBoc-IPDC. This indicates the reaction mechanism of the Boc-carbamate aminolysis is different compared to that of methylcarbamate. A possible cause for such value is the formation of isocyanate intermediates, generated by the deprotonation of the amine of the urethane by the strong base and the dissociation of the bulky *tert*-butyl group.²⁴ These isocyanates then react with the abundant urea moieties to form biurets, thereby introducing branching in the polymer chains, as indicated by the high D_M of 3.1 during the stoichiometric polymerization (Scheme 6).

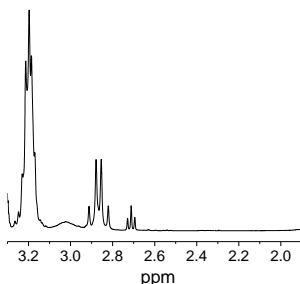
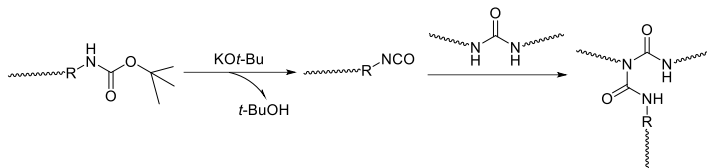


Figure 12. ^1H NMR spectrum of stoichiometric ratio of TOTDDA/Boc-IPDC polymerization at 130 °C under argon flow in the presence of KO*t*-Bu after 20 min.



Scheme 6. Possible biuret formation during the DiBoc-IPDC/TOTDDA polymerization.

4.3.4 M_n optimization

To optimize the M_n of the polyureas, and thereby enhancing their mechanical properties, TOTDDA and IPDMC of different ratios from 1.02:1 to 0.9:1 were copolymerized at 130 °C in the presence of TBD, first under an AFR of 1.2 L/min for 6 hours and then under vacuum for 12 hours to remove the residual methanol. The theoretical and experimental (HFIP-SEC) M_n values of the resulting PUs are presented in Figure 13. The theoretical M_n is calculated by the following equation:

$$M_n = \frac{1}{|1-r|} \times \frac{M_{\text{diamine}} + M_{\text{dicarbamate}}}{2},$$

Where r is the ratio between diamine and dicarbamate, M_{diamine} and $M_{\text{dicarbamate}}$ the molar mass of the diamines and dicarbamate segments in the polymer backbone.

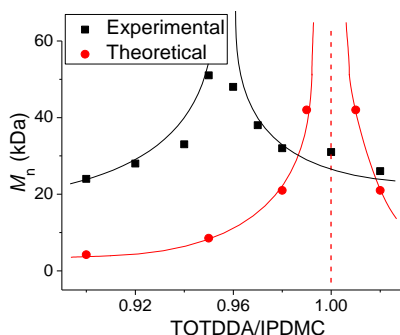


Figure 13. Theoretical and experimental (HFIP-SEC) M_n values of polyureas prepared from different TOTDDA/IPDMC ratios.

The highest M_n ($M_{n-\max}$) of 51 kDa was obtained for a TOTDDA/IPDMC ratio between 0.95/1 to 0.96/1, which deviates from the stoichiometric one due to the partial N -methylation of the end-groups. The use of an excess of IPDMC to reach $M_{n-\max}$ is a prerequisite, as the N -methylation of the primary amine end-groups generates amines upon CO_2 elimination while consuming carbamates (Scheme 4). The degree of N -methylation (D_{me}) is measured by the proportion of the methylated amines, which can be calculated via the following equation:

$$D_{me} = \left(\frac{1}{r_{\max}} - 1 \right) / 2,$$

where r_{\max} is the ratio of diamine/dicarbamate at $M_{n-\max}$. The estimated D_{me} for the TOTDDA/IPDMC polymerization at 130 °C is then between 0.021 and 0.026 according to Figure 10.

Similarly, the copolymerization of TOTDDA and IPDEC with ratios varying from 1.05/1 to

0.95/1 were carried out at the same condition with TOTDDA/IPDMC reactions. The theoretical and experimental M_n s of the obtained PUs are presented in Figure 14.

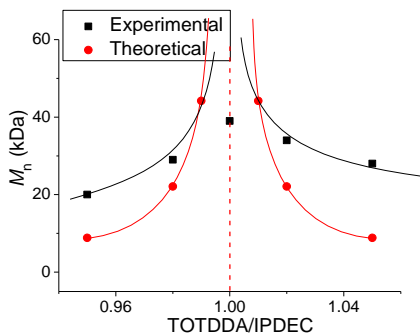


Figure 14. Theoretical and experimental (HFIP-SEC) M_n values of polyureas prepared from different TOTDDA/IPDEC ratios.

An M_{n-max} of 39 kDa is observed for a TOTDDA/IPDEC ratio of 1/1. This is explained by the very slow *N*-alkylation of TOTDDA by IPDEC, leading to little deviation from the stoichiometry. The reduced M_{n-max} achieved during this copolymerization compared to the TOTDDA/IPDMC system is attributed to the lower reactivity of the ethyl-carbamate moieties.

The M_n and the \bar{D}_M values of the PUs prepared from TOTDDA and DiBoc-IPDC with different ratios are presented in Table 3, along with the theoretical M_n s.

Table 3. Theoretical and experimental M_n of PUs prepared from different ratios of TOTDDA and DiBoc-IPDC.

TOTDDA /DiBoc-IPDC	M_n (kDa, HFIP-SEC)	\bar{D}_M	Theoretical M_n (kDa)
1.03	15	1.3	15
1.02	18	1.4	21
1.01	85	2.3	50
1.00	120	3.1	∞
0.98	Gel	N.A.	21

As mentioned in the previous section, the stoichiometric reaction of TOTDDA/Boc-IPDC results in a PU with a very high M_n of 120 kDa and a \bar{D}_M of 3.1, while the polymerization with an excess of Boc-IPDC with respect to TOTDDA leads to gelation. The \bar{D}_M of the polyurea decreases to 2.3 in the presence of a 1 mol% excess of TOTDDA with respect to Boc-IPDC. The M_n then decreases from 120 kDa to 85 kDa, which is most probably still sufficiently high for coating applications without crosslinking. When more than 2 mol% excess of TOTDDA is applied in the polymerization with Boc-IPDC, the M_n values of the polymers are in agreement with the theoretical ones and the \bar{D}_M values are relatively low. This is probably caused by the competition between the excess amines with urea moieties towards the isocyanate intermediates, leading to a limited biuret formation. Detailed investigations on the Boc-carbamate/amine system to prepare PUs are described in Chapter 5.

4.4 Conclusions

In this chapter, the *N*-alkylation of amine during carbamate aminolysis was investigated. Stoichiometric reactions of diamines, i.e. poly(propylene glycol) bis(2-aminopropyl ether) with a molecular weight of 230 Da (PPGda230), 4,7,10-trioxa-1,13-tridecanediamine (TOTDDA) and *N,N'*-dimethyl-1,6-hexanediamine (DMHD), and dicarbamates such as butane dicarbamate (BU2) and isophorone dimethylcarbamate (IPDMC) in a closed set-up at 130 °C showed a decreasing *N*-methylation rate with the order DMHD > TOTDDA > PPGda230. This was due to the higher nucleophilicity of the secondary amines in DMHD compared to the primary amines in TOTDDA, while the methyl groups in PPGda230 sterically hindered the nucleophilic attack of the amine towards the carbamate. Similar *N*-methylation rates were observed with IPDMC and BU2, indicating the limited steric effect of the dicarbamates on the *N*-alkylation. The activation energies of the diamine/IPDMC *N*-methylation reactions follow the order of PPGda230/IPDMC (109.9 kJ/mol) > TOTDDA/IPDMC (93.9 kJ/mol) > DMHD/IPDMC (73.1 kJ/mol). This is in accordance with the proposed mechanism, where an amine attacks the methyl group of a carbamate, resulting in a methyl amine and an unstable carbamic acid, which immediately forms a primary amine and a carbon dioxide molecule.

Both TBD catalyst and efficient removal of methanol were necessary to increase the urea formation rate. The latter raised by a factor of 30 when the argon flow rate increased from 0.3 to 1.2 L/min, while the concentration of the methylated species was reduced more than 50 times.

Optimizations of the M_n of the polyureas were carried out by copolymerization of different ratios of TOTDDA and IPDMC at 130 °C in the presence of TBD. The highest M_n of 51 kDa was obtained at a TOTDDA/IPDMC ratio of 0.95/1 - 0.96/1, indicating an *N*-methylation of 2.1-2.6 mol% of the amine end-groups. The *N*-alkylation rate measured for the TOTDDA/isophorone diethylcarbamate (IPDEC) mixture at 130 °C was 18 times lower than that for the TOTDDA/IPDMC system due to the larger steric effect of the ethyl group compared to the methyl one. The highest M_n of 39 kDa was achieved with a stoichiometric polymerization of TOTDDA and IPDEC. No *N*-alkylation was observed during the copolymerization of isophorone di-*tert*-butylcarbamate (DiBoc-IPDC) and TOTDDA due to the steric effect of the *t*-butyl group. The copolymerization of a slight excess of DiBoc-IPDC towards TOTDDA resulted in a crosslinked structure, probably due to the formation of isocyanates at 130 °C, thereby forming biuret that lead to branching/crosslinking in the polymer chains. The stoichiometric polymerization of TOTDDA and DiBoc-IPDC generates a polyurea with an M_n up to 120 kDa and \bar{D}_M of 3.1, indicating that DiBoc-IPDC is a promising monomer for the preparation of high M_n polyureas.

4.5 References

- (1) Salvatore, R. N.; Yoon, C. H.; Jung, K. W. *Tetrahedron* **2001**, *57*, 7785-7811.
- (2) Liu, X. -F; Ma, R.; Qiao, C.; Cao, H.; He, L. -N. *Chem. Eur. J.* **2016**, *22*, 16489-16493.
- (3) Fang, C.; Lu, C.; Liu, M.; Zhu, Y.; Fu, Y.; Lin, B. -L. *ACS Catalysis*. **2016**, *6*, 7876-7881.
- (4) Chen, W. -C.; Shen, J. -S.; Jurca, T.; Peng, C. -J.; Lin, Y. -H.; Wang, Y. -P.; Shih, W. -C.; Yap, G. P. A.; Ong, T. -G. *Angew. Chem. Int. Ed.* **2015**, *54*, 15207-15212.
- (5) Li, Y.; Sorribes, I.; Vicent, C.; Junge, K.; Beller, M. *Chem. Eur. J.* **2015**, *21*, 16759-16763.
- (6) Dang, T. T.; Ramalingam, B.; Seayad, A. M. *ACS Catalysis*. **2015**, *5*, 4082-4088.
- (7) Tsarev, V. N.; Caner, Y. M.; J.; Wang, Q.; Ushimaru, R.; Kudo, A.; Naka, H.; Saito, S. *Org. Lett.* **2015**, *17*, 2530-2533.
- (8) Yang, Z. -Z.; Yu, B.; Zhang, H.; Zhao, Y.; Ji, G.; Liu, Z. *RSC Adv.* **2015**, *5*, 19613-19619.
- (9) Li, Y.; Sorribes, I.; Vicent, C.; Junge, K.; Beller, M. *Angew. Chem. Int. Ed.* **2013**, *52*, 12156-12160.
- (10) Oku, T.; Arita, Y.; Tsuneki, H.; Ikariya, T. *J. Am. Chem. Soc.* **2004**, *126*, 7368-7377.
- (11) Jung, Y. J.; Bae, J. W.; Yoon, C. -O. M.; Yoo, B. W.; Yoon, C. M. *Synth. Commun.* **2006**, *31*, 3417-3421.
- (12) Barbry, D.; Torchy, S. *Synth. Commun.* **2006**, *26*, 3919-3922.
- (13) Bhattacharyya, S.; Chatterjee, A.; Duttachowdhury, S. K. *J. Chem. Soc., Perkin Trans.* **1994**, *1*, 1-2.
- (14) Calverley, M. J. *Synth. Commun.* **2006**, *13*, 601-609.
- (15) Borch, R. F.; Hassid, A. I. *J. Org. Chem.* **1972**, *37*, 1673-1674.
- (16) Das, S.; Bobbink, F. D.; Bulut, S.; Soudani, M.; Dyson, P. J. *Chem. Commun.* **2016**, *52*, 2497-2500.
- (17) Jiang, X.; Wang, C.; Wei, Y.; Xue, D.; Liu, Z.; Xiao, J. *Chem. Eur. J.* **2014**, *20*, 58-63.
- (18) Liu, J.; Xie, Y.; Ye, L.; Yan, H.; Tu, S. *Org. Prep. Proc. Int.* **2014**, *46*, 453-456.
- (19) Flannigan, J. E.; Mortimer, G. A. *J. Polym. Sci. Polym. Chem. Ed.*, **1978**, *16*, 1221-1228.
- (20) Hellmann, E.; Malluche, Jan.; Hellmann, G. P. *Polym. Eng. Sci.* **2007**, *10*, 1600-1609.
- (21) Dang, T. T.; Ramalingam, B.; Seayad, A. M. *ACS Catalysis*, 2015, *5*, 4082-4088.
- (22) Ma, S.; Liu, C.; Sablong, R. J.; Noordover, B. A. J.; Hensen, E. J. M.; van Benthem, R. A. T. M.; Koning, C. E. *ACS Catalysis*. **2016**, *6*, 6883-6891.
- (23) Hellmann, E.; Malluche, J.; Hellmann, G. P. *Polym. Eng. & Sci.* **2007**, *10*, 1589-1599.
- (24) Knolker, H. -J.; Braxmeier, T.; Schlechtingen, G. *Angew. Chem. Int. Ed.* **1995**, *34*, 2497-2500.
- (25) Clifford, P.; Green, N. J. B.; Pilling, M. J. *J. Phys. Chem.* **1984**, *88*, 4171-4176.
- (26) Calculated from $M_{\text{theoretical}} = 101 * M_{\text{TOTDDA}} + 100 * M_{\text{IPDMC}} - 200 * M_{\text{MeOH}} = 44420 \text{ g/mol}$.

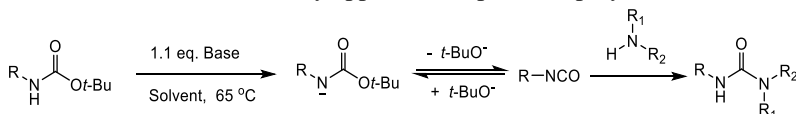
Chapter 5. Isocyanate-free polyurethane/urea coatings with di-*tert*-butyl carbamates as monomer

Summary

In this chapter, di-*tert*-butyl dicarbamates (DiBoc-carbamates) are investigated as dicarbamate monomers for diamine/dicarbamate polymerizations. *Tert*-butyl hexylcarbamate (Boc-HEX) and *N*-hexyl methylcarbamate (NHMC) were reacted with hexylamine (HEX) to study the mechanism of the *tert*-butyl-carbamate (Boc-carbamate)/amine reaction. Potassium *tert*-butoxide (KO*t*-Bu) was the most efficient catalyst for the Boc-HEX/HEX reaction compared to the other investigated catalysts potassium methoxide (KOMe), 4-dimethylaminopyridine (DMAP) and 1,5,7-triazabicyclo[4,4,0]dec-5-ene (TBD). High molecular weight polyureas (PUs) were prepared from stoichiometric polymerizations of short chain diamines with isophorone di-*tert*-butyl dicarbamate (DiBoc-IPDC), while gelation was observed when an excess of DiBoc-IPDC was used with respect to the diamine. Polyurethanes (PURs) were synthesized via the polymerization of diols with either DiBoc-IPDC or isophorone dimethylcarbamate (IPDMC). The PURs prepared from the DiBoc-IPDC had a higher number average molecular weight (M_n) compared to those based on IPDMC, while the reaction of an excess of DiBoc-IPDC with a diol led to gelation. Stable dispersions were obtained from PUs and PURs with 3,3'-diamino-*N*-methyldipropylamine (DMDPA) as internal dispersing agent (IDA). PU coatings with satisfactory mechanical properties and solvent resistance were produced with high M_n PUs with DMDPA as IDA, while polyurethane urea (PUU) coatings were synthesized with diols, DiBoc-IPDC as dicarbamate and DMDPA. These PUU coatings were either too soft or too brittle due to the low molecular weights of the parent resins. Anionically stabilized PU dispersions were prepared by polymerizing diamines with N^2,N^6 -bis(*tert*-butoxycarbonyl) lysine (DiBoc-lysine). However, these reactions generated PUs with low molecular weight and thus resulted in poor coating properties compared to the PU coatings with DMDPA as IDA.

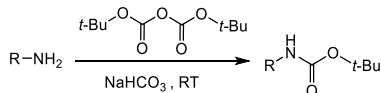
5.1 Introduction

Dicarbamates can potentially be used in the polyurethane (PUR) or polyurea (PU) synthesis as alternatives to the highly toxic diisocyanates.¹⁻⁴ However, conventional dicarbamates such as dimethyl carbamate or dihydroxyl carbamate are considerably less reactive towards diamines or diols compared to diisocyanates, thereby limiting their practical applications.⁵⁻⁸ Therefore, more reactive monomers must be employed for the preparation of polyurethanes and polyureas via isocyanate-free routes. Section 4.3.3.3 in Chapter 4 described the polymerization of isophorone di-*tert*-butyl carbamate (DiBoc-IPDC) and a diamine to a polyurea with high number average molecular weight (M_n). It was proposed that under strong basic conditions, *tert*-butyl carbamate (Boc-carbamate) transforms into an isocyanate intermediate, which immediately reacts with an amine to form a urea moiety. Similar reactions were described by Gastaldi et al., who mixed a series of amines with Boc-arylcabamates in the presence of strong bases like *n*-BuLi or NaH, to generate the corresponding ureas (Scheme 1).⁹ However, such reaction demands a large excess of base to form isocyanates and therefore, is hardly applicable in practical polymerizations.



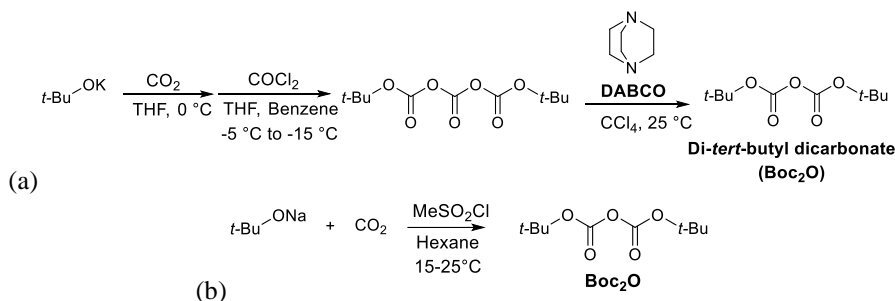
Scheme 1. Mechanisms of urea formation with Boc-carbamate and amine.⁹

The *tert*-butyloxycarbonyl (Boc-carbamate) group is a protective group for amines frequently used in organic chemistry, in particular for protecting the amines of amino acids. The protection proceeds in high yield by addition of di-*tert*-butyl dicarbonate (Boc₂O) in an aqueous solution of amine in the presence of a weak base, such as sodium bicarbonate (Scheme 2).¹⁰ Other strategies of generating Boc-carbamate from either alkyl- or arylamines were also reported, with molecular iodine, sulfamic acid or DMAP as catalysts.¹¹⁻¹³



Scheme 2. Boc-protection of amine using Boc₂O and sodium bicarbonate.¹⁰

Boc₂O is commonly prepared from phosgene, *tert*-butanol and carbon dioxide, with 1,4-diazabicyclo [2.2.2]octane (DABCO) as catalyst (Scheme 3a).¹⁴ Recently, a phosgene-free route to Boc₂O has been developed and adopted by European and Japanese manufacturers, involving the reaction between sodium *tert*-butoxide and carbon dioxide in the presence of *p*-toluene-sulfonic or methanesulfonic acid (Scheme 3b).¹⁵ Such phosgene-free pathway is desired to fulfill the “green strategy” for PU(R) synthesis.



Scheme 3. (a) Conventional and (b) phosgene-free routes to Boc_2O .^{14,15}

Thus, in the present chapter, the Boc-carbamate aminolysis and alcoholysis as polymerization tools for polyurethane/urea synthesis are investigated in more detail. First, the catalysts for such reaction are screened via a model reaction with *tert*-Butyl hexylcarbamate (Boc-HEX) and hexylamine, followed by a mechanistic study of the model reaction using ^1H and ^{13}C NMR. Then, polyureas (PUs) with high molecular weights are synthesized via Boc-dicarbamate/diamine polymerizations. Stable cationic and anionic PU(R) dispersions are produced by copolymerization of diamines, DiBoc-IPDC and IDAs including 3,3'-diamino-*N*-methyldipropylamine (DMDPA) and *N*²,*N*⁶-bis(*tert*-butoxycarbonyl)lysine (DiBoc-lysine). The mechanical properties and solvent resistance of the coatings prepared from these dispersions are evaluated.

5.2 Experimental section

5.2.1 Materials

All reagents were commercially available unless specified otherwise. Sodium bicarbonate (NaHCO_3 , 99%), di-*tert*-butyl dicarbonate (Boc_2O , 99%), L-lysine (98%), poly(propylene glycol) bis(2-aminopropyl ether) with average M_n of 400 and 2000 Da (PPGda400 and PPGda2000), dimethylcarbonate (DMC, 99%), trimethylamine (TEA, 99.5%), 5-amino-1,3,3-trimethylcyclohexanemethylamine (IPDA, mixture of *cis* and *trans*, 99%), 1,5,7-triazabicyclo[4,4,0]dec-5-ene (TBD, 98%), potassium methoxide (KOMe, 95%), potassium *tert*-butoxide ($\text{KO}t\text{-Bu}$, 98%), acetic acid (AA, 99.7%), citric acid (CA, 99.5%), ethylenediaminetetraacetic acid (EDTA, 98%), succinic acid (SA, 99%), hexylamine (HEX, 99%), dimethylacetamide (DMAc, anhydrous), *N*-methylpyrrolidine (NMP, 99%), dimethylformamide (DMF, anhydrous), poly(propylene glycol) with average M_n of 425 and 2000 Da (PPG425 and PPG2000), poly(tetrahydrofuran) with an M_n of 650 Da (pTHF650), triethylene glycol (TEG, 99%), 3,3'-diamino-*N*-methyldipropylamine (DMDPA, 96%), 4,7,10-trioxa-1,13-tridecanediamine (TOTDDA, 98%) and 3-butoxypropylamine (BPA, 99%) were purchased from Sigma Aldrich. A diamine functional pTHF with an average M_n of 1000 Da (pTHFda1000) was purchased from Huntsman. Deuterated solvents were purchased from Buchem BV. All other solvents were purchased from Biosolve. All the chemicals were used without further purification.

5.2.2 Reactions and synthesis

Model reaction of carbamate and hexylamine (HEX)

In a typical experiment, 0.25 mmol of KOMe and 2.5 mmol of HEX were introduced into a 20 mL crimp-cap vial. 0.1 g of toluene was added as the internal standard for GC measurements, followed by the injection of a solution of 25 mmol of carbamate in 4 g of anhydrous DMAc into the vial. The time of injection of the dicarbamate solution was considered as the $t = 0$ of the reaction. The conversion of HEX was monitored by GC-FID.

Synthesis of isophorone dimethylcarbamate (IPDMC)¹⁶

Dimethyl carbonate (DMC, 7 mol) and isophorone diamine (IPDA, 1 mol) were added in 10 min into a 1000 mL three-necked round flask with an argon inlet. Potassium methoxide (1 mol) was then added to the above mixture as the catalyst. The reaction was performed at room temperature for 4 hours, and then at 60 °C for 6 to 8 hours. The mixture was then cooled and poured into an excess of chloroform and washed with brine 3 times. The organic layer was dried with anhydrous sodium sulfate and evaporated to obtain the light yellow solid (208 g, 73%).

¹H NMR (400 MHz, CDCl₃, δ in ppm): 4.75 (d, 1H, -NHCH₂), 4.6 (s, 1H, cy-NHCH), 3.8-3.6 (s, 1H, cy-CHNH, 6H, -OCH₃), 3.3, 2.9 (d, 2H, -CH₂NH), 1.7-0.7 (15H, cy-H). ¹³C{¹H} NMR (100.6 MHz, CDCl₃, δ in ppm): 157.4, 156.3 (C=O), 54.8, 52.1, 51.8, 46.9, 46.3, 44.6, 42.5, 41.8, 36.3, 34.9, 31.7, 29.6, 27.5, and 23.1.

Synthesis of isophorone di-*tert*-butyl dicarbamate (DiBoc-IPDC)

In a 500 mL flask, 68 g (0.4 mol) of IPDA, 192 g (0.88 mol) of Boc₂O and 150 mL water were stirred at room temperature. After 12 hours, the mixture was extracted by 200 mL of chloroform and washed with water (3×200 mL). The organic layer was then dried over anhydrous sodium sulfate and evaporated to dryness to obtain a white powder (135 g, 91%).

¹H NMR (400 MHz, CDCl₃, δ in ppm): 4.6 (d, 1H, -NHCH₂), 4.3 (s, 1H, cy-NHCH), 3.7 (s, 1H, cy-CHNH), 3.2, 2.9 (d, 2H, -CH₂NH), 1.7-0.7 (15H, cy-H, 18H, CCH₃). ¹³C{¹H} NMR (100.6 MHz, MeOD, δ in ppm): 157.4, 156.5 (C=O), 78.6 (C(CH₃)₃), 54.9, 51.8, 46.9, 45.8, 43.7, 41.7, 41.4, 36.3, 34.3, 31.3, 28.8, 26.7, and 26.2 (cy-C), 27.4 (C(CH₃)₃).

(Co)Polymerization of dicarbamates and diamines/diols

In a typical experiment with a 1/1 ratio between the monomers, 2.405 g of DiBoc-IPDC (6.5 mmol) and 1.432 g of TOTDDA (6.5 mmol) were added into a 50 mL crimp-cap vial and mixed under argon flow at 130 °C until the mixture became homogeneous, followed by the addition of 0.0437 g of KO^{*t*}-Bu (0.39 mmol). After the 12 hours, the pressure in the flask was gradually reduced to 5 mmHg and maintained at this value for another 6 hours before quenching the reaction with water. Finally, the precipitated polymer was washed with water 3 times and dried in a vacuum oven for 12 hours to obtain a light yellowish polymer (3.2 g, 84%).

Synthesis of *N*-hexyl methylcarbamate (NHMC)¹⁷

In a 100 mL flask, DMC (90 g, 1 mol), HEX (20.2 g, 0.2 mol), and TBD (0.69 g, 5 mmol) were stirred for 12 hours at room temperature. The reaction mixture was then concentrated by using a rotary evaporator and washed 3 times with a saturated aqueous NaCl solution. The

organic phase was then dried with anhydrous sodium sulfate to obtain NHMC as a colorless oil (28.6 g, 90%).

^1H NMR (400 MHz, CDCl_3 , δ in ppm): 4.95 (s, broad, 1H, NH), 3.65 (s, 3H, OCH_3), 3.16 (m, 2H; NHCH_2), 1.49 (m, 2H; NHCH_2CH_2), 1.29 (m, 6H; $\text{CH}_3\text{CH}_2\text{CH}_2\text{CH}_2$), 0.89 (m, 2H; CH_2CH_3); $^{13}\text{C}\{^1\text{H}\}$ NMR (100.6 MHz, CDCl_3 , δ in ppm): 157.2 ($\text{C}=\text{O}$), 51.9 (OCH_3); 40.9 (NHCH_2); 31.5 ($\text{CH}_3\text{CH}_2\text{CH}_2$); 29.9 (NHCH_2CH_2); 26.2 ($\text{NHCH}_2\text{CH}_2\text{CH}_2$); 22.5 (CH_3CH_2); 14.0 (CH_2CH_3).

Synthesis of *tert*-butyl hexylcarbamate (Boc-HEX)

In a 500 mL flask, 20.2 g (0.4 mol) of HEX, 44 g (0.2 mol) of Boc_2O and 150 mL water were stirred at room temperature. After 12 hours, the mixture was dissolved in 200 mL chloroform and washed with water (3×200 mL). The organic layer was then dried over anhydrous sodium sulfate and evaporated to obtain the product as a colorless liquid (135 g, 91%).

^1H NMR (400 MHz, MeOD, δ in ppm): 0.87 (m, broad, 3H, $-\text{CH}_2\text{CH}_3$), 1.52-1.15 (broad, 18H, $-\text{OCCH}_3$), 3.01 (t, 2H, CHNH); $^{13}\text{C}\{^1\text{H}\}$ NMR (100.6 MHz, MeOD, δ in ppm): 157.8 (CO), 78.4 (OCCH_3); 40.1 (NHCH_2); 27.6 (NHCH_2CH_2), 22.3(CH_2CH_3), 13.2 (CH_2CH_3), 31.3 ($\text{CH}_2\text{CH}_2\text{CH}_3$).

Synthesis of N^2,N^6 -bis(*tert*-butoxycarbonyl)lysine (DiBoc-lysine)¹⁸

In a 500 mL flask, L-lysine (50 mmol) was dissolved in a 1/1 mixture of THF/ H_2O (200 mL). NaHCO_3 (250 mmol) and Boc_2O (100 mmol) were added consecutively into the solution at 0 °C. After 30 min, the solution was heated to room temperature and stirred overnight. The solution was then extracted with Et_2O (3×200 mL) and 20 wt% aqueous solution of citric acid was added into the aqueous layer until pH = 4-5. Then the solution was extracted with CH_2Cl_2 , dried with NaSO_4 , and the solvent was evaporated under reduced pressure to give N^2,N^6 -bis(*tert*-butoxycarbonyl)lysine (DiBoc-lysine) as a light yellowish solid (16.8g, 96%).

^1H NMR (400 MHz, MeOD, δ in ppm): 1.29,1.56 (m, broad, 20H, $-\text{OCCH}_3$, $-\text{CHCH}_2\text{CH}_2$), 1.65 (broad, 2H, $-\text{NHCH}_2\text{CH}_2$), 1.76 (broad, 2H, $-\text{CHCH}_2$), 3.03 (t, 2H, $-\text{NHCH}_2$), 4.05 (broad, 1H, $-\text{NHCH}$); $^{13}\text{C}\{^1\text{H}\}$ NMR (100.6 MHz, MeOD, δ in ppm): 174.9 (COOH), 156.5-157.2 (NHCO), 78.4-79.1 (OCCH_3), 53.5 (NHCH), 40.1 (NHCH_2), 31.1 (NHCH), 29.6 (NHCH_2CH_2), 27.3(OCCH_3), 22.8 (CHCH_2CH_2).

Synthesis of water-borne PUDs with Boc-lysine as IDA

In a crimp cap vial of 50 mL equipped with an argon inlet and a stirring bar, 0.5 g (1.44 mmol) of Boc-lysine was first dissolved in 1 g of anhydrous solvent (DMAc, NMP or DMF). 0.318 g (1.44 mmol) of TOTDDA was then added into the flask together with 5.0 mg (72 μmol) of KOMe or 8.1 mg (72 μmol) of KO t -Bu as catalyst. The polymerization took place under argon flow at 130 °C. After 8 hours, the pressure in the flask was reduced to 5 mmHg and maintained at this value for another 6 hours, before quenching in diethyl ether. Finally, the precipitated polymer was three times washed with diethyl ether and dried in a vacuum oven for 12 hours to obtain the product (65-75%).

Synthesis of polyurea/polyurethane with DMDPA as IDA

Copolymerization reactions were performed using DiBoc-IPDC, diamines/diols and an internal dispersing agent (IDA). In a specific experiment, 10 g (5 mmol) of PPGda2000 and

0.145 g (1 mmol) of DMDPA were added to a 50 mL crimp cap flask together with 1.85 g (6 mmol) of DiBoc-IPDC. The reactor was flushed with argon and the reaction mixture was heated to 130 °C prior to the addition of 40 mg (0.36 mmol) of KO*t*-Bu to the reactor as catalyst. After 12 hours under argon flow at 130 °C, the reaction mixture was poured into an excess of water and washed three times with water before drying in a vacuum oven to obtain the product as a yellow solid (8.9 g, 74%).

Preparation of aqueous dispersions with Boc-lysine as IDA

In a 20 mL crimp-cap vial equipped with a stirring bar, 0.5 gram of PU was dissolved in 4.5 gram of deionized water and stirred for 30 min to obtain a cloudy PU dispersion.

5.2.3 Characterizations

Differential scanning calorimetry (DSC)

DSC measurements were performed on a TA instruments DSC Q100 calorimeter. Samples were first equilibrated at 25 °C, then heated from -80 °C to 200 °C at a heating rate of 10 °C /min followed by an isothermal step for 5 min. A cooling cycle to -80 °C at a rate of 10 °C /min was performed prior to a second heating run to 200 °C at the aforementioned heating rate. The T_g was determined from the second heating run. TA Universal Analysis 2000 software was used for data analysis.

Nuclear magnetic resonance (NMR)

$^{13}\text{C}\{^1\text{H}\}$ NMR (100.62 MHz) and ^1H NMR (400 MHz) spectra were recorded using a Varian Mercury Vx spectrometer at 25 °C. The samples were prepared by dissolving 20 mg of sample in 1 mL MeOD- d_4 as a solvent.

Dynamic light scattering (DLS) and ζ -potential

DLS and ζ -potential measurements were performed on a Malvern ZetaSizer Nano ZS at 25 °C to determine the dispersion characteristics (polyurethane refractive index: 1.59). The average particle size and the particle size distribution of dispersions containing 0.1 wt% solids were determined according to ISO 13321 (1996). The ζ -potential was calculated from the electrophoretic mobility (μ) using the Smoluchowski relationship $\zeta = \eta\mu/\epsilon$ with $\kappa a \gg 1$ and η is the solution viscosity, ϵ the dielectric constant of the medium, κ the Debye-Hückel parameter and a the particle radius. Data acquisition was performed using the ZetaSizer Nano Software.

Gas Chromatography with Flame Ionization Detector (GC-FID)

GC-FID measurements were performed to analyze the kinetic results. A Varian CP-3800 equipped with an FID was used and samples were prepared by quenching 0.05 mL of the reaction mixture with 1 mL of methanol.

The conversion of HEX was monitored by GC-FID measurements with toluene as internal standard. The conversions of the HEX in the model reactions were determined as follows: the GC-FID peak areas of HEX and toluene at time t are denoted as $A_{\text{HEX-}t}$ and C , respectively. The initial concentration ratio between HEX and toluene is designated by I_0 where

$$I_0 = A_{\text{HEX-}0} / A_{\text{toluene-}0}$$

The ratio between HEX and toluene after x minute is designated by I_x where

$$I_x = A_{\text{HEX-}x} / A_{\text{toluene-}x}$$

The concentration of HEX at time x is then

$$C_x = I_x / I_0$$

The conversion of HEX at time x is then

$$p_x = (1 - C_x / C_0) \times 100\%$$

The same calculation method holds for determining the conversion of Boc-HEX.

Attenuated Total Reflection Fourier Transform Infrared (ATR-FTIR) Spectroscopy

ATR-FTIR was performed using a Bio-Rad Excalibur FTS3000MX infrared spectrometer (10 scans per spectrum, spectral resolution of 4 cm^{-1}) with an ATR diamond unit (Golden Gate). The measurement was performed by applying the sample onto the ATR diamond. The spectra were recorded between 4000 and 650 cm^{-1} .

Size Exclusion Chromatography (SEC)

SEC in 1,1,1,3,3,3-hexafluoro-2-propanol (HFIP) was performed at 40°C on a system equipped with a Waters 1515 Isocratic HPLC pump, a Waters 2414 refractive index detector (35°C), a Waters 2707 autosampler, and a PSS PFG guard column followed by 2 PFG-linear-XL ($7 \mu\text{m}$, $8 \times 300 \text{ mm}$) columns in series. HFIP with potassium trifluoroacetate (3 g/L) was used as eluent at a flow rate of 0.8 mL/min . The molecular weights were calculated with respect to poly(methyl methacrylate) standards ($M_p = 580 \text{ Da}$ up to $M_p = 7.1 \times 10^6 \text{ Da}$).

Potentiometric Titration

Potentiometric titrations were performed using a Metrohm Titrino 785 DMP automatic titration device fitted with an Ag electrode. The samples were dissolved in CH_3OH and the $-\text{NH}_x$ groups ($x = 0-2$) were titrated with a normalized 0.1 mol/L HCl isopropanol solution. Blank measurements were carried out using the same amount of CH_3OH .

The molar mass was defined according to the following equation:

$$M_n = \frac{2m_{\text{sample}}}{(V_{\text{sample}} - V_{\text{blank}}) \times C_{\text{HCl}}}$$

The $-\text{NH}_x$ content was defined according to the following equation:

$$N_{\text{NH}_x} = \frac{(V_{\text{sample1}} - V_{\text{blank1}}) \times C_{\text{HCl}}}{m_{\text{sample}}}$$

Where V_{blank} is the volume of HCl solution in mL needed for the blank, (average of two measurements), V_{sample} the volume of HCl solution in mL consumed by the sample, C_{HCl} the HCl concentration in isopropanol in mol/L , N_{NH_x} ($x=0-2$) the molar amount of $-\text{NH}_x$ groups in 1 gram of polymer (mol/g) and m_{sample} the sample weight in gram.

Evaluation of coatings

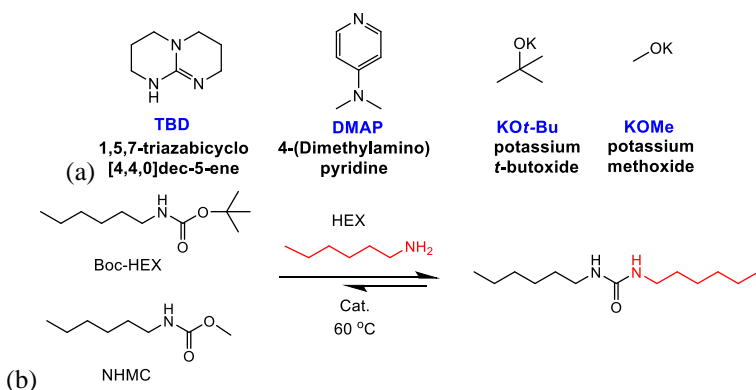
The coating performances were evaluated at room temperature by means of an acetone double rub test, a water resistance test, a reverse impact test and a pencil hardness test. In the acetone double rub test, the sample was rubbed back and forth with a cloth drenched in acetone. If no visual damage was observed after more than 150 rubs (75 double rubs), the acetone resistance of the coating was marked as good. In the water resistance test, the coating was immersed under water for 10 minutes. If no swelling was observed, the water resistance

of the coating was marked as good. The reverse impact test was performed by dropping a 1 kg ball on the backside of a coated panel from a 100 cm height, as described in ASTM D2794. The pencil hardness test (ASTM D3363) was performed via pushing pencils with varying hardness value into the sample and the coating hardness was identified visually by the trace generated. The scale of pencil hardness ranges from 9H, the hardest scale, to 9B, the softest scale.

5.3 Results and discussion

5.3.1 Model reaction of dicarbamates and HEX

Chapter 4 showed that the copolymerization of isophorone di-*tert*-butyl dicarbamate (DiBoc-IPDC) and 4,7,10-trioxa-1,13-tridecanediamine (TOTDDA) results in polyureas (PUs) with high M_n s. However, the high D_M values of these PUs indicate that the mechanism of the reaction between Boc-carbamate/amine and methylcarbamate/amine does not strictly follow that of a linear step growth polymerization. Thus, model reactions were carried out with hexylamine (HEX) and *tert*-butyl hexylcarbamate (Boc-HEX) or *N*-hexyl methylcarbamate (NHMC) to compare the aminolysis rate of Boc- and methylcarbamates. Chapter 2 revealed a limited conversion of the substrates during a stoichiometric reaction of amine and NHMC, indicating that the equilibrium of the carbamate aminolysis favors the left side, i.e. the aminolysis rate is much lower than the urea alcoholysis.¹⁷ Hence, to accurately monitor the consumption of HEX in the model reaction, an excess of carbamate (20/1 ratio) was used with respect to the amine, in the presence of 1 mol% of various catalysts, including alkali bases like KOMe and KO*t*-Bu and organic bases such as TBD and DMAP, the latter being a catalyst for the reaction of arylamines and Boc₂O to arylisocyanates (Scheme 4).¹⁹ The conversion of HEX was monitored by GC-FID (Figure 1).



Scheme 4 (a) Structures of catalyst candidates; (b) Model reaction of Boc-HEX and HEX as substrates (10/1 molar ratio) at 60°C.

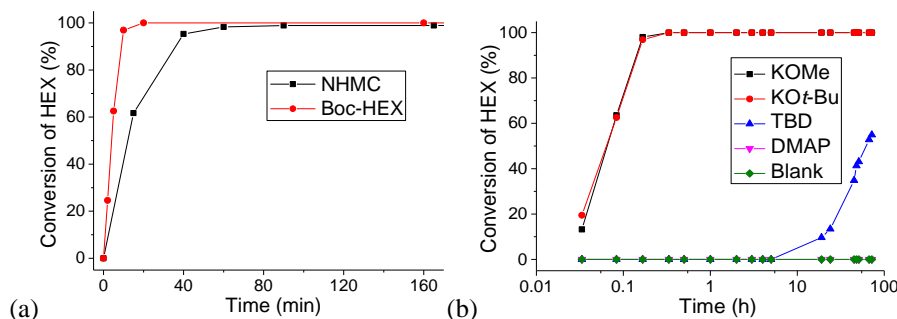
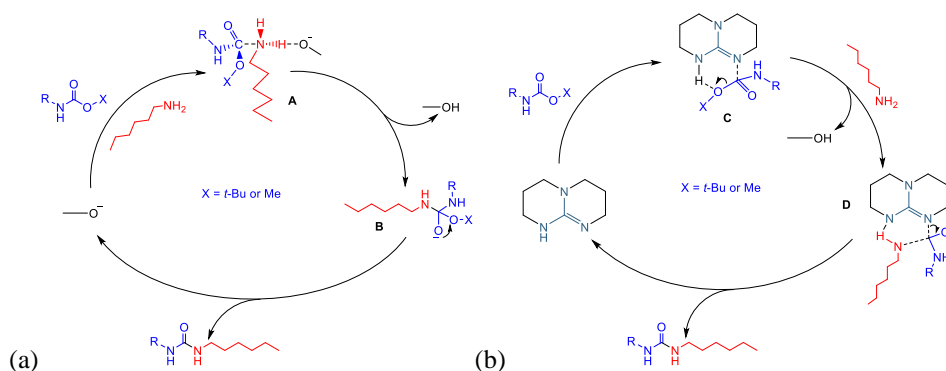


Figure 1. Conversion of HEX as a function of time in model reactions with (a) NHMC or Boc-HEX as carbamate and KOMe as catalyst and (b) Boc-HEX as carbamate in the presence of different catalysts.

The plots in Figure 1a reveal a faster reaction of HEX with Boc-HEX compared to NHMC. This is contradictory with the mechanism of alkali base-catalyzed carbamate aminolysis proposed in Chapter 2 (Scheme 5a, also see Chapter 2). According to such mechanism, the presence of the bulky *tert*-butoxide group in Boc-HEX should enhance the energy level of the transition state **A** compared to the methoxide group of NHMC, thereby reducing the reaction rate. Figure 1b displays a similar catalytic activity of KOMe and KOt-Bu towards the aminolysis of the Boc-carbamate, both much higher than that of TBD, while DMAP is inactive. The activity of TBD in Boc-HEX/HEX model reaction is higher than that reported in Chapter 2 for NHMC/HEX reaction (see Figure 5a in Chapter 2). This is again in contract with the mechanism of TBD-catalyzed carbamate aminolysis proposed in Chapter 2 (Scheme 5b, also see Chapter 2), where the *tert*-butoxide group could lead to higher energy level of the transition state **C**, and consequently slower aminolysis reaction.¹⁷ These results suggest a different mechanism of the Boc-carbamate/amine reaction compared to that proposed in Chapter 2 for the methylcarbamate aminolysis.



Scheme 5. Proposed mechanism for (a) KOMe- and (b) TBD-catalyzed aminolysis (see Chapter 2).

The conversions of Boc-HEX in the Boc-HEX/HEX model reaction with a molar ratio of 1/20 with KOt-Bu and KOMe as catalysts were determined at different temperatures (Figure 2). Above 70 °C, both KOMe- and KOt-Bu-catalyzed reactions achieve full conversion of

Boc-HEX within 30 min. This indicates that the reverse reaction is significantly slower and therefore can be neglected during the calculation of the aminolysis rate.

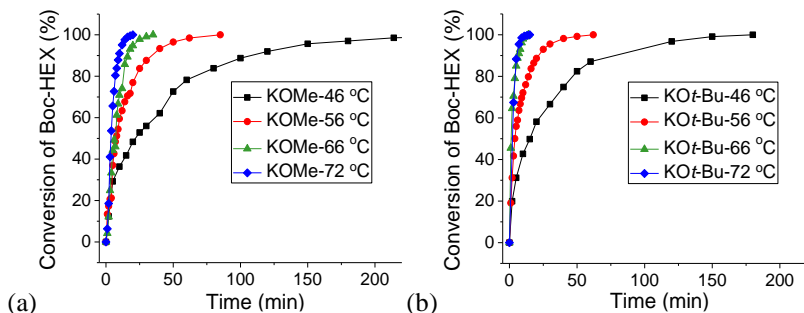


Figure 2. Conversion of Boc-HEX in model reaction with 1/20 ratio of carbamate to amine, catalyzed by (a) KOMe and (b) KOt-Bu at different (measured) temperatures.

Similar catalytic activities were reported for KOMe- and KOt-Bu-catalyzed NHMC/HEX model reactions (see Section 2.3.4 in Chapter 2) due to the deprotonation of methanol by $^-\text{Ot-Bu}$, leading to the same active species (^-OMe) for both reactions. However, a faster conversion of Boc-HEX was observed for the KOt-Bu-catalyzed reaction compared to KOMe-catalyzed one. For example after 40 minutes at 66 °C, the latter reached full conversion of the substrate, which is achieved within 20 minutes for the former. This is caused by a much higher basicity of $^-\text{Ot-Bu}$ ($\text{pK}_a=19$) in the KOt-Bu-catalyzed Boc-carbamate aminolysis compared to the ^-OMe ($\text{pK}_a=15.5$), which is the main catalytic species in the KOMe-catalyzed reaction, as the methoxide anion could hardly protonate the reaction byproduct HOt-Bu into $^-\text{Ot-Bu}$.

If the Boc-carbamate aminolysis reaction is of second order, their reaction rates are determined by the following equation:

$$r = \frac{dC}{dt} = -k(C + 19C_0)C,$$

where k is the reaction rate constant, C the concentration of Boc-HEX at time t and C_0 the starting concentration of Boc-HEX. Through integration, the equation can be expressed as:

$$kt + X = \frac{1}{19C_0} \ln \left| \frac{C + 19C_0}{C} \right|,$$

where X is a constant. A linear relation was observed for the $\ln((C+19C_0)/C)/19C_0$ vs. t plots, indicating that the reaction is indeed of second order (Figure 3a). The reaction rate constants for each reaction at different temperatures can thus be determined from the slope of such plots, while the corresponding activation energy E_a and pre-exponential factor A can be calculated via the corresponding Arrhenius plots (Figure 3c,d). The E_a and $\ln A$ of the NHMC/HEX reaction catalyzed by KOMe and the Boc-HEX/HEX reactions catalyzed by KOMe and KOt-Bu are listed in Table 1. Similar linear relations were also observed in model reactions of 1/20 ratio of NHMC/HEX catalyzed by KOMe (Figure 3b, also see Chapter 2).¹⁷

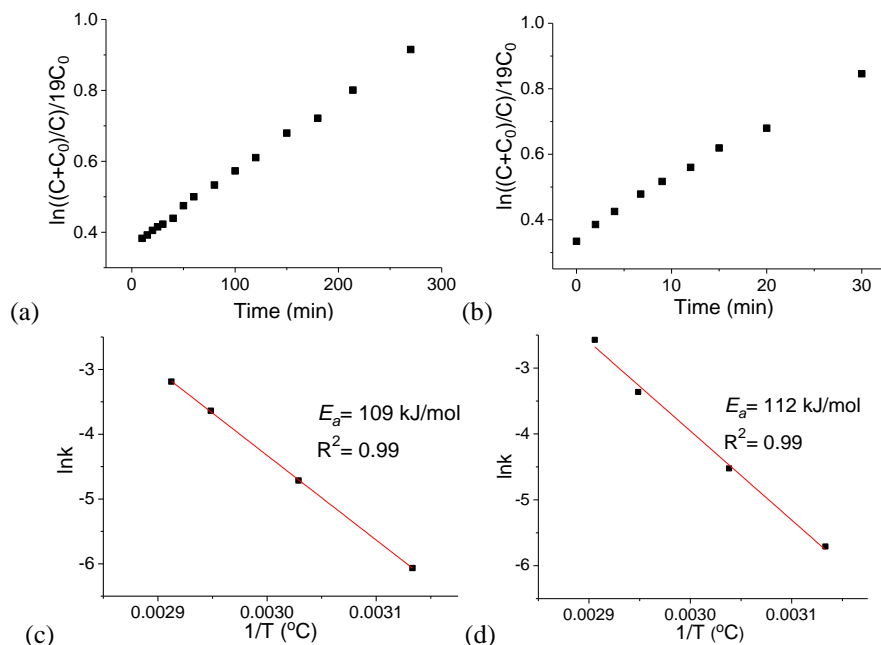


Figure 3. Plots of $\ln((C+C_0)/C)/19C_0$ vs. time plots of (a) KOT-Bu catalyzed Boc-HEX/HEX (1/20) reaction at 46 °C and (b) KOMe catalyzed NHMC/HEX (1/20) reaction at 85 °C. Arrhenius plots of Boc-HEX/HEX (1/20) reactions catalyzed by (c) KOMe and (d) KOT-Bu.

Similar E_a values were observed for KOMe- and KOT-Bu-catalyzed Boc-HEX aminolyses, both higher than the E_a of KOMe-catalyzed NHMC aminolysis (Table 1). As such, this is in agreement with the mechanism of methylcarbamate aminolysis (see Scheme 4 in Chapter 2), as bulkier *tert*-butoxide group could lead to higher energy level of the transition state. However, compared to NHMC, Boc-HEX experiences a higher aminolysis rate ($\ln k = -3.5$ for NHMC and $\ln k = -3.2$ for Boc-HEX, also see Chapter 2) while having a higher activation energy in the presence of KOMe as catalyst.¹⁷ According to the Arrhenius equation,

$$k = Ae^{-E_a/(RT)},$$

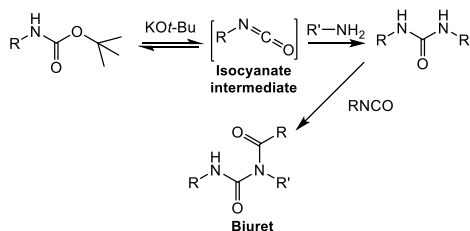
the rate constant is dependent on the absolute temperature T and a pre-exponential factor A related to the orientation of the molecules during collision (see Chapter 2). Given the higher activation energy and rate constant of Boc-HEX compared with NHMC, the factor A of the alkali base-catalyzed aminolysis of Boc-HEX is significantly greater than that of NHMC aminolysis (Table 1). This again indicates different mechanisms between alkali base-catalyzed Boc-carbamate and methylcarbamate aminolysis.

Table 1. Activation energies and pre-exponential factor of NHMC/HEX and Boc-HEX/HEX (1/20 ratio) reactions catalyzed by KOMe or KOt-Bu.

Carbamate	Catalyst	E_a (kJ/ mol)	lnA (pre-exponential factor)
NHMC	KOMe	73 ¹⁷	12 ¹⁷
Boc-HEX	KOMe	109	35
	KOt-Bu	111	37

Hence, a proposed mechanism for the Boc-carbamate aminolysis involves the formation of an isocyanate intermediate under strong basic conditions.²⁰⁻²² During the polymerization between Boc-dicarbamates and diamines, the isocyanate intermediates is formed due to the good leaving group ability of the *tert*-butoxide as a result of its strong steric hindrance, and subsequently react with the urea groups to form biurets, leading to branched structures or even crosslinks (Scheme 6). This explains the faster aminolysis of Boc-HEX with KOt-Bu as catalyst compared to KOMe, as the former has higher basicity ($pK_a = 19$) in comparison with the latter ($pK_a = 15.5$), thereby facilitating the nucleophilic attack of the base catalyst on the carbamate to form isocyanate intermediate.

To further investigate this mechanism, a model reaction with a Boc-HEX/HEX molar ratio of 1.4/1 was carried out at 130 °C under argon flow with KOt-Bu as catalyst. The ¹H NMR spectra of the reaction mixture over a 60 min period are shown in Figure 4.



Scheme 6. Proposed biuret formation in the Boc-carbamate aminolysis.

The spectrum of the reaction mixture at t_0 is characterized by a triplet at 2.65 and 3.04 ppm, assigned to the methylene protons next to the amine end-group in HEX (**c**) and the methylene protons adjacent to the carbamate group in Boc-HEX (**d**). The intensity of those signals decreased with time, while a new resonance attributed to the methylene protons near urea moieties (**a**) appeared at 3.20 ppm. In addition, a minor signal emerged after 10 min at 3.84 ppm (**b**), with an intensity of approximately 6 % with regard to **d** at t_0 , suggesting possible biuret formation.

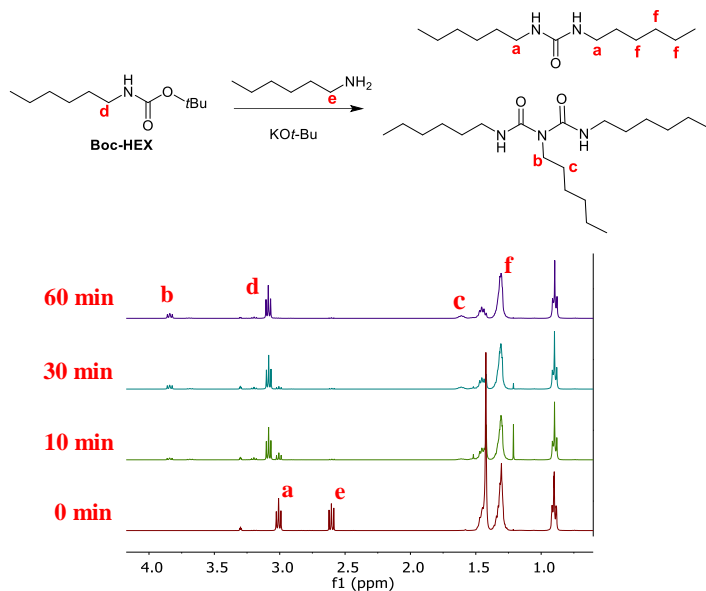


Figure 4. Scheme of the Boc-HEX/HEX (1.4/1) model reaction and ¹H NMR spectra of the reaction mixture at various reaction times.

In order to verify the biuret formation, a two-dimensional ¹H-¹H 2D COSY NMR study was performed to monitor the Boc-HEX/HEX reaction (see Figure 5). The COSY sequence allows to identify the coupling between nearby protons. Thus, the ¹H-¹H 2D COSY NMR spectrum exhibits a correlation between signal **b** and the resonance at 1.61 ppm (**c**), which is also correlated to the methylene resonance of the hexyl moieties at 1.29 ppm (**f**). This suggests that protons **c** and **b** are present in the same hexyl group. The chemical shift at lower field of signal **b** compared to **a** indicates that the methylene protons are connected to a stronger electron withdrawing group than a urea, such as a biuret. This is confirmed by the ¹³C{¹H} NMR spectrum of the reaction mixture after 60 min, which reveals an extra carbonyl signal at 149.2 ppm besides the urea carbonyl and the carbamate signals at 160.0 and 157.2 ppm, respectively.²³ Thus, the resonance **b** is assigned to methylene protons next to the nitrogen of the biuret. The formation of such species could lead to branching and crosslinking during the polymerization.

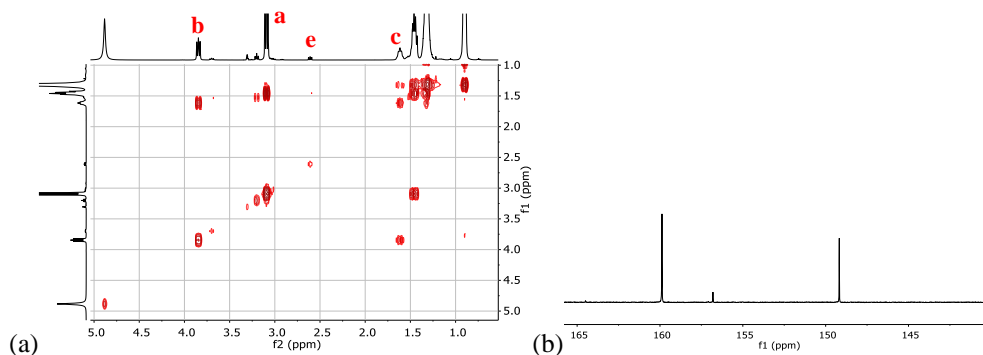
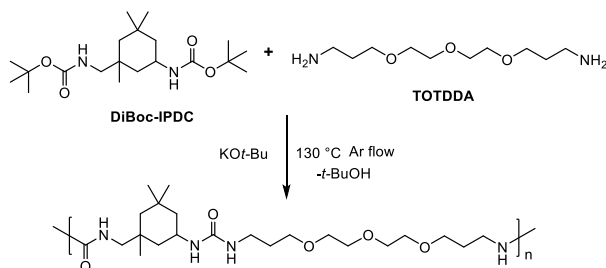


Figure 5. (a) ^1H - ^1H 2D COSY and (b) $^{13}\text{C}\{^1\text{H}\}$ NMR spectra of the Boc-HEX/HEX (1.4/1) model reaction at 60 min (methanol- d_4).

5.3.2 Polyurea synthesis

The insights obtained from the model studies described above were employed in polyurea synthesis. In this section, DiBoc-IPDC and 4,7,10-trioxa-1,13-tridecanediamine (TOTDDA) were polymerized at 130 °C under argon flow with KO t -Bu as catalyst (Scheme 7). An excess of TOTDDA was used with respect to DiBoc-IPDC (TOTDDA/DiBoc-IPDC = 1.2/1) since the stoichiometric polymerization leads to a mixture of too high viscosity for sampling. The reaction was monitored by ATR-IR (Figure 6).



Scheme 7. Reaction scheme of DiBoc-IPDC/TOTDDA polymerization.

Figure 6 shows the FTIR spectra of DiBoc-IPDC and the resulting polyurea product. (Partial) Conversion of the absorption of the carbamate carbonyl was observed at 1700 cm^{-1} into a band at 1640 cm^{-1} , assigned to the C=O vibration of urea moieties.²⁴

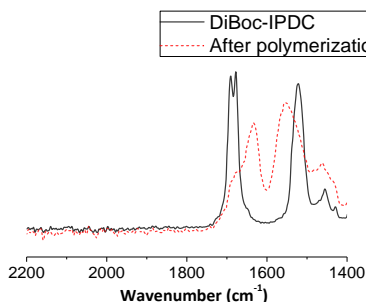


Figure 6. FT-IR spectra of DiBoc-IPDC monomer and polyurea product.

The DiBoc-IPDC/TOTDDA reaction was also followed by ^1H NMR (Figure 7). The spectrum of the reaction mixture at t_0 is characterized by resonances at 0.8-1.1, 1.44 and 2.68 ppm assigned to the methyl and methylene protons on the IPDC ring (**a**), the methyl protons of the di-*tert*-butyl groups (Boc) of DiBoc-IPDC (**b**) and the methylene protons adjacent to the amine end groups (**c**), respectively. The emergence of a signal at 3.20 ppm attributed the methylene protons next to the urea groups (**d**) is accompanied by the reduction of **b** and **c**, indicating the formation of polyurea. The disappearance of **b** after 30 min suggests full conversion of the end-groups. The degree of polymerization (DP) determined from the ratio of the signal intensities of **c** and **a** is about 11 after 60 min, similar to the theoretical value for a 1.2/1 monomer feed ratio.²⁵

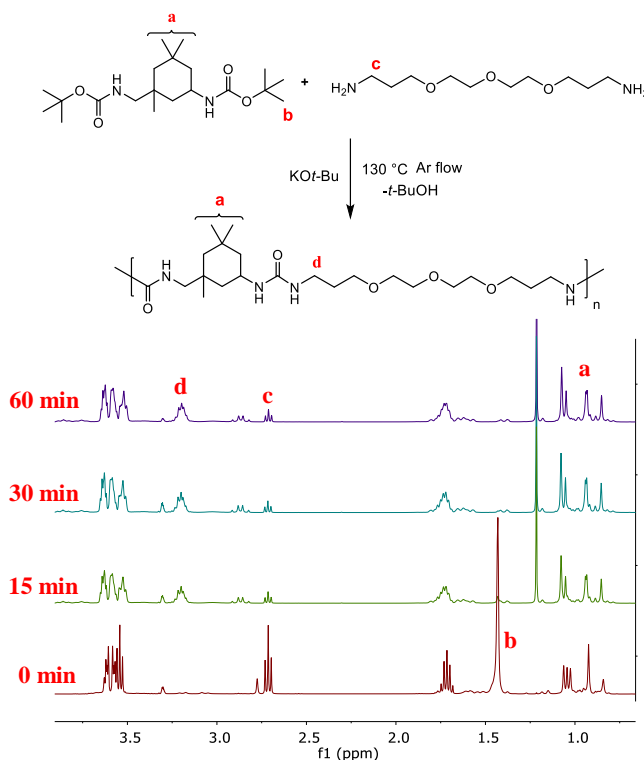


Figure 7. (a) Scheme of DiBoc-IPDC/TOTDDA polymerizations; (b) ^1H -NMR spectra of the polymerization DiBoc-IPDC/TOTDDA (1/1.2) mixtures catalyzed by KOt-Bu.

In chapter 4 it was indicated that the PUs obtained from TOTDDA/DiBoc-IPDC polymerizations could reach high M_n s when TOTDDA was present in slight excess. Besides TOTDDA, commercially available diamine monomers such as PPGda400 and PPGda2000 were also polymerized with DiBoc-IPDC with different amine/carbamate ratios to obtain polyureas with high M_n values. The theoretical²⁷ and experimental (HFIP-SEC) M_n values of the resulting PUs are presented in Table 2.

As observed for the TOTDDA/DiBoc-IPDC system, stoichiometric reactions of PPGda400 or PPGda2000 and DiBoc-IPDC resulted in materials with high D_{MS} and M_n s. However, these

M_n values were lower than those obtained for the polymerization of stoichiometric TOTDDA/DiBoc-IPDC mixtures, especially with PPGda2000, for which gelation was not observed and for which \bar{D}_M values remain low, even for a diamine/DiBoc-IPDC ratio of 0.98. This is probably due to a much lower urea density in PPGda2000-based PUs compared to TOTDDA and PPGda400, thereby leading to reduced biuret formation. Additionally, the lower reactivity of the amines connected to secondary carbons in PPGda compared to the amines connected to primary carbons in TOTDDA also contributes to the lower M_n s of the PUs prepared from the former. The stoichiometric polymerizations of these diamines and DiBoc-IPDC result in PUs with sufficiently high M_n values for coating applications.²⁶ Much higher T_g s of 15 to 77 °C were observed for TOTDDA-based PUs than PPGda400- (8 to 31 °C) and PPGda2000-based (-58 to -61 °C) ones. This is caused by the much lower molar mass of the TOTDDA compared to the other two monomers, leading to higher urea densities in the PU resins and thereby higher T_g s.

Table 2. M_n , \bar{D}_M and T_g of PUs with different ratios of diamines/DiBoc-IPDC (given between parentheses) as comonomers.

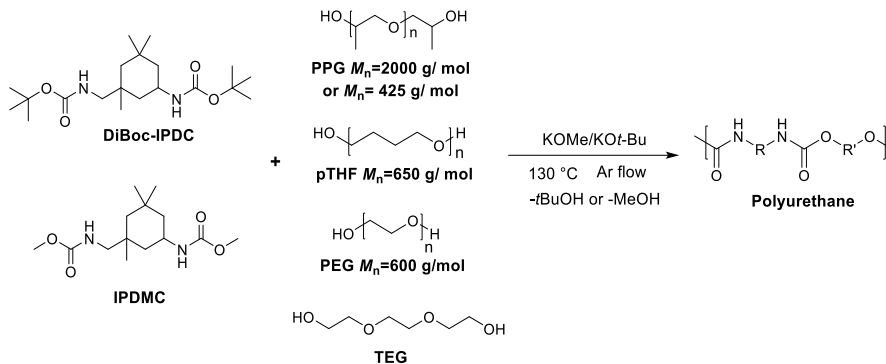
Diamine (Diamine/DiBoc-IPDC)	M_n (kDa) ^a	\bar{D}_M ^a	Theoretical M_n (kDa) ^c	T_g ^d (°C)
TOTDDA (1.03)	15	1.3	15	15
TOTDDA (1.02)	18	1.4	21	20
TOTDDA (1.01)	85	2.3	44	72
TOTDDA (1.00)	120	3.1	∞	75
TOTDDA (0.98)	Gel	N.A. ^b	22	77
PPGda400 (1.02)	33	1.9	31	8
PPGda400 (1.01)	65	2.5	62	23
PPGda400 (1.00)	79	2.9	∞	28
PPGda400 (0.98)	Gel	N.A.	31	31
PPGda2000 (1.02)	45	1.7	100	-60
PPGda2000 (1.01)	52	1.8	200	-61
PPGda2000 (1.00)	62	1.9	∞	-58
PPGda2000 (0.98)	59	1.8	200	-60

^a) Determined by HFIP-SEC; ^b) not available due to gelation; ^c) calculated with Carothers' formula;²⁵ ^d) determined by DSC.

5.3.3 Polyurethane synthesis

Compared to diamines, diols are readily available and less expensive. Thus, PURs were prepared by polymerizing DiBoc-IPDC with five different diols, namely poly(propylene glycol) with M_n of 425 and 2000 Da (PPG425, PPG2000), poly(tetrahydrofuran) with M_n of 650 Da (pTHF650), poly(ethylene glycol) (PEG) with M_n of 600 Da and triethylene glycol

(TEG). These diols are conventional building blocks employed in PUR manufacturing industries to increase the flexibility of the resins. Isophorone dimethylcarbamate (IPDMC) was also used as dicarbamate comonomer to compare with DiBoc-IPDC, as shown in Scheme 8.



Scheme 8. Reaction scheme of dicarbamate/diol polymerizations.

Stoichiometric polymerizations of diols and dicarbamates were performed at 130 °C in the presence of KOt-Bu, first under argon flow for 6 hours and then, under vacuum for 12 hours to remove the residual methanol or *t*-butanol condensation product. The M_n values achieved for each combination are listed in Table 3, together with the corresponding D_M and T_g values.

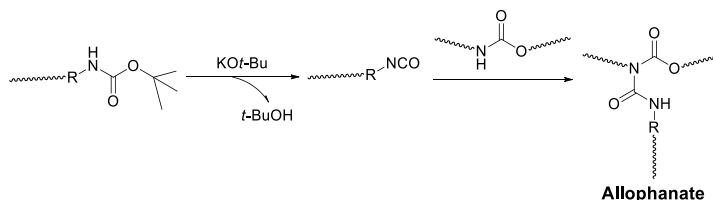
Table 3. M_n , D_M and T_g of PURs prepared from stoichiometric ratios of dicarbamates and diols.

Dicarbamate	Diol	M_n (kDa) ^a	D_M ^a	T_g (°C) ^b
DiBoc-IPDC	PPG2000	49	2.8	-52
	PPG425	34	2.1	-10
	pTHF650	38	2.4	-20
	PEG600	40	2.6	-16
	TEG	30	2.0	56
IPDMC	PPG2000	31	1.6	-58
	PPG425	20	1.6	-28
	pTHF650	13	1.8	-40
	PEG600	17	1.5	-36
	TEG	9	1.2	42

^a) Determined by HFIP-SEC; ^b) determined by DSC.

The M_n values of the PURs with DiBoc-IPDC and PPG2000, PPG425, pTHF650, PEG600 and TEG were 49 kDa, 34 kDa 38 kDa, 40 kDa and 30 kDa, respectively, while the M_n s of PURs prepared from IPDMC were up to 3 times lower due to its lower reactivity towards diols. Higher D_M values were also observed with PURs prepared from DiBoc-IPDC, probably

caused by the allophanate forming side reaction between the earlier-mentioned isocyanate intermediates and urethane moieties (Scheme 9). Such intermediate is absent in IPDMC/diamine polymerization as indicated by the mechanism proposed in Chapter 2. Despite the high M_n s of the PURs, their T_g values are very low ($-52\text{ }^{\circ}\text{C}$ to $-10\text{ }^{\circ}\text{C}$), with the exception of TEG-based PURs ($42\text{--}56\text{ }^{\circ}\text{C}$). Such PURs could potentially be employed in coating applications. The reduced M_n values of PURs compared with PUs prepared from DiBoc-IPDC could result from the lower reactivity of diol than diamine towards isocyanates. The lower M_n value of the TEG-based PURs compared to PPG2000-based ones is most probably related to the higher hydrogen bond density of the urethane moieties in the TEG/DiBoc-IPDC polymerization mixture compared to PPG2000/DiBoc-IPDC, which may result in a higher viscosity and slower reaction. Of course, in addition a similar number of urethane bond formations using a high molar mass polyol results automatically in higher PUR molecular weights compared to the synthesis based on a low MW polyol. It will be obvious that the high urethane densities in the polymer chains of TEG-based PURs could lead to desired material properties, despite the relatively low M_n .



Scheme 9. Possible allophanate formation during DiBoc-IPDC/diol polymerization.

Optimization of the M_n s of the PURs were carried out by polymerization of different ratios of TEG and DiBoc-IPDC or IPDMC at $130\text{ }^{\circ}\text{C}$ under argon flow in the presence of the corresponding alkali bases. The M_n and D_M values of these PURs are displayed in Table 4.

Lower TEG/DiBoc-IPDC ratios led to higher M_n s and D_{MS} . When DiBoc-IPDC was present in excess, gelation was observed due to the possible allophanate formation. The M_n s of the IPDMC-based PURs were below 10 kDa (D_M of 1.1-1.2), and decreased with further deviation from the stoichiometric TEG/IPDMC ratio, suggesting low conversions of functional groups. Obviously, IPDMC is much less reactive than DiBoc-IPDC.

Table 4. Reaction formulation, M_n and \bar{D}_M of polyurethanes based on DiBoc-IPDC and TEG. TEG/dicarbamate ratios are given between parentheses.

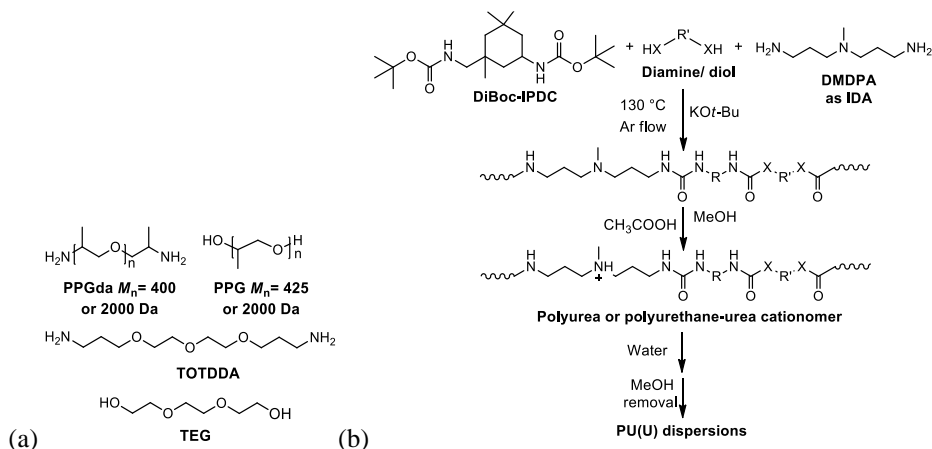
Dicarbamate (TEG/dicarbamate)	M_n (kDa) ^a	\bar{D}_M ^a	Theoretical M_n (kDa) ^c
DiBoc-IPDC (1.02)	14	1.4	19
DiBoc-IPDC (1.01)	21	1.7	37
DiBoc-IPDC (1.00)	30	2.0	∞
DiBoc-IPDC (0.99)	Gel	N.A. ^b	37
DiBoc-IPDC (0.98)	Gel	N.A.	19
IPDMC (1.01)	8	1.1	37
IPDMC (1.00)	9	1.2	∞
IPDMC (0.98)	9	1.2	19
IPDMC (0.96)	9	1.2	9
IPDMC (0.94)	6	1.1	6

^a) Determined by HFIP-SEC; ^b) not available due to gelation; ^c) calculated with Carothers' formula.²⁵

5.3.4. Preparation of water-borne polyurea (PU) and polyurethane urea (PUU) dispersions

The synthesis of PUDs with IPDMC, diamines and DMDPA is described in Chapter 3. Most of the corresponding dispersions generated coatings with unsatisfactory mechanical properties and solvent resistance due to the low molecular weight of the PU resins. The high M_n PUs prepared from DiBoc-IPDC and described in the current chapter could potentially lead to coatings with better material properties.

In this section, PU(U)s containing tertiary amine functionalities were prepared via a one-pot, solvent-free procedure using 3,3'-diamino-*N*-methyldipropylamine (DMDPA) as IDA. Different diamines and diols were employed, including TOTDDA, TEG, PPGda and PPGdiol with different molecular weights (Scheme 10a).



Scheme 10. (a) Structures of diamines and diols employed in PU(U) syntheses. (b) Reaction scheme and dispersion preparation of PU(U) cationomers.

5.3.4.1 Cationic PUDs with DMDPA as IDA

Copolymerizations of DMDPA, PPGda400 and DiBoc-IPDC were performed at 130 °C in the presence of the catalyst KOr-Bu, first under argon flow for 6 hours and then under reduced pressure (3 mmHg) for 12 hours (see also Chapter 3). The produced PUs were then dissolved in methanol and neutralized with acetic acid (one mol equivalent with regard to internal and chain-end amines in the PUs). The solutions were then dispersed in water and methanol was evaporated to generate water-borne PUDs (Scheme 10b). The dispersions were then casted onto aluminum panels and dried overnight in an oven at 50 °C under argon flow to form PU(R) coatings. The mechanical properties and solvent resistance of the resulting coatings are summarized in Table 5.

The M_n values of the PUs synthesized from DiBoc-IPDC and various amounts of DMDPA are between 62–73 kDa, which are almost twice the values of those prepared from IPDMC, DMDPA and PPGda400 (see Table 3 in Chapter 3). The T_g s of the PUs are about 8–12 °C higher than the values of the corresponding IPDMC analogues (see Table 3 in Chapter 3). Despite the high M_n s, stable dispersions with ζ -potentials of about 50 mV (a dispersion is considered stable when the absolute value of the ζ -potential is higher than 30 mV) and particle sizes of ca. 20–90 nm were obtained for these resins. The resulting coatings were slightly harder than those prepared from IPDMC (see Table 3 in Chapter 3). They all passed the impact test and have good acetone and water resistances, probably due to the high entanglement density caused by the high M_n s and strong hydrogen bonding between the PU chains, thus leading to superior mechanical properties.

Table 5. Dispersion and coating properties of PUs with DMDPA as IDA, PPGda400 as diamine and DiBoc-IPDC as dicarbamate (primary amine/carbamate = 1/1).

Mol% of IDA in diamine	M_n (kDa) ^a	T_g (°C) ^b	Av. particle size ^c (nm)	ζ -potential (mV) ^c	Coating hardness	Impact test	Acetone resistance	Water resistance ^d
10	72	24	85	48	3B	+	+	+
20	66	31	30	45	2B	+	+	+
30	62	45	21	52	B	+	+	+
40	73	52	18	50	HB	+	+	+

^{a)} Determined by HFIP-SEC; ^{b)} determined by DSC; ^{c)} determined by DLS; ^{d)} +: no swelling.

PUs based on DiBoc-IPDC, TOTDDA and DMDPA were prepared under the same conditions (Table 6). The resulting resins had sufficiently high M_n s, ranging from 65 kDa to 75 kDa. The T_g s of the PUs raise from 55 to 79 °C with increasing DMDPA content. This is caused by the reduced flexibility of the chains due to the absence of oxygen atoms in DMDPA and the lower molar mass of DMDPA (145.25 g/mol) compared with TOTDDA (220.31 g/mol), leading to higher urea and hydrogen bonding densities. The lower molar mass of TOTDDA compared to PPGda400 also results in higher urea densities in the PUs, and thus in higher T_g s and harder coatings. Similarly, the coatings with TOTDDA-based PUs also passed the impact test and had good acetone resistance. However, these coatings swelled during the water immersion test, probably due to the higher hydrophilicity of the TOTDDA segments in the PU chains compared to the PPG ones in the PPGda400-based PUs. The latter had good water resistance. Additionally, the lower molar mass of TOTDDA compared to PPGda400 also led to a higher concentration of DMDPA segments, and therefore to more tertiary amines (neutralized by acetic acid) within the related TOTDDA-based PUs. This further enhances the hydrophilicity of the material, as indicated by the coating softening during the water immersion test when more than 30 mol% DMDPA was present in the TOTDDA-based PUs.

Table 6. Dispersion and coating properties of PUs with DMDPA as IDA, TOTDDA as diamine and DiBoc-IPDC as dicarbamate (primary amine/carbamate = 1/1).

Mol% of IDA in diamine	M_n (kDa) ^a	T_g (°C) ^b	Av. particle size ^c (nm)	ζ -potential (mV) ^c	Coating hardness	Impact test	Acetone resistance	Water resistance ^d
10	68	55	156	43	B	+	+	±
20	72	68	24	45	HB	+	+	±
30	65	71	23	41	F	+	+	-
40	75	79	18	46	F	+	+	-

^{a)} Determined by HFIP-SEC; ^{b)} determined by DSC; ^{c)} determined by DLS; ^{d)} ±: swelling without softening, -: swelling and softening.

Soft PUs were prepared from DMDPA, PPGda2000 and DiBoc-IPDC. The corresponding dispersion and coating properties are displayed in Table 7. As those polymers have much

lower densities of ionic groups in the polymer chain compared to the TOTDDA- or PPGda400-based PUs, precipitation occurred during the preparation of PUDs with low DMDPA contents of 10-20 mol% of the amine monomers. At higher DMDPA content, stable PUDs were formed with particle sizes below 200 nm and ζ -potentials above 40 mV. The low T_g s of these PUs are caused by the soft PPGda2000 chain segments, which dominates over the contributions of the rigid isophorone and DMDPA units. The poor acetone and water resistance are probably the result of low urea densities in the polymer matrices, which swell upon contact with solvents. As expected, the coatings prepared from PPGda2000 and DiBoc-IPDC are softer (< 6B) compared to those with PPGda400 (3B). In principle, a high loading of DMDPA in the diamine feed would lead to an enhanced T_g . However, the T_g s of the PPGda2000-based PUs are hardly influenced by the DMDPA contents. This could be attributed to a microphase separation of the polymer, whose T_g measured by DSC would only represent the soft segment part (PPGda2000 segments). With regard to the reverse impact test, no cracking was observed for PU coatings with 30 and 40 % IDA in the amine feed due to the softness of the materials. However, the hardnesses of the coatings are all below 6B, which is undesired for most industrial applications.

Table 7. Dispersion and coating properties of PUs with DMDPA as IDA, PPGda2000 as diamine and DiBoc-IPDC as dicarbamate (primary amine/carbamate = 1/1).

Mol% of IDA in diamine	M_n (kDa) ^a	T_g (°C) ^b	Av. particle size ^c (nm)	ζ -potential (mV) ^c	Coating hardness	Impact test	Acetone resistance	Water resistance ^d
10	59	-62	N.A. ^d	N.A.	N.A.	N.A.	N.A.	N.A.
20	57	-60	N.A.	N.A.	N.A.	N.A.	N.A.	N.A.
30	53	-63	143	47	<6B	+	-	+
40	55	-62	40	45	<6B	+	-	+

^{a)} Determined by HFIP-SEC; ^{b)} determined by DSC; ^{c)} determined by DLS; ^{d)} decipitation during dispersion; ^{e)} +: no swelling.

5.3.4.2 Cationic polyurethane urea dispersions (PUUDs) with DMDPA as IDA

Polyurethane ureas (PUUs) were synthesized by copolymerization of diols, DiBoc-IPDC and DMDPA, first at 130 °C for 6 hours under argon flow in the presence of KO^t-Bu, then under a vacuum of 3 mm Hg for another 12 hours. The properties of PUU dispersions (PUUDs) and related coatings based on PPG2000, PPG425 and TEG, together with DiBoc-IPDC and different loadings of DMDPA as IDA are displayed in Table 8.

PUUs obtained from PPG2000 and DiBoc-IPDC with 10 to 20 mol% of DMDPA in the amine feed led to precipitation during the preparation of the dispersions, probably due to an insufficient neutralized amine loading to stabilize the particles. Similarly, precipitation was observed during dispersion of PPG425-based PUU with 10 mol% of DMDPA, while PUUs with higher DMDPA contents generated dispersions with ζ -potentials above 50 mV and particle sizes below 50 nm. The T_g values of the PPG425- and PPG2000-based PUUs are far below room temperature, leading to soft coatings. Their solvent resistances are also poor due

to a combination of low urea densities and insufficient molecular weights.

The TEG-based PUUs exhibit low M_n values of 24-28 kDa with T_g s between 56-60 °C, which resulted in hard coatings with pencil hardnesses above B. The T_g s of these PUUs are barely influenced by the DMDPA content, probably due to the similar molar masses of DMDPA (145 g/mol) and TEG (150 g/mol), and consequently similar contribution to the T_g of the material. Despite their high T_g s, the low M_n s of these compounds result in insufficient entanglement formation in the polymer matrices, leading to failures in reverse impact tests. The poor solvent resistance of the coatings is attributed to an abundant amount of hydrophilic TEG segments in the PUUs.

Despite the similar building blocks, the T_g s of the PUUs produced from PPG425 are lower than the corresponding T_g s of the PPGda400-based PUs (see Table 5 and Table 8). This is on the one hand caused by the higher M_n s of the PUs compared to PUUs, as a result of the higher reactivity of diamines towards DiBoc-IPDC compared to diols. Additionally, the stronger hydrogen bonds between the urea moieties in PUs in comparison to those between urethanes in PUUs reduces the chain mobility in the polymer matrices, further enhancing the T_g of the material.

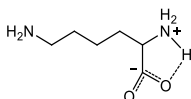
Table 8. Dispersion and coating properties of PUUs with DMDPA as IDA, DiBoc-IPDC as dicarbamate and different diols (primary amine/carbamate = 1/1).

Diol	IDA mol%	M_n (kDa) a	T_g (°C) b	Av. particle size (nm) ^c	ζ -potential (mV) ^c	Coating hardness	Impact test	Acetone resistance	Water resistance ^e
PPG 425	10	33	-12	N.A. ^d	N.A.	N.A.	N.A.	N.A.	N.A.
	20	32	-2	42	52	<6B	+	-	+
	30	34	7	23	59	6B	+	-	+
	40	37	11	35	50	5B	+	-	+
PPG 2000	10	28	-57	N.A.	N.A.	N.A.	N.A.	N.A.	N.A.
	20	30	-56	N.A.	N.A.	N.A.	N.A.	N.A.	N.A.
	30	34	-58	120	51	<6B	+	-	+
	40	31	-55	95	49	<6B	+	-	+
TEG	10	24	56	135	41	B	-	-	-
	20	28	59	46	45	B	-	-	-
	30	25	57	22	40	B	-	-	-
	40	28	60	20	44	HB	-	-	-

a) Determined by HFIP-SEC; b) determined by DSC; c) determined by DLS; d) precipitation during dispersion; e) +: no swelling, -: swelling and softening.

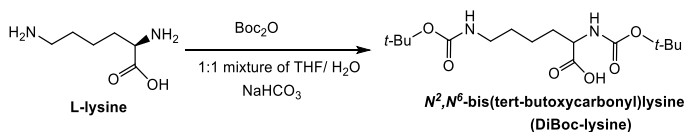
5.3.4.3 Anionic PUDs with Boc-lysine as IDA

Anionic PUDs could also be synthesized by employing IDAs with carboxylic acid groups. The conventionally used dimethylol propionic acid (DMPA) could not be incorporated into the polymer backbone via diol/dicarbamate reaction due to the low reactivity of the hydroxyl groups. Therefore, the diamine-functional amino acid lysine was used as an alternative. However, the polymerization of lysine and IPDMC resulted in oligomers due to the low reactivity of the α -amine, which forms (internal) hydrogen bonds with the carboxylic acid group (Scheme 11).²⁷ Similarly, the dimethylcarbamate form of lysine could not be synthesized via the melt transurethanization method developed by Deepa et al., as a result of the low reactivity of the α -amine of lysine towards dimethyl carbonate.⁷



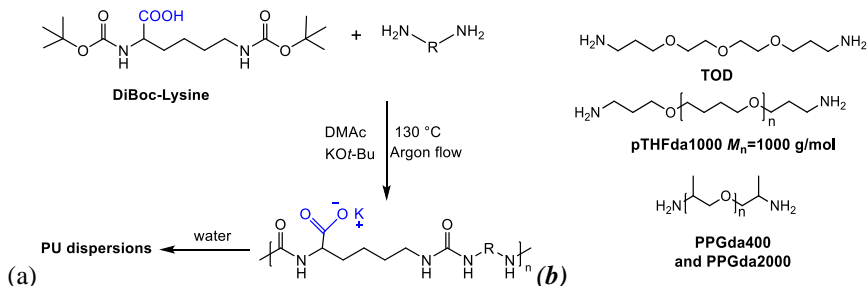
Scheme 11. Hydrogen bond formation between the α -amine and carboxylic acid group in lysine.²⁶

Alternatively, lysine Boc-dicarbamate (DiBoc-lysine) was successfully synthesized from lysine and Boc₂O in the presence of sodium bicarbonate as catalyst, as shown in Scheme 12.



Scheme 12. Synthesis of N^2,N^6 -bis(tert-butoxycarbonyl)lysine (DiBoc-lysine).

DiBoc-lysine was incorporated into PU backbones via stoichiometric polymerizations in DMAc solvent of DiBoc-lysine and diamines at 130 °C under argon flow (Scheme 13). An excess of KO t -Bu was used to neutralize the pending carboxylic acid groups and to catalyze the polymerization. The resulting polyurea solutions were then washed with diethyl ether and dried at 80 °C under vacuum overnight. Since the carboxylic acid groups in these PUs were already neutralized by KO t -Bu during the reaction, they can directly disperse in water to form PUDs. The properties of the PUDs and the corresponding coatings based on the diamines TOTDDA, PPGda400, PPGda2000 and pTHFda1000 are summarized in Table 9.



Scheme 13. (a) Preparation of PU(U)D with Boc-lysine as IDA. (b) Structures of diamines employed in the polymerizations.

Table 9. Dispersion and coating properties of the PUs prepared from a stoichiometric ratio of DiBoc-lysine and diamines.

Diamine/diol	M_n^a (kDa)	\bar{D}_M^a	T_g^b (°C)	Av. particle diameter (nm) ^c	ζ - potential (mV) ^c	Coating hardness	Impact test
PPGda400	13	1.7	8	N.A. ^d	N.A.	N.A.	N.A.
PPGda2000	21	1.6	-61	146.6	-40	<6B	+
pTHFda1000	11	1.8	-75	N.A.	N.A.	N.A.	N.A.
TOTDDA	5	1.5	2	N.A.	N.A.	N.A.	N.A.

^{a)} Determined by HFIP-SEC; ^{b)} determined by DSC; ^{c)} determined by DLS; ^{d)} precipitation during dispersion.

The M_n s of the PUs prepared from DiBoc-lysine were relatively low, with \bar{D}_M values below 2, and no clear indications for branching were obtained. The low M_n s of the PUs also suggest a slow reaction between DiBoc-lysine and diamines. As a result, limited amounts of IDAs are incorporated in the PU chains, leading to unstable dispersions. Nevertheless, the PU prepared from DiBoc-lysine and PPGda2000 yielded a stable dispersion with a high ζ -potential of -40 mV. The coating generated from such dispersion is soft (< 6B) due to the low T_g of the resin.

To enhance the mechanical properties of lysine-based PUs, the rigid IPDC building block was introduced via a two-step method. Firstly, diamine-functional PU prepolymers of various M_n values were synthesized from different ratios of DiBoc-IPDC and PPGda230. Then, the incorporation of Boc-lysine was achieved by copolymerizing DiBoc-lysine and the prepolymers at 130 °C under argon flow in the presence of an excess of KO^t-Bu to neutralize the acid groups. The M_n s of the prepolymers with different PPGDa230/IPDMC ratios and the resulting lysine-based PUs as well as the average particle sizes and ζ -potentials of the PUDs are displayed in Table 10.

Table 10. Dispersion and coating properties of the PUs prepared from a stoichiometric ratio of DiBoc-lysine and diamine-functional PUs with different PPGda230/IPDMC ratios.

Entry	PPGda230/IPDMC (molar ratio)	M_n of prepolymer (Da) ^a	M_n of lysine- based PU (kDa) ^b	Av. particle size ^c (nm)	ζ -potential (mV) ^c
1	1.10/1	4,900	10	N.A. ^d	N.A.
2	1.25/1	2,900	7	N.A.	N.A.
3	1.30/1	2,800	6	53	-45
4	1.35/1	2,200	6	59	-56
5	1.40/1	1,800	6	68	-54

^{a)} Determined by potentiometric titration; ^{b)} determined by HFIP-SEC; ^{c)} determined by DLS; ^{d)} precipitation during dispersion.

The M_n s of the prepolymers range from 2 to 5 kDa (determined from potentiometric titration of the end groups), while the PUs prepared from stoichiometric polymerization of DiBoc-lysine and the diamine-terminated prepolymers had low M_n s of approximately 6-10 kDa. PUs

prepared from entries 1 and 2 precipitated during dispersion preparation, probably due to an insufficient number of neutralized carboxylic acid groups present per polymer chain (Note: the longer the prepolymer segments, the lower the DiBoc-lysine content of the final polymer). The dispersions of entries 3-5 were rather stable with ζ -potentials lower than -40 mV and particle sizes between 53-68 nm. Side reactions such as transamidation between DMAc solvent and diamines could take place during the DiBoc-lysine aminolysis, leading to off-stoichiometry between diamine and DiBoc-lysine.²⁸ This side reaction can at least partially explain the low M_n values of the PUs obtained. Due to the low M_n s of the lysine-based PUs, their coatings have poor mechanical strength. Therefore, an alternative method for incorporating acid groups along the PU backbones will be introduced in the next chapter, which involves poly(amic acid urea) formation via polymerization of diamine-functional PUs and a dianhydride.

5.4 Conclusions

In this chapter, di-*tert*-butyl carbamates (DiBoc-carbamates) were employed as monomers in isocyanate-free syntheses of polyureas (PUs) and polyurethanes (PURs). Potassium *tert*-butoxide (KO^t-Bu) proved to be most efficient catalyst compared to the other investigated catalysts, *viz.* potassium methoxide (KOMe), 4-dimethylaminopyridine (DMAP) and 1,5,7-triazabicyclo[4,4,0]dec-5-ene (TBD) in model reactions with *tert*-butyl hexylcarbamate (Boc-HEX) and hexylamine (HEX) as substrates. Higher values of activation energies and pre-exponential factors as well as faster reaction rates were observed for Boc-HEX/HEX model reactions in the presence of KOMe compared to the *N*-hexylmethylcarbamate (NHMC)/HEX model reactions with the same catalyst reported in Chapter 2. This is likely due to the presence of isocyanate intermediates during the base-catalyzed Boc-carbamate/amine reaction, as further evidenced by the formation of biuret during the reaction of an excess of Boc-HEX with HEX.

Polyureas (PUs) with M_n values up to 120 kDa were prepared from 4,7,10-trioxa-1,13-tridecanediamine (TOTDDA), poly(propylene glycol) bis(2-aminopropyl ether)s with average M_n s of 400 and 2000 Da (PPGda400 and PPGda2000, respectively) and isophorone di-*tert*-butyl dicarbamate (DiBoc-IPDC). Gelation was observed when an excess of DiBoc-IPDC was used with respect to the diamine. Polyurethanes (PURs) were synthesized from poly(propylene glycol)s with M_n s of 425 and 2000 Da (PPG425, PPG2000), poly(tetrahydrofuran) with M_n of 650 Da (pTHF650), poly(ethylene glycol) (PEG) with M_n of 600 Da (PEG600) and triethylene glycol (TEG) with either DiBoc-IPDC or isophorone dimethylcarbamate (IPDMC). Higher M_n and D_M values were measured for PURs prepared from DiBoc-IPDC compared to those based on IPDMC, due to the higher reactivity of DiBoc-IPDC and the possible formation of allophanates during the polymerization, respectively.

Stable dispersions with low particle sizes and high ζ -potentials were obtained from PUs and PURs with 3,3'-diamino-*N*-methyldipropylamine (DMDPA) as internal dispersing agent (IDA), with the notable exception of PURs based on PPG425 and PPG2000 with low DMDPA content. The resulting PU coatings based on both TOTDDA and PPGda400 diamines showed high pencil hardness (up to HB and F for PPGda400 and TOTDDA,

respectively), good impact and solvent (and water) resistance. PU coatings produced from TOTDDA and DMDPA exhibited poorer water resistance compared with the PPGda400-based ones, probably due to the more hydrophilic nature of TOTDDA. PU coatings obtained from PPGda2000 displayed low pencil hardness (< 6B) and poor acetone resistance due to the low T_g (-60 °C) and low urea densities in the polymer chains. Polyurethane urea (PUU) coatings were prepared from PUUs with M_n s between 30-50 kDa were synthesized with PPG2000, PPG425 and TEG as diols, DiBoc-IPDC as dicarbamate and DMDPA as IDA. These PUU coatings with PPG2000 and PPG425 were soft (5B-6B) and had a poor acetone resistance, while the TEG-based PUU coatings were brittle and exhibited poor water and acetone resistances due to the hydrophilicity of TEG and the low molecular weights of the resins.

Anionically-stabilized PU dispersions were obtained from N^2,N^6 -bis(*tert*-butoxycarbonyl) lysine (DiBoc-lysine) and diamines including PPGda400, PPGda2000, pTHFda1000 and TOTDDA, or diamine-functional PUs synthesized with PPGda230 and DiBoc-IPDC. However, because of the low M_n s of these lysine-based PUs, their coatings displayed poorer mechanical properties compared to the PU coatings from diamines, DMDPA and DiBoc-IPDC.

All in all we tend to conclude that the chemistry discussed in this chapter and the dispersions and coatings based on the generated, isocyanate-free PUs and PUUs show encouraging results. The reader should bear in mind that the mechanical and solvent and water resistance tests were all performed on coating systems without added external curing agents. It can be expected that the coating properties can be further enhanced when such curing agents are mixed with the stable PU and PUU emulsions. We come back to the effect of applying curing chemistry to our PU(U)s in Chapter 7.

5.5 References

- (1) Rokicki, G.; Piotrowska, A. *Polymer* **2002**, *43*, 2927-2935.
- (2) Ochiai, B.; Utsuno, T. *J. Polym. Sci., Part A: Polym. Chem.* **2013**, *51*, 525-533.
- (3) Deng, Y.; Li, S.; Zhao, J. B.; Zhang, Z.; Zhang, J.; Yang, W. *RSC Adv.* **2014**, *4*, 43406-43414.
- (4) Li, C.; Li, S.; Zhao, J.; Zhang, Z.; Zhang, J.; Yang, W. *J. Polym. Res.* **2014**, *21*, 1-10.
- (5) Li, S.; Zhao, J.; Zhang, Z.; Zhang, J.; Yang, W. *RSC Adv.* **2014**, *4*, 23720-23729.
- (6) Deng, Y.; Li, S.; Zhao, J.; Zhang, Z.; Zhang, J.; Yang, W. *Chin. J. Polym. Sci.* **2015**, *33*, 880-889.
- (7) Deepa, P.; Jayakannan, M. *J. Polym. Sci., Part A: Polym. Chem.* **2007**, *45*, 2351-2366.
- (8) Deepa, P.; Jayakannan, M. *J. Polym. Sci., Part A: Polym. Chem.* **2008**, *46*, 5897-5915.
- (9) Gastaldi, S.; Weinreb, S. M.; Stien, D. *J. Org. Chem.* **2000**, *65*, 3239-3240.
- (10) Prashad, M.; Har, D.; Hu, B.; Kim, H. -Y.; Girgis, M. J.; Chaudhary, A.; Repič, O.; Blacklock, T. *J. Org. Proc. Res. Dev.* **2004**, *8*, 330-340.
- (11) Varala, R.; Nuvula, S.; Adapa, S. R. *J. Org. Chem.* **2006**, *71*, 8283-8286.
- (12) Upadhyaya, D. J.; Barge, A.; Stefania, R.; Cravotto, G. *Tetrahedron Lett.* **2007**, *48*, 8318-8322.
- (13) Sikchi, S. A.; Hultin, P. G. *J. Org. Chem.* **2006**, *71*, 5888-5891.

- (14) Pope, B. M.; Yamamoto, Y.; Tarbell, D. S. *Org. Synth.* **1977**, *57*, 45-46.
- (15) Kurimoto, I.; Minai, M. US Patent 5151542 A, **1992**.
- (16) Deepa, P.; Jayakannan, M. *J. Polym. Sci., Part A: Polym. Chem.* **2008**, *46*, 2445-2458.
- (17) Ma, S.; Liu, C.; Sablong, R. J.; Noordover, B. A. J.; Hensen, E. J. M.; van Benthem, R. A. T. M.; Koning, C. E. *ACS Catalysis* **2016**, *6*, 6883-6891. See also Chapter 2.
- (18) Shendage, D. M.; Fröhlich, R.; Haufe, G. *Org. Lett.* **2004**, *6*, 3675-3678.
- (19) Knolker, H. -J.; Braxmeier, T.; Schlechtingen, G. *Angew. Chem. Int. Ed. Engl.* **1995**, *34*, 2497-2500.
- (20) Lamothe, M.; Perez, M.; Colovray-Gotteland, V.; Halazy, S. *Synlett* **1996**, *1*, 507-508.
- (21) Agami, C.; Couty, F. *Tetrahedron* **2002**, *58*, 2701-2724.
- (22) Spyropoulos, C.; Kokotos, C. G. *J. Org. Chem.* **2014**, *79*, 4477-4483.
- (23) Kaji, A.; Arimatsu, Y.; Murano, M. *J. Polym. Sci., Part A: Polym. Chem.* **1992**, *30*, 287-297.
- (24) Teo, L. -S.; Chen, C. -Y.; Kuo, J. -F. *Macromolecules* **1997**, *30*, 1793-1799.
- (25) Carothers, W. H. *Trans Faraday Soc.* **1936**, *1*, 39-49.
- (26) Jang, J. Y.; Jhon, Y. K.; Cheong, I. W.; Kim, J. H. *Colloid. Surf. A: Physicochem. Eng. Asp.* **2002**, *196*, 135-143.
- (27) Nagy, P. I. *Int. J. Mol. Sci.* **2014**, *15*, 19562-19633.
- (28) Zhang, Q.; Chen, Q. *J. Saudi Chem. Soc.* **2016**, *20*, 114-119.

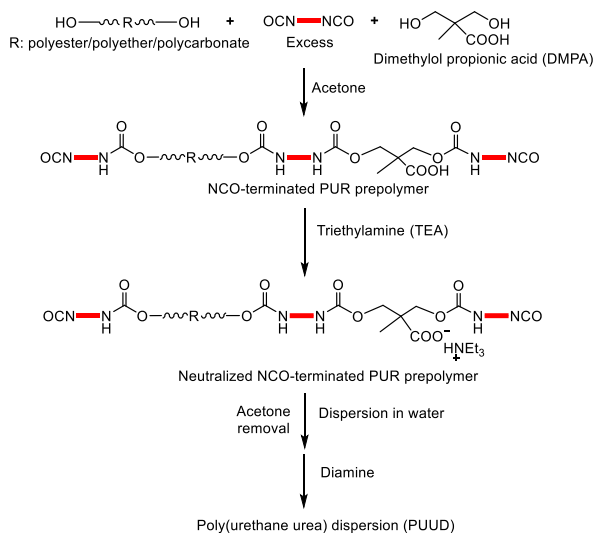
Chapter 6. Anionic polyurea dispersions with ethylenediaminetetraacetic dianhydride as internal dispersing agent

Summary

In this chapter, the synthesis of poly(amic acid urea)s (PAAUs) and their evaluation in water-borne coating systems are reported. Ethylenediaminetetraacetic dianhydride (EDTAD) was employed together with diamine-functional polyureas (PUdas) as building blocks for the production of carboxylic acid-containing PAAUs. A model reaction with diamine-functional poly(propylene glycol) and EDTAD successfully generated poly(amic acid)s (PAAs) with M_n s of about 30 kDa. Imidization of the amic acid moieties was observed during polymerization, and was promoted by removal of water. Poly(amic acid urea)s (PAAUs) were synthesized via polymerization of PUdas and EDTAD. The factors that affected the particle sizes of the corresponding PAAU dispersions (PAAUDs) were investigated. Dispersions with larger particle sizes were obtained by decreasing the neutralization agent concentration or the carboxylic acid content in the PAAUs, which could be tailored by varying either the molecular weight of the PUdas or the PUda/EDTAD ratio. Water-borne PAAU coatings were prepared from PAAUDs with various diamines. Coatings with satisfactory mechanical properties and solvent resistance were obtained via the combination of diamines with backbones based on a hydrophobic poly(tetrahydrofuran)/poly(propylene glycol) copolymer and a poly(propylene glycol).

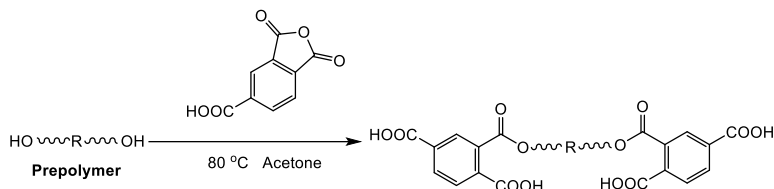
6.1 Introduction

Water-borne polyurethane urea dispersions (PUUDs) have gained increasing attention during the past decades due to their significantly lower volatile organic compound (VOC) contents compared to solvent-borne polyurethane (PUR) solutions.¹ The conventional production of PUUDs consists of three steps. The PUR prepolymers are first synthesized with diols and an excess of diisocyanates, together with an internal dispersing agent (IDA) such as dimethylolpropionic acid (DMPA). The diisocyanate-functional prepolymers are then neutralized by triethylamine (TEA) and dissolved in a low boiling point solvent like acetone, followed by addition of water to form the aqueous dispersion, after which the organic solvent is evaporated. Finally, diamine chain extenders are added to the dispersion to enhance the number average molecular weight (M_n) of the prepolymers to yield the PUUD with particle sizes of 50-300 nm and pH between 7-8 (Scheme 1).²⁻⁴ For such process, a minimum amount of IDA is required for the preparation of stable PUUDs. This minimum value depends on different parameters such as the polymer structure,^{5,6} the degree of neutralization⁷ and the preparation temperature.^{8,9}



Scheme 1. Industrial synthesis of high molecular weight poly(urethane urea) dispersions.²

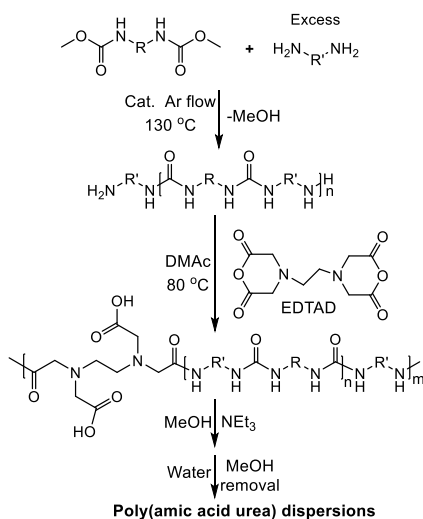
Apart from DMPA, dimethylol butanoic acid (DMBA),¹⁰ organic sulfonic acid¹¹ and organic phosphonic acid¹² are also employed as IDAs in PUUD synthesis. Another interesting strategy to disperse PURs is via the modification with anhydrides. The production of such water-dispersible PURs involves the synthesis of hydroxyl-functional PUR prepolymers, followed by the end group modification with trimellitic anhydride (TMA) to afford water-dispersible PURs with neutralizable carboxylic acid end-groups (Scheme 2).¹³⁻¹⁵ This method is not suitable for the preparation of PUR resins of high MW, since in that case the concentration of the dispersing ionic groups would be too low to stabilize the polymers in an aqueous medium.



Scheme 2. Modification of hydroxyl-functional PURs with trimellitic anhydride.¹⁵

The two most popular diisocyanate monomers for PUR synthesis are the aromatic toluene diisocyanate (TDI) and methylene diphenyl diisocyanate (MDI), employed mostly in the production of rigid PURs.¹⁶ However, aromatic diisocyanates are sensitive to UV radiation, which causes yellowing of the PURs in outdoor applications. An alternative for the aromatic diisocyanates is isophorone diisocyanate (IPDI), which bears an aliphatic ring with enhanced UV stability and pending methyl groups to enhance the rigidity of the PURs.^{17,18} Traditional diols for PUR synthesis include poly(tetrahydrofuran) (pTHF), poly(propylene glycol) (PPG) and poly(ethylene glycol) (PEG), which act as soft-segments (SSs) in the PURs to increase the flexibility of the materials.

In Chapters 3 and 5, cationically stabilized polyurea dispersions (PUDs) were investigated and the resulting PU coatings were evaluated. However, conventional PUUDs are normally anionically stabilized by -COOH groups in the backbone, with TEA as neutralization agent. The pH values of these systems are higher than 7. They are compatible with other components in the coating formulations.¹⁹ Thus, to mimic the industrial PUUDs, water dispersible poly(amic acid urea)s (PAAUs) are synthesized in this chapter via reaction of ethylenediaminetetraacetic dianhydride (EDTAD) and diamine-functional polyureas (PUs). The latter are prepared from dicarbamates and an excess of diamine (Scheme 3). Factors that influence the particle sizes and stabilities of the PAAU dispersions (PAAUDs) are investigated. The properties of the corresponding PAAU-based coatings are evaluated and optimized.



Scheme 3. Preparation of poly(amic acid urea) dispersions.

6.2 Experimental Section

6.2.1 Materials

All reagents were commercially available unless specified otherwise. 1,4-Diaminobutane (99%), 1,3-cyclohexanebis(methylamine) (CHBMA, mixture of isomers, 99%), isophorone diamine (IPDA, *cis* and *trans* mixture, 99%), 4,7,10-trioxa-1,13-tridecanediamine (TOTDDA, 97%), poly(propylene glycol) bis(2-aminopropyl ether) with average M_n of 230 and 2000 Da (PPGda230 and PPGda2000), ethylenediaminetetraacetic dianhydride (EDTAD, 99%), diethylenetriamine-pentaacetic dianhydride (DETPAD, 98%), triethylamine (TEA, 99%), potassium methoxide (KOME, 95%), 1,5,7-triazabicyclo[4.4.0]dec-5-ene (TBD, 98%), dimethyl carbonate (DMC, 99%), dimethylformamide (DMF, anhydrous, 99.8%) and sodium sulfate (99%, anhydrous) were purchased from Sigma Aldrich. A diamine-functional pTHF/PPG copolymer with an average M_n of 1000 Da (pTHF1000) was purchased from Huntsman. Deuterated solvents were purchased from Buchem BV. Other common solvents were purchased from Biosolve. All the chemicals were used without further purification.

6.2.2 Reactions and synthesis

Synthesis of butane diurethane (BU2)²⁰

In a 500 mL flask, a mixture of DMC (90 g, 1 mol), molten DAB (35.2 g, 0.4 mol) and TBD (1.39 g, 10 mmol) was stirred for 1 hour at room temperature. During this period, 100 mL of diethylether (Et₂O) were added at the moment a precipitation was observed. The precipitate was then isolated by filtration. The residue was recrystallized from chloroform and dried overnight at 60 °C in a vacuum oven to obtain BU2 as a colorless crystalline solid (70 g, 86%).

¹H NMR (400 MHz, CDCl₃, δ in ppm): 4.9 (s, broad, 2H, **NH**), 3.6 (s, 6H, **OCH₃**), 3.2 (m, 4H, **NHCH₂**), 1.5 (m, 4H, **NHCH₂CH₂**). ¹³C{¹H} NMR (100.6 MHz, CDCl₃, δ in ppm): 157.2 (**C=O**), 51.9 (**OCH₃**); 40.6 (**NHCH₂**); 27.2 (**NHCH₂CH₂**).

Synthesis of isophorone dimethylcarbamate (IPDMC)

In a 2000 mL three-neck flask equipped with a condenser, 170 g (1 mol) of IPDA, 630 g (7 mol) of DMC and 70 g (1 mol) of potassium methoxide were mixed under argon flow and stirred at room temperature. After 4 hours, the mixture was heated up to 60 °C for 6 hours. The solution was then cooled and poured into an excess of chloroform and subsequently washed with brine. The organic layer was dried over anhydrous sodium sulfate. The solvent was evaporated to dryness to obtain the product as a yellowish solid (196 g, 69%).

¹H-NMR (400 MHz, CDCl₃ δ in ppm): 4.8 (d, 1H, **-NHCH₂**), 4.6 (s, 1H, **cy-NHCH**), 3.8-3.6 (s, 1H, **cy-CHNH**, 6H, **-OCH₃**), 3.3, 2.9 (d, 2H, **-CH₂NH**), 1.7-0.7 (15H, **cy-H**). ¹³C{¹H} NMR (100.6 MHz, CDCl₃ δ in ppm): 157.4, 156.3 (**C=O**), 54.8 and 52.1 (**OCH₃**), 51.8, 46.9, 46.3, 44.6, 42.5, 41.8, 36.3, 34.9, 31.7, 29.6, 27.5, and 23.1 (**cy-C**).

Synthesis of 1,3-cyclohexanebis(methylcarbamate) (CHBMC)

In a 500 mL flask, a mixture of DMC (90 g, 1 mol), molten CHBMA (56.8 g, 0.4 mol) and TBD (1.39 g, 10 mmol) was stirred for 1 hour at room temperature. During this period, 100 mL of diethyl ether (Et₂O) were added when a precipitation was observed. The precipitate

was then isolated by filtration. The residue was recrystallized from chloroform and dried in a vacuum oven overnight at 60 °C to obtain CHBMC as a colorless crystalline solid (81 g, 78%).

^1H NMR (400 MHz, CDCl_3 δ in ppm): 4.77 (s, 2H, $-\text{CH}_2\text{NH}$), 3.66 (s, 6H, $-\text{OCH}_3$), 3.02 (s, 4H, $-\text{CH}_2\text{NH}$), 1.81-0.55 (10H, cy-**H**). $^{13}\text{C}\{^1\text{H}\}$ NMR (100.6 MHz, CDCl_3 δ in ppm): 157.4, 156.3 (C=O), 53.1 and 52.3 (OCH_3), 51.3, 49.5, 48.6, 47.4, 38.8, 38.5, 37.7, 37.5, 34.0, 33.6, 31.8, 31.2, 30.7, 30.2, 29.7, 29.2, 25.9, and 24.6 (cy-**C**).

Preparation of diamine-functional polyureas (PUDas)

In a typical experiment, 2.86 g (10 mmol) of IPDMC, 2.99 g (13 mmol) of PPGda230 and 0.07 g (0.5 mmol) of TBD were mixed in a 50 mL crimp-capped vial under argon flow and stirred at 130 °C for 12 hours. The pressure in the flask was then gradually reduced to 5 mmHg and maintained at this value for another 6 hours before quenching the mixture in water. Finally, the precipitated polymer was washed with water 3 times and dried in a vacuum oven for 12 hours to obtain a light yellowish polyurea (6.32 g, 86.7%).

Model reaction with PPGda2000 and EDTAD

In a typical experiment, a mixture of 1 g (0.5 mmol) of PPGda2000, 0.128 g (0.5 mmol) of EDTAD and 4 g of DMF was stirred at 80 °C in a 20 mL crimp-capped vial. Samples were taken during the reaction at a set time.

Copolymerization of PUDas and dianhydrides

In a typical experiment, 4.00 g (2 mmol) of PUda with molecular weight of 2150 Da (determined by potentiometric titration) was dissolved in 4.00 g of anhydrous DMAc. Then, 0.51 g (2 mmol) of EDTAD was added into the solution which was stirred at 80 °C for 30 minutes. The mixture was then precipitated in water and washed with water 3 times, and subsequently dried in a vacuum oven at 80 °C for 12 hours to obtain a yellowish poly(amic acid urea) (3.12 g, 69.2%).

Preparation of water-borne PAAU dispersions (PAAUD)

In a typical experiment, 1 gram of PAAU was dissolved in 1 mL of methanol. An equivalent amount of trimethylamine (TEA) was added according to the concentration of the $-\text{COOH}$ groups determined from potentiometric titration. The mixture was stirred for 10 minutes and then slowly added to 8 mL of water under vigorous stirring to obtain a PAAU dispersion with solid content of 10 wt%.

Preparation of PAAU coatings

In a typical experiment, 1.5 gram of PAAUD was casted on an aluminum panel. A wet film of 250 μm thickness was applied using a doctor blade, followed by drying at 50 °C under argon flow to form a colorless PAAU coating with thickness of 25 μm .

6.2.3 Characterization

Size exclusion chromatography (SEC)

SEC in 1,1,1,3,3,3-hexafluoro-2-propanol (HFIP) was performed at 40 °C on a system equipped with a Waters 1515 Isocratic HPLC pump, a Waters 2414 refractive index detector (35 °C), a Waters 2707 autosampler, a PSS PFG guard column followed by 2 PFG-linear-XL

(7 μ m, 8*300 mm) columns in series. HFIP with potassium trifluoroacetate (3 g/L) was used as eluent at a flow rate of 0.8 mL/min. The molecular weights were calculated with respect to poly(methyl methacrylate) standards (Polymer Laboratories, Mp = 580 Da up to Mp = 7.1*10⁶ Da).

Nuclear magnetic resonance spectroscopy (NMR)

¹³C{¹H} NMR (100.62 MHz) and ¹H NMR (400 MHz) spectra were recorded using a Varian Mercury Vx spectrometer at 25 °C. The samples were prepared by dissolving 20 mg of polymer in 1 mL MeOD-d₄ or 50 mg/ml using dimethylsulfoxide (DMSO-d₆) or dimethylformamide (DMF-d₇) as a solvent.

Dynamic light scattering (DLS) and ζ -potential measurements

DLS and ζ -potential measurements were performed to determine the dispersion characteristics on a Malvern ZetaSizer Nano ZS at 25 °C (polyurethane refractive index: 1.59). The average particle size and the particle size distribution of dispersions containing 0.1 wt% solids were determined according to ISO 13321 (1996). The ζ -potential was calculated from the electrophoretic mobility (μ) using the Smoluchowski relationship $\zeta = \eta\mu/\epsilon$ with $\kappa\alpha \gg 1$ and η is the solution viscosity, ϵ the dielectric constant of the medium, κ the Debye-Hückel parameter and α the particle radius. Data acquisition was performed using the ZetaSizer Nano Software.

Differential scanning calorimetry (DSC)

DSC measurements were performed on a TA Instruments DSC Q100. Samples were heated from -80 to 180 °C at a heating rate of 10 °C/min followed by an isothermal step for 5 min. A cooling cycle to -80 °C at a rate of 10 °C/min was performed prior to a second heating run to 180 °C at the aforementioned heating rate. The T_g was determined from the second heating run. The Universal Analysis 2000 software was used for data acquisition.

Potentiometric titration

Potentiometric titrations were performed using a Metrohm Titrino 785 DMP automatic titration device fitted with an Ag titrode. The samples were dissolved in CH₃OH, and the -NH_x groups (x=0-2) were titrated with a normalized 0.1 N HCl isopropanol solution, while the -COOH groups were titrated with a normalized 0.1 N KOH isopropanol solution. Blank measurements were carried out using the same amount of CH₃OH.

The molar mass of PUda was defined according to the following equation:

$$M_n = \frac{2m_{sample}}{(V_{sample} - V_{blank}) \times C_{HCl}},$$

the -NH_x content was defined according to the following equation:

$$N_{NHx} = \frac{(V_{sample1} - V_{blank1}) \times C_{HCl}}{m_{sample}},$$

the -COOH content was defined according to the following equation:

$$N_{COOH} = \frac{(V_{sample2} - V_{blank2}) \times C_{KOH}}{m_{sample}},$$

where V_{blank1} and V_{blank2} are the volumes of HCl and KOH solutions in mL needed for the blank experiment (average of two measurements), respectively; $V_{sample1}$ and $V_{sample2}$ the volumes of HCl and KOH solutions in mL consumed by the sample, respectively, C_{HCl} the

HCl concentration in isopropanol in mol/L, C_{KOH} the KOH concentration in isopropanol in mol/L, N_{NH_x} ($x=0-2$) the molar amount of $-\text{NH}_x$ groups in 1 gram of polymer (mol/g), N_{COOH} the molar amount of $-\text{COOH}$ groups in 1 gram of polymer (mol/g) and m_{sample} the sample weight in gram.

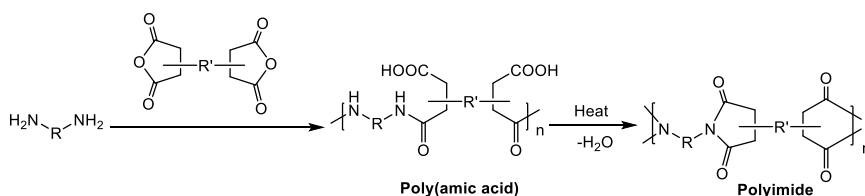
Evaluation of coatings

The coating performances were evaluated at room temperature by means of an acetone double rub test, a water resistance test, a reverse impact test and a pencil hardness test. In an acetone double rub test, the sample was rubbed back and forth with a cloth drenched in acetone. If no visual damage was observed after more than 150 rubs (75 double rubs), the acetone resistance of the coating was marked as good. In the water resistance test, the coating was immersed under water for 10 minutes. If no swelling was observed visually, the water resistance of the coating was marked as good. The reverse impact test was performed by dropping a 1 kg ball on the backside of a coated panel from a 100 cm height, as described in ASTM D2794. The pencil hardness test (ASTM D3363) was performed via pushing pencils with varying hardness value into the sample and the coating hardness was identified visually by the trace generated. The scale of pencil hardness ranges from 9H, the hardest scale, to 9B, the softest one.

6.3 Results and discussion

6.3.1 Model reaction study with diamine and dianhydride

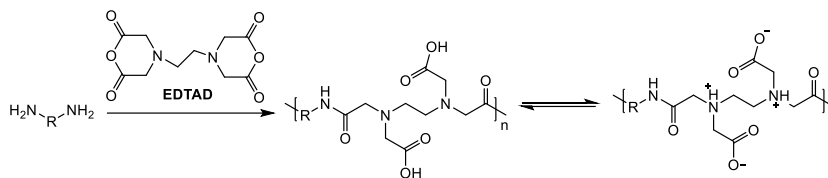
The reaction of a diamine and a dianhydride is commonly employed in polyimide production (Scheme 4).^{21,22} The intermediate poly(amic acid) (PAA) contains abundant carboxyl groups and could be utilized in the production of water-borne dispersions. Hence, water-dispersible PAAUs with pending carboxyl groups could be synthesized by polymerizing diamine-functional polyureas with a dianhydride and preventing full conversion into the corresponding polyimides.



Scheme 4. Preparation of polyimide from diamine and dianhydride.²¹

To investigate the rates of the diamine/dianhydride reactions and the corresponding M_n build up, model reactions were performed with a dianhydride and a long chain diamine PPGda2000 to mimic the diamine-functional polyureas. Ethylenediaminetetraacetic dianhydride (EDTAD) was selected as the dianhydride monomer since it is non-aromatic and therefore will not cause yellowing of the coating formulation during outdoor exposure. Additionally, the EDTAD molecule has two tertiary amines, which could be protonated by the carboxylic acid groups to generate potentially self-dispersible zwitterionic polymers (Scheme 5). For simplicity, the amic acid form of the EDTAD-based polymer will be drawn in the rest of the thesis, instead of the zwitterionic form. The bulk polymerization of PPGda2000/EDTAD

results in a highly viscous mixture, leading to inefficient stirring and to inhomogeneity. Thus, the reactions were performed in dimethylformamide (DMF), since it is a good solvent for EDTAD and PUs, which are used for preparing water-borne PAAUDs.²³ Polymerizations of PPGda2000/ EDTAD with different molar ratios were carried out at 80 °C in DMF for 1 hour. The M_n values of the various mixtures determined by HFIP-SEC are displayed in Figure 1.



Scheme 5. Polymerization of EDTAD and diamine to form zwitterionic PAAU.

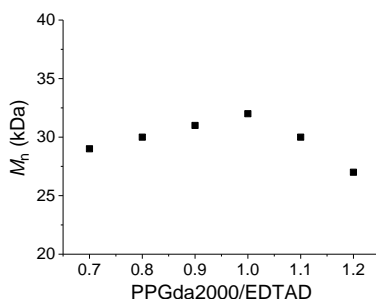
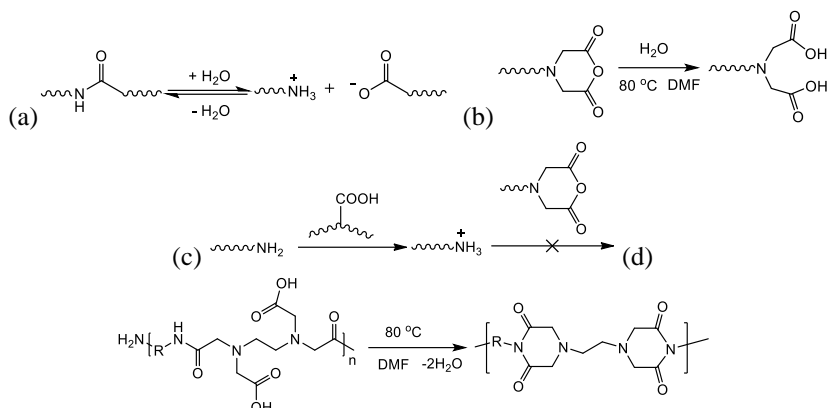


Figure 1. M_n values of PPGda2000/EDTAD mixtures with various molar ratios after 1 hour polymerization at 80 °C (HFIP-SEC).

For each combination, the M_n value reached approximately 30 kDa immediately after the dissolution of EDTAD in the solvent, and remained constant afterwards. This indicates a fast reaction between diamine and EDTAD. The M_n of 32 kDa measured for the PAA produced under stoichiometric conditions was lower than expected. This could be explained either by the hydrolysis of amide bonds present within the polymer, which would lead to the formation of ammonium carboxylate salts (Scheme 6a),²⁴ by the hydrolysis of anhydride end-groups into non-reactive diacids, resulting in an off-stoichiometry between the amine and anhydride groups (Scheme 6b) or by the reduction of the nucleophilicity of amine end-groups after protonation by the abundant COOH moieties (Scheme 6c). The water responsible for hydrolysis would originate from some imide formation, often observed during the synthesis of PAAs (Scheme 6d).²¹



Scheme 6. Hydrolysis of (a) amide bonds and (b) anhydride end-groups in PPGda2000/EDTAD mixture at 80 °C. (c) Loss of amine reactivity via protonation by –COOH moieties. (d) Generation of water via imide formation from PAA in DMF solution at 80 °C.^{21,24}

To further identify the side reactions occurring during the preparation of PAAs, a stoichiometric polymerization of PPGda2000 and EDTAD was carried out at 80 °C in deuterated DMF (DMF-*d*₆). A sample was collected after 1 hour and analyzed by ¹H and ¹³C{¹H} NMR. The presence of PAA was confirmed by a singlet at 8.01 ppm assigned to the amide proton (a) of the amic acid moiety in the ¹H NMR spectrum and two singlets at 170.2 and 172.8 ppm in ¹³C{¹H} NMR attributed to the carbonyl of the amide group (b) and the carboxyl group near the amide moiety (c), respectively (Figure 2). In addition, the hydrolysis of the anhydride end-groups was shown, evidenced by the presence of a resonance at 173.4 ppm, probably due to the carbonyls of a diacid end group (d), thereby limiting the *M_n* of PAA.

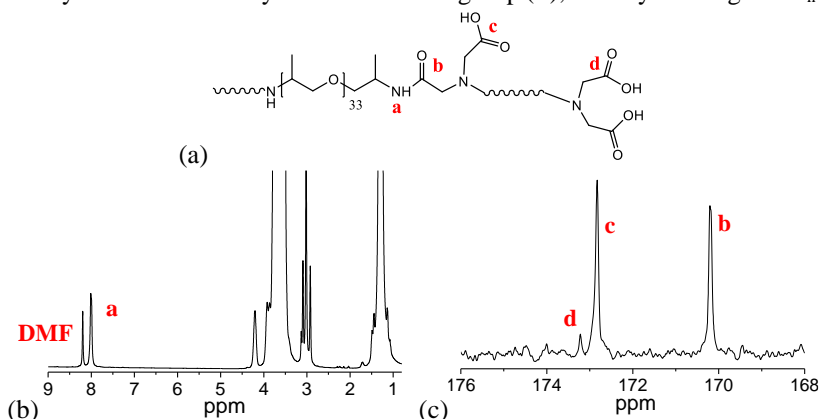


Figure 2. (a) PAA prepared from PPGda2000 and EDTAD. (b) ¹H and (c) ¹³C{¹H} NMR of a stoichiometric PPGda2000/ EDTAD mixture after 1 hour in DMF-*d*₇.

The possible formation of imide was investigated via model reactions with 3-butoxypropylamine (BPA) and EDTAD in 2/1 molar ratio in DMF-*d*₇ at 80 °C in a closed set-up or under argon flow (Figure 3a). Both reactions were monitored by ¹H NMR. Figures 3b

and 3c present the ^1H NMR spectra of the reaction mixture at t_0 and after 12 hours reaction in a closed set-up, respectively. The latter was characterized by two triplets at 3.95 and 1.1 ppm, assigned to the methylene protons next to the imide (**a**) and the methyl protons in BPA (**b**). The much lower intensity of **a** compared to **b** indicates a limited formation of imide during the polymerization in a closed set-up. However, applying an argon flow for 12 hours led to a significant increase of the intensity of **a** (Figure 3d). This is caused by the shift of the equilibrium of imidization to the imide side due to removal of water by the argon flow.

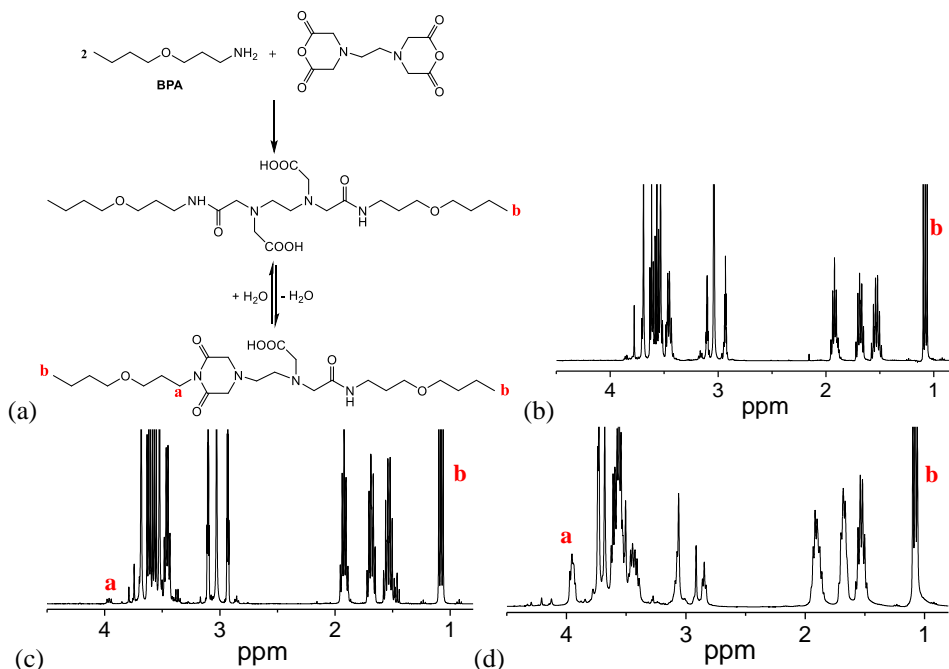
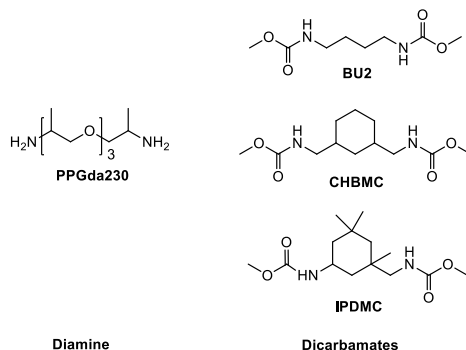


Figure 3. (a) Reaction scheme of 2/1 ratio of BPA/EDTAD. ^1H NMR of BPA/EDTAD (2/1 ratio) reaction in a closed set-up at (b) 0 h and (c) 12 hours. (d) ^1H NMR of BPA/EDTAD (2/1 ratio) under argon flow after 12 hours.

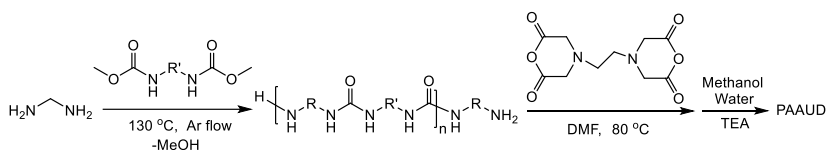
6.3.2 Poly(amic acid urea) dispersions (PAAUDs)

Similarly to the synthesis of PAAs from diamines and EDTAD, poly(amic acid urea)s (PAAUs) were produced via polymerization of EDTAD and diamine-functional polyureas (PUDas). The latter were obtained from polymerization of dicarbamates and a molar excess of diamines. To increase the hydrophobicity of the PAAUs, and thereby enhancing the stability of the dispersions, PPGda230 was used as diamine. Three dicarbamates were employed including the linear BU2, the cyclic ring-containing 1,3-cyclohexanebis(methylamine) (CHBMA) and isophorone dimethylcarbamate (IPMDC) (Scheme 6).



Scheme 6. Diamine and dicarbamates used in the synthesis of PUDas.

Thus, PUDas with M_n values between 1,780 and 2,150 Da, determined by potentiometric titration, were synthesized from polymerizations of PPGda230 and one of the dicarbamates presented in Scheme 6 with a molar ratio of 1.3/1. The absence of carbamate signals in the corresponding $^{13}\text{C}\{^1\text{H}\}$ NMR spectrum indicates that the PUDas were (predominantly) diamine-functional. These PUDas were then dissolved in DMF and reacted with EDTAD. However, the DMF solutions of both BU2- and CHBMC-based PUDas showed physical gelling at room temperature due to the strong hydrogen bond interactions between BU2 or CHBMC segments. Such interactions were much weaker for IPDMC-based PUDas, due to the asymmetric structure and the pending methyl groups of the isophorone backbone that disrupt the hydrogen bond formation between the urea moieties. These IPDMC-based PUDas were then polymerized with stoichiometric amounts of EDTAD to form PAAU solutions. The solutions were then precipitated in water and washed with water to remove DMF, followed by drying in a vacuum oven overnight at 80 °C (Scheme 7).



Scheme 7. General preparation procedure of a PAAUD.

Similarly to PAAs, the successful preparation of PAAUs was confirmed by the presence of amic acid moieties within the polymer chains, as evidenced by ^1H and $^{13}\text{C}\{^1\text{H}\}$ NMR. (Figure 4). However, due to the overlapping of proton signals of the isophorone fragments and the end-groups of PPGda units, ^1H NMR proved to be unsuitable to determine the M_n s of the polymers (see also Chapter 3). HFIP-SEC measurements indicated that the M_n s of the obtained PAAUs were around 30 kDa, which are close to the M_n s of commercial PUUD systems (Table 1).²⁵ These PAAUs were then dissolved in methanol and neutralized with trimethylamine (TEA, one molar equivalent with respect to the carboxyl groups as determined by potentiometric titration), followed by dispersion into water and evaporation of methanol to generate PAAUDs. As expected, partial dissolution of the low M_n part of both BU2- and CHBMC-based PAAUDs in water resulted in physical gelation of the dispersions after 24 hours. Such gelation can cause wrinkling or rough surfaces during coalescence of

coating films due to the inhomogeneity of the dispersions. Therefore, only the IPDMC-based PAAUDs were used for further investigations.

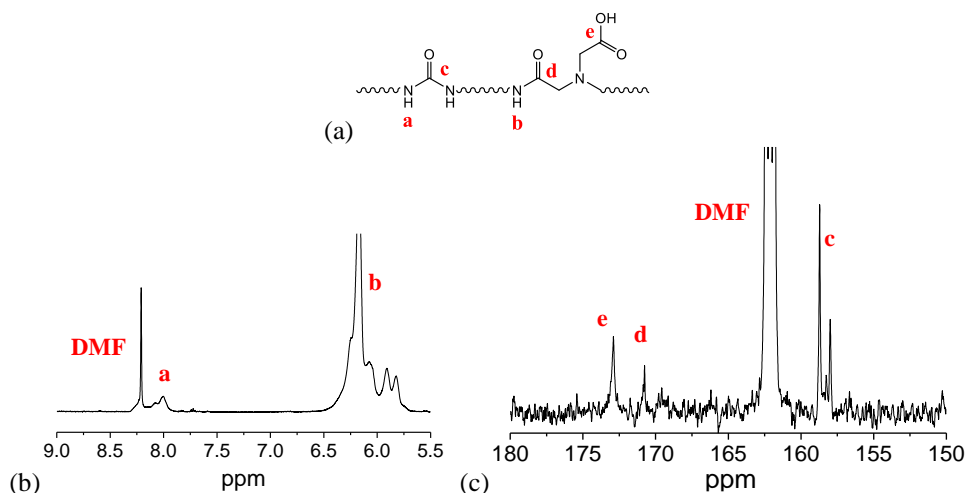


Figure 4. (a) Simplified structure of PAAU. (b) ¹H and (c) ¹³C{¹H} NMR of PAAUs prepared from PUda and EDTAD (DMF-*d*₇).

The IPDMC-based PAAU generated a stable dispersion, as expected in view of the ζ -potential of -41 mV, with an average particle size of 14 nm, much smaller than the commercially available PUUDs (> 50 nm). Particles of small sizes can give highly viscous dispersions especially at high solid contents, which is not favored during coating formation.^{26,27} However, the particle sizes can be adjusted to desired values by varying the concentration of either the neutralization agent (TEA) or the ionic groups, by using PUdas of different M_n s or varying the PUdas/EDTAD ratios.²⁸

Table 1. Properties of the PAAU resins and resulting dispersions prepared from EDTAD and PUdas with different dicarbamate building blocks and PPGda230 as monomers.

Dicarbamates	M_n of PUda ^a (Da)	M_n of PAAU ^b (kDa)	Av. particle size (nm) ^c	ζ -potential (mV) ^c
IPDMC	2,150	28	14	-41
BU2	1,950	36	N.A. ^d	N.A.
CHBMC	1,780	31	N.A.	N.A.

^a) Determined by potentiometric titration; ^b) determined by SEC in HFIP; ^c) determined by DLS;

^d) not available due to physical gelation.

6.3.3 Effect of the TEA/-COOH molar neutralization ratio on the PAAUD particle sizes

As discussed in section 6.3.1, the PAAUs prepared from EDTAD are zwitterionic due to the presence of tertiary amines in the backbone, which can pick up protons from the pendent COOH groups, and therefore can self-disperse in water. However, the absence of TEA results

in precipitation during the dispersion process. Thus, various amounts of TEA were employed to neutralize the carboxylic acid groups of a PAAU, obtained via stoichiometric polymerization of EDTAD and a PUda, to different degrees. The applied PUda was produced from excess PPGda230 and IPDMC with a molar ratio of 1.3/1. The plots of the average particle sizes and the ζ -potentials of the PAAUDs vs. the TEA/-COOH ratio are displayed in Figure 5.

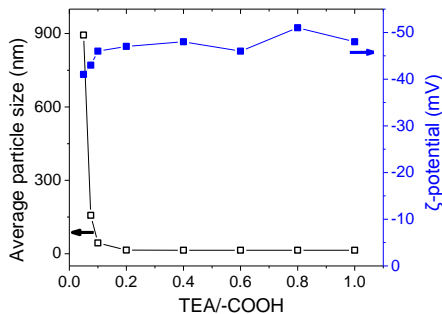


Figure 5. Particle sizes and ζ -potentials of PAAUDs prepared via stoichiometric polymerization of EDTAD and PUda (synthesized using a 1.3/1 molar ratio of PPGda230/IPDMC) and neutralized with different TEA/-COOH molar ratios.

An average particle size of 900 nm was observed upon addition of 5 mol% of TEA with regard to the -COOH groups. The dispersion partially agglomerated after 24 hours at room temperature. This is probably caused by the depletion interaction, an attraction force arising from an increase in osmotic pressure of the surrounding solution when colloidal particles get close enough such that the excluded co-solutes, such as PAAUs with low M_n s, do no longer fit in between these colloidal particles.²⁹ Increasing the TEA/-COOH molar ratio to 0.075 caused a drastic decrease of the particle size to 160 nm. For this and higher TEA/-COOH molar ratios, the dispersion was stable and no precipitation occurred even after 30 days. The particle sizes remained constant at a value of 14 nm for TEA/-COOH molar ratios above 0.1. Although the ζ -potentials of all these PAAUDs studied were below -40 mV, the abrupt change of particle sizes within a small variation of TEA/-COOH molar ratio indicates that the size of the particles cannot be readily controlled by simply changing the concentration of the neutralization agent.

6.3.4 Effect of PUda/EDTAD molar ratio on the PAAUD particle size

Another strategy to increase the particle sizes, and accordingly reduce the viscosity of the emulsions, is based on the reduction of the concentration of ionic groups in the PAAUs, but still target 100% neutralization of the pendent COOH groups, which can be achieved by increasing the PUda/EDTAD molar ratio. Thus, a PUda with an M_n of 2150 Da (determined by potentiometric titration) was synthesized from a 1.3/1 molar ratio of PPGda230 and IPDMC, followed by polymerization with different amounts of EDTAD to generate PAAUs of different molecular weights, which were subsequently neutralized with one equivalent of TEA with regard to the amount of carboxylic acid groups present and finally dispersed in water. The M_n s and the -COOH concentrations (mmol/g) of the PAAUs as well as the particle sizes of the dispersions are displayed in Table 2.

As expected, an increase of the PUda/EDTAD molar ratio results in a reduction of the –COOH content of the PAAU and accordingly in dispersions with larger particles. The dispersions have high ζ -potentials of -40 to -50 mV, and remained stable after 30 days at 40 °C. However, the M_n values of the PAAUs decreased from 30 kDa to 12 kDa with increasing PUda/EDTAD molar ratio from 1.0/1 to 2.0/1. Although the particle sizes of the dispersion of the resin produced from the high PUda/EDTAD molar ratio of 2/1 are comparable to those in commercial PUR systems, the M_n value of the PAAU of 12 kDa is much lower than those of the PURs used in conventional coatings (above 30 kDa with D_M higher than 3).²⁵ Thus, these PAAUDs are not suitable for the preparation of coatings exhibiting the desired mechanical properties.

Table 2. Properties of the PAAU resins and resulting dispersions prepared from various molar ratios of PUda/EDTAD

PUda/ EDTAD	M_n^a (kDa)	D_M^a	-COOH content ^b (mmol/g)	Av. particle size ^c (nm)	ζ -potential ^c (mV)
2.0/1	12	1.1	0.33	48	-45
1.8/1	14	1.2	0.38	42	-50
1.6/1	18	1.3	0.43	36	-48
1.4/1	23	1.5	0.48	20	-49
1.2/1	25	1.5	0.54	16	-42
1.0/1	30	1.6	0.59	14	-48

^{a)} Determined by SEC in HFIP; ^{b)} determined by potentiometric titration; ^{c)} determined by DLS.

6.3.5 Effect of the molecular weight of PUda on the PAAUD particle size

An alternative approach to reduce the ionic group density in PAAUs involves enhancing the M_n of the PUDas. This would enable us to reduce the concentration of ionic groups and at the same time retain the desired high M_n values. Additionally, PUda with PPGda and IPDMC segments are hydrophobic. One should realize that longer PUda chains lead to PAAUs with higher hydrophobicity and consequently request more ionic groups for stabilization. By controlling the ionic group concentration along the PAAU chains it should be possible to control the particle sizes of the corresponding PAAUDs and accordingly tune the viscosity of the emulsions. PUDas with different PPGda230/IPDMC ratios were synthesized with M_n s ranging from 950 to 4750 Da as determined by potentiometric titration. These PUDas were then polymerized with a stoichiometric amount of EDTAD. The resulting PAAUs were then neutralized with a stoichiometric amount of TEA and dispersed in water to generate PAAUDs. The M_n s of the PUDas, the glass transition temperature (T_g), M_n and –COOH content of the PAAUs as well as the particle sizes of the corresponding PAAUDs are presented in Table 3.

Table 3. Properties of the PAAU resins and the resulting dispersions prepared from stoichiometric amounts of PUDas and EDTAD

PPGda230 /IPDMC	M_n of PUda (Da) ^a	M_n of PAAU (kDa) ^b	T_g (°C) ^c	-COOH content of PAAU ^a (mmol/g)	Av. particle size (nm) ^d	ζ -potential (mV) ^d
1.1/1	4,750	34	96	0.20	61	-42
1.2/1	2,950	32	88	0.43	38	-40
1.3/1	2,150	28	73	0.59	14	-41
1.4/1	1,700	26	65	0.83	9	-47
1.7/1	1,200	26	49	1.25	8	-50
2.0/1	950	25	41	1.54	8	-52

^{a)} Determined by potentiometric titration; ^{b)} determined by SEC in HFIP; ^{c)} determined by DSC; ^{d)} determined by DLS.

Higher molar ratios of PPGda230/IPDMC, deviating more and more from the stoichiometric ratio, led to PUDas³⁰ and consequently PAAUs of lower M_n s. The T_g s of these PAAUs decreased from 96 to 41 °C with decreasing M_n of PUDas, as a result of the lower content of isophorone moieties, the presence of which significantly contributes to the increase of the T_g s of these PAAUs (see Chapter 3). PUDas with higher M_n s, which contain less amine end-groups, react with less EDTAD to build up high molecular weight materials. These high M_n polymers contain relatively low amounts of dispersing EDTAD groups and therefore gave large particles during dispersion. Higher conversion of functional groups are required for the reaction between EDTAD and PUDas with lower M_n s during the same polymerization time. This may result in somewhat lower M_n values of the resulting PAAUs, which have relatively high EDTAD contents, leading to smaller particles. In addition, higher EDTAD contents in the PAAU synthesis may result in a higher amount of M_n -limiting side reactions (see Scheme 6 a-c).

To further adjust the particle sizes of the dispersions to the requirements for industrial PUUDs, the PAAUs described in Table 3 were neutralized with various amounts of TEA and then dispersed in water. The particle sizes of the resulting dispersions, measured by DLS, are reported in Figure 6.

Thus, longer PUda segments led to more hydrophobic PAAUs and consequently larger particles, as indicated in Figure 6a. Moreover, the increase of the hydrophobicity of the PAAUs also resulted in a less drastic change of the particle size upon small variations of the TEA/-COOH ratio. The particle sizes of the PAAUDs prepared from a PUda with M_n of 4,750 Da (PUda₄₇₅₀) varied from 60 to 100 nm when the molar ratio of TEA/-COOH decreased from 1/1 to 0.5/1. The influence of the TEA/-COOH ratio on the pH of the PUda₄₇₅₀-based PAAUDs was investigated and displayed in Figure 6b. As expected, a linear relation was observed between TEA loading and pH. The latter raised from 7 to 8.1 as the TEA/-COOH molar ratio increased from 0.66-1. These pH values of the PAAUDs were close to those of the commercial PUUDs (pH = 7-8) and accordingly are expected to be compatible with the corresponding additives in the standard formulations.⁴

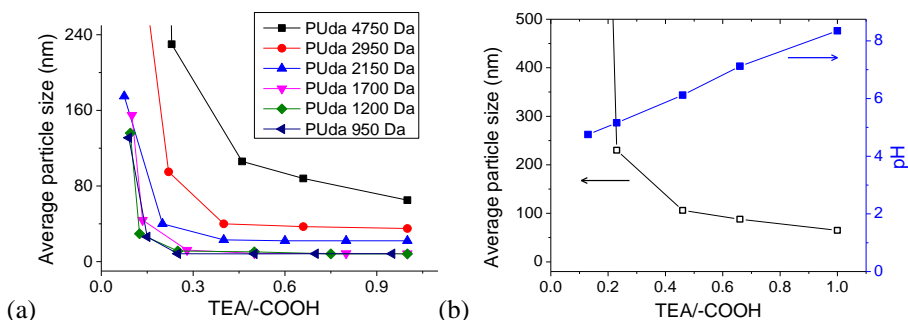


Figure 6. (a) Particle sizes of PAAUDs with different lengths of PUda segments and different molar ratios of TEA/-COOH. (b) Particle sizes and pH of PAAUDs prepared from PUda₄₇₅₀ with different molar ratios of TEA/-COOH.

Another noticeable observation is the difference between the theoretical and experimental carboxylic acid contents in the PAAUs. For a stoichiometric PUda/EDTAD reaction, each amine generates one carboxylic acid group in the resulting PAAU. Thus, the theoretical carboxylic acid content in the PAAUs coincides with the number of amines in the corresponding PUda. The theoretical and experimental carboxylic acid contents for each PAAU presented in Table 3 are listed in Table 4.

The theoretical -COOH contents of PAAUs are 1.5-2 times higher than the experimental ones, indicating a reduction of the number of carboxylic acid groups during the preparation of the resins. This is most probably caused by the loss of material with high -COOH contents, especially the low molecular weight fractions, during the purification of PAAUs and the formation of imide moieties, which consumes carboxylic acids as shown in Scheme 5c. As indicated in Figure 3, the imidization probably takes place during the drying process of the PAAU at 80 °C under vacuum rather than during the diamine/EDTAD reaction, which proceeds in a closed set-up without water elimination. Please note that the carboxylic acid content of a PAAU resin based on PUda₄₇₅₀ and EDTAD could be increased from 0.20 to 0.33 mmol/g upon freeze-drying, thereby avoiding the treatment at elevated temperature and limiting the imidization side reaction.

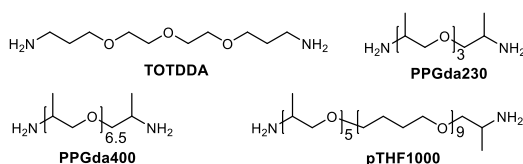
Table 4. Theoretical and experimental carboxylic acid content of PAAUs prepared from PUDas with different molecular weights

M_n of PUda ^a (Da)	Experimental -COOH content of PAAU ^a (mmol/g)	Theoretical -COOH content of PAAU (mmol/g)
4,750	0.20	0.42
2,950	0.43	0.68
2,150	0.59	0.93
1,700	0.83	1.18
1,200	1.25	1.67
950	1.54	2.11

^{a)} Determined by potentiometric titration.

6.3.6 Water-borne poly(amic acid urea) coatings

PUDas were synthesized with various diamines *viz.* 4,7,10-trioxa-1,13-tridecanediamine (TOTDDA), PPGda400, PPGda230 and pTHF1000, a PPG/pTHF block copolymer with amine end-groups, in combination with different ratios of IPDMC (Scheme 8). These PUDas were then polymerized with stoichiometric amounts of EDTAD to generate PAAUs. After neutralization with TEA and dispersion into water, stable PAAUDs of 10 wt% solid content were obtained with high ζ -potential close to -50 mV and particle sizes between 40-150 nm. By applying the PAAUDs on aluminum panels and drying at 50 °C overnight, PAAU-based coatings with thicknesses of 20-30 μ m were produced. The coatings were evaluated by means of pencil hardness, impact resistance, acetone and water resistance tests. The results are summarized in Table 5.



Scheme 8. Diamines employed in the synthesis of PAAU coatings.

The M_n s of the PAAUs range from 28 to 42 kDa. The coatings prepared from TOTDDA-based PAAUs have moderate T_g s between 16-32 °C, with hardnesses of 3B and good impact resistance, with the exception of the coating prepared from the resin obtained when applying a TOTDDA/IPDMC ratio of 1.1/1. Although the high density of urea moieties in the TOTDDA-based PAAUs promotes a good resistance against acetone, the resulting coatings swell in water due to the hydrophilicity of the TOTDDA-based urea segments. The low T_g s of the PPGda400-based resins led to soft coatings (< 4B) with good impact resistance. The low urea density of these coatings also results in poor acetone resistance, while moderate water resistance was observed as a result of the hydrophobicity of the PPG segments and the lower urea content in comparison with the TOTDDA-based system. The T_g s of PAAUs based on PPGda230 were much higher than those produced from PPGda400 (75-96 °C *vs.* -4-10 °C) due to the higher urea density of PPGda230-based PAAUs, as a result of the lower molar mass of PPGda230. The high T_g values also give rise to coatings hardnesses higher than the F qualification. However, the latter were brittle and failed the reverse impact tests as a result of high moduli and low entanglement densities of the materials due to their high T_g s and insufficiently M_n s, respectively. The pTHF1000-based PAAU coatings were very soft (< 6B) due to the low T_g values of the parent resins. Their resistance towards acetone was poor because of the low urea density. However, the strong hydrophobicity of the pTHF segments provided coatings with good water resistance. Thus, to compensate the moderate water resistance and poor impact resistance of the PPGda230-based PAAU coatings, mixtures of 10-20 mol% of pTHF1000 and 90-80 mol% PPGda230 were employed as diamines for the preparation of PAAUs. The resulting coatings had moderate T_g s and hardness but passed the impact tests due to the flexible pTHF1000 segments. The high density of urea moieties issued from the short PPGda230 moiety and the hydrophobic pTHF chain resulted in PAAU coatings with good acetone and water resistance.

Table 5. M_n , T_g and coating properties of PAAUs prepared with TOTDDA, PPGda400, PPGda230 and pTHF1000 as diamines, IPDMC as dicarbamate and EDTAD as dianhydride.

Diamines	Diamine/ IPDMC	M_n (kDa) ^a	T_g (°C) ^b	Pencil hardness	Impact test	Acetone resistance	Water resistance ^c
TOTDDA	1.1/1	36	32	3B	-	+	-
TOTDDA	1.2/1	35	23	3B	+	+	-
TOTDDA	1.3/1	38	16	3B	+	+	-
PPGda400	1.1/1	39	10	4B	+	-	±
PPGda400	1.2/1	34	3	5B	+	-	±
PPGda400	1.3/1	31	-4	5B	+	-	±
PPGda230	1.1/1	34	96	H	-	+	±
PPGda230	1.2/1	32	88	F	-	+	±
PPGda230	1.3/1	28	73	HB	-	+	±
pTHF1000	1.1/1	42	< -60	< 6B	+	-	+
pTHF1000	1.2/1	36	< -60	< 6B	+	-	+
pTHF1000	1.3/1	39	< -60	< 6B	+	-	+
pTHF1000 (10 mol%) +PPGda230 (90 mol%)	1.1/1	37	57	HB	+	+	+
pTHF1000 (20 mol%) +PPGda230 (80 mol%)	1.1/1	35	42	B	+	+	+

^a) Determined by HFIP-SEC; ^b) determined by DSC; ^c) +: no swelling, ±: swelling without softening, -: swelling and softening.

6.4 Conclusions

In this work, ethylenediaminetetraacetic dianhydride (EDTAD) was employed for the synthesis of water-dispersible poly(amic acid urea)s (PAAUs). Model reactions with a stoichiometric ratio of EDTAD and poly(propylene glycol) bis(2-aminopropyl ether) with molecular weight 2000 Da (PPGda2000) generated poly(amic acid)s (PAAs), as evidenced by ¹H and ¹³C{¹H} NMR. Imidization was observed during the PAA formation and was promoted by removal of water from the system. Poly(amic acid urea)s (PAAUs) were synthesized by polymerization of EDTAD and diamine-functional polyureas (PUDas), which were produced from poly(propylene glycol) bis(2-aminopropyl ether) with a molecular weight of 230 Da (PPGda230) and isophorone dimethylcarbamate (IPDMC). These PAAU resins generated stable water-borne dispersions (PAAUDs), the particle sizes of which could be adjusted by varying either the concentration of neutralization agent or the carboxyl content

in PAAU. The latter was influenced by the M_n of the PUda and by the PUda/EDTAD ratio. PAAU coatings were prepared from different diamines including 4,7,10-trioxa-1,13-tridecanediamine (TOTDDA), poly(propylene glycol) bis(2-aminopropyl ether) with a molecular weight of 400 Da (PPGda400), PPGda230 and poly(tetrahydrofuran)/PPGda block copolymer with a molecular weight of 1000 Da (pTHF1000). PAAU coatings with optimum properties were obtained by using PPGda230/pTHF1000 mixtures as diamines. These coatings have good solvent resistance and mechanical properties, as a result of their high urea density, chain flexibility and hydrophobicity.

6.5 References

- (1) Zhou, X.; Li, Y.; Fang, C.; Li, S.; Cheng, Y.; Lei, W.; Meng, X. *J. Mater. Sci. & Technol.* **2015**, *31*, 708-722.
- (2) Dieterich, D. *Prog. Org. Coat.* **1981**, *9*, 281-340.
- (3) Sardon, H.; Irusta, L.; Fernández-Berridi, M. J. *Prog. Org. Coat.* **2009**, *66*, 291-295.
- (4) Markus, P. H.; Rosthauser, J. W.; Beatty, M. C. US Patent 4501852 A, **1985**.
- (5) Nanda, A. K.; Wicks, D. A. *Polymer* **2006**, *47*, 1805-1811.
- (6) Wey, Y.; Luo, Y.; Li, B. *Colloid Polym. Sci.* **2005**, *283*, 1289-1297.
- (7) Saw, L. K.; Brooks, B. W.; Carpenter, K. J.; Keight, D. V. *J. Colloid Interface Sci.* **2003**, *257*, 163-172.
- (8) Saw, L. K.; Brooks, B. W.; Carpenter, K. J.; Keight, D. V. *J. Colloid Interface Sci.* **2004**, *279*, 235-243.
- (9) Sardon, H.; Irusta, L.; Fernández-Berridi, M. J.; Luna, J.; Lansalot, M.; Bourgeat-Lami, E. J. *J. Appl. Polym. Sci.* **2011**, *120*, 2054-2062.
- (10) Lee, D. -K.; Tsai, H. -B.; Yang, Z. -D.; Tsai, R. -S. *J. Appl. Polym. Sci.* **2012**, *126*, E275-E282.
- (11) Dochniak, Y. D.; Michael, J.; Stammler, S. US Patent 5703158 A, **1997**.
- (12) Breucker, L.; Landfester, K.; Taden, A. *ACS Appl. Mater. Interfaces*, **2015**, *7*, 24641-24648.
- (13) Bullermann, J.; Spohnholz, R.; Friebe, S.; Salthammer, T. *J. Polym. Sci., Part A: Polym. Chem.* **2014**, *52*, 680-690.
- (14) Kim, C. K.; Kim, B. K.; Jeong, H. M. *Colloid. Polym. Sci.* **1991**, *269*, 895-900.
- (15) Lorenz, O.; August, H. -J.; Hick, H.; Triebs, F. *Angew. Makromol. Chem.* **1977**, *63*, 11-22.
- (16) Kreye, O.; Mutlu, H.; Meier, M. A. R. *Green Chem.* **2013**, *15*, 1431-1455.
- (17) Noble, K. L. *Prog. Org. Coat.* **1997**, *32*, 131-136.
- (18) Sugano, S.; Chinwanitchaen, C.; Kanoh, S.; Yamada, T.; Hayashi, S.; Tada, K. *Macromol. Symp.* **2006**, *239*, 51-57.
- (19) Manvi, G. N.; Jagtap, R. N. *J. Disper. Sci. Technol.* **2010**, *31*, 1376-1382.
- (20) Tang, D.; Mulder, D. J.; Noordover, B. A. J.; Koning, C. E. *Macromol. Rapid Commun.* **2011**, *32*, 1379-1385.
- (21) Tian, X.; Jiang, X.; Lu, H.; Huang, D. *Ind. J. Chem. Tech.* **2012**, *19*, 271-277.
- (22) Ando, S.; Matsuura, T.; Sasaki, S. *Macromolecules* **1992**, *25*, 5858-5860.
- (23) Bower, G. M.; Frost, L. *J. Polym. Sci., Part A: Polym. Chem.* **1963**, *10*, 3135-3150.
- (24) Dine-Hart, R. A.; Wright, W. W. *J. Appl. Polym. Sci.* **1967**, *11*, 609-627.

- (25) Jang, J. Y.; Jhon, Y. K.; Cheong, I. W.; Kim, J. H. *Colloid. Surf. A: Physicochem. Eng. Asp.* **2002**, *196*, 135-143.
- (26) Luckham, P. F.; Michael, A. U. *J. Colloid Interface Sci.* **1999**, *220*, 347-356.
- (27) Wang, T.; Ni, M.; Luo, Z.; Shou, C.; Cen, K. *Chin. Sci. Bull.* **2012**, *57*, 3644-3651.
- (28) Chattopadhyay, D. K.; Raju, K. V. S. N. *Prog. Polym. Sci.* **2007**, *32*, 352-418.
- (29) Tuinier, R.; Rieger, J.; de Kruif, C. G. *Adv. Colloid Interface Sci.* **2003**, *103*, 1-31.
- (30) Carothers, W. H. *Trans. Faraday Soc.* **1936**, *1*, 39-49.

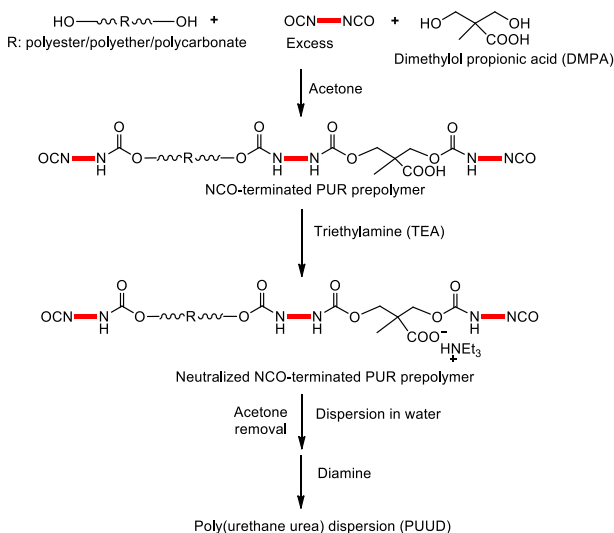
Chapter 7. Curing of polyurea coatings

Summary

The curing of polyureas (PUs) and the evaluation of the corresponding coating systems are reported in this chapter. The complicated curing mechanism of amine- and amic acid groups containing poly(amic acid urea) dispersions (PAAUDs), using ethylenediaminetetraacetic dianhydride (EDTAD) as internal dispersing agent, was investigated via a model reaction with 3-butoxypropylamine (BPA) and ethylenediaminetetraacetic dianhydride (EDTAD) as substrates at 150 °C under argon flow. The reaction exhibited the formation of cyclic and noncyclic imides, amides and imidines. The formation rates of both the noncyclic imide and the amide were enhanced by the addition of phosphoric acid (H_3PO_4) as catalyst. Curing of poly(amic acid urea) (PAAU) coatings in the presence of H_3PO_4 resulted in significant improvements of mechanical properties and solvent resistance. PUs prepared from poly(propylene glycol) bis(2-aminopropyl ether) with an M_n of 400 Da (PPGda400), 3,3'-diamino-*N*-methyldipropylamine (DMDPA) and isophorone dimethylcarbamate (IPDMC) were neutralized by polyacids and dispersed in water. Stable polyurea dispersions (PUDs) were obtained with ethylenediaminetetraacetic acid (EDTA) and succinic acid (SA) as neutralization agents. Curing of EDTA-based PU coatings resulted in enhanced hardness, impact and acetone resistance due to the formation of amide bonds between the carboxylic acids in EDTA and the amine end-groups in PUs.

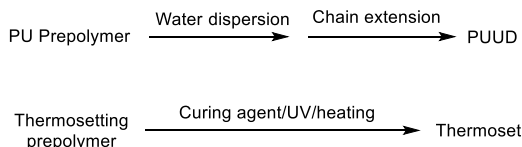
7.1 Introduction

Water-borne polyurethane urea dispersions (PUUDs) are generally prepared in four steps. First, an isocyanate-terminated PUR prepolymer is synthesized in a volatile organic solvent like acetone via the reaction of a diol with an excess of diisocyanate and an internal dispersing agent (IDA), usually carrying a carboxylic acid group. The prepolymers are then neutralized by a volatile amine such as triethylamine (TEA) and dispersed in water, followed by acetone evaporation and chain extension with a diamine to obtain high molecular weight PUUDs (Scheme 1).¹ These PUUDs can be applied on various substrates, like steel, plastics and wood, to form polyurethane (PUR) coatings with satisfactory material properties.

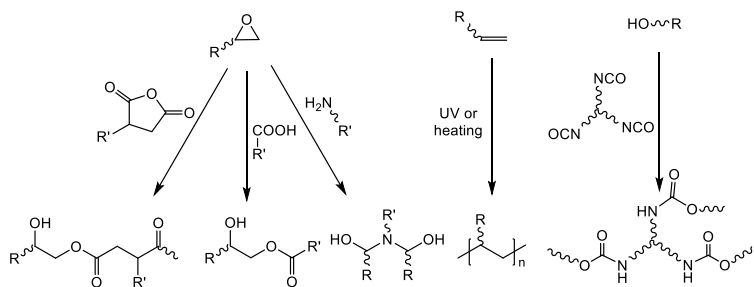


Scheme 1. Industrial synthesis of high molecular weight poly(urethane urea) dispersions.¹

Alternatively, if the MWs of the synthesized polymers are insufficiently high, crosslinking reactions can be used for improving the material properties, similarly to thermosets, which are produced via curing of thermosetting prepolymers by irradiation, heating or addition of curing agents (Scheme 2). For example, epoxy resins are commonly cured by di- or polyamines,² polycarboxylic acids³ or anhydrides,⁴ acrylic resins via UV radiation or heating⁵ and hydroxyl-functional polymers by multi-functional (blocked) isocyanates^{6,7} (Scheme 3). The increase of polymer molecular weight or crosslink density is accompanied by a raise of tensile and shear moduli and, thereby, enhanced mechanical properties.^{8,9}

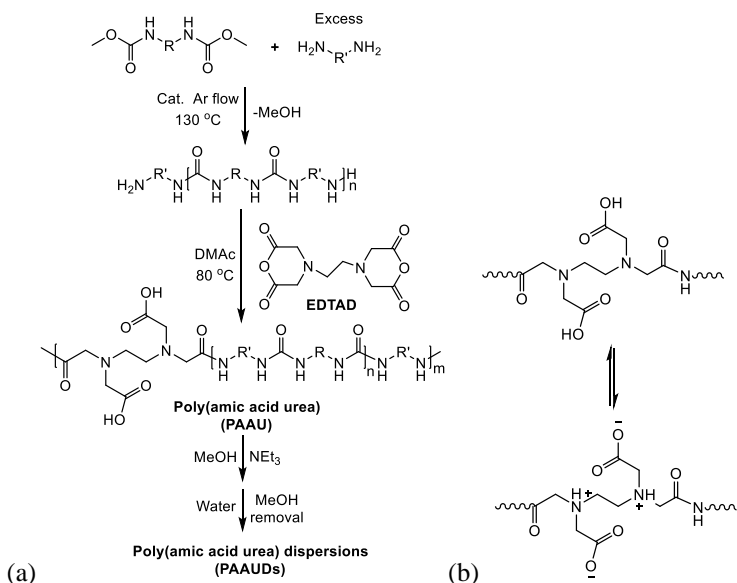


Scheme 2. Chain extension and curing of prepolymers to improve the material properties of resins.

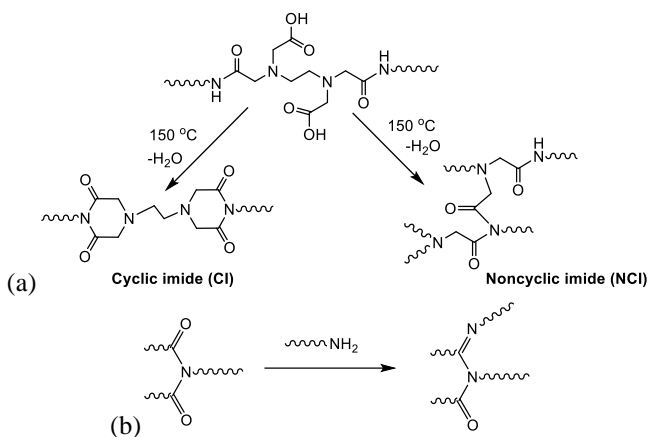


Scheme 3. Crosslinking of epoxides, acrylics and hydroxyl-functional polymers.²⁻⁷

The production of anionically stabilized aqueous poly(amic acid urea) dispersions (PAAUDs) with ethylenediaminetetraacetic dianhydride (EDTAD) as internal dispersing agent was described in Chapter 6 (Scheme 4a). The amic acids in the PAAUs could form zwitterionic species by proton exchange between the carboxylic acids and the tertiary amines of EDTAD-derived moieties (Scheme 4b). The reaction between the carboxylic acids and primary/secondary amines in the corresponding PAAU coatings can lead to crosslinked structures. Such an amide formation reaction normally occurs above 100 °C, which is also favorable for efficient water removal,¹⁰ and can be catalyzed by phosphoric acid-¹¹ and boric acid derivatives^{12,13}. In addition to the formation of cyclic imide structures mentioned in Chapter 6, intermolecular imidization between carboxylic acids and amides^{14,15} as well as the generation of imidine structures from amines and imides¹⁶ could also take place during the curing of PAAU, promoting the crosslinking of the material (Scheme 5). Hence, the possibly complicated curing chemistry of PAAUD at elevated temperatures was studied via model reactions between 3-butoxypropylamine (BPA) and EDTAD. Similarly, the crosslinking of cationically stabilized PUDs, synthesized in Chapter 3, was carried out with polyacids, acting also as neutralization agents for the corresponding PUDs. Both types of dispersions were cured at temperatures ranging from 50 to 150 °C and then evaluated.



Scheme 4. (a) Preparation of poly(amic acid urea) dispersions. (b) Proton exchange between the tertiary amine and the carboxylic acid in the EDTAD-derived moiety in PAAU.



Scheme 5. (a) Cyclic and noncyclic imide formation from poly(amic acid)s. (b) Imidine formation from imides.

7.2 Experimental Section

7.2.1 Materials

All reagents were commercially available unless specified otherwise. Ethylenediaminetetraacetic dianhydride (EDTAD, 99%), isophorone diamine (IPDA, *cis* and *trans* mixture, 99%), 1,2,4,5-cyclohexanetetracarboxylic dianhydride (CHTCD, 99%), 3,3'-diamino-*N*-methyl dipropylamine (DMDPA, 96%), 4,7,10-trioxo-1,13-tridecanediamine

(TOTDDA, 97%), 3-butoxypropylamine (BPA, 99%), poly(propylene glycol) bis(2-aminopropyl ether) with average M_n of 230 and 2000 Da (PPGda230 and PPGda2000), ethylenediaminetetraacetic dianhydride (EDTAD, 99%), triethylamine (TEA, 99%), acetic acid (99.7%), 1,5,7-triazabicyclo[4.4.0]dec-5-ene (TBD, 98%), dimethyl carbonate (DMC, 99%), tin(II) chloride (SnCl_2 , 99.99%), zinc chloride (ZnCl_2 , 98%), aluminum chloride (AlCl_3 , 99.99%), magnesium chloride (MgCl_2 , 99.9%), boric acid (H_3BO_3 , 99.5%), phosphoric acid (H_3PO_4 , 99%), sulfuric acid (H_2SO_4 , 98%), dimethylformamide (DMF, anhydrous, 99.8%) and sodium sulfate (99%, anhydrous) were purchased from Sigma Aldrich. A diamine-functional pTHF/PPG copolymer with a molecular weight of 1000 Da (pTHF1000) was purchased from Huntsman. Deuterated solvents were purchased from Buchem BV. Other common solvents were purchased from Biosolve. All the chemicals were used without further purification.

7.2.2 Reactions and synthesis

Synthesis of isophorone dimethylcarbamate (IPDMC)

In a 2000 mL three-neck flask equipped with a condenser, 170 g (1 mol) of IPDA, 630 g (7 mol) of DMC and 70 g (1 mol) of potassium methoxide were mixed under argon flow and stirred at room temperature. After 4 hours, the mixture was heated up to 60 °C for 6 hours. The solution was then cooled and poured into an excess of chloroform and subsequently washed with brine. The organic layer was dried over anhydrous sodium sulfate. The solvent was evaporated to dryness to obtain the product as a yellowish solid (196 g, 69%).

^1H -NMR (400 MHz, CDCl_3 δ in ppm): 4.8 (d, 1H, $-\text{NHCH}_2$), 4.6 (s, 1H, cy- NHCH), 3.8-3.6 (s, 1H, cy- CHNH , 6H, $-\text{OCH}_3$), 3.3, 2.9 (d, 2H, $-\text{CH}_2\text{NH}$), 1.7-0.7 (15H, cy- H). $^{13}\text{C}\{^1\text{H}\}$ NMR (100.6 MHz, CDCl_3 δ in ppm): 157.4, 156.3 (C=O), 54.8 and 52.1 (OCH_3), 51.8, 46.9, 46.3, 44.6, 42.5, 41.8, 36.3, 34.9, 31.7, 29.6, 27.5, and 23.1 (cy- C).

Preparation of diamine-terminated cationically dispersible polyureas

Water-dispersible polyureas were prepared from diamines, IPDMC and various amounts of DMDPA. In a typical experiment, PPGda230 (3.68 g, 16 mmol), DMDPA (1.45 g, 10 mmol), IPDMC (5.72 g, 20 mmol) and TBD (0.14 g, 1 mmol) were introduced into a 100 mL 3-neck flask and stirred under argon flow at 130 °C for 12 hours. The pressure in the flask was then gradually reduced to 5 mmHg and maintained at this value for another 6 hours before quenching the mixture with water. Finally, the precipitated polymer was washed 3 times with water and dried in a vacuum oven for 12 hours to obtain a light yellowish polymer (8.10 g, 85%).

Preparation of cationically stabilized polyurea dispersions

In a typical experiment, 1 gram of prepolymer was dissolved in 1 mL of methanol. One equivalent of acetic acid was added according to the concentration of the amines determined from the potentiometric titration. The mixture was stirred for 10 minutes and then slowly added to 8 mL of water under vigorous stirring.

Preparation of diamine-functional polyureas (PUdas)

In a typical experiment, 2.86 g (10 mmol) of IPDMC, 2.99 g (13 mmol) of PPGda230 and 0.07 g (0.5 mmol) of TBD were mixed in a 50 mL crimp-capped vial under argon flow and

stirred at 130 °C for 12 hours. The pressure in the flask was then gradually reduced to 5 mmHg and maintained at this value for another 6 hours before quenching the mixture in water. Finally, the precipitated polymer was washed 3 times with water and dried in a vacuum oven for 12 hours to obtain a light yellowish polyurea (6.32 g, 87%).

Copolymerization of PUdas and dianhydrides

In a typical experiment, 4.00 g (2 mmol) of PUda with molecular weight of 2,000 Da (determined by potentiometric titration) was dissolved in 4.00 g of anhydrous dimethylformamide (DMF). 0.51 g (2 mmol) of EDTAD was added into the solution and stirred at 80 °C for 30 minutes. The mixture was then precipitated in water and washed 3 times with water and subsequently dried in oven at 80 °C for 12 hours to obtain a yellowish poly(amic acid urea) (3.12 g, 69%).

Model reaction of EDTA and BPA

The reactivities of the carboxylic acid groups towards amines were evaluated by monitoring the reaction between EDTA and BPA. In a typical experiment, 52 mg (0.4 mmol) of BPA and 4.9 g of DMSO-*d*₆ were introduced into a 20 mL crimp-cap vial, followed by addition of 58 mg (0.2 mmol) of EDTA. The time of EDTA addition was considered as the *t* = 0 of the reaction.

Preparation of BPA-based diimide

A mixture of 2.56 g (10 mmol) of EDTAD, 2.62 g (20 mmol) of BPA and 20 g of *p*-xylene was stirred in a three-neck flask under reflux for 48 hours. The reaction was then quenched into water and washed five times with an 0.5 M aqueous NaOH solution, followed by drying with Na₂SO₄ and concentrating via a rotary evaporator. The resulting viscous liquid was then dried overnight at 80 °C under vacuum (5 mmHg) to obtain a brownish solid (2.45 g, 51%).

¹H-NMR (400 MHz, CDCl₃, δ in ppm): 3.7 (t, CH₂NCOCH₂-), 3.5 (s, -NCH₂CON), 3.3 (m, 8H CH₃CH₂CH₂CH₂O-, NHCH₂CH₂CH₂O-), 2.6 (NCH₂CH₂N-), 1.6 (NHCH₂CH₂CH₂O-), 1.5 (CH₃CH₂CH₂CH₂O-), 1.3 (CH₃CH₂CH₂CH₂O-), 0.9 (CH₃CH₂-). ¹³C{¹H} NMR (100.6 MHz, CDCl₃, δ in ppm): 170.6 (-NCOCH₂), , 70.2 (CH₃CH₂CH₂CH₂O), 68.3 (NHCH₂CH₂CH₂O), 56.2 (NCH₂CH₂N), 52.3 (NCH₂CO), 36.4 (CH₂NHCO), 31.8 (CH₃CH₂CH₂CH₂O), 28.2 (NHCH₂CH₂CH₂O), 19.3 (CH₃CH₂CH₂CH₂O), 14.4 (CH₃CH₂-).

Preparation of BPA-based diamic acid (DAA)

In a typical experiment, 2.56 g (10 mmol) of EDTAD was dissolved in 8.00 g of anhydrous DMF. 2.62 g (20 mmol) of BPA was added into the solution which was stirred at 80 °C for 2 minutes, followed by precipitation in a mixture of diethyl ether/hexane (5/1) and washed three times with the same mixture. The resulting solid was then dried at room temperature under 2 mmHg for 2 hours to obtain a white DAA solid (3.22 g, 62%).

¹H-NMR (400 MHz, CDCl₃, δ in ppm): 3.3-3.4 (12H, CH₃CH₂CH₂CH₂O-, -NCH₂COOH), 3.2 (s, NCH₂CO), 3.1 (-CONHCH₂), 2.7 (NCH₂CH₂N-), 1.6 (NHCH₂CH₂CH₂O-), 1.5 (CH₃CH₂CH₂CH₂O-), 1.3 (CH₃CH₂CH₂CH₂O-), 0.9 (CH₃CH₂-). ¹³C{¹H} NMR (100.6 MHz, CDCl₃, δ in ppm): 174.7 (-COOH), 171.4 (CONH), 70.2 (CH₃CH₂CH₂CH₂O), 68.2 (NHCH₂CH₂CH₂O), 59.6 (NCH₂COOH), 53.6 (NCH₂CH₂N), 37.4 (CH₂NHCO), 31.8

(CH₃CH₂CH₂CH₂O), 29.4 (NHCH₂CH₂CH₂O), 19.3 (CH₃CH₂CH₂CH₂O), 14.4 (CH₃CH₂).

Preparation of water-borne PAAU dispersions

In a typical experiment, 1 gram of PAAU was dissolved in 1 mL of methanol. One equivalent of trimethylamine (TEA) was added according to the concentration of the -COOH groups determined from potentiometric titration. The mixture was stirred for 10 minutes and then slowly added to 8 mL of water under vigorous stirring.

Catalyst selection for amide formation

Catalyst activities for amide formation between carboxylic acid groups of amic acids and amines were assessed by monitoring the reaction between BPA and EDTAD. In a typical experiment, 105 mg (0.8 mmol) of BPA and 4.9 g of DMSO-*d*₆ were introduced into a 20 mL crimp-cap vial, followed by addition of 51 mg (0.2 mmol) of EDTAD and 4 mg (40 μmol) of H₃PO₄. The time of EDTAD addition was considered as the *t* = 0 of the reaction.

Preparation of PAAU coatings

In a typical experiment, 1.5 gram of PAAUD was casted on an aluminum panel. A wet film of 250 μm thickness was applied using a doctor blade, followed by drying at 50 °C under argon flow to form a colorless PAAU coating.

7.2.3 Characterization

Size exclusion chromatography (SEC)

SEC in 1,1,1,3,3,3-hexafluoro-2-propanol (HFIP) was performed at 40 °C on a system equipped with a Waters 1515 Isocratic HPLC pump, a Waters 2414 refractive index detector (35 °C), a Waters 2707 autosampler, a PSS PFG guard column followed by 2 PFG-linear-XL (7 μm, 8*300 mm) columns in series. HFIP with potassium trifluoroacetate (3 g/L) was used as eluent at a flow rate of 0.8 mL/min. The molecular weights were calculated with respect to poly(methyl methacrylate) standards (Polymer Laboratories, Mp = 580 Da up to Mp = 7.1*10⁶ Da).

Nuclear magnetic resonance spectroscopy (NMR)

¹³C{¹H} NMR (100.62 MHz) and ¹H NMR (400 MHz) spectra were recorded using a Varian Mercury Vx spectrometer at 25 °C. The samples were prepared by dissolving 20 mg of polymer in 1 mL MeOD-*d*₄ or 50 mg/ml using dimethylsulfoxide (DMSO-*d*₆) or dimethylformamide (DMF-*d*₇) as solvent.

Dynamic light scattering (DLS) and ζ-potential measurements

DLS and ζ-potential measurements were performed on a Malvern ZetaSizer Nano ZS at 25 °C (polyurethane refractive index: 1.59) to determine the dispersion characteristics. The average particle size and the particle size distribution of dispersions containing 0.1 wt% solids were determined according to ISO 13321 (1996). The ζ-potential was calculated from the electrophoretic mobility (μ) using the Smoluchowski relationship $\zeta = \eta\mu/\epsilon$ with $\kappa\alpha \gg 1$ and where η is the solution viscosity, ε the dielectric constant of the medium, κ the Debye-Hückel parameter and α the particle radius. Data acquisition was performed using the ZetaSizer Nano Software.

Differential scanning calorimetry (DSC)

DSC measurements were performed on a TA Instruments DSC Q100. Samples were heated from -80 to 180 °C at a heating rate of 10 °C/min followed by an isothermal step for 5 min. A cooling cycle to -80 °C at a rate of 10 °C/min was performed prior to a second heating run to 180 °C at the aforementioned heating rate. The T_g was determined from the second heating run. The Universal Analysis 2000 software was used for data acquisition.

Calculation of amine end-groups in PAAU

The concentration of amine end-groups in PAAUs was calculated according to the following equation, which is deduced from the Carothers' equation.¹⁷

$$F = \frac{4 - \frac{8C_c}{C_a + C_c}}{M_a + M_c},$$

where F is the concentration of amine end-groups in the polymer (mol/g), C_a and C_c the concentration of amine and carbamate in the monomer mixture, respectively, M_a and M_c the molar mass of diamine and dicarbamate monomers, respectively.

Potentiometric titration

Potentiometric titrations were performed using a Metrohm Titrino 785 DMP automatic titration device fitted with an Ag titrode. The samples were dissolved in CH₃OH and the -NH_x groups ($x = 0-2$) were titrated with a normalized 0.1 mol/L HCl isopropanol solution while the -COOH groups were titrated with a normalized 0.1 mol/L KOH isopropanol solution. Blank measurements were carried out using the same amount of CH₃OH.

The molar mass of PUda was defined according to the following equation:

$$M_n = \frac{2m_{sample}}{(V_{sample} - V_{blank}) \times C_{HCl}}.$$

The -NH_x content was defined according to the following equation:

$$N_{NHx} = \frac{(V_{sample1} - V_{blank1}) \times C_{HCl}}{m_{sample}}.$$

The -COOH content was defined according to the following equation:

$$N_{COOH} = \frac{(V_{sample2} - V_{blank2}) \times C_{KOH}}{m_{sample}},$$

where V_{blank1} and V_{blank2} are the volumes of HCl and KOH solutions in mL needed for the blank experiment (average of two measurements), respectively, $V_{sample1}$ and $V_{sample2}$ the volumes of HCl and KOH solutions in mL consumed by the sample, respectively, C_{HCl} the HCl concentration in isopropanol in mol/L, C_{KOH} the KOH concentration in isopropanol in mol/L, N_{NHx} the molar amount of -NH_x ($x = 0-2$) groups in 1 gram of polymer (mol/g), N_{COOH} the molar amount of -COOH groups in 1 gram of polymer (mol/g) and m_{sample} the sample weight in gram.

Gel fraction measurement

In a typical experiment, 50 mg of cured polymer sample was immersed in methanol at 50 °C for 24 h. The sample was then filtered and dried in a vacuum oven at 50 °C until constant weight. The gel fraction was calculated by the following equation:

$$\text{Gel fraction (\%)} = (W_t/W_0) \times 100\%,$$

where W_0 is the original weight of the sample and W_t the weight after drying.

Evaluation of the coatings

The coating performances were evaluated at room temperature by means of an acetone double rub test, a reverse impact test and a pencil hardness test. In an acetone double rub test, the sample was rubbed back and forth with a cloth drenched in acetone. If no damage was observed after more than 150 rubs (75 double rubs), the acetone resistance of the coating was marked as good. In the water resistance test, the coating was immersed in water for 10 minutes. If no swelling was observed, the water resistance of the coating was marked as good. The reverse impact test was performed by dropping a 1 kg ball on the backside of a coated panel from a 100 cm height, as described in ASTM D2794. The pencil hardness test (ASTM D3363) was performed by pushing pencils with varying hardness value into the sample. The coating hardness was identified by the trace generated. The scale of pencil hardness ranges from 9H, the hardest scale, to 9B, the softest one.

7.3 Results and discussion

7.3.1 Catalysts for amic acid/amine reaction

The poly(amic acid urea)s (PAAUs) prepared in Chapter 6 contain amine and carboxylic acid groups. The reaction between these moieties at elevated temperature could form amide bonds and therefore result in crosslinked resins. Thus, to study the mechanism of the possible curing reactions, involving amine and amic acid groups present in the PAAUs, a model reaction was performed with 3-butoxypropylamine (BPA) and EDTAD in a 4/1 ratio in DMSO- d_6 at 150 °C under argon flow (model reaction **A**, Figure 1a). The reaction of 1 eq. of EDTAD with 2 eq. of BPA generates a diamic acid (DAA), which can either self-condense to afford a cyclic- (CI) or a noncyclic imide (NCI), or react further with BPA to produce tri- or even tetraamides. While amidation and the noncyclic imidization reactions imply crosslinking of the PUs, the generation of CI does not. To follow the conversions of DAA into these three species, samples of the reaction mixture were taken over 6 hours and analyzed by NMR. The ^1H NMR spectra of these samples are presented in Figure 1b.

The spectrum of the sample at t_0 was characterized, among others, by a triplet at 0.87 ppm assigned to the methyl protons (**a**) and two multiplets at 1.62 ppm and 1.75 ppm attributed to the β -methylene protons close to amide (**b**) or imide moieties of CI (**b'**) or NCI (**b''**), and the β -methylene protons next to the amine group of BPA (**c**), suggesting that 1 eq. of DAA was immediately generated from 1 eq. of EDTAD and 2 eq. of BPA. The decrease of **c** was accompanied by the rise of **b/b'/b''** and the emergence of triplets at 3.15 ppm and 3.67 ppm representing the methylene proton next to the amide (**d**) and imide groups of CI (**e**) or NCI (**e'**), respectively. The assignment of signal **e** to imide was confirmed by the similarity with the methylene resonance of the diimide prepared from BPA/EDTAD in a 2/1 ratio (see experimental section).

To increase both amidation and noncyclic imidization rates and thereby to enhance the crosslink densities of the material, a series of catalysts including Brønsted acids such as phosphoric (H_3PO_4), boric (H_3BO_3) and sulfuric acids (H_2SO_4), Lewis acids like zinc chloride

(ZnCl₂), tin (II) chloride (SnCl₂), magnesium chlorides (MgCl₂) and aluminum chlorides (AlCl₃) and the Lewis base 1,5,7-triazabicyclo[4.4.0] dec-5-ene (TBD, Figure 2), were evaluated for the model reaction **A** depicted in Figure 1a, with a catalyst loading of 15 mol% with regard to the initial EDTAD amount. The conversion of BPA at time *t* was calculated by the intensity ratio of signal **c** at *t* and *t*₀, while the conversion of DAA into imide at time *t* equaled to the ratio of intensity of **e** at *t* and intensity of **c** at *t*₀ (Figure 1). Both the conversion of BPA and the conversion of DAA into imide over a period of 4 hours were determined from ¹H NMR and are depicted in Figure 2. The conversion of DAA into amide was equal to the conversion of BPA, based on the assumption that the BPA was only consumed via reaction with DAA to form amide. Hence, the conversions and selectivities of DAA towards amide and imide after 4 hours of reaction time are listed in Table 1.

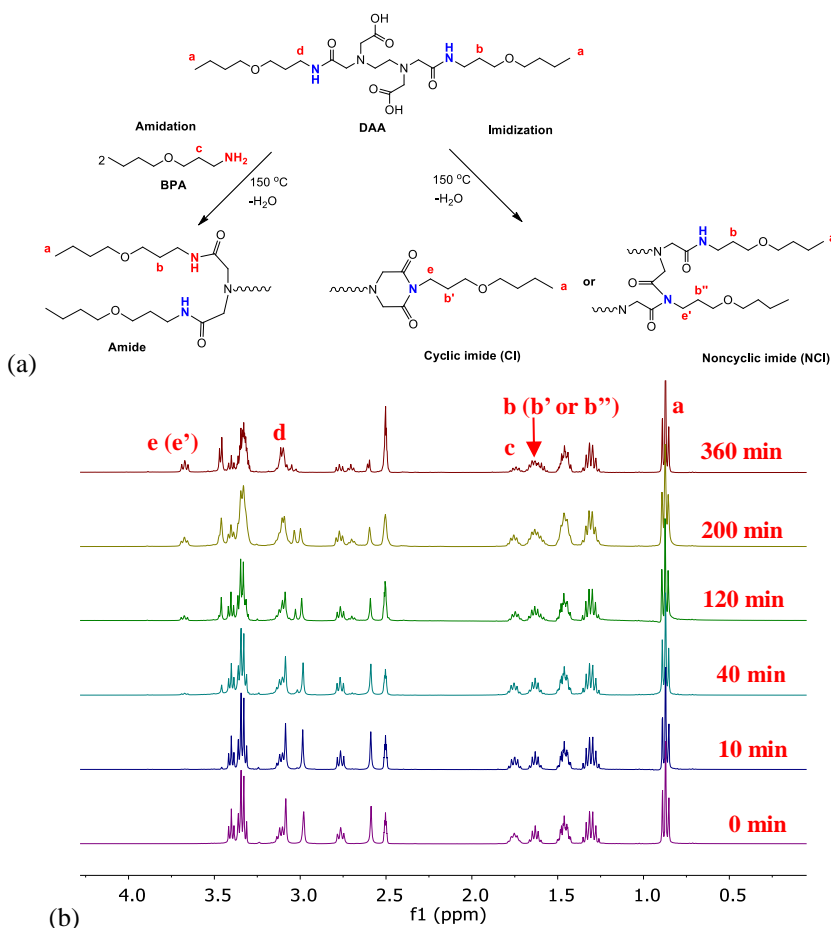


Figure 1. (a) BPA/EDTAD model reaction **A** with 4/1 ratio. (b) ¹H NMR of BPA/EDTAD (4/1 ratio) reaction at 150 °C over 6 hours (DMSO-*d*₆).

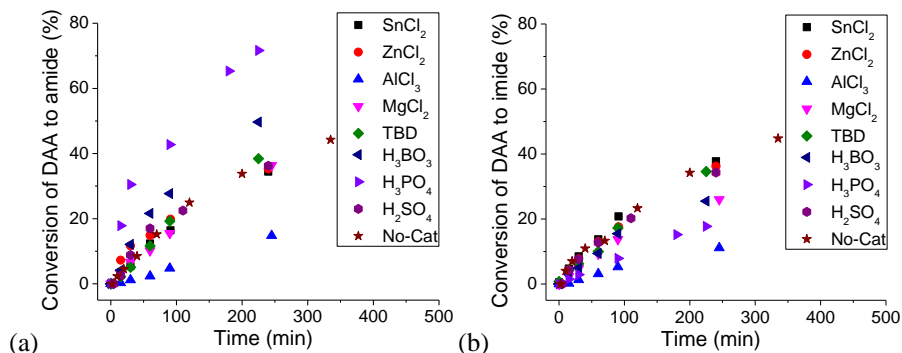


Figure 2. Conversions of DAA into (a) amide and (b) imide as a function of time in a BPA/EDTAD mixture in a 4/1 ratio in DMSO- d_6 at 150 °C under argon flow with 15 mol% of various catalysts, determined by ^1H NMR.

In the absence of catalyst, the conversions of BPA into amide and imide in the model reaction **A** were comparable after 4 hours (Table 1). Similar conversions of BPA and selectivities towards amide were observed for the model reactions with and without SnCl_2 , ZnCl_2 , TBD and H_2SO_4 as catalysts. The use of H_3PO_4 and H_3BO_3 led to an increase of the catalytic activity towards amidation, with the order $\text{H}_3\text{PO}_4 > \text{H}_3\text{BO}_3$. The model reactions catalyzed by these two acids exhibited higher selectivities towards amide than towards imides. The reduced selectivities for imidizations observed in the model reactions with these two catalysts compared to the non-catalyzed ones is ascribed to the competition between amidation and imidization, as both consume carboxylic acid moieties. Slow imidizations were found for the MgCl_2 - and AlCl_3 -catalyzed model reactions, in agreement with the results reported by Ali. et al.¹⁷

To verify whether H_3PO_4 , the most active amidation catalyst in reaction **A**, also catalyzes imidization reactions, model reactions between BPA and EDTAD with a 2/1 ratio were carried out in DMSO- d_6 at 150 °C under argon flow with or without H_3PO_4 (model reaction **B**, Figure 3). Under such conditions, BPA and EDTAD were fully reacting into DAA upon mixing. The subsequent conversion of DAA into the corresponding mono-or diimide in these model reactions was determined by ^1H NMR and is displayed in Figure 3.

Table 1. Conversions of DAA and selectivities towards amide and imide in model reaction A in the presence of various catalysts at 150 °C under argon flow after 4 hours, determined by ^1H NMR.

Catalyst	Total conversion of amine (mol%)	Selectivity towards amide (mol%)	Selectivity towards imide (mol%)
SnCl_2	73	48	52
ZnCl_2	72	49	51
AlCl_3	24	58	42
MgCl_2	61	59	41
TBD	74	51	49
H_3BO_3	80	66	34
H_3PO_4	93	78	22
H_2SO_4	70	51	49
No catalyst	74	50	50

Similar conversions of DAA into imide were observed for model reaction **B** with or without H_3PO_4 , indicating the lack of catalytic activity of H_3PO_4 towards imidization. It should be noted that intramolecular cyclic imidization is favored compared to intermolecular noncyclic imidization under the applied conditions, due to the low concentration of DAA (0.08 mol/L). Hence, this does not rule out the possibility that H_3PO_4 may catalyze NCI formation in the PAAU resin, where the concentration of $-\text{COOH}$ and amides are significantly higher than in solution.

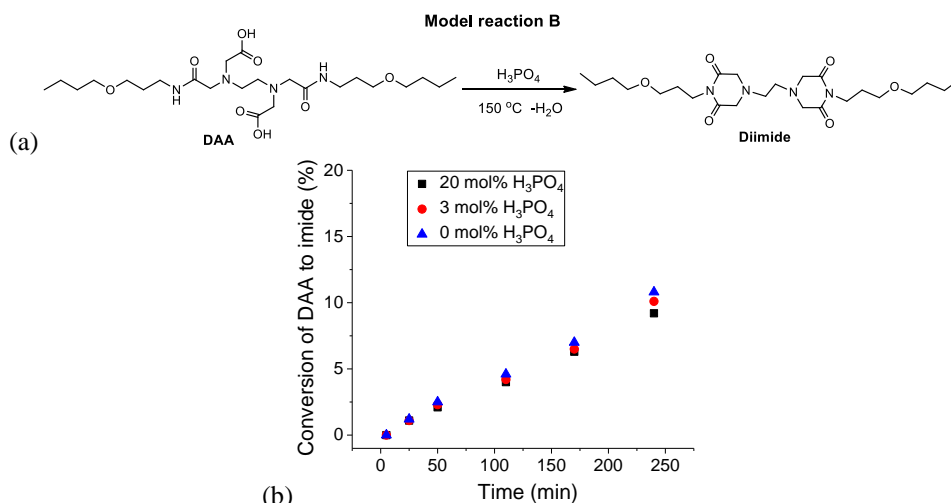


Figure 3. (a) Model reaction B with a 2/1 ratio of BPA/EDTAD. (b) Conversion of DAA into mono- or diimide as a function of time in model reaction B in $\text{DMSO}-d_6$ under argon flow with or without H_3PO_4 as catalyst, determined by ^1H NMR.

Thus, further investigations on imidization at higher concentrations were carried out by heating DAA in bulk, with or without addition of 3 wt% (15 mol%) of H_3PO_4 at 150 °C under argon flow. DAA was prepared via the reaction of BPA and EDTAD in a 2/1 ratio in dimethylformamide (DMF) at 80 °C for 2 minutes, followed by precipitation in a diethyl ether/hexane mixture (1/5 volume ratio) and drying under vacuum at room temperature. The conversions of DAA into imide in these two reactions were determined by ^1H NMR and are displayed in Figure 4.

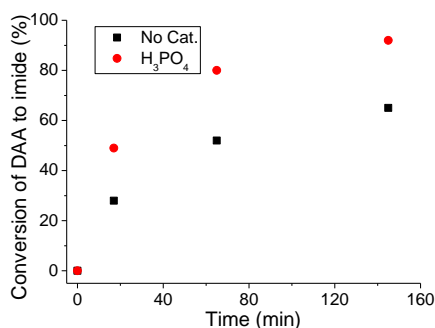


Figure 4. Conversion of DAA into imide as a function of time in bulk under argon flow with or without H_3PO_4 as catalyst at 150 °C, determined by ^1H NMR ($\text{DMSO}-d_6$).

A significantly faster conversion of DAA into mono- or diimide was observed in bulk compared to the reaction in solution (Figure 3). This is contradictory to the zero-order kinetics of CI formation, where the conversion into imide is not influenced by the concentration of amic acid. Moreover, the ^1H NMR spectrum of the reaction mixture after 2.5 hours exhibits a splitting of the signal of the methylene protons next to the imide at 3.68 ppm compared to the spectrum of the pure diimide (Figure 5a). In addition, the corresponding $^{13}\text{C}\{^1\text{H}\}$ NMR spectrum displays multiple signals between 170.4–170.7 ppm (**m'**), close to the carbonyl signal (**m**) of the diimide (Figures 5b and 1). These data suggest the formation of NCI from DAA upon heating at 150 °C. The faster DAA conversion in the presence of H_3PO_4 indicates its high catalytic activity towards NCI formation (Figure 4). The proposed mechanisms for NCI and CI formation in the presence of H_3PO_4 can be found in the Appendix of Chapter 7. Such mechanisms indicate the high selectivity of H_3PO_4 towards intermolecular noncyclic imidization instead of intramolecular cyclic imidization.

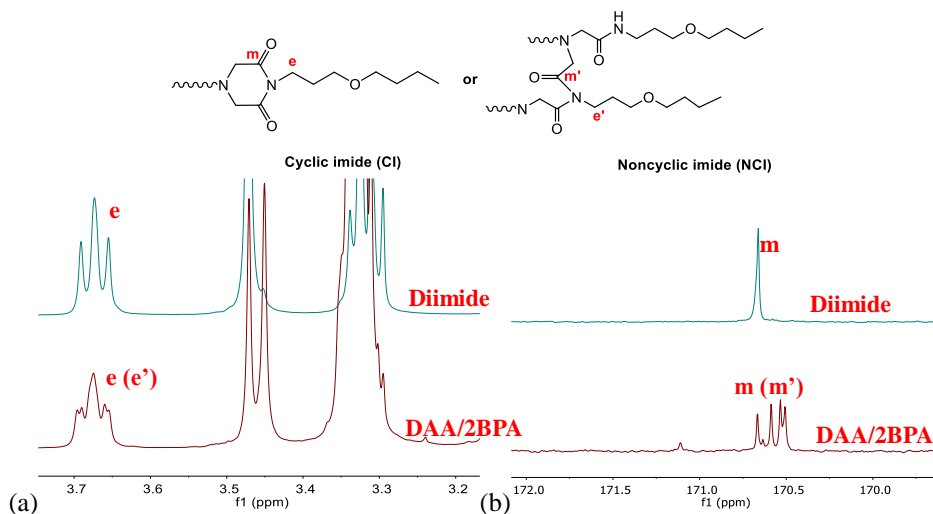


Figure 5 (a) ^1H NMR and (b) $^{13}\text{C}\{^1\text{H}\}$ NMR ($\text{C}=\text{O}$ region) of diimide (upper) and BPA/DAA (2/1 ratio) reaction in bulk at $150\text{ }^\circ\text{C}$ over 2.5 hour (lower, $\text{DMSO}-d_6$)

The selectivity towards amidation and imidization in a BPA/DAA (2/1 ratio) reaction was also investigated in bulk. The reactions were performed at $150\text{ }^\circ\text{C}$ under argon flow with or without addition of 3 wt% of H_3PO_4 . However, precipitation was observed during the catalyzed reaction, possibly due to the formation of salt from H_3PO_4 and BPA. Therefore, only the conversions of BPA and DAA into imide for the non-catalyzed DAA/BPA reaction over a period of 22 hours were determined by ^1H NMR (Figure 6).

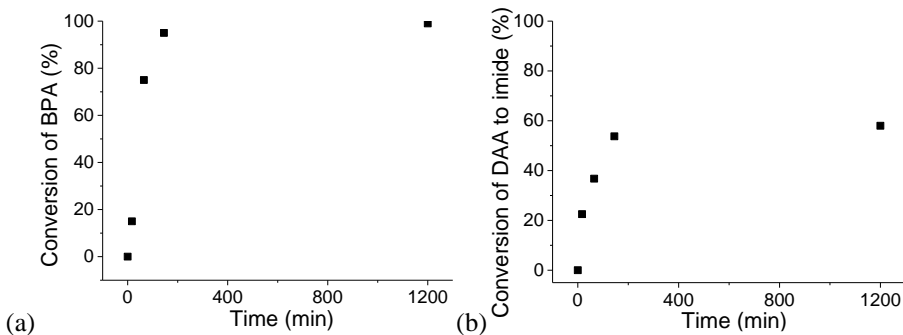


Figure 6. (a) Conversions of BPA and (b) conversion of DAA into imide for BPA/DAA (2/1 ratio) reaction mixture in bulk at $150\text{ }^\circ\text{C}$ under argon flow, determined by ^1H NMR ($\text{DMSO}-d_6$).

The conversion of BPA reached more than 90% after 2.5 hours, while 55% of the amic acids in DAA generated imide moieties. The higher summation than 100% of these two conversions is contradictory to the reaction depicted in Figure 1a, where DAA either undergoes amidation with BPA or forms imides. A possible explanation lies in the formation of imidine from an imide and BPA (Scheme 7), as indicated by two singlets at 3.45 ppm assigned to the methylene protons next to imide (a) and imidine (b, Figure 7).¹⁶ The formation

of imidine could also enhance crosslinking during the curing of PAAUs at high temperature.

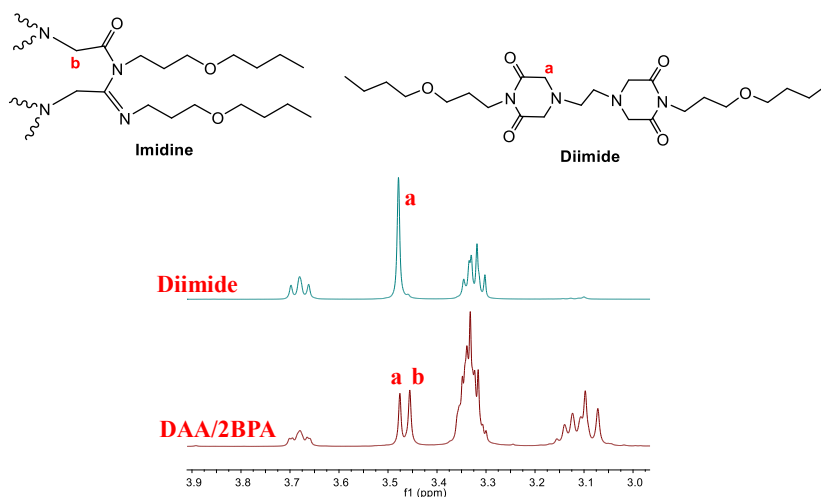
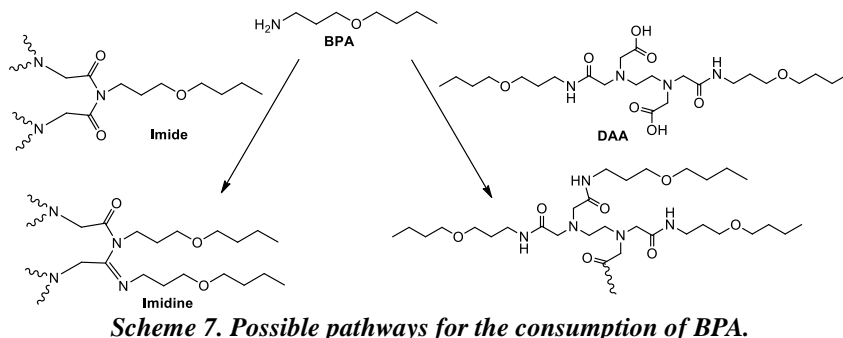


Figure 7. ^1H NMR spectra of diimide and BPA/DAA (2/1 ratio) reaction after 2.5 hours (in the 3.0-4.0 ppm region, DMSO-d_6).

7.3.2 Crosslinking of anionically stabilized PUDs

The influence of the M_n s of PUDs and the amine/carboxylic acid ratios in the PAAUs (Scheme 4a) on the effectiveness of the crosslinking during high temperature-curing of PAAUs were assessed by gel fraction measurements. Thus, PAAUs were produced via polymerization of EDTAD and diamine-functional polyureas (PUDs), synthesized from various ratios of poly(propylene glycol) bis(2-aminopropyl ether) with an average M_n of 230 Da (PPGda230) and isophorone dimethyl carbamate (IPDMC). These PAAUs were then dissolved in methanol and neutralized by TEA (one molar eq. per carboxyl group), followed by dispersion in water and removal of methanol to form PAAUDs. Next, the PAAUDs were casted on a Teflon sheet and dried at 150 °C for 20 hours with and without the presence of H_3PO_4 . Since the non-crosslinked PAAUs are soluble in methanol, the resulting free standing films of weight W_0 were immersed in methanol at 50 °C for 24 h, followed by drying in a vacuum oven at 50 °C overnight to obtain crosslinked polymers of weight of W . The gel fractions W/W_0 and the $-\text{COOH}$ contents of the polymers are displayed in Table 2.

The primary/secondary amine end-groups could not be quantified from potentiometric titration, due to the presence of tertiary amines in the EDTAD-derived moieties within the PAAU. Hence, only the -COOH contents were determined for these PAAUs. Lower M_n s of the PUda resulted in higher (amine) end-group concentrations and also in greater amine and -COOH contents in the corresponding PAAUs after reaction with 0.7 molar eq. of EDTAD (entries 1-5), and consequently in faster amide formation and accordingly in a larger gel fraction during the curing at 150 °C. The PAAUs prepared in entries 6 and 7 bear limited amounts of amine end-groups due to the stoichiometric and over-stoichiometric EDTAD/PUda ratios. However, the corresponding cured resins have significantly higher gel fractions compared to the PAAU of entry 3, of which the amine end-groups are more abundant. This is attributed to the greater -COOH contents in entries 6 and 7 that leads to more NCI formation than in the case of entry 3, resulting in a higher crosslinking density of the materials of entries 6 and 7 (Scheme 8a). Such reaction could also be catalyzed by H_3PO_4 , as indicated by entries 8-10, where the gel fractions of the corresponding cured PAAUs are much higher than for the non-catalyzed curing processes (entries 6,7), in agreement with the model reactions studied.

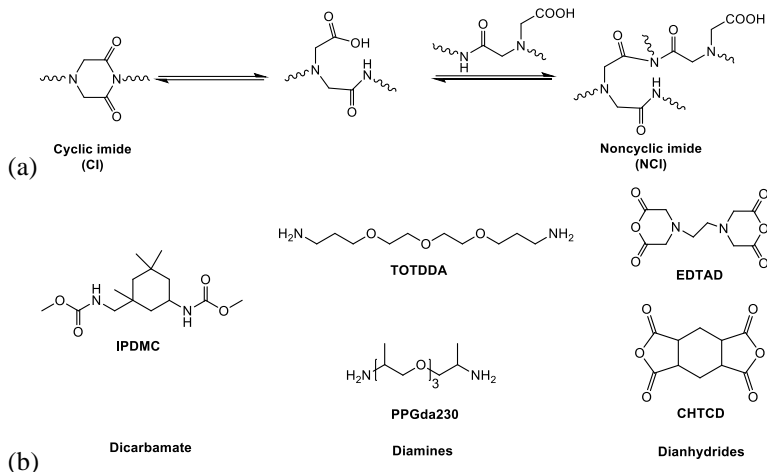
Table 2. -COOH content of the PAAU resins prepared from PUDas and EDTAD in various dianhydride/amine ratios and gel fraction of the PAAU casted film after curing at 150 °C for 24 h with or without H_3PO_4 as catalyst.

Entry	M_n of PUda ^a (Da)	Addition of H_3PO_4 (mol% to -COOH)	Anhydride /amine	-COOH content ^a (mmol/g)	Gel fraction (%)
1	4,750	0	0.7/1	0.14	1
2	2,950	0	0.7/1	0.30	3
3	2,150	0	0.7/1	0.41	6
4	1,500	0	0.7/1	0.65	20
5	1,200	0	0.7/1	0.88	27
6	2,150	0	1.0/1	0.59	16
7	2,150	0	1.3/1	0.72	20
8	2,150	5	0.7/1	0.41	11
9	2,150	5	1.0/1	0.59	34
10	2,150	5	1.3/1	0.72	36

^{a)} Determined by potentiometric titration.

The results obtained for free standing films were then applied to coatings. Thus, PUDas were produced by polymerizing PPGda230 or 4,7,10-trioxa-1,13-tridecanediamine (TOTDDA, Scheme 8b) with various amounts of IPDMC. These materials were then reacted with stoichiometric amounts of EDTAD or 1,2,4,5-cyclohexanetetracarboxylic dianhydride (CHTCD) to form PAAUs. After dissolution in methanol and addition of 3 wt% of H_3PO_4 , the resins were neutralized with TEA and dispersed into water to generate stable PAAUDs of 10 wt% solid contents with high ζ -potential values close to -50 mV and particle sizes between 50-200 nm. The PAAUDs were applied on aluminum panels and dried at 50 °C overnight,

generating coatings with thicknesses of 20-30 μm . Finally, curing at elevated temperatures for 24 hours led to light yellowish coatings, which were evaluated by means of pencil hardness, water and acetone resistances, reverse impact resistance and cross adhesion tests. The results are summarized in Table 3.



Scheme 8. (a) Cyclic imide and noncyclic imide formation during curing of PAAUs.¹⁴ (b) Building blocks employed in PAAU coatings

PAAU coatings cured at 150 $^{\circ}\text{C}$ have, compared to those cured at 50 $^{\circ}\text{C}$, improved coating hardness, good impact and solvent resistances and strong adhesion to the aluminum substrate, with the exception of the coating based on PUda with high M_n of 4750 Da (PUda₄₇₅₀). The poor impact resistance probably results from insufficient crosslinking due to the low -COOH content and the poor adhesion to the substrate is most likely due to the low -COOH concentration as well. Although PAAUs based on PUDas with lower M_n s have lower amounts of isophorone moieties, and thereby lower T_g values, their corresponding cured coatings have higher crosslink densities (see Table 2) which results in enhanced T_g s. As a result, similar T_g s were measured for these cured coatings. Lower curing temperatures gave less crosslinking of the resins, as reflected by the lower T_g values of the coatings, poor impact and poor acetone resistances due to limited crosslinking densities, in particular when curing was done at 110 $^{\circ}\text{C}$. The substitution of EDTAD by CHTCD afforded a cured coating with slightly higher T_g due to the more rigid structure of the CHTCD residues. Significant enhancement of impact and solvent resistances as well as substrate adhesion were observed for the cured PAAU coating based on TOTDDA compared to the uncured one. These coatings were softer than those prepared from PPGda230 due to their lower T_g s. In conclusion, curing at elevated temperatures proved to be a useful method for improving the coating properties of PAAUs.

Table 3. M_n , T_g and coating properties of cured PAAUs prepared with PPGda230 or TOTDDA as diamines, IPDMC as dicarbamate and EDTAD or CHTCD as dianhydride.

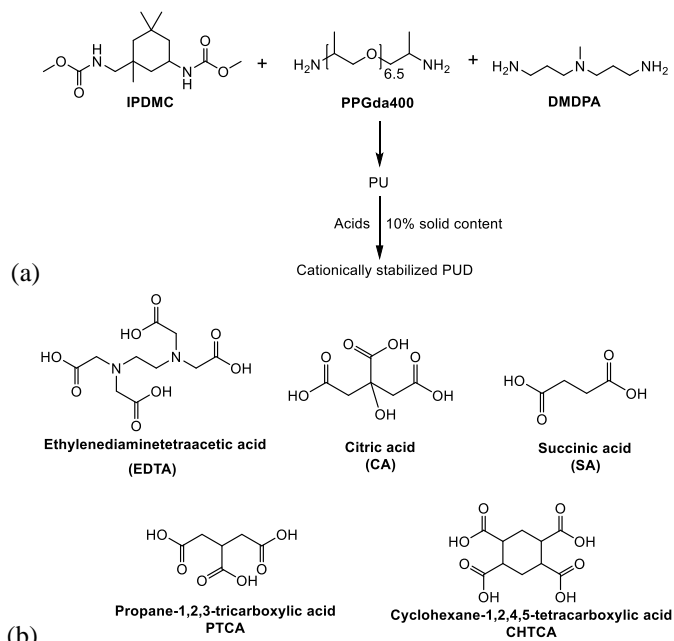
Diamine	M_n of PU ^a (Da) ^a	T_{cure} (°C)	T_g^b (°C)	Pencil hardness	Impact test	Cross adhesion test	Water Resistance ^c	Acetone Resistance
PPGda230	4,750	150	101	H	-	-	±	+
PPGda230	2,950	150	95	H	+	+	+	+
PPGda230	2,150	150	88	F	+	+	+	+
PPGda230	2,150	50	73	HB	-	-	±	-
PPGda230	1,500	150	91	F	+	+	+	+
PPGda230	1,200	150	90	F	+	+	+	+
PPGda230	2,150	140	86	F	+	+	+	+
PPGda230	2,150	125	82	F	+	+	+	+
PPGda230	2,150	110	77	HB	-	-	+	-
PPGda230	2,080 ^d	150	91	F	+	+	+	+
PPGda230	2,080 ^d	50	75	HB	-	-	±	-
TOTDDA	2,050	150	81	F	+	+	+	+
TOTDDA	2,050	50	18	3B	-	-	-	-

^{a)} Determined by potentiometric titration; ^{b)} determined by DSC; ^{c)} +: no swelling, ±: swelling without softening, -: swelling and softening; ^{d)} With CHTCD as dianhydride.

7.3.3 Crosslinking of cationically stabilized PUDs

Chapter 3 describes the synthesis of PUs with isophorone dicarbamate (IPDMC) and diamines as monomers, one of these being 3,3'-diamino-*N*-methyldipropylamine (DMDPA, Scheme 9a). The corresponding cationically stabilized PUDs with acetic acid (AA) as neutralization agent generated coatings with unsatisfactory mechanical properties and solvent resistance as a result of the relatively low molecular weights of the PU resins. Hence, these PUDs were neutralized with polyacids, which could also act as crosslinking agents during the curing of the resulting coatings at elevated temperatures.¹⁸

In this section, AA was substituted by five different polyacids, *viz.* ethylenediaminetetraacetic acid (EDTA), citric acid (CA), succinic acid (SA), propane-1,2,3-tricarboxylic acid (PTCA) and cyclohexane-1,2,4,5-tetracarboxylic acid (CHTCA, Scheme 9b). Their potential as crosslinking agents was evaluated by curing the PU coatings at 150 °C.



Scheme 9. (a) Synthetic scheme of PUD. (b) Polyacids used in this section as neutralization and curing agents.

PUDas were prepared via polymerization of PPGda400, IPDMC and the internal dispersing agent (IDA) DMDPA, with a 1.3/1 amine/carbamate ratio and either 20 or 30 mol% IDA. The concentrations of the ionizable amine groups, either as end-groups or incorporated within the backbone, were determined by potentiometric titration. Then, the PUDas were dissolved in methanol and neutralized with various concentrations of the above-mentioned acids, followed by addition of water and removal of methanol to obtain PUDs (Scheme 9a). The particle sizes and ζ -potentials of these dispersions are summarized in Table 4.

Precipitation occurred during the preparation of PUDs neutralized by CA, PTCA and CHTCA, while dispersions without visible macrophase separation were obtained with EDTA and SA, with the exception of the PUD with 20 mol% IDA in entry 1, where the amines in the polymer were neutralized by a stoichiometric amount of -COOH groups of EDTA. The low solubility of entry 1 is probably due to the lack of sufficient surface charges for stabilization. PUDs neutralized by AA were synthesized via the procedure described above for comparison. The dispersions had small particle sizes of 8-32 nm and remained stable even after 30 days at 40 °C. The PUDs neutralized by AA have high ζ -potentials of about 50 mV, while slightly lower ζ -potentials of 34-41 mV were observed for the PUDs neutralized by EDTA and SA, probably due to the lower mobility of the bulkier EDTA and SA that hinders the rearrangement of the electron double layer of the particles.¹⁹

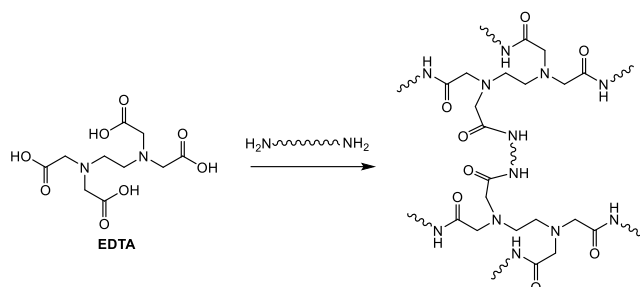
Table 5. Formulation and characteristics of PUDs based on PPG400 and IPDMC with DMDPA as IDA (amine/carbamate= 1.3/1) and (poly)acids as neutralization agents.

Entry	mol% of IDA	Acid	-COOH/-NH _x ^a	Av. particle diameter (nm) ^b	ζ-potential (mV) ^b
1	20	EDTA	1/1	N.A. ^c	N.A.
2	20		2/1	18	35
3	20	CA	1/1	N.A.	N.A.
4	20		2/1	N.A.	N.A.
5	20	SA	1/1	20	39
6	20	PTCA	1/1	N.A.	N.A.
7	20		2/1	N.A.	N.A.
8	20	CHTCA	1/1	N.A.	N.A.
9	20		2/1	N.A.	N.A.
10	20	AA	1/1	26	56
11	30	EDTA	1/1	12	34
12	30		2/1	8	41
13	30	CA	1/1	N.A.	N.A.
14	30		2/1	N.A.	N.A.
15	30	SA	1/1	16	36
16	30	PTCA	1/1	N.A.	N.A.
17	30		2/1	N.A.	N.A.
18	30	CHTCA	1/1	N.A.	N.A.
19	30		2/1	N.A.	N.A.
20	30	AA	1/1	32	49

^{a)} Determined by potentiometric titration; ^{b)} determined by DLS; ^{c)} not available due to precipitation.

The PUDs containing 30 mol% IDA and neutralized by either EDTA, SA or AA were then casted onto aluminum panels and dried at room temperature for 12 hours before curing at 150 °C in an oven under argon flow for 8 hours. The hardness and impact resistance of the cured coatings were evaluated and compared to the corresponding values of the non-cured materials. The results are summarized in Table 6. The M_n s of the PUs based on SA only slightly increased after curing due to insufficient crosslinking, leading to poor impact and acetone resistances. The curing of PU coatings with EDTA as neutralization agent improved the hardness and the acetone resistance as well as the impact resistance, probably because of intermolecular amidation between the carboxyls of the neutralization agent and the amine end-groups of the polyureas during the curing process (Scheme 10). As expected, the M_n s of the PU coatings with AA as neutralization agent remained constant after curing at 150 °C.

The coatings with EDTA and SA were harder (3B to 2B), compared to the one with AA (6B), illustrating the significant effect of the counter ion on the coating properties. This is likely caused by the salt formation between amines and the polyacids EDTA and SA, providing additional intermolecular interactions between the chains, and therefore leading to higher hardnesses.



Scheme 10. Possible amidation between EDTA and diamine-functional polyureas.

Table 6. Properties of PU coatings based on PPG400 and IPDMC with 30 mol% MeBAPA as IDA (primary amine/carbamate= 1.3/1) and (poly)acids as neutralization agents, before and after curing at 150 °C.

Acid	M_n (kDa) ^a (\bar{M}_n)		Pencil hardness		Impact test		Acetone resistance	
	Before	After	Before	After	Before	After	Before	After
EDTA		N.A. ^b	3B	2B	F	P	-	+
SA	9 (1.4)	11 (1.6)	3B	3B	F	F	-	-
AA	9 (1.4)		6B	6B	F	F	-	-

^{a)} Determined by HFIP-SEC; ^{b)} not available due to gelation.

Figure 8 shows deformed aluminum substrates covered with coatings prepared from PPGda400 and IPDMC and neutralized by EDTA. The coating before curing failed the impact test, as evidenced by visible cracks on the surface, while the one after 8 hours of curing at 150 °C exhibited a good impact resistance. The enhanced coating properties obtained after curing of these PUs are likely due to the increase of crosslink density as a result of an amide-forming condensation reaction between amine end-groups and carboxylic acid groups of the neutralizing agent. Similar curing mechanisms as described in the previous section may also take place in the curing process of these PUDs due to presence of comparable functional groups. The yellowish appearance of the cured coating is probably caused by the formation of imide structures during the process (see Chapter 6).

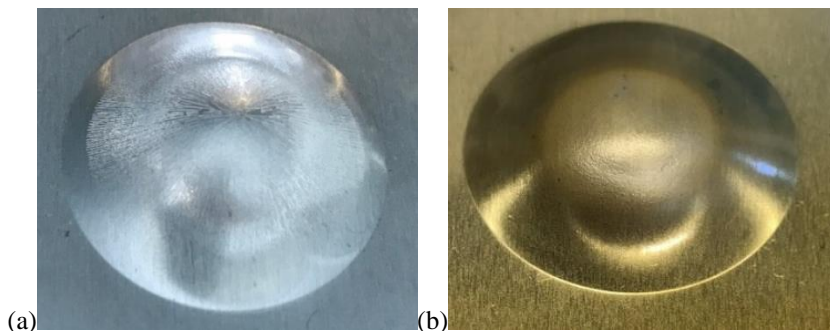
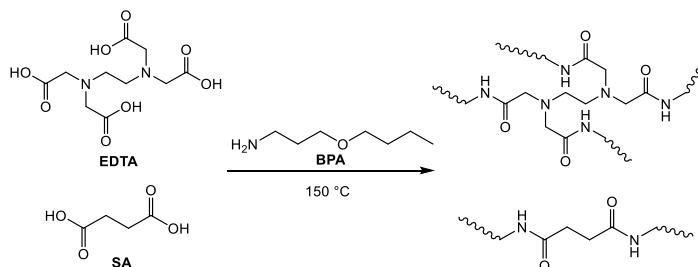


Figure 8. Deformed aluminum substrates covered with PU coatings based on PPGda400 and IPDMC (molar ratio: 1.3/1), neutralized by EDTA after reverse impact test, (a) before and (b) after curing at 150 °C for 8 hrs.

The enhanced coating properties obtained after curing of these PUs are likely due to the increase of crosslink density as a result of an amide-forming condensation reaction between amine end-groups and carboxylic acid groups of the neutralizing agent. Thus, model reactions were carried out at the temperature at which the curing was realized, using EDTA or SA and 3-butoxypropylamine (BPA) as substrates to verify this hypothesis (Scheme 11). The same concentration of BPA was used for each reaction with a stoichiometric acid/amine ratio.



Scheme 11. Model reactions with EDTA/SA and BPA as substrates with a 1/1 ratio of carboxylic acid and amine groups at 150 °C over 4 hours.

The limited M_n increase of SA-neutralized PUDs after curing at 150 °C was probably caused by the formation of the butoxypropyl-*N*-succinimide (Figure 9a). To verify such assumption, a model reaction with a 2/1 ratio of BPA/SA was carried out at 150 °C under argon flow, and monitored by $^{13}\text{C}\{^1\text{H}\}$ NMR (Figure 9b). The spectrum at t_0 was characterized by a singlet at 175.5 ppm assigned to the carbonyl of the SA (**a**). The decrease of intensity of **a** was accompanied by the emergence of two signals at 174.5 and 178.2 ppm attributed to the carbonyls of amide (**b**) and imide (**c**), respectively.²⁰ The formation of succinimide end-caps the amines and accordingly prohibits their further reaction with carboxylic acids, and therefore limits molecular weight growth or crosslinking during the curing of PUs, as indicated in Table 6. On the other hand, the tetra-functional EDTA is more efficient in promoting the crosslinking density of the PUs compared to di-functional SA.²¹

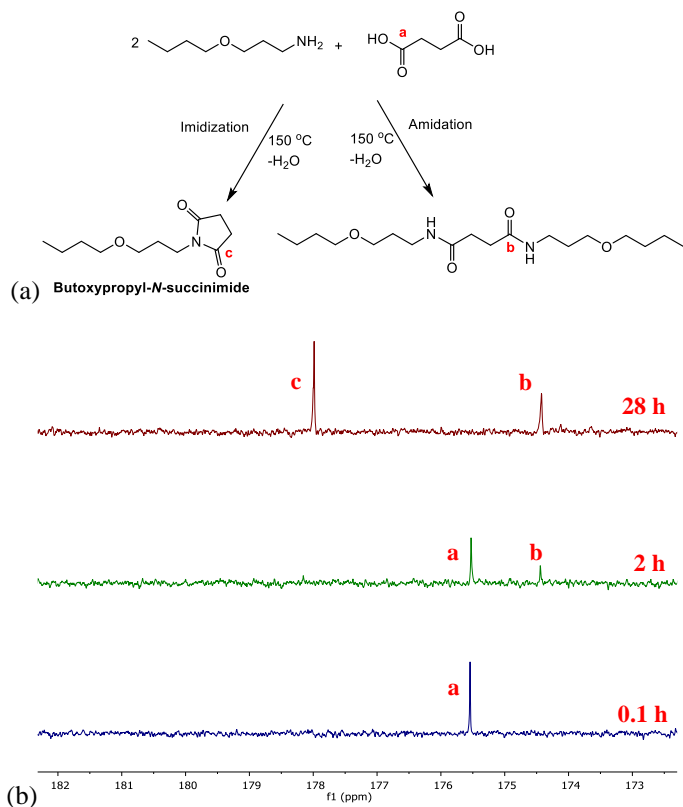


Figure 9. (a) Imide and amide formation in SA/BPA model reaction performed for 0-28 h at 150 °C. (b) ¹H NMR spectra of SA/BPA (1/2) mixtures, recorded in DMSO-*d*₆.

7.4 Conclusions

In this work, the curing of polyurea dispersions via reactions between carboxylic acids and amines was investigated. A first model reaction with 3-butoxypropylamine (BPA) and ethylenediaminetetraacetic dianhydride (EDTAD) as substrates in a 4/1 ratio revealed the formation of amides, noncyclic imides (NCI), cyclic imides (CI) and imidines. The formation rates of both amides and NCI was enhanced by the presence of H₃PO₄. Poly(amic acid urea)s (PAAUs) were synthesized from EDTAD and diamine-functional polyureas (PUDas). The latter were produced by polymerization of poly(propylene glycol) bis(2-aminopropyl ether) with an average *M*_n of 230 Da (PPGda230) and IPDMC with different ratios. Curing of PAAU dispersions at 150 °C with H₃PO₄ catalyst promoted the gel fraction compared to those without catalyst. PAAU coatings were prepared from 4,7,10-trioxa-1,13-tridecanediamine (TOTDDA) or PPGda230 as diamines, IPDMC as dicarbamate and EDTAD or 1,2,4,5-cyclohexanetetracarboxylic dianhydride (CHTCD) as dianhydrides. The coatings cured above 125 °C in the presence of H₃PO₄ exhibited significant improvements of mechanical properties and solvent resistance compared to those cured at 50 °C.

Cationically stabilized PUDs were prepared from 3,3'-diamino-*N*-methyldipropylamine

(DMDPA), isophorone dimethylcarbamate (IPDMC) and poly(propylene glycol) bis(2-aminopropyl ether) with an M_n of 400 Da (PPGda400) with polyacids as neutralization agents, viz. ethylenediaminetetraacetic acid (EDTA), citric acid (CA), succinic acid (SA), propane-1,2,3-tricarboxylic acid (PTCA) and cyclohexane-1,2,4,5-tetracarboxylic acid (CHTCA). Only EDTA- and SA-based PUDs remained stable with small particle sizes of about 20 nm and ζ -potential values between 34 and 41 mV. Curing of EDTA-based PU coatings at 150 °C resulted in enhanced hardness, impact and acetone resistances, due to the formation of amide bonds between the carboxylic acids in EDTA and the amine end-groups in PUs, which was evidenced by suitable model reactions. Curing of EDTA-based PU coatings at 150 °C resulted in enhanced hardness, impact and acetone resistances, while limited improvements in material properties were observed in SA-based PU coatings cured at the same temperature due to the formation of cyclic-succinimide.

7.5 References

- (1) Dieterich, D. *Prog. Org. Coat.* **1981**, 9, 281-340.
- (2) Cawse, J. US Patent B2 8981033, **2011**.
- (3) Jailliet, F.; Desroches, M.; Auvergne, R.; Boutevin, B.; Caillol, S. *Eur. J. Lipid Sci. Technol.* **2013**, 115, 698-708.
- (4) Ampudia, J.; Larrauri, E.; Gil, E. M.; Rodríguez, M.; León, L. M. *J. Appl. Polym. Chem.* **1999**, 71, 1239-1245.
- (5) Park, Y. -J.; Lim, D. -H.; Kim, H. -J.; Park, D. -S.; Sung, I. -K. *Int. J. Adhes.* **2009**, 29, 710-717.
- (6) Yeganeh, H.; Mehdizadeh, M. R. *Euro. Polym. J.* **2004**, 40, 1233-1238.
- (7) Moeini, H. R. *J. Appl. Polym. Chem.* **2009**, 112, 3714-3720.
- (8) Fetters, L. J.; Lohse, D. J.; Richter, D.; Witten, T. A.; Zirkelt, A. *Macromolecules* **1994**, 27, 4659-4647.
- (9) Wool, R. P. *Macromolecules* **1993**, 26, 1564-1569.
- (10) Allen, C. L.; Chhatwal, A. R.; Williams, J. M. J. *Chem. Commun.* **2012**, 48, 666-668.
- (11) Montalbetti, C. A. G. N.; Falque, V. *Tetrahedron* **2005**, 61, 10827-10852.
- (12) Lanigan, R. M.; Starkov, P.; Sheppard, T. D. *J. Org. Chem.* **2013**, 78, 4512-4523.
- (13) Tang, P. W. *Org. Synth.* **2005**, 81, 262-263.
- (14) Konieczny, J. M.; Wunder, S. L. *Macromolecules* **1996**, 29, 7613-7615.
- (15) Sacher, E. *J. Macromol. Sci.-Phys. B* **1986**, 25, 405.
- (16) Funke, W.; Horning, K.; Möller, M. H.; Würthwein, E.-U. *Chem. Ber.* **1993**, 126, 2069-2077.
- (17) Ali, M. A.; Siddiki, S. M. A. H.; Kon, K.; Hasegawa, J. *Chem-Eur. J.* **2014**, 20, 14256-14260.
- (18) Zhao, F.; Repo, E.; Yin, D.; Meng, Y.; Jafari, S.; Sillanpää, M. *Environ. Sci. Technol.* **2015**, 49, 10570-10580.
- (19) Bijsterbosch, B. H.; van Leeuwen, H. P.; Overbeek, J. T. G.; Vincent, B.; van der Wal, A. *Fundamentals of Interface and Colloid Science* Lyklema, J. **1995**, vol. 2, p 3.208.
- (20) Matsubara, K.; Nakato, T.; Tomida, M. *Macromolecules* **1997**, 30, 2305-2312.
- (21) Carothers, W. *Trans. Faraday Soc.* **1936**, 32, 39-49.

Appendix

Proposed mechanisms of intermolecular noncyclic and intramolecular cyclic imidizations

The proposed mechanisms for both cyclic and noncyclic imidization of EDTAD-based amic acid in the presence of H_3PO_4 are displayed in Figure S1. The H_3PO_4 initially is proposed to form a carboxylic-phosphoric anhydride intermediate with the amic acid. For intramolecular cyclic imidization, the nitrogen in the amide could directly attack the carbonyl of the carboxylate and accordingly forms an imide (blue arrows). Alternatively, the nitrogen of the amide could attack the phosphorus and result in an eight-membered transition state **A**, which could transform into a transition state **B** via an attack of amide nitrogen on the carbonyl of the carboxylate, followed by addition of water and dissociation of phosphoric acid to form the imide (green arrows). Such route is energetically less favored than the direct imide formation (blue arrows) due to the high ring strain of the transition state **B**. Similarly, an attack of the oxygen of the amide on the phosphorus would result in a transition state **C**. The next step involves the formation of a [3.3.1] transition state **D**, followed by addition of water and dissociation of phosphoric acid to form the imide (red arrows). Again, the high ring strain of the transition state **D** disfavors its presence during the reaction.

These mechanisms could also be valid for the intermolecular noncyclic imidization. Consequently, transition states **E**, **F**, **G** and **H** are formed instead of **A**, **B**, **C** and **D**, respectively. The energy levels of the four- and six-membered rings in the transition states **F** and **H** are much lower than those for **B** and **D**. Therefore, these species are much more likely to be present during the imidization of amic acid, and hence suggest a much higher rate for intermolecular noncyclic imidization than for intramolecular cyclic imidization.

In conclusion, the proposed mechanisms indicate a high selectivity of H_3PO_4 towards intermolecular noncyclic imidization rather than intramolecular cyclic imidization.

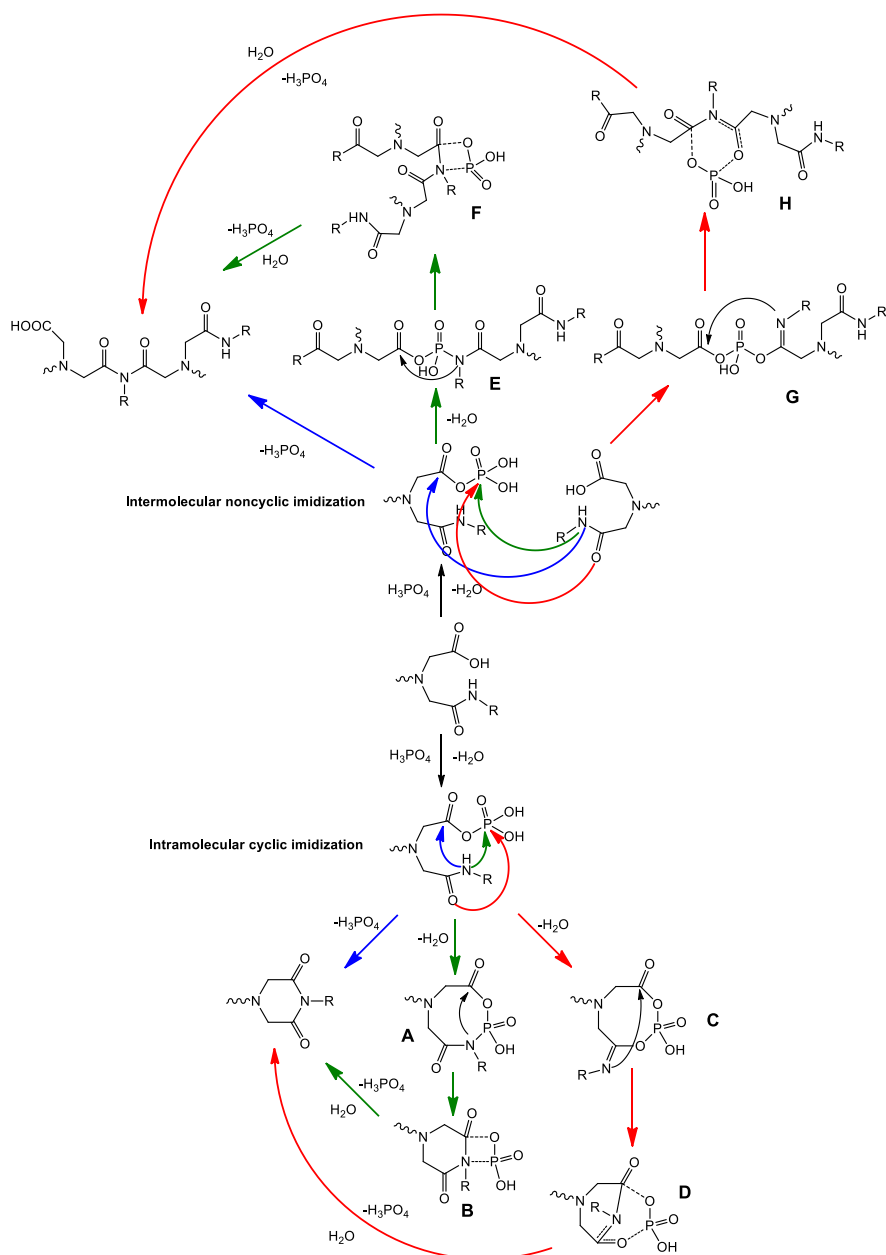


Figure S1. Proposed mechanisms of intermolecular noncyclic and intramolecular cyclic imidizations.

Chapter 8. Epilogue

8.1 Highlights

This work concerning the development of an isocyanate-free approach to water-borne polyurethane (PUR) and polyurea (PU) dispersions (PU(R)Ds) and coatings has provided a broad range of insights into the chemistry and reactivity of dicarbamates as isocyanate-free building blocks, the colloidal properties of PU(R) dispersions and the properties of coating materials derived from non-isocyanate monomers.

In this study, efficient catalysts for carbamate aminolysis were screened and the mechanisms of the reactions catalyzed by the most active ones, i.e. alkali bases and 1,5,7-triazabicyclo[4.4.0]dec-5-ene (TBD), were investigated via model reactions and computational simulations. PUs with high molecular weights (MWs) were successfully synthesized from diamine/dimethylcarbamate polymerizations catalyzed by alkali bases.

Besides the addition of a catalyst, the MWs of the PUs were enhanced by mitigation of the *N*-alkylation side reaction during the dicarbamate/diamine polymerization via an efficient removal of the byproduct methanol. This side reaction was also limited by employing the more sterically hindered diethyl- or di-*tert*-butyl carbamates (DiBoc-carbamate) as monomers. The polymerization of DiBoc-carbamates with diamines in the presence of an alkali base at 130 °C generated isocyanate intermediates, which led to PUs with MWs up to 120 kDa, along with branching as a result of biuret formation.

Cationically stabilized PU(R)Ds with good dispersion stability were prepared via incorporation of the tertiary amine-containing internal dispersing agent (IDA) 3,3'-diamino-*N*-methyldipropylamine (DMDPA) in the PU(R)s, followed by dissolution in the co-solvent methanol and neutralization with volatile acids and finally, dispersion in water and removal of the methanol. The hardness of the corresponding PU(R) coatings were dependent on the glass transition temperatures (T_g s) and urea contents of their parent resins, which could be modulated by employing different types and contents of building blocks and various amounts of DMDPA. In addition, the coatings prepared from PU(R)s of MWs above 50 kDa showed improved impact and solvent resistances compared to those issued from PU(R)s with MWs below 30 kDa.

Anionically stabilized PUDs were produced from N^2,N^6 -bis(*tert*-butoxycarbonyl) lysine (DiBoc-lysine) and diamines. Combination of DiBoc-lysine and a series of diamines lead to PUs with MWs up to 20 kDa, which can be dispersed in water without addition of neutralization agents. Another approach for the preparation of anionically stabilized PUDs involved the reaction of dianhydrides such as ethylenediaminetetraacetic dianhydride (EDTAD) with a series of diamine-functional polyureas (PUdas). The resulting poly(amic acid urea)s (PAAUs) with MWs up to 40 kDa were dissolved in methanol and neutralized by trimethylamine (TEA), followed by dispersion in water and removal of methanol to form PAAU dispersions (PAAUDs). The particle sizes of these dispersions could be tailored by varying the neutralization agent concentration, the molecular weight of the PUdas or the PUda/EDTAD ratio. The PAAU coatings prepared from the corresponding PAAUDs

exhibited satisfactory mechanical properties and solvent resistances.

Curing of PAAU coatings at elevated temperatures ($> 125\text{ }^{\circ}\text{C}$) significantly improved their mechanical properties and solvent resistances as a result of crosslinking between the polymer chains via amidation between the free primary/secondary amines and amic acids and intermolecular imidization between carboxylic acids and amides. Both these reactions can be catalyzed by H_3PO_4 . Similarly, the curing at $150\text{ }^{\circ}\text{C}$ of PU coatings based on diamines, dicarbamates and DMDPA with ethylenediaminetetraacetic acid (EDTA) as neutralization and crosslinking agent improved their impact and solvent resistances.

8.2 Technology assessment

This work employs dicarbamates as alternative building blocks to diisocyanates for the synthesis of PU(R)s. While the types of commercially available diisocyanate monomers are limited, dicarbamates could be readily obtained from the reaction between various diamines and dialkylcarbamates, thereby providing more versatility for the PU(R) industry and allowing a more extensive tailoring of properties. Whereas diisocyanates are prepared from diamines and phosgene, dicarbamates are synthesized from diamines and dicarbonates such as dimethyl carbonate (DMC) and di-*tert*-butyl dicarbonate (Boc_2O). DMC is cheaper than both phosgene and Boc_2O , while the prices of the latter two are comparable. Therefore, the prices of the dicarbamates described in this thesis may be comparable with or even lower than the prices of diisocyanates. Most of the polymerizations proceed in bulk, thereby avoiding the use of toxic and/or volatile organic solvents. All diamines, dicarbamates and internal dispersing agents used in this work are commercially available. Their combination results in PU(R) coatings with satisfactory mechanical properties and solvent resistances, suitable for real life applications. Additionally, the T_g s of these materials can be tailored by employing different structures and contents of the building blocks. As a result, PU(R)s coatings with different hardnesses could be prepared for various application purposes. Therefore, this study is interesting for paint producing companies, some of which were actively involved in the project within the framework of the Dutch Polymer Institute (DPI). Furthermore, the PU(R)Ds described in this work are prepared according to an industrially applied solvent-assisted dispersion (SAD) process, substituting acetone by methanol, a better solvent for the PUs used during our investigations. These PU(R)Ds can easily form smooth coatings on substrates at ambient temperature. Finally, the poly(amic acid urea) dispersions (PAAUDs) mentioned in this thesis do not require additional chain extenders for molecular weight enhancement. Instead, the dispersions can be cured at elevated temperatures ($>125\text{ }^{\circ}\text{C}$) to form crosslinked materials with enhanced mechanical properties and solvent resistance.

Three drawbacks can be mentioned of the approach described in this study. First of all, although the alkali bases are very active catalysts for dicarbamate/diamine polymerizations, they have poor solubility in many monomers and solvents, resulting in low catalytic activities. Secondly, the curing rates of the PU coatings are relatively slow, as a result of slow amidation and imidization reactions at the applied curing temperatures. Such slow curing processes are undesired in industry, due to the excessive consumption of energy and time. Finally, the low solid contents of around 10 wt% for the PU(R)Ds prepared in this work are much lower than the 35-50 wt% for the commercially available PURDs. These could result in much thinner

coatings after application and thus be less beneficial for protective purposes.

8.3 Outlook

Based on the isocyanate-free method for PU(R) production developed in this thesis, bio-based monomers such as isosorbide, 1,4-butanediol or the fatty acid-based diamine Priamine® (Croda) could also be integrated in the PU(R) backbone. Their combination with lysine-based monomers could potentially generate fully renewable PU(R)s dispersible in water. The properties of the resulting coatings could be further enhanced either by employing DiBoc-functional monomers or via curing at elevated temperatures.

Additionally, analytical techniques such as ^{31}P NMR and mass spectroscopy could be employed to identify the possible intermediates during the phosphoric acid-catalyzed noncyclic imidization, and consequently verify the mechanisms proposed in Chapter 7. Such investigations could give insights into the curing mechanism of the PAAUs and may provide potential solutions to reduce the time of curing. Alternatively, the slow curing rate of PAAU coatings could be mitigated by addition of amine- or activated hydroxyl-containing compounds such as diethylene triamine or Primid® (Ems-Chemie AG), and the differences in curing rates between the coatings with and without addition of curing agent could be studied via FT-IR or gel fraction measurements.

Since cyclic imides could potentially improve the thermal stabilities of the material,¹ it would also be interesting to quantify the cyclic imides in the cured PU coatings and investigate their influence on the thermal properties of the material via DSC and TGA.

The quaternization of tertiary amines in DMDPA-based PUs with a halogenated acid such as chloroacetic acid could produce zwitterionic moieties with quaternary ammonium and carboxylates.² These modified PUs could be dispersed in water without addition of neutralization agent. The properties of the corresponding PUDs could be modulated by varying the carbon numbers between the carboxylic acid to the quaternary amine.

As all the anionically stabilized PUDs produced in this study contain carboxylic acids, it is also worthwhile to explore and incorporate other IDAs containing sulfonic acid such as Vestamin® (Evonik) or phosphoric acid-derivatives in the PU backbone and study the corresponding dispersions and coating properties.

While side reactions such as allophanate or biuret formations are expected during industrial PU(R) production between diisocyanates and diamines or diols, the aminolysis and alcoholysis of dicarbamates described in this work afford more control over the polymer structures. Thus, it would be interesting to study the difference in properties of PU(R)s based on similar building blocks prepared via isocyanate and non-isocyanate approaches.

Silicon monomers such as tetraethyl orthosilicate (TEOS) could also be incorporated in the PU chains via reaction with diamine-functional PUs prepared in this study. The resulting polyurea silicates could have improved thermal and mechanical properties compared to PUs.

Furthermore, PUDs with higher solid contents could be prepared by dispersing the methanol solution of PU in lower amounts of water. The influence of the size of the dispersed particles of the PUDs on their viscosities could also be investigated, as the latter is a crucial parameter for almost all coating applications.

Finally, the abundant urethane/urea moieties in PU(R)s with low MWs and T_g s prepared in

this work could provide good adhesion to polar surfaces such as glass or steel. Hence, further investigations are recommended to explore the properties of these PU(R)s as adhesives.

8.4. References

- (1) Chattopadhyay, D. K.; Raju, K. V. S. N. *Prog. Polym. Sci.* **2007**, *32*, 352-418.
- (2) Kazantsev, O. A.; Baruta, D. S.; Shirshin, K. V.; Sivokhin, A. P.; Kamorin, D. M. *Rus. J. Phys. Chem. A* 2011, *85*, 413-418.

Glossary

ΔH	enthalpy of activation
ΔS	entropy of activation
$^{13}\text{C}\{^1\text{H}\}$ NMR	Carbon-13 nuclear magnetic resonance spectroscopy
^1H NMR	proton nuclear magnetic resonance spectroscopy
^1H - ^1H 2D COSY NMR	proton-proton two-dimensional homonuclear correlation spectroscopy
AFR	argon flow rate
ATR-FTIR	attenuated total reflection Fourier transform infrared
BAC	bis-alkylcarbamate
BAEC	bis(2-aminoethyl) carbamate
BAPA	bis(3-aminopropyl)amine
BAPC	bis(3-aminopropyl) carbamate
BCC	bis-cyclic carbonate
BDO	1,4-butanediol
BHC	bis-hydroxyalkylcarbamate
BMC	bis-methylcarbamate
Boc ₂ O	di-tert-butyl dicarbonate
Boc-carbamate	<i>tert</i> -butyl carbamate
Boc-HEX	<i>tert</i> -butyl hexylcarbamate
BPA	3-butoxylpropylamine
BPC	bis-phenylcarbamate
BU2	butylene biscarbamate
C	concentration
CA	citric acid
CHBMA	1,3-cyclohexanebis(methylamine)
CHBMC	1,3-cyclohexanebis(methylcarbamate)
CHTCA	cyclohexane-1,2,4,5-tetracarboxylic acid
CHTCD	1,2,4,5-cyclohexanetetracarboxylic dianhydride
CI	cyclic imide
DAA	diamic acid
DAB	1,4-diaminobutane
DBTDL	di-butyltin-dilaurate
DBU	1,8-diazabicyclo(5.4.0)undec-7-ene
DCC	dicyclohexylcarbodiimide
DCMPA	3,3'-dicarbamate- <i>N</i> -methyl-dipropylamine
DCTB	trans-2-[3-(4- <i>tert</i> -butylphenyl)- 2-methyl-2-propenylidene] malononitrile
DEC	diethyl carbonate
DETA	diethylene triamine
DETPAD	diethylenetriamine-pentaacetic dianhydride
DFT	density functional theory

DiBoc-carbamate	di- <i>tert</i> -butyl dicarbamate
DiBoc-IPDC	di- <i>tert</i> -butyl isophorone dicarbamate
DiBoc-lysine	<i>N</i> ² , <i>N</i> ⁶ -bis(<i>tert</i> -butoxycarbonyl) lysine
DLS	Dynamic light scattering
\bar{D}_M	polydispersity index for molecular weight
DMAc	dimethylacetamide
DMAP	dimethylaminopyridine
DMBA	dimethylol butanoic acid
DMC	dimethyl carbonate
DMDPA	3,3'-diamino- <i>N</i> -methyldipropylamine
D_{me}	degree of methylation
DMF	dimethylformamide
DMHD	<i>N,N'</i> -dimethyl-1,6-hexanediamine
DMPA	dimethylolpropionic acid
DMSO	dimethyl sulfoxide
DODD	4,9-dioxa-1,12-dodecane-diamine
DSC	Differential scanning calorimetry
E_a	activation energy
EDTA	ethylenediaminetetraacetic acid
EDTAD	ethylenediaminetetraacetic dianhydride
EWG	electron-withdrawing group
GC-FID	gas chromatography with flame ionization detector
h	Planck's constant
HAD	1,7-diaminoheptane
HC	hydroxyl carbamate
HDC	1,6-hexamethylene dicarbamate
HDI	hexane-1,6-diisocyanate
HEX	hexylamine
HFIP	1,1,1,3,3,3-hexafluoro-2-propanol
HS	hard segment
IDA	internal dispersing agent
IDAa	diamine-functional IDA
IDAc	dicarbamate functional IDA
IPDEC	diethylcarbamate
IPDI	isophorone diisocyanate
IPDMC	isophorone dimethylcarbamate
IRC	intrinsic reaction coordinate
k_{2Me}	reaction rate constant of methylation of secondary amine
K_a	equilibrium constant
$k_{alcoholysis}$	rate constant of carbamate alcoholysis
$k_{aminolysis}$	rate constant of carbamate aminolysis
k_B	Boltzmann constant
KHMDS	potassium bis(trimethylsilyl)amide
k_{Me}	reaction rate constant of methylation of primary amine

KOMe	potassium methoxide
KO <i>t</i> -Bu	Potassium <i>tert</i> -butoxide
KTFA	Potassium trifluoroacetate
k_{urea}	urea generation rate
lnA	frequency factor
MALDI-ToF-MS	matrix-assisted laser desorption ionization time-of-flight mass spectrometry
MDI	methylene diphenyl diisocyanate
M_n	number average molecular weight
MTBD	7-methyl-1,5,7-triazabicyclo[4.4.0]dec-5-ene
MW	molecular weight
NAC	neutralization agent concentration
NCI	noncyclic imide
NHMC	<i>N</i> -hexyl methylcarbamate
NMP	<i>N</i> -methylpyrrolidine
P ₂ -Et	tetramethyl(tris(dimethylamino)phosphoranylidene) phosphoric triamid-ethyl-imine
PAA	poly(amic acid)
PAAU	poly(amic acid urea)
PAAUD	poly(amic acid urea) dispersion
PC	propylene carbonate
PCMD	poly(carbonate macrodiol)
PEG	poly(ethylene glycol)
PHU	poly(hydroxyl urethane)
PPG	poly(propylene glycol)
PPGda	poly(propylene glycol) bis(2-aminopropyl ether)
Priamine ® 1074	fatty acid-based diamine
PTCA	propane-1,2,3,-tricarballic acid
PTCA	propane-1,2,3-tricarboxylic acid
pTHF	poly(tetrahydrofuran)
pTHF1000	diamine functional pTHF/PPG copolymer with an average M_n of 1000 Da
pTHFda1000	diamine-functional pTHF with an average M_n of 1000 Da
PU	polyurea
PUD	polyurea dispersion
PUda	diamine-functional polyurea
PUR	polyurethane
PURD	polyurethane dispersion
PUU	polyurethane urea
PUUD	polyurethane/urea dispersion
R	gas constant
<i>r</i>	ratio between dicarbamate and diamine
ROMP	ring-opening polymerization
SA	succinic acid

Sc(OTf) ₃	scandium triflate
SEC	size exclusion chromatography
SrO	strontium oxide
SS	soft segment
TBD	1,5,7-triazabicyclo-[4.4.0]dec-5-ene
TDI	toluene diisocyanate
TEA	triethylamine
TEG	triethylene glycol
T_g	glass transition temperature
THF	tetrahydrofuran
Ti(Obu) ₄	titanium(IV) butoxide
TMA	trimellitic anhydride
TMG	1,1,3,3-tetramethyl-guanidine
TMP	trimethylolpropane
TOTDDA	4,7,10-trioxa-1,13-tridecanediamine
TS	transition state
VOC	volatile organic compounds
W	weight of the sample
ZPE	zero-point energie
α	particle radius
ΔE^\ddagger	energy barrier
ϵ	dielectric constant
η	solution viscosity
κ	Debye-Hückel parameter
μ	electrophoretic mobility

Summary

Polyurethane (PURs) and polyureas (PUs) are classes of polymers in which the segments are connected by urethane or urea moieties, respectively. The hydrogen bonds between those groups result in strong physical crosslinks between the polymer chains, leading to materials exhibiting superior mechanical properties compared to other polymers such as polyethers or polyesters. Important applications of PURs and PUs are the water-borne PU(R) dispersions and coatings based thereon, the standard preparation of which utilizes extremely toxic diisocyanates. Alternatively, PU(R) could be produced from dicarbamates or cyclic carbonates, contributing to the global drive for green chemistry. This thesis focuses on developing isocyanate-free routes for water-borne PU dispersions, with the emphasis on understanding the structure-property relations of these polymers.

For this study, dicarbamates were employed as alternatives to react with diamines to form polyureas. An extensive experimental study was performed to determine the most active and practically usable catalysts for such polymerization. The results suggested that metal alkoxides and amides were the best performers in terms of promoting the carbamate and carbonate aminolysis. More specifically, potassium methoxide (KOMe), potassium ethoxide (KO i -Bu), potassium bis(trimethylsilyl)amide (KHMDs) as well as the previously studied 1,5,7-triazabicyclo[4.4.0]dec-5-ene (TBD) were the best catalysts for these reactions. Activation energies for the formation of carbamates and ureas were determined through kinetic experiments at different temperatures. The obtained results were in good agreement with computational modeling calculations.

Aqueous dispersions of PUs were prepared by incorporation of internal dispersing agents (IDAs) within the PU backbones. Thus, the polyamines diethylenetriamine (DETA), bis(3-aminopropyl)amine (BAPA) and 3,3'-diamino-*N*-methyldipropylamine (MeBAPA) were incorporated into PUs. However, both DETA- and BAPA-based PUs resulted in gelation during polymerization due to reactions between carbamates and the secondary amines in the IDA moieties, while moderate molecular weight (MW) were observed for MeBAPA-based PUs. The residual secondary/tertiary amine groups present along the PU backbones were neutralized with volatile acids, such as acetic acid, and the resulting neutralized polymers were dispersed in water to form stable PUDs with particle sizes below 300 nm and high ζ -potentials (>40 mV). The coatings prepared from commercially available diamine-functional poly(propylene) glycol (PPGda400), isophorone dicarbamate (IPDMC) and MeBAPA showed satisfactory properties such as sufficient impact resistance and solvent resistance against acetone and water.

PUs generated from dicarbamate/diamine polymerization have lower MWs than those produced from isocyanate chemistry. Thus, an in-depth study regarding the limitations of the MW growth during dimethylcarbamate/diamine polymerization was provided. Undesired methylation of the amines by the methylcarbamate monomers was observed during polymerization, and was considered to be the limiting factor for reaching high conversions and high molecular weights during the polymerization. Suppression of the methylation, either by efficient removal of the methanol from the reaction mixture or by substitution of

dimethylcarbamates with the more sterically hindered diethylcarbamates, results in polyureas with high MW.

Compared to dimethylcarbamates, faster polymerization was observed for highly sterically hindered di-*tert*-butylcarbamates (DiBoc-carbamates) and diamines. This was explained by the formation of isocyanate intermediates under basic conditions at high temperatures, as evidenced by both proton and carbon NMR (^1H and ^{13}C NMR). Consequently, stoichiometric polymerizations of DiBoc-carbamates and diamines or diols lead to branched structures of high number average molecular weights (M_n s) up to 100 kDa (polydispersity of 3.1) (or even to gelation), due to the formation of allophanates or biurets from isocyanates and urethanes or ureas, respectively. These high molecular weight DiBoc-carbamate-based PU(R) coatings exhibited excellent mechanical properties and solvent resistance.

A key step in the development of high MW, water-borne PU systems is the chain extension of relatively low MW prepolymers dispersed in water. As the carbamate-amine chemistry used for prepolymerization was not sufficiently reactive to achieve chain extension under mild conditions, the anhydride-amine coupling appeared to be a promising option, which accordingly was explored in depth. The reaction of the cyclic anhydride ethylenediaminetetraacetic dianhydride (EDTAD) with a primary amine generated an amic acid structure, i.e. an amide bond and a free carboxylic acid. The latter could then potentially be used as an IDA through neutralization with e.g. triethylamine or a non-amine base. Although the reaction between amines and anhydrides was very fast, the observed MW build-up was rather limited, probably due to the hydrolysis of amide bonds or anhydride moieties. The latter generates diacid groups, which are not reactive towards amines, thereby acting as chain stoppers during the polymerization and limiting the MW growth. Imidization between carboxylic acid groups and amides was also observed from both ^1H and ^{13}C NMR studies, and could be mitigated by lowering the drying temperature of the polymer. The particle sizes of these poly(amic acid urea) dispersions (PAAUDs) could be adjusted via changing the concentration of the neutralization agent or by changing the carboxylic acid content in the PAAUs, which could be tailored by varying either the MW of the diamine-functional polyurea prepolymers (PUDas) or the PUDa/EDTAD ratio.

To further improve the material properties of the PU coatings, crosslinking of the PU coatings was also investigated by first preparing diamine-functional PAAUDs via the copolymerization of an excess of diamine-functional polyureas and a dianhydride, followed by drying at elevated temperature on an aluminum panel. The resulting materials were cured above 120 °C overnight to obtain crosslinked polyurea coatings with improved solvent and impact resistance compared to those cured at ambient temperatures. The crosslinking was found to originate from the reaction between the pending carboxylic acid groups and the end-amine functions as well as amide moieties. The latter resulted in non-cyclic imides formed between the polymer chains. Both these reactions can be catalyzed by H_3PO_4 .

Similar crosslinking reactions were also applied to non-amic acid-containing PUs. These PUDs, produced from polymerization of diamines, dicarbamates and MeBAPA, were neutralized with multi-functional acids such as ethylenediaminetetraacetic acid (EDTA). Curing of these dispersions at 150 °C resulted in crosslinked structures with satisfactory

coating properties.

Overall, this thesis screened and investigated the most efficient catalysts for the isocyanate-free polyurea synthesis with dicarbamates and diamines. Moreover, it also demonstrated the preparation of stable water-borne polyurea dispersions with high MW as well as polyurea-based coatings with desired material properties. In conclusion, this work described the use non-toxic raw materials in polyurea synthesis, and established novel isocyanate-free routes towards high performance PU applications.

Acknowledgement

The past four years have been an exiting and pleasant journey, filled with joy and sweat. I wish to thank everyone that accompanied and helped me during this period, without them I can never finish this adventure.

I would like to thank my first promotor Cor Koning for providing me this precious opportunity to dive deep into the coating science and helped me during the four years. You are a great promotor, and a nice friend. During my second year, when things went chaotic and I was quite desparate in finding solutions for the difficult problems in this project, you constantly encouraged me and gave me advices, and even contacted resources in industries to help me tackle the problems. Despite the long trip from Zwolle to Eindhoven, you always manage to get to the University every other week to have a meeting with us. You gave me with many valuable advices, but you also allow me to have enough freedom for carrying out my own ideas, and build up my independence as a researcher. It is a great pleasure working by your side.

Secondly, I wish to express my gratitude to my second promotor Rolf van Benthem. Your extensive knowledge and experience in organic chemistry, material science and coating technology proved to be a crucial asset to this project, and I'm still nourishing from that after 4 years. You are always able to provide a solution for every single problem we encounterd, and it turned out to be a right one for most of the times (I wonder if you get bored of being right). The way of critical thinking is something I learned most from you, and it helped me build up an analytical mind for my future careers.

I also like to thank my daily supervisor Rafaël Sablong for the great help during my last two years. You are a great person to work with, and I learned a lot from your experimental skills in organic and polymer chemistry. I truly admire your responsible and cautious attitude towards work. This is especially true when it comes to writing, which I improved significantly (maybe not as good as you expect yet) under your guidance. You are very kind to everyone, and no matter how busy you are, you can always spare some time for the helpless rookies.

My first daily supervisor, Bart Noordover had been guiding me from the very beginning of my PhD career, and I can't tell how grateful I am to you, as you not only recruited me in this project, but also supported me during the difficult times. I've never feel desparate when you leave us in the second year, because you've already taken us so far that we could continue on our own. I'm very happy to know that you are now live close to your family and have a comfortable life there.

Dutch Polymer Institute (DPI) are greatly acknowledged for the funding of this project. I was very lucky to meet and work with many experienced researchers in industries and academia: Keimpe, Ronald, Roel, Ron, Ronald, Monique, Bert, Caterina, Peter, Ping, Mauro and Isabel. I'm specially thankful to Ron, who helped me greatly in tacking one of the most important problems in the project, and Peter (also as my paranimf), who went to almost all the conferences and meetings with me, you are a great person to work with, and I wish you find

a nice job soon .

I cannot finish my thesis without the help from the master student who worked with me during the past three years, and I would like to thank you for that. Ellen, your creative mind and independent working spirit has inspired me a lot during your stay in our group, and I wish you a great success in the following years. Cheng, you are a good friend and work mate, and I hope you will get a perfect job for your future career. Huiyi, your solid background in chemistry and hard working spirit are very helpful in the project, and I'm sure you will have a great time working with Hans in the coming years.

It is my great privilege to be a member in both the amazing SPM and blooming SPC groups, and I would like to thank all the awesome colleagues for the friendly and open environment. Lily, it is a great pleasure to work by your side, since you're so helpful and kind and always filled with positive energy, which inspires me at my lowest moments. I wish you a great success in finding a nice job! Cristina, you have extensive experience in polymer science are very helpful to us, and I really admire your efficiency in doing scientific research. Juliën, you are a genius in NMR, and I'm sure you're have a great time in working on the instruments. Remco, thank you very much for take us under your wings in the last two years, and provide us with such a friendly working environment and letting me chair the group meeting for a month, which is really helpful in my personal skill development. Caterina, your knowledge in surface chemistry and polymer science has always been a great asset to the group, and I learned a lot from you. Martin, Marco and Ton, you have made the research in floor 1 and 2 a lot easier by maintaining a well organized working environment. Pleunie and Caroline, you have always been so helpful to everyone that come to your offices. I wish to show my thanks to the other SPM and PTG/e members: Karel, Geert, Erik, Mark, Judith, Benny, Pim, Timo, Stefan, Mohammad, Olessya, Silvia, Joice, Hans, Han and Cees. As currently a part of the growing SPC group, I would also like to express my gratitude to many other SPCers: Jos, Alessandro, Chiara, Leo, Jaap, Ilja, Ping, Mauro, Isabel, Peter, Dilek, Kirill, Vincent, Mark, Jelena, Dannie, Laura, Adriaan, Marieke, Emma, Tahoorra. Thank you all to make SPC a warm family.

一晃七年就过去了，在这七年里我有幸结识了各路中华英杰。首先，感谢宇晶，在我这几年最艰难的几道坎上都提供了有力的帮助和指点，祝愿你和薇姐以及将要出生的小宝宝今后生活越来越美好。感谢已经在国内的陈于蓝师姐，我很高兴能在硕士期间认识你，你对工作认真的态度以及科研的前瞻性令我拜服，祝愿你和龙哥在国内发越来越多的好文章。颖渊师姐，感谢你对我找工作的支持和帮助，非常羡慕你有一个可爱活泼的小 Daniel 和爱你的 John。感谢姜长这几年的照顾和帮忙，以及午饭时分带来的欢声笑语，希望埃因霍恩午饭小队在你的领导下越来越壮大。春亮，感谢你这几年对我的帮助，你对科研的专注精神让我敬佩，从你那我学到很多东西，祝愿你和女朋友今后的事业一帆风顺。彦武，感谢你能做我的答辩嘉宾，以及这些年的慷慨帮助，祝你很快能找到一份好工作，家庭美满幸福。德磊，你天生的幽默感总是给大家带来无限的欢乐，祝你接下来在这座城市的工作顺利。小宝，我的大学校友，感谢你多次请客吃饭，你精湛的刀法让我记忆犹新，希望你能尽快毕业，并且找到一个自己喜欢的工作。刘浩，感谢你一直以来的帮助，祝你在国内事业爱情美满。礼华，感谢多次

请客和组织的“德扑”局，每次都玩的非常开心，也谢谢你多次帮我做测试。一流，祝你在新的岗位上事业蒸蒸日上。强哥，你精湛的乒乓技术征服了大半个荷兰，让我等羡慕不已，祝你很快能找到好工作，并和女朋友聚首。刘冲，我的邻居以及合作伙伴，感谢你对我的帮助。另外，也感谢博士期间遇到的中国朋友：杨芸，蒙潇，谢杰，段春辉，林良良，宋诗冬，丁子然，潘继凯，苏心如，汪捷，李思雨，迟梦，顾家镭，以及在体育馆遇到的好朋友：王昕，大明，小安，吴疆，英哲，毋凡，荣哥，叶一舟，冯驰，孟晨，老贾，陶林凯，谢谢你们对我的帮助。

Finally, I would like to thank my family and girlfriend for their support and unconditional love during the past years. 爸爸妈妈，感谢这么多年的养育之恩以及无私奉献的关爱，谢谢老妈从小培养我的英语，直到来这边才明白您的苦心。吴寅和赵伟，我的好兄弟，谢谢这几年的鼓励和支持，希望我们很快又能相聚。最后，to my dearest Angelyrao，遇见你是我最美丽的意外，感谢你让我的苦闷的学术生活充满光明和动力，相信我们互补的性格一定能让生活越来越好，我爱你！

Shuang Ma 麻爽

13th-November-2017

List of publications

Peer-reviewed journal publications

S. Ma, E. P. A. van Heeswijk, B. A. J. Noordover, R. J. Sablong, R. A. T. M. van Benthem, C. E. Koning. "Isocyanate-free approach to water-borne polyurea dispersions and coatings" (submitted).

S. Ma, R. J. Sablong, R. A. T. M. van Benthem, C. E. Koning. "Non-isocyanate strategy for anionically stabilized water-borne polyurea dispersions and coatings" (submitted)

S. Ma, H. Zhang, R. J. Sablong, R. A. T. M. van Benthem, C. E. Koning. "Di-*tert*-butyl carbamate for isocyanate-free polyurethane/urea dispersions and coatings" (to be submitted).

S. Ma, C. Liu, R. J. Sablong, B. A. J. Noordover, E. J. M. Hensen, R. A. T. M. van Benthem, C. E. Koning. "Catalysts for isocyanate-free polyurea synthesis: mechanism and application" *ACS Catalysis*. 2016, 6, 6883–6891.

Conference proceedings

Ma, S., Sablong, R.J., Hensen, E.J.M., van Benthem, R.A.T.M., Koning, C.E. "Isocyanate-free strategies to polyurethane/ureas" *12th Coating science international* (2016)

Ma, S., Sablong, R.J., Hensen, E.J.M., van Benthem, R.A.T.M., Koning, C.E. "Water-borne polyurethane/urea dispersions and coatings in isocyanate-free routes" *13th Coating science international* (2017)

Publications and patents not related to this thesis

Robert T. M. Jakobs., Shuang Ma., Rint P. Sijbesma. "Mechano-catalytic polymerization and cross-linking in a polymeric matrix." *ACS Macro Lett.* 2013, 2, 613–616.

Curriculum Vitae

Shuang Ma was born on December 26th 1988 in LongQuan China. After finishing high school in 2006, he started the Bachelor Chemical Engineering at Zhejiang University, China. In 2010 he graduated within the group of Chemical Engineering and continued his Master study in the Chemistry and Chemical Engineering department of Eindhoven University of Technology in the Netherlands. He graduated within the group of Prof. Rint Sijbesma on the research topic of “Mechanically activated metathesis catalyst in solid state”. From August 2013, he started a PhD project at in Eindhoven University of Technology under the supervision of Prof. dr. Cor Koning and Prof. dr. Rolf A.T.M. van Benthem from the Laboratory of Physical Chemistry. Dr. Bart A.J. Noordover and dr. Rafaël J. Sablong became his coach later. His PhD research topic was focused on the development of isocyanate-free polyurea dispersions for coating applications. The most important results obtained in this research are described in this dissertation.

